Physical Processes Controlling the Surface Layer Dynamics in the Stratified Gulf of Finland: An Application of Ferrybox Technology

VILLU KIKAS

TUT
PRESS

TALLINN UNIVERSITY OF TECHNOLOGY
Marine Systems Institute

Dissertation was accepted for the defence of the degree of Doctor of Philosophy in Earth Sciences on November 15, 2016.

Supervisor: Prof. Urmas Lips, Marine Systems Institute at Tallinn University of Technology

Opponents: Dr. Seppo Kaitala, Marine Research Centre, Finnish Environment Institute, Finland

                   Dr. Piia Post, Institute of Physics, Faculty of Science and Technology, University of Tartu, Estonia

Defence of the thesis: December 15, 2016 at the Marine Systems Institute, Tallinn University of Technology, Akadeemia tee 15a, Tallinn, Estonia

Declaration:

Hereby I declare that this doctoral thesis, my original investigation and achievement, submitted for the doctoral degree at Tallinn University of Technology has not been submitted for doctoral or equivalent academic degree.

/Villu Kikas/

Pinnakihi muutlikkust kontrollivad füüsikalised protsessid kihistunud Soome lahes: Ferrybox tehnoloogia rakendus

VILLU KIKAS

TABLE OF CONTENTS

LIST OF ORIGINAL PUBLICATIONS

I   Kikas, V., Lips, U. (2016). Upwelling characteristics in the Gulf of Finland (Baltic Sea) as revealed by Ferrybox measurements in 2007–2013. *Ocean Science*, 12, 843–859, doi: 10.5194/os–12–843–2016.

II   Kikas, V., Norit, N., Meerits, A., Kuvaldina, N., Lips, I., Lips, U. (2010). High–resolution monitoring of environmental state variables in the surface layer of the Gulf of Finland (during a dynamic spring bloom in March–May 2010). *IEEE Conference Publications: Baltic International Symposium (BALTIC), 2010 IEEE/OES US/EU, Riga, 24–27 August 2010*, 1–9, doi: 10–1109/BALTIC.2010.5621627.

III   Lips, U., Kikas, V., Liblik, T., Lips, I. (2016). Multi-sensor in situ observations to resolve the sub-mesoscale features in the stratified Gulf of Finland, Baltic Sea. *Ocean Science*, 12, 715–732, doi:10.5194/os–12–715–2016.

IV   Lips, I., Rünk, N., Kikas, V., Meerits, A., Lips, U. (2014). High-resolution dynamics of spring bloom in the Gulf of Finland, Baltic Sea. *Journal of Marine Systems*, 129, 135–149, doi: 10.1016/j.jmarsys.2013. 06.002.

V   Lips, U., Lips, I., Kikas, V., Kuvaldina, N. (2008). Ferrybox measurements: a tool to study meso-scale processes in the Gulf of Finland (Baltic Sea). *IEEE Conference Publications: 2008 IEEE/OES US/EU– Baltic International Symposium, Tallinn, 27–29 May 2008*, 1–6, doi: 10–1109/BALTIC.2008.4625536.

AUTHOR'S CONTRIBUTION

I   The author was responsible for everyday maintenance of the Ferrybox system, data collection, data analysis and interpretation of the results and writing of the manuscript.

II   The author was responsible for everyday maintenance of the Ferrybox system, data collection, data analysis and interpretation of the results and he participated in the writing of the manuscript.

III   The author was responsible for processing and statistical analysis of Ferrybox data, combined presentation and analysis of Ferrybox and buoy data and he participated in the writing of the manuscript.

IV   The author was responsible for processing and analysis of Ferrybox data and he participated in the writing of the manuscript.

V   The author was responsible for processing and analysis of Ferrybox data and he participated in the writing of the manuscript.

APPROBATION OF THE RESULTS

1. 7th FerryBox Workshop, 06 – 09.04.2016, Heraklion, Crete. Continuous Ferrybox measurements create new knowledge on essential processes in the marine environment.

2. 6th Warnemünde Turbulence Days (WTD), 11 – 15.08.2013, Rostock, Germany. Mesoscale and submesoscale variability in the Gulf of Finland (Baltic Sea) as revealed by autonomous in-situ observations.

3. 4th IEEE/OES Baltic Symposium, 24 – 28.08.2010, Riga, Latvia. High-resolution monitoring of environmental state variables in the surface layer of the Gulf of Finland (during a dynamic spring bloom in March-May 2010).

INTRODUCTION

The Baltic Sea is a young and vulnerable brackish inland sea surrounded by many different countries. Human activities have a great impact on the sea and its ecosystem mainly through the land based activities such as industry and agriculture, but also due to different uses of the sea, among them ship traffic. On the other hand, the latter also creates possibilities to monitor the human impact and maybe even more importantly discover new knowledge about the Baltic Sea ecosystem and processes influencing the state of the marine environment.

There are many ships regularly crossing the Baltic Sea and its sub-basins from one port to another, for instance, Tallinn and Helsinki in the Gulf of Finland. The ferries serving this regular passenger line provide a suitable monitoring platform for autonomous flow-through systems already since 1997. In 2006, a new more complex and sophisticated measurement system referred as "Ferrybox" was installed on board a passenger ferry cruising between Tallinn and Helsinki.

It took some time, but the system is in operation since May 2007. It measures different environmental parameters, like temperature, conductivity, chlorophyll *a* fluorescence and for some time pCO_2, not forgetting numerous water samples collected. The measurements are done in a way that more data in time and space are provided than regular monitoring cruises (conducted not very often) or satellite images (limited availability due to quite a cloudy region) could do. Of course, Ferrybox technology has its limitations as well, e.g. the measurements are conducted along a fixed ferry line and depend on the ferry schedule. Nevertheless, collected high-quality data prove to be a very good addition to conventional measuring/monitoring platforms.

In this thesis along the published papers, the experiences of conducting measurements with a flow-through system installed on passenger ships traveling along the same transect, on a daily basis, nearly a decade, are presented. Most of the examples, comparisons and phenomena noted are from the spring–summer period in 2007–2013. However, the data collection and transmitting is still a daily routine, which regularly goes on.

The main scientific question studied during the Ph.D. work was related to the dynamics of coastal upwelling events. The results show that the classical scheme of coastal upwelling/downwelling in elongated basins (Krauss and Brügge 1991) has to be updated if applied in the Gulf of Finland. The estuarine character of this basin (closed at one end where the fresh water input exists and open water exchange with a larger basin at the other end) leads to clear differences in upwelling behavior near the northern and southern coasts of the gulf. These differences are recognized in upwelling frequencies and intensities in relation to the wind forcing, as well as a manifestation of sub-mesoscale variability.

1. BACKGROUND

1.1 Forcing and physical processes

The Baltic Sea is a relatively small, but at the same time one of the largest brackish water areas with the following dimensions: area of 393000 km^2 and volume of 21200 km^3 (Leppäranta and Myrberg 2009). It is a semi-enclosed sea connected to the North Sea via the narrow and shallow Danish Straits, and it consists of several sub-basins. The main physical forcing components for the Baltic Sea system are: the atmospheric forcing (including wind forcing and atmospheric pressure gradients), heat exchange through the sea surface, freshwater input/output due to precipitation and evaporation, freshwater discharge from rivers, and the water exchange with the North Sea (Omstedt et al. 2014).

Tidal forcing has been considered low (Lilover et al. 2011), but the ice cover also affects the dynamics of the sea in winter when all the sea might be frozen (Omstedt et al. 2014). The freshwater input into the surface layer amounts to annual river discharge of 440 km^3 and surplus of freshwater due to the difference in precipitation (215 km^3) and evaporation (175 km^3) (Leppäranta and Myrberg 2009). This freshwater input and saltier water inflows into the sub-surface and deep layers create a strong vertical haline stratification of the water column with a permanent halocline at the depths of 60–80 m in the deep basins of the sea. The vertical stratification is strengthened in summer due to the development of the seasonal thermocline at the depths of 10–20 m.

General circulation in the Baltic Sea is characterized by a cyclonic pattern in the surface layer (Leppäranta and Myrberg 2009). In the deeper layers, the main factors maintaining the circulation are gale-forced barotropic or baroclinic salt water inflows and vertical mixing of deeper, saltier waters with the surface, fresher waters (Meier et al. 2006). The saltier water inflows from the North Sea form a gravity-driven dense bottom flow, which transports these waters (while mixing with the surrounding Baltic Sea waters) through the southern sub-basins and deep channels to the Gotland Deep and Northern Baltic Proper (Kõuts and Omstedt 1993). Due to the deep connection with the Baltic Proper, the Gulf of Finland is part of the Baltic thermohaline circulation (Elken and Matthäus 2008) while the Gulf of Bothnia and Gulf of Riga are separated from the Baltic Proper by narrow and shallow straits, and thus the quasi-permanent halocline is not developed there (Omstedt and Axell 2003).

Mesoscale processes have been observed and studied since the 1970's and 1980's when eddy-resolving CTD surveys were introduced in the Baltic Proper. These studies revealed that the Baltic Sea has rich mesoscale variability with spatial scales $O(10)$ km through the whole water column (Aitsam et al. 1984). Those measurements with high horizontal resolution revealed the patchiness in the horizontal distribution of thermohaline fields in the upper layer and occurrence of sharp thermohaline fronts. The observations showed a clear similarity between the physical processes in the Baltic Sea and the ocean,

although the scales of features and processes were different (Aitsam et al. 1984). After that, various mesoscale structures have been revealed across the Baltic Sea among them intra-pycnocline anticyclonic lenses (similar to Mediterranean water lenses in the Atlantic – Meddies), sub-surface cyclonic eddies (negative lenses), and "ordinary" upper layer cyclonic and anticyclonic eddies (Elken 1996, Reissmann 2005). A number of studies provide evidence that these mesoscale features create remarkable changes in the Baltic Sea pelagic ecosystem functioning (Kahru et al. 1984, Nausch et al. 2009).

Upwelling is a common mesoscale phenomenon in the Baltic Sea, redistributing both the heat and salt in coastal regions and replenishing the surface layer with nutrients, especially in summer when the surface layer is depleted of nutrients (Lehmann et al. 2012). Bychkova et al. (1988) have identified 22 areas of upwelling occurrences in the Baltic Sea under favorable atmospheric forcing conditions. Model simulations and satellite images have shown that the annual-averaged frequency of strong upwelling may be as high as 30–40% in some parts of the Baltic Sea (Kowalewski and Ostrowski 2005, Lehmann et al. 2012). During upwelling, temperature difference up to 10 °C can be observed, and upwelling duration varies from 1–2 days up to a month (Myrberg et al. 2008). The coastal upwelling events transport nutrient-rich deep water to surface with an excess of phosphorus (lowering N/P ratio), which favors cyanobacterial blooms (Vahtera et al. 2005). Most prominent upwelling areas with favorable wind conditions are the Swedish south and east coast (30%), off the southern tip of Gotland (15%) and on the northern side of the Gulf of Finland (14%) (Lehmann and Myrberg 2008).

The Gulf of Finland is an elongated basin in the northeastern part of the Baltic Sea (Fig. 1) with a length of about 400 km and a maximum width of 135 km (Alenius et al. 1998). Due to the prevailing wind forcing, freshwater input mainly in the east and saltier water inflow in the west, the estuarine circulation with an up-estuary flow in the deeper layers and down-estuary flow in the surface layer exist in the gulf. The wind-induced alterations and even reversals of this circulation pattern can occur (Elken et al. 2003, Liblik et al. 2013). The long-term residual circulation in the surface layer of the gulf is characterized by an inflow of the saltier water of the northern Baltic Proper along the southern coast and the seaward flow of gulf water along the northern coast (Andrejev et al. 2004). The circulation is more complex at time scales from days to weeks mainly due to the variable wind forcing. A variety of mesoscale processes, including upwelling events, have been observed in the Gulf of Finland (Talpsepp et al. 1994, Pavelson et al. 1997, Lips et al. 2009).

A seasonal thermocline forms in the Gulf of Finland in spring–summer at the depths of 10–20 m separating the upper mixed layer and intermediate cold water layer (Alenius et al. 1998, Liblik and Lips 2011). On average (based on data from 1987–2008), the upper mixed layer depth was 11.4 in June, 12.1 m in July and 14.1 m in August in the western and central gulf (Liblik and Lips 2011). It has been shown that quasi–stationary thermohaline stratification patterns influenced by the external forcing exist in the gulf (Liblik and Lips 2012). The observed

changes in the stratification (except in case of upwelling/downwelling events) could be explained by a simple conceptual model where the heat flux, wind mixing, estuarine circulation and its alteration due to the wind forcing were accounted (Liblik and Lips 2012).

While high concentrations of dissolved inorganic nitrogen (DIN) and phosphorus (DIP) are observed in winter, the DIN and DIP concentrations decline fast in April–May and are usually below the detection limit in summer in the upper mixed layer. The nutriclines are associated with the seasonal thermocline in summer in the Gulf of Finland, whereas the phosphates are available at shallower depths than the inorganic nitrogen compounds (Laanemets et al. 2004). Thus, vertical flux of nutrients due to mixing or upward movement is required to support the phytoplankton growth in the euphotic layer. In the elongated Gulf of Finland, where the coastal upwelling events occur frequently, they could remarkably contribute to such transport of nutrients (Lips et al. 2009). For instance, due to the excess transport of phosphorus, the upwelling events are considered as a major contributor to the cyanobacterial blooms in the gulf (Vahtera et al. 2005, Laanemets et al. 2006, Lips and Lips 2008).

Coastal upwelling events are generated in the Gulf of Finland by strong enough wind impulses from west – south-west near the northern coast and from east – north-east near the southern coast. According to a principal model of upwelling in elongated basins (Krauss and Brügge 1991), first, the cross-shore Ekman transport is created in the surface layer, which produces cross-shore sea level and density gradient (the latter due to upwelling of denser waters), and in turn along-shore jet current. The wind impulse needed to create an upwelling is estimated as large as 4000–9000 N m^{-2} s for strong thermal stratification and 10500–14000 N m^{-2} s for weak stratification based on the following formula:

$$WI = \int_0^t C_a \rho_a U_a^2 dt \qquad (1)$$

where ρ_a is the air density, C_a is the drag coefficient, U_a is the wind speed (upwelling favorable component) at a 10 m height, and t is the wind duration (Haapala 1994). The analysis of wind data (Lehmann et al. 2012) and model experiments suggest that one of the major upwelling areas exists in the north-western part of the Gulf of Finland along the Finnish coast (Myrberg and Andrejev 2003, Lehmann et al. 2012). The analysis of remote sensing images in combination with the wind data revealed 1–4 upwelling events near the southern coast and 3–5 upwelling events near the northern coast of the gulf per year in June–September (Uiboupin and Laanemets 2009). In the latter study, a criterion based on cumulative wind stress of 0.1 N m^{-2} d (corresponds to 8640 N m^{-2} s) for potential occurrence of an upwelling event was applied, calculated using wind data with the 3-h time step (Δt) as:

$$CWS = \sum_{i=1}^{n} C_a \rho_a \, \Delta t |U_i| U_i^{70} \qquad (2)$$

where U_i is the wind velocity at time step t_i and U_i^{70} its projection to the along-gulf axis of 70°.

Model experiments by Laanemets et al. (2009) have suggested that a steeper bottom slope and greater sea depths along the southern coast can cause larger nutrient inputs along the southern coast than the inputs along the northern coast under the same magnitude of wind forcing. Furthermore, the upwelling events enhance the coastal offshore exchange (and related transport of nutrients), especially during their relaxation (Laanemets et al. 2011). Model simulations by Zhurbas et al. (2008) showed that the instability of along-shore baroclinic jets leads to the development of filaments/squirts remarkably increasing the lateral eddy diffusivity. In this respect, the sub-mesoscale processes could play an important role, as it has been suggested by recent studies based on high–resolution in situ (Lips et al. 2011), numerical modeling (Laanemets et al. 2011) and remote sensing (Uiboupin et al. 2012) data. The relevant sub-mesoscale features are the upwelling filaments and intra-thermocline intrusions with lateral scales less than the internal Rossby radius of deformation, which is about 2–5 km in the Gulf of Finland (Alenius et al. 2003).
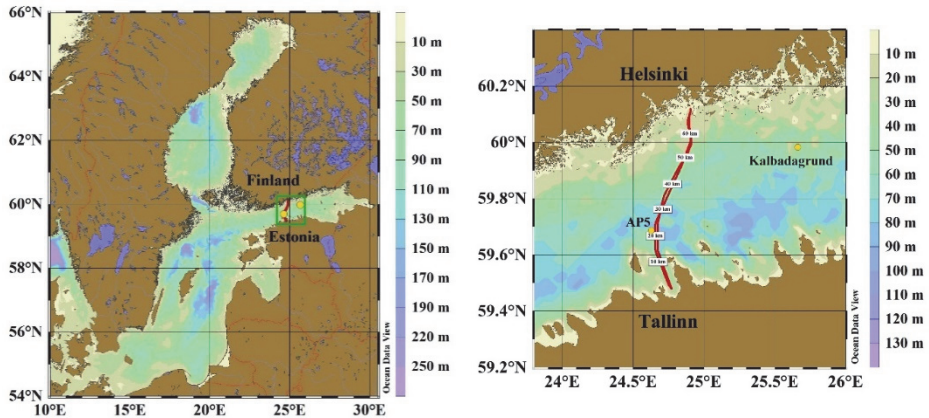
Figure 1. Map of the Baltic Sea and the ferry route between Tallinn and Helsinki in the Gulf of Finland (maps were prepared using ODV software; Schlitzer, 2010).

While essential contribution of mesoscale processes to the vertical exchanges of nutrients in the marine environment has been suggested and proved by a number of studies (McGillicuddy et al. 1998, Martin and Pondaven 2003), the role of sub-mesoscale processes is still not clear. Recent studies suggest that the sub-mesoscale processes significantly contribute to the vertical exchange of water mass properties between the upper and deep ocean (Bouffard et al. 2012). These sub-mesoscale processes are characterized by order-one ($O(1)$) Rossby and Richardson numbers (Thomas 2008), large vertical velocity and vorticity fluctuations and large vertical buoyancy flux, resulting in considerable intermittency of oceanographic properties in the upper ocean (Capet et al. 2008).

1.2 Ferrybox technology

Unattended monitoring of marine environment using ships of opportunity, where autonomous measurement systems (so-called "Ferryboxes") are installed, has been implemented in many regions of the World Ocean (Kahru and Brown 1999). First trials of using ships of opportunity for the environmental monitoring in the Baltic Sea were made by Estonian and Finnish scientists in the Gulf of Finland between Tallinn and Helsinki in 1990–1991 (Rantajärvi 2003). Regular measurements of temperature, salinity and chlorophyll *a* (Chl *a*) fluorescence along this route started in 1997 (Kanoshina et al. 2003) while the longest data series in the Baltic (since 1993) is available along the ferry route Helsinki – Travemünde (Petersen 2014).

Ferrybox systems have been successfully used to register different physical and biological parameters in locations where other conventional measurements are too expensive to acquire data with necessary resolution or which are not convenient for remote sensing due to cloudiness. A principal scheme of the Ferryboxes is shown in Fig. 2.

Figure 2. Principal scheme of the Ferrybox system.

Ferrybox flow-through system is proven to be cost-effective and reliable – constant power supply, easy maintenance, near real time data transfer (via GSM or satellite connection), high resolution in time and space, a variety of sensor that can be added. Eighteen regularly going passenger and merchandise ships with installed Ferryboxes cover large areas in the Baltic Sea and the North Sea, giving vital environmental background information (Petersen 2014). The limitations of Ferrybox technology are related to the measurements and water sampling only from the surface layer and some disturbances that the ferry itself could cause for the water parameters taken in and forced to flow through the tubes to the sensor

package. In addition, on the negative side, the ship routes or the ships could change, creating caps in the data flow. However, the Ferryboxes have evolved into more compact systems and therefore adding more mobility to transfer them from one to other ship (of course, this requires negotiations with the shipping company) (Aiken et al. 2011).

Unattended measurements of physical parameters (i.e. temperature, salinity, etc.) and Chl *a* fluorescence and water sampling (using attached autonomous water sampler) are successfully applied in the Baltic Sea to monitor late summer cyanobacteria blooms and environmental factors influencing the bloom intensities (Leppanen et al. 1995, Kanoshina et al. 2003, Lips and Lips 2008). Less attention has been paid to the studies of the dynamics of spring bloom using unattended measurements (Paper **IV**), although a spring bloom intensity index is developed and applied (Fleming and Kaitala 2006).

In some cases, the ferry routes and schedules provide a perfect opportunity to follow certain processes if the measurements are repeatedly conducted for a long period. For instance, Buijsman and Ridderinkhof (2007) estimated the water and suspended matter exchange between the Wadden Sea and the North Sea using data collected along the Den Helder–Texel ferry route. Similarly, the Tallinn–Helsinki ferry route across the elongated Gulf of Finland and the schedule consisting of two cruises a day and a short 1.5 h stay in Helsinki are convenient for coastal upwelling studies. Two crossings a day allow to study the daily changes in the surface layer. Since the data along the ferry route are recorded frequently enough (20 s, see Chapter 3 for more details), the spatial variability from basin scale to less than 1 km can be analyzed. The measurements from both the open sea and two coastal areas reveal well the coastal-offshore gradients and, based on regular daily data, enable to analyze statistical characteristics of the upwelling events.

Being a technology used by ships of opportunity (SOOP), this particular Ferrybox system (4H-Jena FerryBox I; obtained by the Marine Systems Institute in 2006) has been on board many ships crossing the same route in the Gulf of Finland: 2006–2008 "Galaxy", 2008–2013 "Baltic Princess", 2013–2014 "Silja Europa", 2015–2016 "Baltic Queen". All the before mentioned are sister ships, except "Silja Europa", this means that the flow-through system was installed in the same place and way over the years. On board "Silja Europa" it was installed more into the middle section, which did not influence the data quality (comparing the daily crossings); also other characteristics remained similar to other ships i.e. water intake to the system, ship speed, etc.

1.3 Motivation and objectives

To assess the state of the Gulf of Finland ecosystem and to quantify the impact of various factors/processes, in situ measurements with high enough resolution, duration and extent have to be conducted. Conventional monitoring programs have too low frequency and spatial resolution of sampling while special investigations using the research vessels are conducted episodically. Therefore,

new autonomous measurement methods, among them in situ observations using voluntary platforms such as ferries, have to be applied. Several studies have shown how the Ferrybox measurements are successfully used for different applications (Petersen et al. 2011) among them for the analysis of abiotic factors influencing the cyanobacterial bloom intensities in the Gulf of Finland (Lips and Lips 2008). The combination of Ferrybox measurements and remote sensing is suggested as an important monitoring method of coastal waters (Petersen et al. 2008).

Mesoscale processes as major factors controlling the spatial and temporal variability of environmental variables as well as the vertical exchange of nutrients in the Baltic Sea have been suggested and proved by a number of studies and reports in the recent two decades (Elken 1996, BACC 2015). One among the mesoscale processes contributing to the vertical transport is upwelling that can occur anywhere in the semi-enclosed Baltic Sea (Omstedt et al. 2014) and is a prominent feature in the Gulf of Finland (Uiboupin and Laanemets 2009). Leading to a significant vertical transport of nutrients into the euphotic layer (Lips et al. 2009, Laanemets et al. 2011), it also influences the phytoplankton growth and species composition (Lips and Lips 2010).

Dynamics and characteristics of upwelling events have been studied in the Gulf of Finland based on in situ measurements (Haapala 1994), remote sensing (Uiboupin and Laanemets 2009) and modeling (Myrberg and Andrejev 2003). Most prominent upwelling events that were captured by measurements are an event along the northern coast in July 1999 (Vahtera et al. 2005) and an event along the southern coast in August 2006 (Lips et al. 2009). The following characteristic features of upwelling events in the Gulf of Finland are suggested:

- the Finnish coastal sea in the north-western part of gulf is one of the main upwelling areas in the Baltic Sea (Myrberg and Andrejev 2003) where upwelling frequency in May–September 1990–2009 has been up to 15% (Lehmann et al. 2012); almost the same upwelling frequency is suggested by the latter authors for the central part of gulf along the Estonian (southern) coast;

- mean upwelling area detected on the basis of 147 maps during the period of 2000–2009 was 5642 km^2 (19% of the gulf surface area) along the northern coast and 3917 km^2 (13% of the gulf surface area) along the southern coast (Uiboupin and Laanemets 2015), while the largest area covered by the upwelling water was identified as 12140 km^2 (data from 2000–2006; (Uiboupin and Laanemets 2009); the authors' estimate of the mean cross–shore extent of upwelling area was 20–30 km off the northern coast and varied between 7 and 20 km off the southern coast;

- the intensity of upwelling events depends on the values of cumulative upwelling-favorable wind stress and strength of vertical stratification; Haapala (1994) suggested that at least a 60-h long wind event has to exist to create an upwelling event; based on the wind data analysis from 2000 – 2005 and taking the threshold value for cumulative wind stress of 0.1 N m^{-2} d, on

average, about two upwelling events should appear off the southern coast and four events off the northern coast (Uiboupin and Laanemets 2009);

- it is suggested that the difference in topography off the southern and northern coast of the gulf results in differing upwelling dynamics along the opposite coasts – in the case of similar wind stress (but in opposite directions) the transport of waters from deeper layers starts earlier and is larger along the southern coast (Väli et al. 2011).

Thus, we know quite a lot about the dynamics and characteristics of the upwelling events in the Gulf of Finland. However, there is a discrepancy between the frequency estimates based on remote sensing and those based on wind forcing arguments. According to the wind statistics and modeling experiments, more upwelling events should occur near the northern coast than near the southern coast. The greater impact of upwelling events along the southern coast has been attributed to the steeper bottom slopes there. Various methods have been applied to reveal characteristic features of coastal upwelling events in the Baltic Sea, but high-resolution long-term in situ data have not been analyzed with this aim until now. The collected Ferrybox data along the Tallinn–Helsinki ferry route serve the first opportunity to estimate upwelling statistics based on in situ observations with a large number of events captured.

According to high-resolution profiling at a fixed position in the Gulf of Finland, quasi-stationary stratification patterns of the thermocline occurred there at timescales of 4–15 days (Liblik and Lips 2012) and the vertical dynamics of phytoplankton were largely defined by these patterns (Lips et al. 2011). At the same time, the layered structure of the major basins of the Baltic Sea, with the seasonal thermocline and the halocline situated at different depths – about 10–30 m and 60–80 m, respectively, is a challenge to be accurately described by numerical models (Tuomi et al. 2012). One possible reason for poor estimates could be the lack of knowledge on the role of sub-mesoscale processes in regard to energy transfer from the mesoscale to small scales. These processes could contribute to the vertical material exchange as well as re-stratification of the water column (Brannigan 2016).

Sub-mesoscale features, including eddies with diameters of less than Rossby radius of deformation, are mostly not captured by traditional oceanographic methods due to their fast appearance, nonstationary nature and short lifetimes (Lavrova et al. 2012). Sources of their generation are still not well known, but fronts and current instability have been suggested to play a significant role (Lavrova et al. 2012, Karimova and Gade 2015). An analysis of SAR imagery for the period from 2009 to 2011 discovered almost 7000 sub-mesoscale eddies in the Baltic Sea in 2009–2011 (Karimova and Gade 2015). It can be hypothesized that under certain conditions, such as the development and relaxation of coastal upwelling events in a stratified estuary, the sub-mesoscale processes are more energetic than predicted by the theory of quasi-geostrophic turbulence in the ocean interior.

A major impact of coastal upwelling events on phytoplankton growth has been documented by several studies (e.g. Vahtera et al. 2005, Lips and Lips 2010).

There are examples showing the influence of sub-mesoscale features on phytoplankton growth and distribution (Lips et al. 2011, Uiboupin et al. 2012). The regular Ferrybox measurements at Tallinn–Helsinki ferry route could enable to show that these observations can be a valuable source of information and a good basis for descriptive and statistical analysis of meso- to sub-mesoscale features and physical-biological coupling.

The main objectives of the study are:

- to develop a method for detection and quantitative description of coastal upwelling events based on Ferrybox measurements;
- to describe the occurrence of coastal upwelling events and their characteristic parameters along the two opposite coasts of the gulf statistically;
- to explain the dependence of revealed upwelling characteristics on the forcing and prevailed meteorological and hydrographic conditions in the gulf in summer;
- to characterize the sub-mesoscale processes in the gulf and their role in energy transfer from the mesoscale to smaller scales;
- to demonstrate the ability of Ferrybox technology to track the phytoplankton dynamics and to describe the link between the physical forcing and the variability of biogeochemical parameters in the surface layer of the gulf.

2. MATERIAL AND METHODS

2.1 Ferrybox data

2.1.1 The system and sensors

The applied flow-through system is a commercial product, "Ferrybox I" from 4H-Jena (Germany). For current passenger ship "Baltic Queen" (and its former sister ships) the water intake for measurements and sampling is attached to the sea chest that is located on starboard side close to the bow and is meant to take in large amounts of seawater for various tasks. The water enters the sea chest through a grating with a total surface area of 0.84 m^2, where the openings have the dimensions of 20 x 90 mm and form in total an open area of 0.32 m^2. The grating is 0.5 m in height, and the center of it is located 4.1 m below the waterline while the maximum draught of the ferry is 6.4 m. The total volume of the sea chest is approximately 8 m^3 and the time interval to flush it through is depending on the cruising speed of the ferry. For "Silja Europa" the sea chest was located more in the middle section of the ship, and the intake faced downward.

The water flow from the sea chest into the system is forced by the hydrostatic pressure since the Ferrybox is located on the lower deck about 4–5 meters below the waterline. To restrict larger particles to get into the measurement system a mud filter (pore size 1 mm) is used just after the water intake. The filter is cleaned regularly to prevent clogging of the water flow. Before the sensors, a debubbler is installed to avoid air bubbles to affect the measurements of conductivity, turbidity, and Chl a fluorescence. The rate of water inflow from the sea chest into the debubbler varies between 12 and 15 $l\,min^{-1}$. The flow rate through the sensors is stabilized by an internal pump, which is controlled by a pressure sensor in the system. The feedback loop between the internal pump and the pressure sensor guarantees an average pressure of 180 mbar and flow rate of 6–7 $l\,min^{-1}$.

For temperature measurements, a Pico Technology high accuracy platinum covered sensor PT100 is used. It is installed close to the water intake to diminish the effect of warming of water while flowing through the tubes onboard. For salinity measurements, an FSI Excell thermosalinograph (temperature and conductivity meter) is used. For Chl a fluorescence and turbidity measurements, a SCUFA submersible fluorimeter (Turner Designs) with a flow-through cap is used. The fluorimeter is equipped with a temperature sensor to correct the fluorescence values for temperature influence. Water samples are taken by a sampling device Hach Sigma 900 MAX (starting from November 2013, ISCO 5800 Refrigerated Sampler), whereas the water is pumped from the debubbler into the bottles using an internal pump of the water sampler.

Start and stop of the measuring cycle is automatically controlled by a GPS (Garmin 16HVS) device installed on board. The system starts the measurements and data recording when the ferry is away from the harbor more than a control distance of 0.7 nautical miles and stops when it is closer than this distance, in order to avoid the sediments getting into the system. Temperature, salinity, Chl a

fluorescence and turbidity data are recorded during every crossing (twice a day) every 20 s that corresponds to a horizontal resolution of approximately 160 m. Same applies to GPS and household data which are used for a preliminary data quality control.

The system and sensors are kept clean by an acid washing procedure performed automatically every night. Additional manual cleaning for SCUFA sensors is conducted weekly during the productive season.

2.1.2 Data handling and quality control

The Ferrybox data handling and quality control are described in detail in (Paper I). The sensors have been calibrated at the factory before the installation and, if necessary, sent for an additional laboratory calibration. Since the system contains two temperature sensors, the performance of them is routinely followed by the comparison of data acquired from the sensors. The quality of thermosalinograph data is guaranteed by taking a series of water samples and analyzing them using a high-precision salinometer AUTOSAL 2–4 times a year. The analyses have shown, that a stable correction of 0.08 (units in Practical Salinity Scale; the value has been stable over the years) must be added to the recorded salinity.

The SCUFA fluorimeter is calibrated at the laboratory once every winter, usually an intercalibration event held by Alg@line consortium (see more information about the Alg@line in Rantajärvi, (2003)). However, due to the dependence of fluorescence values upon the varying optical properties of the sea water and phytoplankton species composition, weekly or bi-weekly sampling and laboratory analyses for Chl *a* content is performed to convert the fluorescence values into Chl *a* (the procedure is described below).

A predefined time interval (usually 10 or 15 min) is set for water sampling along the route when the ferry is traveling from Helsinki to Tallinn. Depending on the task, from 11 to 17 samples were collected weekly or bi-weekly (during one crossing) in 2007–2013. After sampling, the water samples are kept in cool (4 °C) and dark conditions until collecting them for the laboratory analyses. In order to calibrate the measured fluorescence values against Chl *a* content in the water, the collected water samples are analyzed using a spectrophotometer Thermo Helios γ. The concentration of Chl *a* is determined by filtering the water samples through glass-fiber filters (Whatman GF/F or Millipore APFF filter with pore size of 0.7 μm), extracting the pigments 24 h at room temperature with ethanol (96%) and measuring the absorption at the wavelength of 665 nm. A linear regression between fluorescence and Chl *a* content detected spectrophotometrically is found to convert fluorescence values into the Chl *a* concentrations.

The data acquired by the Ferrybox system recorded with a time step of 20 s are stored in an onboard terminal. To synchronize the measurements performed by the sensors having different sampling frequencies and GPS, the acquired data within every 19 s interval are averaged and recorded as the measurements at every

20th s. The data are automatically delivered to the on-shore FTP-server once a day when the ferry is in the harbor using a GSM connection.

The performance of the system is validated by the control parameters, such as the flow rate and pressure in the system, and the data are checked for unrealistic values against the criteria set for every parameter on the basis of known natural variation of them in the Gulf of Finland. In order to use the data for the assimilation into operational models, automatic procedures for preliminary processing and quality check have been applied. One of the procedures, which have to be carried out when using the Ferrybox data, is the shifting of data points to the actual positions of the water intake. The problem arises since the coordinates attached to a data record correspond to the location of the ferry at the time of measurement, but the water is taken in earlier at a different position. Since various systems of water intake are applied, this procedure is unique for each combination of a Ferrybox and a ferry.
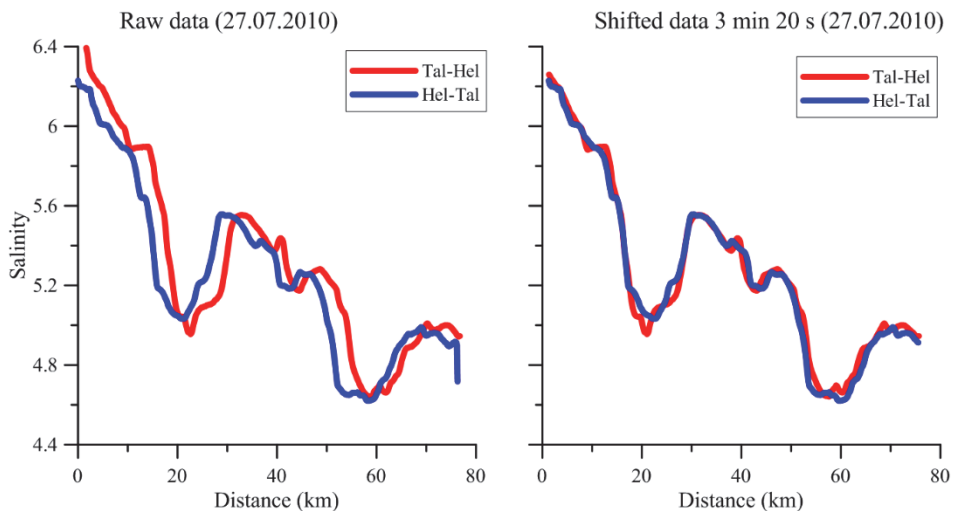
Figure 3. Measured salinity distribution along the ferry route Tallinn–Helsinki from the forth and backward journeys on 27 July 2010. Raw data are presented in the left panel and the processed data in the right panel where the shifting of data points by 3 min and 20 s was applied; x-axis shows the distance from the Tallinn Bay (latitude 59.48° N) in km along the meridional transect.

The problem of the time lag between the intake and measurement was solved by the analysis of data from forth and backward journeys – a position correction procedure was introduced to get the best match between the two profiles a day. For the all used sister ferries, the time shift of 3 min 20 s was applied. This relatively long period is obviously related to the water exchange in the sea chest. Due to an almost constant cruising speed of the ferry outside the harbor areas (16 knots), the applied procedure gives acceptable results (Fig. 3). The comparison of data from Tallinn to Helsinki and back from Helsinki to Tallinn obtained on the same day is one of the used quality assurance procedures – the profiles

containing unexpected deviations are marked by a quality flag indicating a possible quality problem.

2.1.3 Analyzed Ferrybox data

Altogether data of more than 1000 crossings have been collected along the Tallinn–Helsinki ferry route in 2007–2013 and in the present study (by 4H-Jena system "Ferrybox 1"). In (Paper **I**), temperature and salinity data collected from May to September in 2007–2013 are used. Since in 2008 and 2013, the system was transferred from one ferry to the new ferry brought to Tallinn–Helsinki route and a failure of measurements in September 2012 occurred, data from not all crossings were available. Nevertheless, the data from all months from May to September were analyzed at least for six years in 2007–2013.

Part of the same data set was applied for analysis of sub-mesoscale variability and influence of physical processes to Chl *a* distribution in the surface layer (Paper **III**). The period of July–August in 2009–2012 was chosen to match the buoy profiler data from the same area (see in next sub-chapter). The data from May–September 2007 were applied to draw the conclusions about the average distribution of temperature, salinity, and Chl *a* in the surface layer across the Gulf of Finland (Paper **II**).

The spatial and temporal variability of thermohaline fields and phytoplankton dynamics in spring were studied based on data from March–May 2009 and 2010 (Papers **IV** and **V**). In (Paper **IV**) data on nutrient concentrations and phytoplankton species composition and biomass were incorporated into the analysis. The water samples were collected weekly and analyzed in the laboratory next day after sampling (the methods are described in Paper **IV**). In addition, in spring 2010, a pCO_2 sensor was attached to the Ferrybox system to identify the changes in CO_2 concentration related to phytoplankton growth and physical processes, including upwelling events (Paper **V**).

To convert Chl *a* fluorescence data measured by the Ferrybox system to Chl *a* content values, a linear regression line between those two data sets was found separately for spring and summer each year. While in spring, good consistency of Chl *a* fluorescence and Chl *a* was obtained (e.g. Paper **V**), the summer communities of phytoplankton are more diverse in the sense of pigment characteristics, and therefore the fluorescence data have to be used very carefully if the goal is to describe the variability of phytoplankton biomass. The same applies to other systems, which were equipped with fluorimeters. See the used equations for estimating Chl *a* content based on fluorimeters data in (Paper **III**).

2.2 Data from other observing systems

The data from an autonomous buoy profiler (Idronaut S.r.l.; surface buoy designed by Flydog Solutions Ltd.), which was deployed in the central Gulf of Finland (see location in Fig. 1) in summers 2009–2012, were used in the study (Paper **III**). The system recorded vertical profiles of temperature, salinity, and

Chl *a* fluorescence in the water layer from 2 to 45 (50) m with a time resolution of 3 h and a vertical resolution of 10 cm using an OS316*plus* CTD probe (Idronaut S.r.l.) equipped with a Seapoint Chl *a* fluorimeter. Ship-borne measurements and sampling close to the buoy profiler were arranged bi-weekly to check the quality of data (compare the vertical profiles from the buoy with those from the research vessel) and to calibrate the fluorimeter by laboratory analyses of Chl *a* content from the water samples (Paper **III**).

The used dataset also includes vertical profiles of temperature, salinity, and Chl *a* fluorescence conducted with a towed undulating vehicle (Scanfish). The horizontal distributions of T, S, and Chl *a* in the water column from 2 to 45 m (see location of sections in Fig. 1; Paper **III**) were mapped. Scanfish sensor set consisted of a Neil Brown Mark III CTD probe and TriOS microFlu-chl-A fluorimeter. Data were recorded continuously (both down- and upcast are used) and the processed data were stored with a vertical resolution of 0.5 m. The average distance between the consecutive Scanfish cycles, including down- and upcast while the vessel was moving with a speed of 7 knots, was 600 m.

It is very challenging to study sub-mesoscale processes in the coastal, relatively shallow but vertically stratified sea areas where the characteristic baroclinic Rossby radius is on the order of a few kilometers. A combination of autonomous and research-vessel-based devices, such as Ferryboxes, moored profilers, and towed undulating instruments (Scanfish) was applied in the present study. For instance, the dataset from July–August 2009–2012 analyzed in (Paper **III**) comprised data from 461 Tallinn–Helsinki ferry crossings, 968 CTD and Chl *a* profiles collected at station AP5 and six Scanfish surveys.

In addition to the autonomous devices and towed vehicle, ship-borne measurements were conducted in the area throughout all seasons analyzed in the present study. For instance, in spring 2010 altogether seven surveys close to the ferry route (and station AP5) were conducted in April and May (Paper **IV**). CTD measurements using an Ocean Seven 320*plus* CTD probe (Idronaut S.r.l.) equipped with a Seapoint Chl *a* fluorimeter and water sampling aboard the research vessel were performed. Such application of several systems in parallel increased the confidentiality that the autonomous systems (including Ferrybox) were operating well.

2.3 Forcing and remote sensing data

As the forcing data, mostly the wind data from the region were used; it means the other forcing factors, such as the heat flux through the sea surface and fresh water and saltier water inflows were not considered. This approach is justified by the characteristic temporal scales of analyzed processes from a day to several weeks.

Both, the measured and the modeled wind data were applied. The measured wind data were obtained from the Kalbådagrund meteorological weather station (Finnish Meteorological Institute) with a time step of 3 h. For modeled data, the closest model point to Kalbådagrund was used when extracting data from the HIRLAM (High-Resolution Limited Area Model). The modeled data source was

the HIRLAM version of the Estonian Meteorological and Hydrological Institute with the spatial resolution of 11 km and the time interval of 3 h (Männik and Merilain 2007).

The data from Kalbådagrund weather station or the closest HIRLAM model point have also been used in the earlier studies of coastal upwellings in the Gulf of Finland (Lips et al. 2008, Uiboupin and Laanemets 2009). According to Keevallik and Soomere (2010), the HIRLAM output matches well with the observations at Kalbådagrund (the wind is measured at 32 m), although the modeled wind direction (at 10 m height) is turned by 20° counter-clockwise from the measured wind direction.

Remote sensing data were acquired as MERIS L2 product data along the ferry route (Paper **II**).

2.4 Calculations

Various methods have been applied to reveal characteristic features of coastal upwelling events in the Baltic Sea (Paper **I**). A certain temperature isoline as the boundary of the upwelling area was used by Uiboupin and Laanemets (2009) and a temperature deviation (2 °C) from the mean temperature along zonal transects was employed by Lehmann et al. (2012). In the former study, the remote sensing data and in the latter one both the remote sensing and modeled data were applied. In the present study, the data of high-resolution long-term Ferrybox measurements are analyzed with this aim first time.

An upwelling index is introduced based on the temperature deviations from the average value for each crossing. First, the measurements were converted into horizontal profiles with a constant step of 0.5 km. The upwelling index for the southern gulf (UI_S) and the northern gulf (UI_N) were calculated as a sum of negative temperature deviations in the respective coastal areas (0–20 km offshore) as:

$$UI_S = \sum_{\Delta T_i < 0}^{i=1\ldots40} \Delta T_i \text{ and } UI_N = \sum_{\Delta T_i < 0}^{i=101\ldots140} \Delta T_i \qquad (3)$$

where ΔT_i is the temperature deviation of 0.5-km cell i from the average temperature of the crossing. The selection of the 20-km wide area is explained in sub–chapter 3.1 (see also Paper **I** for more details). A cumulative upwelling index (*CUI*) is calculated by summing up daily upwelling index values (which were obtained by averaging of two values a day) for certain periods. The obtained *CUI* values were divided by 40, which is the number of data cells in the 20-km wide coastal area, to keep the meaning of *CUI* as the sum of average negative temperature deviations, having a unit of [°C d]:

$$CUI_S(n1 \ldots n2) = \sum_{j=n1}^{j=n2} \left(\frac{1}{40} UI_{Sj}\right)$$
$$CUI_N(n1 \ldots n2) = \sum_{j=n1}^{j=n2} \left(\frac{1}{40} UI_{Nj}\right) \qquad (4)$$

where $n1$ and $n2$ are the start and the end day number of the selected period, for which the cumulative upwelling index is calculated, and UI_{Sj} and UI_{Nj} are the upwelling indexes at day j off the southern and northern coast, respectively (Paper **I**).

The introduced indices are similar to those used previously in the studies of upwelling events and their influence on the phytoplankton dynamics in the Gulf of Finland (Lips and Lips 2008, Myrberg et al. 2008). Since in the present study, horizontal distributions and deviations from the average in the surface layer were used, it is similar to the approach applied by Lehmann et al. (2012). The main difference between the two approaches is that here meridional while in Lehmann et al. (2012) zonal distributions were used. The results of the present study indicate that the use of meridional distributions is more appropriate in the Gulf of Finland. This conclusion is justified by the fact that, on average, the north–south temperature gradient is negligible in the gulf (see sub-chapter 3.1), while the west–east temperature gradient could exist between the shallower and narrower Gulf of Finland and the deeper and wider northern Baltic Proper due to differential warming and cooling (Paper **I**).

To characterize the role of sub-mesoscale processes in energy transfer from the mesoscale to the smaller scales, horizontal wavenumber spectra of temperature variance were calculated. The spectra were calculated using fast Fourier transform algorithm and discrete horizontal temperature profiles based on the Ferrybox and Scanfish data (Paper **III**). The use of spatial spectra of temperature (instead of density) was based on the assumptions that in summer in the surface and thermocline layer of the gulf the water density is mainly controlled by temperature and it is measured by one sensor while density has to be estimated from the readings of two separate sensors. An assumption was made that the distance between the data points along the ferry route was constantly 160 m. The mean spectra for a certain period with quasi-stationary variability were obtained by averaging of single spectra over the selected periods. The spectral slopes between the spatial scales of 10 and 0.5 km were estimated, and the results were compared to some theoretical slope estimates (Paper **III**).

3. RESULTS AND DISCUSSION

3.1 General characteristics of thermohaline fields

The Ferrybox data collected twice a day along the Tallinn–Helsinki ferry route (central Gulf of Finland) since 2007 enable to characterize a wide range of variability – from synoptic scale to seasonal scale in time and from sub-mesoscale to basin-scale in space. Examples of the variability of temperature and salinity distributions expose both the seasonal course and shorter-scale variations in the study area (Fig. 4). The typical seasonal course of the surface layer temperature is characterized by temperature about 5 °C at the beginning of May, a maximum > 20 °C in late July–early August and a drop below 15 °C in late September (Paper **I**). The seasonal course of the surface layer salinity is not well pronounced on the background of variability at shorter scales. While usually, the lowest surface layer salinity was observed in June–July, the salinity was the lowest in May in 2008, and it was the lowest in August in 2010 and 2011 (Paper **I**). This more distinct seasonal course in temperature and less distinct in salinity could be a result of different main forcing factors affecting temperature and salinity distributions. While in temperature, the seasonal cycle dominates due to the seasonal cycle in solar radiation, the changes in salinity distribution are largely controlled by the intensity of convective mixing in winter (Liblik et al. 2013, Lips et al. 2016) and wind-induced alterations in the estuarine circulation (Elken et al. 2003, Liblik and Lips 2012, Liblik and Lips 2017).

Both, the surface layer temperature and salinity had quite large inter-annual variations with the highest temperature in summer 2010 (up to 22 °C) and the highest salinity in 2011 and the lowest in 2009 (Fig. 4). Nevertheless, the analysis of 7-year data series revealed some general features, which could be linked to the prevailed circulation scheme and dynamics of the surface layer (Paper **I**). For this purpose, the average deviations of temperature and salinity from the cross-gulf mean values were calculated (Fig. 5).

On average, the surface layer temperature did not have any horizontal gradient while the surface layer salinity was higher in the southern than in the northern part gulf (Paper **I**). The result that the surface water with the lowest salinity was on average at about 20 km from the northern coast supports the known general circulation scheme in the Gulf of Finland (Palmen 1930, Andrejev et al. 2004). Thus, although some recent modeling studies have suggested that the residual circulation scheme could be reversed for some periods (up to five years; e.g. Soomere et al. (2011)), the high-resolution, long-term salinity measurements support the classical view of the residual circulation in the Gulf of Finland (Paper **I**).
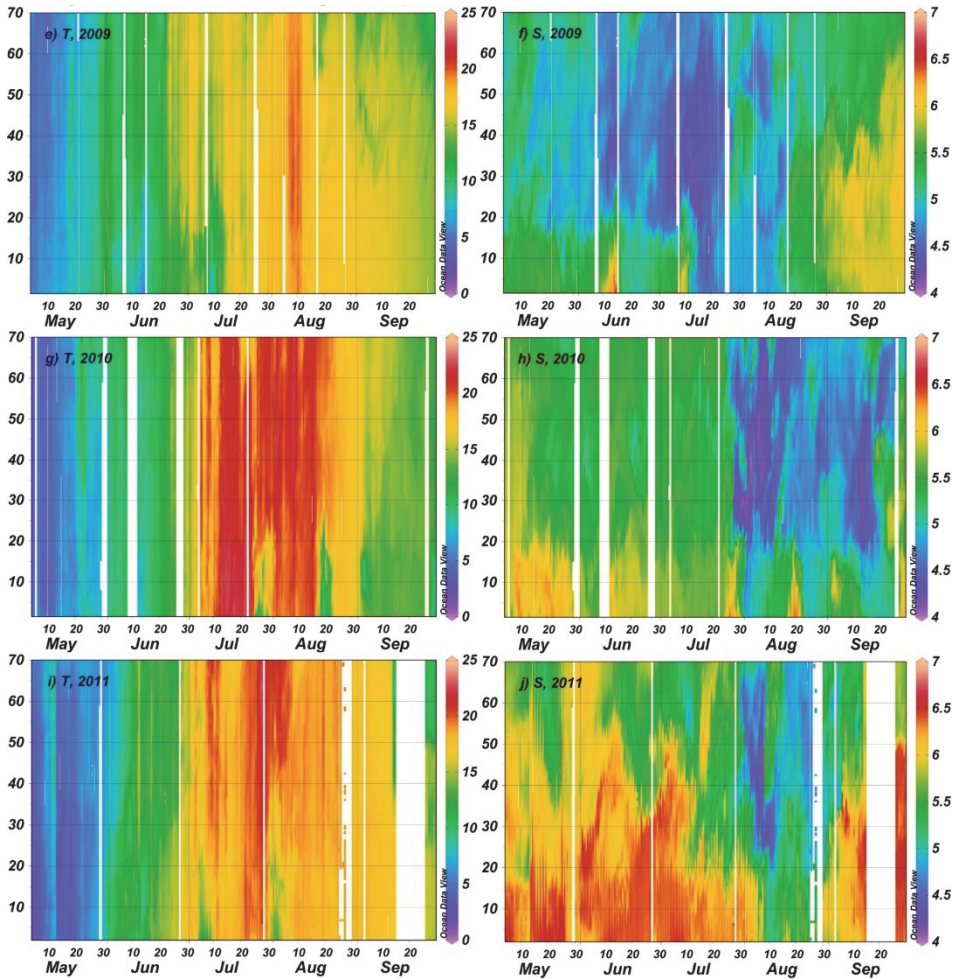
Figure 4. Examples of temporal changes in temperature (in °C) and salinity (in g kg⁻¹) distributions across the Gulf of Finland based on Ferrybox measurements between Tallinn and Helsinki in May–September 2009–2011: 2009, (e, f), 2010 (g, h) and 2011 (i, j); y-axis shows the distance from Tallinn Bay (latitude 59.48 N) in km along the meridional transect.

At the same time, if the wind forcing favorable for upwelling events near the southern coast prevailed (as it was observed in summer 2010) the low salinity water appeared in the southern part of the open gulf, close to the upwelling front (Paper **I**). This phenomenon was also observed during an intense upwelling event in August 2006 (Lips et al. 2009); it was modeled by Laanemets et al. (2011) and noted by Liblik and Lips (2017) based on an analysis of CTD data from surveys across the gulf in 2006–2013.

In summer 2007, on average, the lowest salinity in the surface layer was observed close to the northern shore, and a salinity front was visible in the central part of the study transect (Paper **V**). It is interesting to note that a local maximum

in Chl *a* distribution was revealed in association with this salinity front as it has been noted by several other studies in the Baltic Sea and the Gulf of Finland (e.g. (Pavelson et al. 1997).
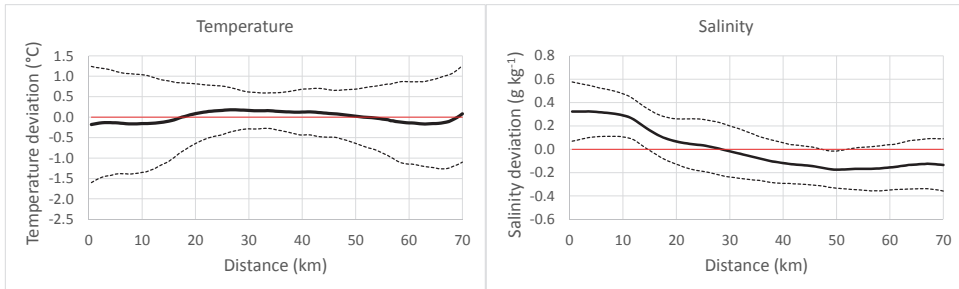
Figure 5. Average distributions of temperature and salinity deviations (from the cross–gulf average) across the Gulf of Finland based on Ferrybox measurements between Tallinn and Helsinki in May–September 2007–2013. Mean values are shown as solid lines and mean plus and minus r.m.s. are shown as dotted lines.

Occasionally the periods with distinctly lower surface layer temperature were observed off the northern or southern shore (Fig. 4). Such situations are related to the coastal upwelling events – their characteristic time scale was several days to 1–2 weeks, and they extended towards the open sea by 15–20 km (Paper **I**). The coastal upwelling events off the southern shore were also accompanied by an increase in surface salinity while in the case of coastal upwelling events seen in the temperature distributions off the northern coast, a simultaneous increase in salinity was not well visible.

It is remarkable that, on average, the variability of temperature deviations was much higher near the coasts than in the central part of the study transect (Fig. 5). In the case of upwelling events off the southern coast and their absence off the northern coast (in 2010), this high variability of temperature was concentrated only in the 20 km wide coastal area off the southern shore (Paper **I**). This high variability of temperature in the coastal areas is mostly related to the upwelling activity and, therefore, the intensity of upwelling events can be estimated based on data from the 20 km wide coastal zones (see next sub-chapter).

The differences in seasonal course and distinct features observed in the surface layer were also associated with corresponding changes and features in the sub–surface layers (Fig. 6). For instance, the upper mixed layer was warmer and thinner in 2010 when the easterly winds were more frequent than usually, and it was colder and thicker in 2012 when westerly winds clearly prevailed (Paper **III**). Such dependence of the vertical stratification in the gulf on the local wind forcing was also shown by Liblik and Lips (2012) based on buoy profiler data and Liblik and Lips (2017) based on temperature and salinity cross-section data. This result is in accordance with the estuarine dynamics where up-estuary winds cause deepening of the thermocline and weakening of the stratification while down-

estuary winds lead to a shallower upper mixed layer and strengthening of the stratification (Chen and Sanford 2009).
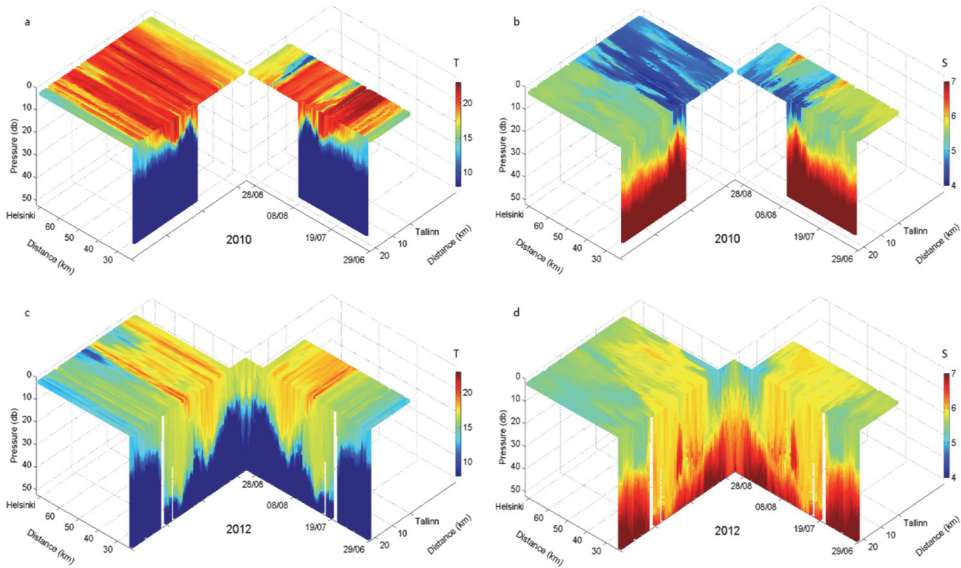
Figure 6. Temporal changes in horizontal and vertical distributions of temperature (°C) and salinity (g kg^{-1}) in the Gulf of Finland measured by the Ferrybox system between Tallinn and Helsinki and the autonomous buoy profiler at station AP5 from 29 June to 31 August in 2010 (a and b, respectively) and 2012 (c and d). The Ferrybox data are split into two parts at the position of the buoy profiler AP5. The x-axis shows the distance along the ferry route from a starting point off Tallinn harbor at the latitude of 59.48º N.

3.2 Coastal upwelling events

3.2.1 Characteristics and occurrence of upwelling events

The most prominent mesoscale process in the elongated and stratified Gulf of Finland is coastal upwelling. In the present study, the criterion of an upwelling occurrence was selected as the value of the upwelling index (*UI*) exceeding 40 °C (in absolute values, while *UI* is by definition a negative number; Paper **I**). It corresponds to an average negative temperature deviation of at least –1 °C in a 20 km wide coastal area. The upwelling events found using the selected criterion were also the occasions when the maximum negative temperature deviation from the transect mean value was at least –2 °C. Thus, the criterion *UI* < –40 °C gives similar results on upwelling presence to the criterion based on the maximum negative temperature deviation of –2 °C (which was used e.g. by Lehmann et al. (2012)).

Table 1. Characteristics of detected upwelling events; dates, coastal area (N – off the northern coast; S – off the southern coast), type, maximum temperature deviation from the transect mean value, cumulative upwelling index calculated for each event and cumulative along-gulf wind stress calculated for upwelling favorable winds before and during the upwelling event.

No	Dates	Coast	Type	Maximum temperature deviation (°C)	Cumulative upwelling intensity (°C day)	Cumulative wind stress (N m^{-2} d)
1.	3–14 June 2007	S	UF	–4.12	–19.8	–0.49
2.	8–16 July 2007	S	GD	–3.02	–12.6	–0.34
3.	21–27 July 2007	N	UF	–4.02	–13.9	0.93
4.	29 July–8 August 2007	N	GD	–3.64	–16.5	0.38
5.	10–17 September 2007[*]	N	GD	–1.97	–7.5	0.75
6.	26–28 May 2008[*]	S	UF	–2.52	–3.9	–0.20
7.	11–15 June 2008	N	UF	–2.73	–7.2	0.62
8.	27–29 June 2008	N	UF	–2.27	–6.2	0.53
9.	10–17 September 2008	S	UF	–5.42	–23.0	–1.08
10.	9–16 June 2009	S	UF	–4.77	–14.8	–0.27
11.	24 June – 14 July 2009	S	GD	–5.78	–36.1	–0.42
12.	16–22 August 2009	N	UF	–3.20	–10.7	0.54
13.	28 August – 9 September 2009	N	UF	–2.74	–14.1	0.56
14.	17–30 September 2009[*]	N	UF	–3.09	–19.3	1.28
15.	20–24 May 2010	S	GD	–2.21	–5.1	–0.56
16.	12–13 June 2010[*]	S	UF	–2.60	–2.3	–0.19
17.	20–24 July 2010	N	UF	–4.70	–9.3	0.31
18.	26 July – 1 August 2010	S	UF	–6.19	–15.7	–0.34
19.	17–23 August 2010	S	UF	–7.78	–20.8	–0.66
20.	2–12 September 2010	S	GD	–5.27	–16.0	–0.25
21.	4–12 May 2011[*]	S	GD	–2.22	–9.3	–0.09
22.	31 May – 8 June 2011	N	UF	–2.32	–10.3	0.60
23.	11–15 June 2011	S	UF	–3.12	–6.0	–0.38
24.	24–27 June 2011	N	UF	–2.40	–4.8	0.41
25.	5–10 July 2011	S	GD	–5.05	–10.6	–0.38
26.	29 July – 7 August 2011	S	GD	–4.69	–22.2	–0.62
27.	14 September 2011[*]	N	UF	–4.90	–3.1	0.47
28.	26–30 September 2011[*]	N	UF	–3.27	–13.8	1.26
29.	18–27 July 2012[*]	N	GD	–4.55	–22.4	1.37
30.	2–13 August 2012	N	UF	–4.17	–22.2	0.58
31.	17 July – 1 August 2013[0]	N	UF	–6.15	–26.0	0.63
32.	11–31 August 2013	N	GD	–5.03	–39.7	0.92
33.	15–30 September 2013	S	UF	–7.34	–40.2	–0.71

[*] see the comments in (Paper **I**)

In total 33 upwelling events were found in May–September 2007–2013 (Table 1). On average, five events a year were registered, and the maximum number of events (eight) was observed in 2011. This result is similar to the results by Uiboupin and Laanemets (2009), but the Ferrybox data from 2007–2013 revealed an almost equal number of events near the northern coast (17) and the southern coast (16) (Paper **I**). Since the upwelling near the northern coast was detected for 150 days and near the southern coast for 140 days, the upwelling occurred at 18 and 17% of the time, respectively, off these two coasts (altogether data from 838 days were available). The result is similar to the findings by (Lehmann et al. 2012)

when they analyzed the remote sensing data. However, it is quite different from the results based on numerical models (Myrberg and Andrejev 2003, Lehmann et al. 2012), which have indicated much higher upwelling occurrences (up to 30%) near the northern coast and prevalence of downwelling near the southern coast. Both, the maximum temperature deviation and the average of these maximum deviations during the identified upwelling events were larger near the southern coast (Paper **I**). The maximum negative temperature deviation from the transect mean value near the southern coast was -7.78 °C (during the event on 17 to 23 August 2010) and near the northern coast -6.15 °C (during the event on 17 July–1 August 2013). The average of maximum temperature deviations for all detected events was -4.64 °C and -3.60 °C, respectively.

The introduced cumulative upwelling index (*CUI*) summarizes both, the total extent of an upwelling in space and its duration in time. The average value for 17 upwelling events off the northern coast was -14.5 °C day and off the southern coast -16.2 °C day (Paper **I**). Summing up *CUI* values for all detected upwelling events gave the total *CUI* for the events off the northern coast of -247.0 °C day and off the southern coast of -258.4 °C day. It was found that the negative temperature deviations from the transect mean are more common for the northern coastal sea area while the upwelling events were more intense in the southern coastal sea area. A larger impact of the upwelling events near the southern coast has also been noted in the earlier studies (Laanemets et al. 2009, Väli et al. 2011), and it was explained by a higher position of the thermocline, steeper bottom slope and greater depths in the southern part.

The highest monthly number of upwelling events was observed in July, and the sum of *CUI* values of all events in July and August (-185.3 °C day and -187.9 °C day) clearly exceeded the respective values in the other months (Paper **I**). Obviously, the revealed seasonal course was partly related to the temperature difference between the surface layer and the cold layer beneath the seasonal thermocline, which has its maximum in the Gulf of Finland in July–August (Liblik and Lips 2011).

3.2.2 Relation to wind forcing

The occurrence of coastal upwelling events in the Gulf of Finland can be related quite well to the variations of the along-gulf wind stress (Paper **I**). The upwelling events appeared after a certain favorable wind pulses with long enough duration and magnitude (Fig. 7). The estimated cumulative wind stress for the detected upwelling events varied between 0.31 and 1.37 N m^{-2} d for westerly winds and between -0.09 and -1.08 N m^{-2} d for easterly winds (Table 1). The average value of the cumulative wind stress for an upwelling event off the northern coast was 0.71 N m^{-2} d and off the southern coast -0.44 N m^{-2} d. Since the upwelling events along the two coasts had, on average, similar magnitude, this result suggests that the required favorable along-gulf wind stress has to be larger for the upwelling events off the northern coast than for the similar events off the southern coast. This suggestion is also supported by a comparison of relationships between the

CUI and cumulative wind stress (*CWS*) related to the upwelling events near the opposite coasts (Fig. 8). The linear regression lines between the *CUI* and *CWS* indicate that at the same *CWS* values, the upwelling events had higher intensities off the southern coast than off the northern coast.
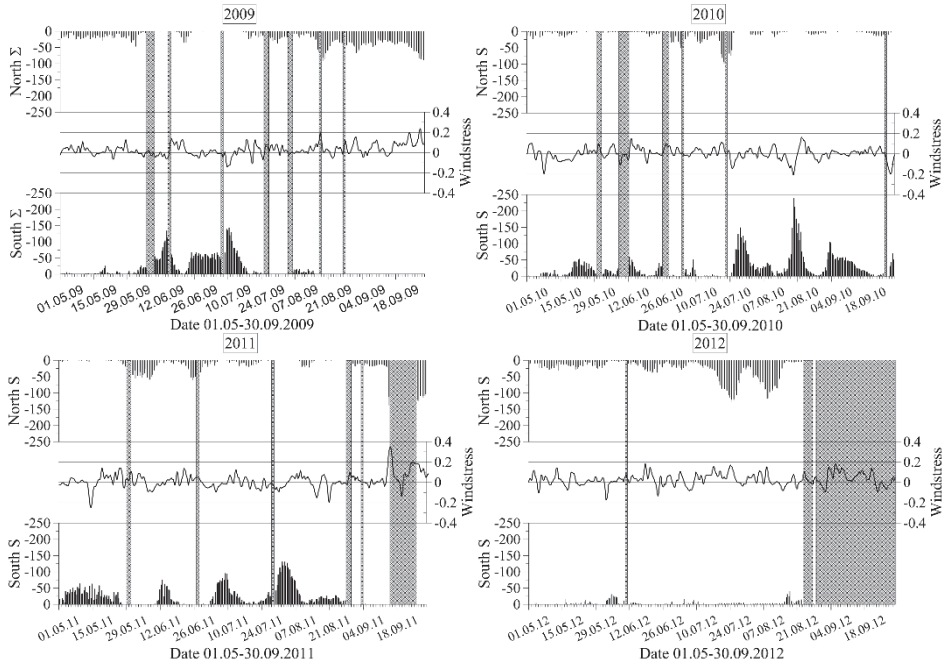
Figure 7. Temporal changes in upwelling index off the northern coast (at the top of each subplot; °C) and off the southern coast at the bottom of each subplot; °C) and along-gulf wind stress (black curve in the middle; N m^{-2}) in May–September 2009, 2010, 2011, and 2012.

Laanemets et al. (2009) suggested that the steeper slope and greater depths near the southern coast could be the reasons for a more intense outcome of the upwelling events there. This suggestion was based on a simple theory of upwelling dynamics linking the position of the onshore return flow with the bottom slope and stratification (Lentz and Chapman 2004). Since near the both coasts, the onshore return flow should occur in the near-bottom layer, but the slope is steeper and depths are greater in the south, the vertical transport of cold and nutrient rich waters could be more intense in the southern gulf (Laanemets et al. 2009, Väli et al. 2011).

An additional explanation comes from the estuarine character of the Gulf of Finland – it is open in the west with free water exchange and closed in the east with the main freshwater source. Prevailing winds together with Coriolis force create a general cyclonic circulation in the surface layer (Alenius et al. 1998); due to the geostrophic balance, it results in a higher sea level and deeper thermocline in the northern part of the gulf. Such an average thermocline inclination across

31

the gulf was shown by Liblik and Lips (2017) based on an analysis of 35 temperature and salinity cross-sections. Thus, weaker wind impulse is needed for upwelling initiation on the southern side of the gulf.

Furthermore, a longer and stronger southwesterly wind impulse can cause 'filling-up' of the gulf and is counteracting to the estuarine circulation (Elken et al. 2003). This wind impulse creates an inflow in the surface layer and downward movement of the thermocline (Liblik and Lips 2017), which in turn may reduce the upwelling outcome near the northern coast and makes it more energy demanding to maintain the event. Opposite process is taking place with down–estuary winds (easterly) – outflow in the surface layer and, therefore, a general upward movement of the thermocline and strengthening of the stratification (Liblik and Lips 2012). Thus, in the latter case, the estuarine circulation is supporting an upward movement of the thermocline in the entire gulf (Lips et al. 2008) and easier generation of upwelling events near the southern coast.
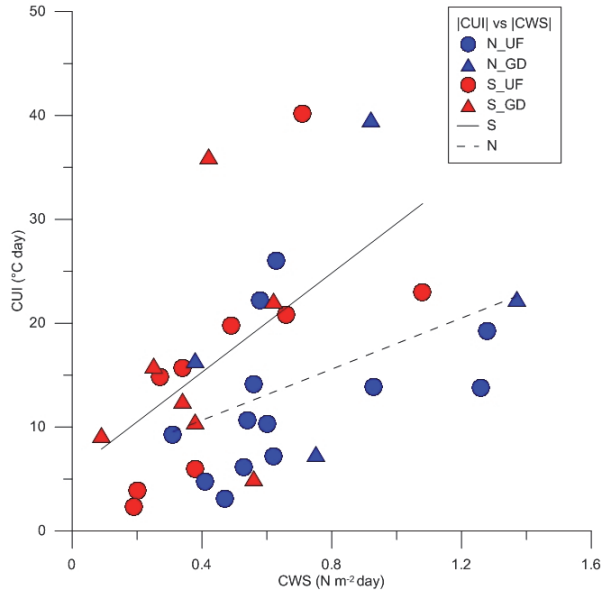
Figure 8. The relationship between the cumulative upwelling index (CUI) and cumulative along-gulf wind stress (CWS) based on 33 detected upwelling events in May–September 2007–2013. Red symbols indicate the events off the southern coast and blue symbols the events off the northern coast; circles correspond to the events with pronounced upwelling front (N_UF and S_UF) and triangles the events with a gradual decrease in temperature towards the coast (N_GD and S_GD). The linear regression lines for southern (solid line) and northern upwelling events (dashed line) are shown.

3.2.3 Two types of upwelling events

Two characteristic shapes of upwelling events in the surface layer temperature distribution were identified near the both coasts (Paper **I**). Most of the upwelling

events were characterized by a sharp and intense temperature front between the upwelling waters and the rest of the transect (Fig. 9; red curves). The sharp upwelling fronts are usually associated with strong along-front jet currents, for instance, as measured by Suursaar and Aps (2007) in the Gulf of Finland in summer 2006. Typical for such events were an almost uniform temperature outside the upwelling area and the temperature minimum (maximum temperature deviation) close to the upwelling front. The other distribution pattern (Fig. 9; dark blue curves) exposed a gradual decrease in temperature towards the upwelling waters. Typical for the latter events were the irregularities in temperature distribution with a characteristic scale of a few kilometers and the temperature minimum (maximum temperature deviation) in the cell closest to the shore. The mentioned irregularities could be associated with the development of upwelling filaments, which occurred under certain conditions and stayed in our measurement window (Uiboupin and Laanemets 2009).

Zhurbas et al. (2008) have shown based on a numerical experiment that the cold/warm water squirts and filaments could develop after the weakening of the upwelling favorable winds. Similarly, the sub-mesoscale squirts and filaments could develop if the wind forcing is strong enough to initiate an upwelling event but not as strong as needed to retain the mesoscale frontal dynamics. This situation could be relevant for the southern upwelling events with a gradual decrease in temperature toward the coast developed in case of upwelling favorable, but relatively weak winds (Paper **I**; see also Fig. 8).

The prevailing westerly to southwesterly winds, which cause an inflow in the upper layer and a compensating outflow in the deeper layers (Elken et al. 2003, Liblik and Lips 2012), could lead to the deepening of the seasonal thermocline in the gulf in 2012 and 2013. The two very intense upwelling events with the gradual temperature decrease were observed in these summers along the northern coast. Thus, even if the wind forcing stays constant, the deepening of the thermocline could counteract to the upwelling development, and it could lead to instabilities and appearance of filaments. The occurrence of more filaments related to intense upwelling events near the northern coast (in comparison to those near the southern coast) could also be related to the differences in the bottom topography near the northern and southern coasts. Zhurbas et al. (2006) have shown that the baroclinic instability of the upwelling jet is expected to occur when the bottom slope is smaller than the isopycnal slope, which could be the case more often near the northern coast where the slope is less steep.

The spatial distribution of salinity in the surface layer from coast to coast drastically differed between the upwelling events near the northern coast and the events near the southern coast (Fig. 9). In the latter case, the spatial variability was much larger than in the former case. In addition, in the case of southern upwelling events, the salinity minimum along the transect was often situated very close to the upwelling front. Although such diversity in salinity distribution could partly be related to the history of water movements in the gulf, the local salinity minimum close to the upwelling front might be caused by the westward current jet along the front as also revealed by model experiments (Laanemets et al. 2011).

A similar decrease in horizontal salinity gradient across the gulf due to westerly winds and an opposing increase of the gradient due to easterly winds was noted by Liblik and Lips (2017) based on an analysis of salinity cross-section data from summers 2006–2013.
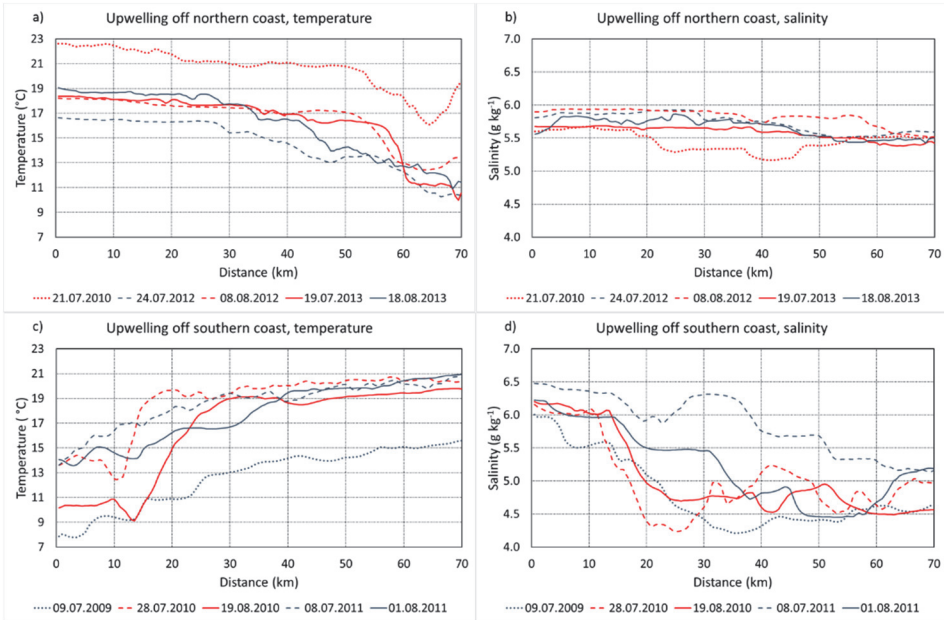
Figure 9. Characteristic distributions of temperature and salinity along the ferry route Tallinn–Helsinki with coastal upwelling events off the northern coast (a, b) and off the southern coast (c, d); x-axis shows the distance from the Tallinn Bay (latitude 59.48º N) in km along the meridional transect.

3.3 Surface layer sub-mesoscale variability

According to the theory of quasi-geostrophic turbulence in the ocean interior, the shape of the energy spectrum should follow the –3 slope (in log-log space) at the spatial scales below the mesoscale (Charney 1971). It has been shown that if the spatial resolution of numerical models was increased the spectral slope converted rather to –2 than –3 (Capet et al. 2008) suggesting that sub-mesoscale processes play an important role in the energy cascade from larger to smaller scales. In the present study, in situ observations, using both autonomous devices and research vessel were applied to map the distribution patterns of temperature and salinity (at meso- and sub-mesoscale) in the Gulf of Finland. The analysis of Ferrybox data revealed that, under certain conditions, upwelling events existed with a gradual decrease of surface layer temperature from the open sea towards the coast characterized by a relatively high spatial variability at scales of a few to 10 km (Paper **I**). This spatial variability could be a sign of sub-mesoscale dynamics in the case of wind forcing not strong enough to produce an Ekman transport in the entire surface layer and maintain the mesoscale upwelling front.

Overall horizontal variability of temperature characterized as the standard deviation of temperature along the ferry route was varying in quite large ranges in time – from 0.2 °C to 3.7 °C (Fig. 10), however, the seasonal averages for analyzed four years were quite close to each other (Table 2). The calculated horizontal wavenumber spectra of temperature variance had also relatively large variability in the spectral level, but the spectral curves could be approximated as straight lines between the lateral scales of 10 and 0.5 km (Paper **III**). Within the periods of high spatial variability of temperature, mostly related to upwelling events affecting the distribution of temperature in the surface layer, the estimated spectral slopes (scales from 10 km to 0.5 km) were between –1.8 and –2 (Table 2).

Table 2. Standard deviations of temperature and slopes of wavenumber spectra of temperature variance based on the data collected in the surface layer along the ferry route between Tallinn and Helsinki. Average values for each year over the study period from 29 June to 31 August and within the selected periods with similar spatial variability are given. Numbers of the periods correspond to the periods marked in Fig. 10.

Year No	Dates	Standard deviation (°C)	Spectral slope (10 km – 0.5 km)
2009	**29 June–31 August**	**0.71**	**–2.1**
1	29 June–15 July	1.26	–1.9
2	16 July–14 August	0.37	–2.3
3	15 August–31 August	0.78	–1.9
2010	**29 June–31 August**	**0.83**	**–2.2**
1	29 June–18 July	0.52	–2.3
2	19 July–31 July	1.46	–2.0
3	1 August–16 August	0.48	–2.2
4	17 August–24 August	1.89	–1.9
2011	**29 June–31 August**	**0.73**	**–2.2**
1	29 June–12 July	0.93	–2.1
2	13 July–25 July	0.38	–2.6
3	26 July–9 August	1.43	–1.9
4	10 August–31 August	0.34	–2.2
2012	**29 June–22 August**	**0.76**	**–2.2**
1	29 June–16 July	0.32	–2.6
2	17 July–13 August	1.16	–2.0
3	14 August–22 August	0.35	–2.4

The found conversion of wavenumber spectra of temperature variance to –2 slope has been identified earlier in other sea areas by high-resolution modeling (Capet et al. 2008) and in situ measurements (Hodges and Rudnick 2006). Kolodziejczyk et al. (2015) showed that if the spatial variability of surface density in the north-eastern subtropical Atlantic Ocean was analyzed then the –2 spectral slope was obtained in summer conditions when the salinity and temperature variations did not compensate each other. In the Gulf of Finland in summer, the wavenumber spectra of both temperature and density variance corresponded to –2 slope when the spatial variability was dominated by coastal upwelling events

(or their relaxation). Similar tendency towards –2 slope was obtained for the wavenumber spectra of temperature variance in the thermocline layer between the spatial scales of 10 and 1 km estimated based on data from Scanfish surveys (Paper **III**).
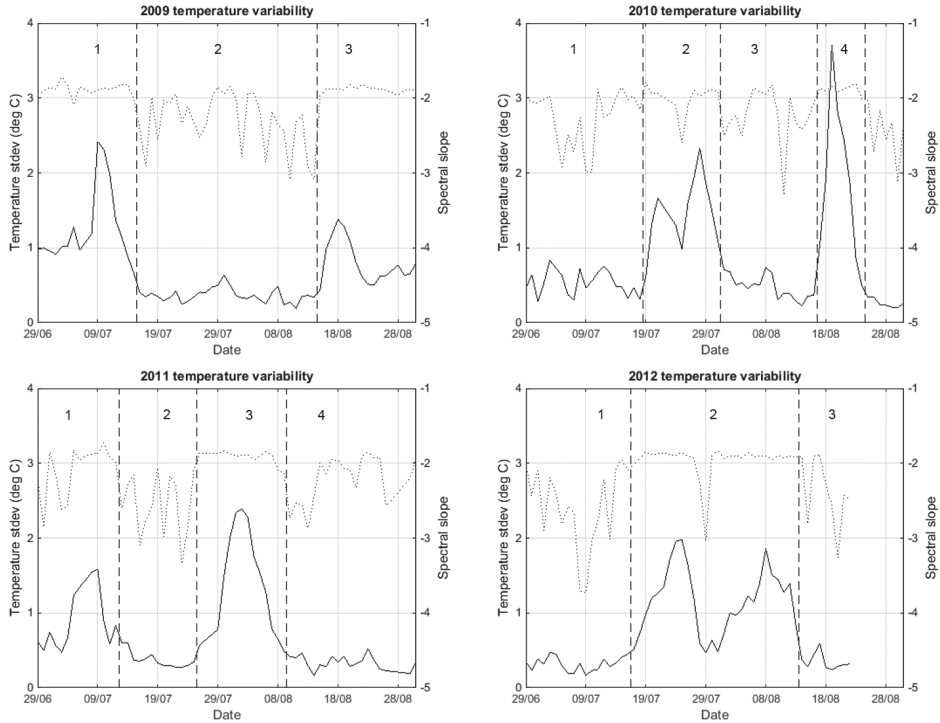
Figure 10. Statistical characteristics of the temperature variability in the surface layer of the Gulf of Finland along the ferry route Tallinn–Helsinki from 29 June to 31 August in 2009, 2010, 2011, and 2012. Standard deviations of temperature are shown as solid lines and spectral slopes of temperature variance between the horizontal scales of 10 and 0.5 km as dotted lines. The vertical dashed lines denote the borders between the selected distinct periods with similar variability patterns (numbers of periods are shown in the upper part of the panels).

According to these findings, the sub-mesoscale processes have to be more energetic than suggested by the quasi-geostrophic theory of turbulence in the ocean interior. Recent high-resolution modeling studies (grid spacing of 0.125 nautical miles was used; Väli et al. (2016)) also showed the occurrence of diverse sub–mesoscale features in relation to the development and relaxation of upwelling events in the Gulf of Finland. Väli et al. (2016) noticed the following features: the high Rossby number threads (typical width and length of 2–3 km and 10–50 km, respectively), cyclonic vortices with a diameter of 4–6 km, and spiral cyclonic eddies with a diameter of 10–15 km. The signs of such sub-mesoscale features could be seen in the sub-surface layer at the vertical profiles

of temperature and/or salinity as intrusions of waters with different thermohaline characteristics (see e.g. Fig. 6d and Paper **III**). Based on the Scanfish data, these patches were usually inclined in relation to a horizontal plane and isopycnals as it was found for filamentary sub-mesoscale structures in the upwelling system off southern Peru (Pietri et al. 2013). The intrusions had characteristic vertical scales of 5–15 m and lateral scales of about 5 km (Paper **III**).

3.4 Biogeochemical signal dynamics

3.4.1 Spring bloom dynamics derived from Ferrybox observations

Spring bloom in the Baltic Sea is mostly controlled by the winter pool of inorganic nutrients and prevailing physical conditions during the bloom period. The bloom is very dynamic, and high-resolution observations have to be applied to follow the bloom development and influencing factors, among them mesoscale processes and development of vertical stratification (Kahru and Nõmmann 1990). An example, how the Ferrybox technology is applied to describe the spring bloom in the Baltic Sea, is presented by Fleming and Kaitala (2006), who derived the spring bloom intensity index based on Chl *a* fluorescence measurements.

The Marine Systems Institute at Tallinn University of Technology has established a marine environmental observatory in the Gulf of Finland with Ferrybox measurements along the Tallinn–Helsinki ferry line in its core (Papers **II**–**IV**). The analyzed Ferrybox data collected in spring 2009 and 2010 indicated that the Chl *a* concentration >5 mg m^{-3} (considered as the start of the bloom; Paper **IV**) was reached in the Gulf of Finland before the surface temperature exceeded the temperature of maximum density (2.5 °C). The earlier bloom development in 2009 compared with 2010 could be related to the slightly earlier warming of the surface waters and/or stronger haline stratification in 2009 (similarly to findings by Kahru and Nõmmann (1990)). This suggestion assumes that the lower salinity in the surface layer in spring 2009 indicates a stronger vertical stratification (Paper **IV**). After passing the temperature of maximum density, the Chl *a* peaks coincided with the periods of relatively fast temperature increase (Fig. 11). It shows indirectly the positive role of the buoyancy flux (leading to a strengthening of the vertical stratification) for phytoplankton growth in spring (Paper **II**).

Based on flow-through data and laboratory analyses, two more characteristic features of the spring bloom were detected. The bloom started to decline when the inorganic nitrogen was depleted from the surface layer (Fig. 11). The secondary peak of the bloom dominated by dinoflagellates (Paper **IV**) occurred in the second half of May after a relatively rapid increase of the surface temperature (Fig. 11).

To extend the Ferrybox observations to a larger area, remote sensing data could be used, but for the Gulf of Finland, it is not easy to find cloud-free images. Two images as reduced resolution MERIS L2 products were available from the bloom development period on 12 and 14 April 2010 (Paper **II**). Based on the

remote sensing data, the Chl *a* levels were higher on 14 April than those on 12 April pointing to the phytoplankton growth (bloom development) as also revealed by the Ferrybox data for the same period (Fig. 11). The Chl *a* levels were somewhat higher in the central and southern parts than those close to the northern shore and clear spatial variability in mesoscale was detected on 14 April (Paper **II**).
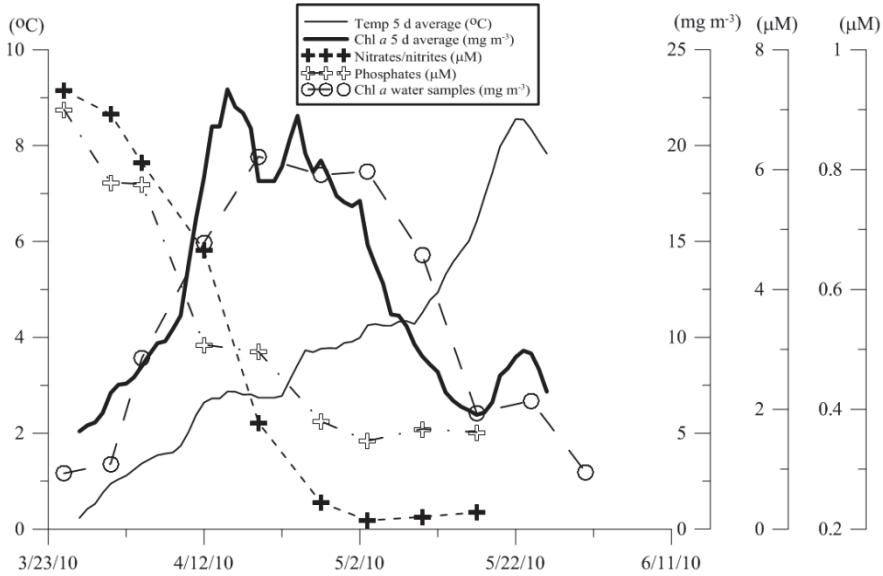
Figure 11. Temporal variations of environmental parameters in the Gulf of Finland in March–May 2010 presented as daily averages for water sample analyses and 5-d running mean values for flow-through data. Axes represent Ferrybox water temperature (left y-axis), Chl *a* content from Ferrybox flow-through and water samples (first y-axis on the right), NO_3+NO_2 concentration (second y-axis on the right side) and PO_4 concentration (third y-axis on the right).

Both, the Ferrybox data and extracted MERIS L2 product data along the ferry route were calibrated against Chl *a* content measured from the water samples. A comparison of the two datasets showed that the remote sensing data qualitatively agree well with the Ferrybox and water sample analysis data. The quantitative comparison revealed that the correlation between MERIS data and water samples analysis results was low, although significant (Fig. 12; Paper **II**). One reason for the latter could be the time lag between the satellite image and ground measurements – more than 10 hours, which might lead to some shifts of borders between the water masses with high and low Chl *a* content. Another reason could be the stratification, which as shown by (Uiboupin and Laanemets 2015) influences the match of remote sensing and Ferrybox data (acquired from the 4–5 m depth) if the wind speed is <5 m s^{-1}.

A challenge of using Chl *a* fluorescence data for the estimates of the Chl *a* content is related to the chlorophyll quenching (e.g. Halverson and Pawlowicz

2013). As seen from Fig. 12, the Chl *a* fluorescence data from two crossings differ, whereas the Chl *a* values from the water sample analyses are well correlated with the data from Helsinki to Tallinn (made after 6:30 p.m.). To avoid the quenching effect, the data only from evening crossings are used in the present study.
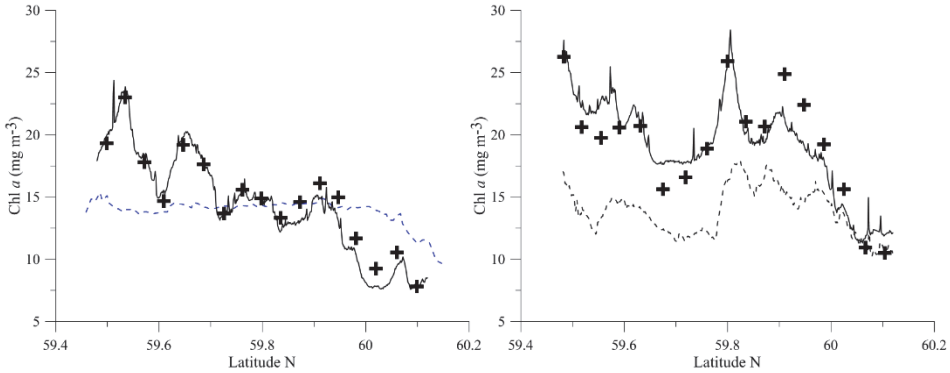
Figure 12. Comparison between Chl *a* data – MERIS L2 product (dashed line), Ferrybox data (solid line) and water samples analysis results (crosses) obtained along the ferry route on 12 April 2010 (left panel). Comparison between Ferrybox Chl *a* data acquired on 19 April 2010 (right panel) when the ferry was traveling from Tallinn to Helsinki (dashed line) and from Helsinki to Tallinn (solid line) and water samples analysis results (crosses) collected from Helsinki to Tallinn.

The standard Ferrybox sensor set can be complemented with various other sensors – nutrient analyzers, pCO_2 sensors and others. In spring 2010, a pCO_2 sensor was attached to the Ferrybox system on board "Galaxy". It was demonstrated that spatiotemporal distribution of pCO_2 was in a good accordance with the Chl *a* dynamics confirming that the pCO_2 measurements can be used for estimates of phytoplankton productivity (Paper **II**).

3.4.2 Dynamics of summer phytoplankton from Ferrybox observations

Since the surface layer of the Gulf of Finland is usually depleted of inorganic nutrients in summer, the growth of phytoplankton to a large extent depends on physical processes creating vertical nutrient fluxes (Lips and Lips 2008) or producing favorable conditions for certain phytoplankton groups (Lips et al. 2011). The two examples, shown in Fig. 13, represent the situation of an increase of Chl *a* content in the near-coast convergence zone – in late July 2010 near the northern coast and in the second half of July–early August near the southern coast.

Before the biomass increase in late July 2010, the cyanobacteria dominated in the surface layer under strongly stratified conditions in the first half of July (Lips and Lips 2014). Later, the sub-surface Chl *a* maxima were observed in the central and northern part of the gulf (based on Scanfish data; Paper **III**). When the wind

favorable for cross-gulf Ekman transport from south to north appeared, the bloom developed in the northern gulf (Fig. 13). Since the species, which dominated in the sub-surface Chl *a* maxima layer (*Heterocapsa triquetra*), was abundant in the bloom area, it was suggested that the bloom could not be explained by pure convergence in the surface layer and did benefit from the sub-surface biomass (Lips and Lips 2014; Paper **III**). Consequently, the ageostrophic sub-mesoscale processes, which could be responsible for vertical transport and re-stratification of the surface layer, might also contribute to the growth enhancement (Levy et al. 2012).
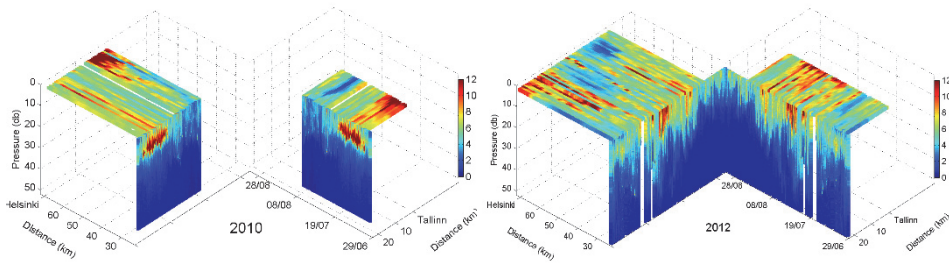
Figure 13. Temporal changes in horizontal and vertical distribution of Chl *a* (mg m^{-3}) in the Gulf of Finland measured by the Ferrybox system between Tallinn and Helsinki and the autonomous buoy profiler at station AP5 from 29 June to 31 August in 2010 and 2012. The Ferrybox route and the location of station AP5 are shown in Fig. 1.

CONCLUSIONS

Ferrybox technology has been proven as a cost-effective environmental monitoring approach as well as a method of in situ measurements for studying processes controlling the upper layer dynamics in the sea. The value of the data is increasing in time when this high-resolution observation method is applied for a long time, e.g. for decades covering the variability in all seasons in a certain sea area. The data collected along the Tallinn–Helsinki ferry route from coast to coast in the elongated Gulf of Finland characterize the variability in transversal thermohaline structure within a large range of temporal and spatial scales. The analysis allows to draw conclusions on the dynamics of this estuarine-like basin. Among the other issues the suggestions from short-time experiments on the causes of variability of the thermohaline and biogeochemical fields can be tested on this long-term but high-resolution data set.

The main scientific question of this study was related to the dynamics of coastal upwelling events. The results show that the classical scheme of coastal upwelling/downwelling in elongated basins (Krauss and Brügge 1991) has to be updated to take into account the estuarine character of the Gulf of Finland. The gulf is closed at the eastern end, where the freshwater input exists, and it has open water exchange with a larger basin through the western border. This configuration leads to clear differences in upwelling behavior near the northern and southern coasts of the gulf. The main differences are seen in upwelling frequencies and intensities in relation to the wind forcing.

The main results of the present thesis can be summarized as follows:

- Ferrybox measurements from Tallinn to Helsinki can be successfully used to describe the surface layer dynamics in the Gulf of Finland, including coastal upwelling events.
- An average cross-gulf salinity distribution in the surface layer with the salinity minimum in the northern gulf confirms that, in general, an outflow of fresher waters dominates along the northern coast (with the core at a distance of 20 km from the northern shore) in summer.
- Upwelling index based on the temperature data from a single crossing and cumulative upwelling index were introduced and applied on collected Ferrybox data from May–September 2007–2013.
- The upwelling occurrences and average intensities of the events are similar near the northern and southern coasts while the wind impulse needed to generate an upwelling event of certain intensity differs between the two coastal areas.
- This different response to the wind forcing in the southern and northern coastal areas could be related to the estuarine character of the basin with only one open border in the west and prevailing winds from west – south-west.
- A deeper position of the thermocline (on average) in the northern gulf could be a reason why a stronger wind impulse is needed to initiate the upwelling

by the westerly (up-estuary) winds near the northern coast than in the case of the easterly (down-estuary) winds and the upwelling near the southern coast.

- Secondly, dominating long-term easterly (down-estuary) winds cause an outflow of the surface layer waters and a compensating upward movement of the thermocline in the gulf that intensifies the upwelling near the southern coast. The effect is reversed in the case of long-term westerly (up-estuary) winds, working against the upwelling intensification near the northern coast.

- Two types of upwelling events were identified – one characterized by a strong upwelling front and the other revealing a gradual decrease in temperature from the open sea to the coastal area. The spatial variations in temperature with scales of a few kilometers, which were characteristic for the second type, could be signs of the sub-mesoscale features (filaments and squirts) associated with the upwelling dynamics.

- The identified pronounced sub-mesoscale features in the surface and subsurface layer (filaments and intra-thermocline intrusions) and estimated slopes of horizontal wavenumber spectra of temperature variance between the lateral scales of 10 and 0.5 km (being close to –2) indicate that ageostrophic sub-mesoscale processes contribute considerably to the energy cascade from larger to smaller spatial scales in this stratified sea basin.

- Both the variations in vertical stratification and mesoscale hydrodynamic processes have been employed to explain the observed spring bloom evolution and its spatial and temporal variability. The observed coincidence of Chl *a* peaks with the periods of relatively fast temperature increase indirectly shows the importance of positive buoyancy fluxes (vertical stratification) for phytoplankton growth in spring.

- High-resolution measurements and sampling revealed the high spatial and temporal variability in Chl *a* distribution, the phytoplankton growth enhancement related to the convergence in the surface layer near the coasts and the possible contribution of sub-mesoscale processes to the formation of surface blooms.

REFERENCES

Aiken, C. M., W. Petersen, F. Schroeder, M. Gehrung & P. A. R. von Holle (2011) Ship-of-Opportunity Monitoring of the Chilean Fjords Using the Pocket Ferry Box. *Journal of Atmospheric and Oceanic Technology,* 28**,** 1338–1350.

Aitsam, A., H. P. Hansen, J. Elken, M. Kahru, J. Laanemets, M. Pajuste, J. Pavelson & L. Talpsepp (1984) Physical and chemical variability of the Baltic Sea: a joint experiment in the Gotland Basin. *Continental Shelf Research,* 3**,** 291–310.

Alenius, P., K. Myrberg & A. Nekrasov (1998) The physical oceanography of the Gulf of Finland: a review. *Boreal Environment Research,* 3**,** 97–125.

Alenius, P., A. Nekrasov & K. Myrberg (2003) Variability of the baroclinic Rossby radius in the Gulf of Finland. *Continental Shelf Research,* 23**,** 563–573.

Andrejev, O., K. Myrberg, P. Alenius & P. A. Lundberg (2004) Mean circulation and water exchange in the Gulf of Finland – a study based on three-dimensional modelling. *Boreal Environment Research,* 9**,** 1–16.

BACC (2015) Second Assessment of Climate Change for the Baltic Sea Basin. *Second Assessment of Climate Change for the Baltic Sea Basin***,** 1–501.

Bouffard, J., L. Renault, S. Ruiz, A. Pascual, C. Dufau & J. Tintore (2012) Sub-surface small–scale eddy dynamics from multi–sensor observations and modeling. *Progress in Oceanography,* 106**,** 62–79.

Brannigan, L. (2016) Intense submesoscale upwelling in anticyclonic eddies. *Geophysical Research Letters,* 43**,** 3360–3369.

Buijsman, M. C. & H. Ridderinkhof (2007) Long–term ferry–ADCP observations of tidal currents in the Marsdiep inlet. *Journal of Sea Research,* 57**,** 237–256.

Bychkova, I.A., S.V. Viktorov & D.A. Shumakher (1988) A relationship between the large scale atmospheric circulation and the origin of coastal upwelling in the Baltic. *Meteorol. Gidrol., 10 (1988), pp. 9–98 (in Russian)*.

Capet, X., J. C. McWilliams, M. J. Mokemaker & A. F. Shchepetkin (2008) Mesoscale to submesoscale transition in the California current system. Part I: Flow structure, eddy flux, and observational tests. *Journal of Physical Oceanography,* 38**,** 29–43.

Charney, J. G. (1971) Geostrophic Turbulence. *Journal of the Atmospheric Sciences,* 28**,** 1087–1095.

Chen, S. N. & L. P. Sanford (2009) Axial Wind Effects on Stratification and Longitudinal Salt Transport in an Idealized, Partially Mixed Estuary. *Journal of Physical Oceanography,* 39**,** 1905–1920.

Elken, J. 1996. *Deep Water Overflow, Circulation and Vertical Exange in the Baltic Prober*.

Elken, J. & W. Matthäus (2008) Baltic Sea oceanography. *Regional Climate Studies, Assessment of climate change for the Baltic Sea Basin. Annex A,* 1**,** 379–385.

Elken, J., U. Raudsepp & U. Lips (2003) On the estuarine transport reversal in deep layers of the Gulf of Finland. *Journal of Sea Research,* 49**,** 267–274.

Fleming, V. & S. Kaitala (2006) Phytoplankton spring bloom intensity index for the Baltic Sea estimated for the years 1992 to 2004. *Hydrobiologia,* 554**,** 57–65.

Haapala, J. (1994) Upwelling and its Influence on Nutrient Concentration in the Coastal Area of the Hanko Peninsula, Entrance of te Gulf of Finland. *Estuarine Coastal and Shelf Science,* 38**,** 507–521.

Halverson, M. J. & R. Pawlowicz (2013) High–resolution observations of chlorophyll *a* biomass from an instrumented ferry: Influence of the Fraser River plume from 2003 to 2006. *Continental Shelf Research,* 59**,** 52–64.

Hodges, B. A. & D. L. Rudnick (2006) Horizontal variability in chlorophyll fluorescence and potential temperature. *Deep–Sea Research Part I–Oceanographic Research Papers,* 53**,** 1460–1482.

Kahru, M. & C. Brown (1999) Monitoring algal blooms: New techniques for detecting large–scale environmental change. *Photosynthetica,* 36**,** 50–50.

Kahru, M., J. Elken, I. Kotta, M. Simm & K. Vilbaste (1984) Plankton distributions and processes across a front in the open Baltic Sea. *Marine Ecology Progress Series,* 20**,** 101–111.

Kahru, M. & S. Nõmmann (1990) The phytoplankton spring bloom in the Baltic Sea in 1985, 1986: multitude of spatio–temporal scales. *Continental Shelf Research,* 10**,** 329–354.

Kanoshina, I., U. Lips & J. M. Leppanen (2003) The influence of weather conditions (temperature and wind) on cyanobacterial bloom development in the Gulf of Finland (Baltic Sea). *Harmful Algae,* 2**,** 29–41.

Karimova, S. & M. Gade (2015) Analysis of sub-mesoscale eddies in the Baltic Sea based on SAR imagery and model wind data. *2015 Ieee International Geoscience and Remote Sensing Symposium (Igarss)***,** 1227–1230.

Keevallik, S. & T. Soomere (2010) Towards quantifying variations in wind parameters across the Gulf of Finland. *Estonian Journal of Earth Sciences,* 59**,** 288–297.

Kolodziejczyk, N., G. Reverdin, J. Boutin & O. Hernandez (2015) Observation of the surface horizontal thermohaline variability at mesoscale to submesoscale in the north–eastern subtropical Atlantic Ocean. *Journal of Geophysical Research–Oceans,* 120**,** 2588–2600.

Kowalewski, M. & M. Ostrowski (2005) Coastal up- and downwelling in the southern Baltic. *Oceanologia,* 47**,** 453–475.

Krauss, W. & B. Brügge (1991) Wind–produced water exchange between the deep basins of the Baltic Sea. *J. Phys. Oceanograp.J. Phys. Oceanograp.,* 21**,** 373–384.

Kõuts, T. & A. Omstedt (1993) Deep water exchange in the Baltic Proper. *Tellus Series a–Dynamic Meteorology and Oceanography,* 45A**,** 311–324.

Laanemets, J., K. Kononen, J. Pavelson & E. L. Poutanen (2004) Vertical location of seasonal nutriclines in the western Gulf of Finland. *Journal of Marine Systems,* 52**,** 1–13.

Laanemets, J., M. J. Lilover, U. Raudsepp, R. Autio, E. Vahtera, I. Lips & U. Lips (2006) A fuzzy logic model to describe the cyanobacteria Nodularia spumigena blooms in the Gulf of Finland, Baltic Sea. *Hydrobiologia,* 554**,** 31–45.

Laanemets, J., G. Vali, V. Zhurbas, J. Elken, I. Lips & U. Lips (2011) Simulation of mesoscale structures and nutrient transport during summer upwelling events in the Gulf of Finland in 2006. *Boreal Environment Research,* 16**,** 15–26.

Laanemets, J., V. Zhurbas, J. Elken & E. Vahtera (2009) Dependence of upwelling–mediated nutrient transport on wind forcing, bottom topography and stratification in the Gulf of Finland: model experiments. *Boreal Environment Research,* 14**,** 213–225.

Lavrova, O., A. Serebryany, T. Bocharova & M. Mityagina. 2012. Investigation of fine spatial structure of currents and submesoscale eddies based on satellite radar data and concurrent acoustic measurements. In *Conference on Remote Sensing of the Ocean, Sea Ice, Coastal Waters and Large Water Regions*. Edinburgh, SCOTLAND: Spie–Int Soc Optical Engineering.

Lehmann, A. & K. Myrberg (2008) Upwelling in the Baltic Sea – A review. *Journal of Marine Systems,* 74**,** S3–S12.

Lehmann, A., K. Myrberg & K. Hoflich (2012) A statistical approach to coastal upwelling in the Baltic Sea based on the analysis of satellite data for 1990–2009. *Oceanologia,* 54**,** 369–393.

Lentz, S. J. & D. C. Chapman (2004) The importance of Nonlinear cross-shelf momentum flux during wind-driven coastal upwelling. *Journal of Physical Oceanography,* 34**,** 2444–2457.

Leppanen, J. M., E. Rantajärvi, S. Hallfors, M. Kruskopf & V. Laine (1995) Unattended monitoring of potentially toxic phytoplankton species in the Baltic Sea in 1993. *Journal of Plankton Research,* 17**,** 891–902.

Leppäranta, M. & K. Myrberg (2009) Physical Oceanography of the Baltic Sea. *Physical Oceanography of the Baltic Sea***,** 1–378.

Levy, M., R. Ferrari, P. J. S. Franks, A. P. Martin & P. Riviere (2012) Bringing physics to life at the submesoscale. *Geophysical Research Letters,* 39**,** 13.

Liblik, T., J. Laanemets, U. Raudsepp, J. Elken & I. Suhhova (2013) Estuarine circulation reversals and related rapid changes in winter near–bottom oxygen conditions in the Gulf of Finland, Baltic Sea. *Ocean Science,* 9**,** 917–930.

Liblik, T. & U. Lips (2011) Characteristics and variability of the vertical thermohaline structure in the Gulf of Finland in summer. *Boreal Environment Research,* 16**,** 73–83.

Liblik, T. & U. Lips (2012) Variability of synoptic scale quasi-stationary thermohaline stratification patterns in the Gulf of Finland in summer 2009. *Ocean Science,* 8**,** 603–614.

Liblik, T. & U. Lips (2017) Variability of pycnoclines in a three-layer, large estuary: the Gulf of Finland. *Boreal Environmental Research,* 22**,** 27 – 47.

Lilover, M. J., J. Pavelson & T. Kõuts (2011) Wind forced currents over the shallow Naissaar Bank in the Gulf of Finland. *Boreal Environment Research,* 16**,** 164–174.

Lips, I. & U. Lips (2008) Abiotic factors influencing cyanobacterial bloom development in the Gulf of Finland (Baltic Sea). *Hydrobiologia,* 614**,** 133–140.

Lips, I. & U. Lips (2010) Phytoplankton dynamics affected by the coastal upwelling events in the Gulf of Finland in July–August 2006. *Journal of Plankton Research,* 32**,** 1269–1282.

Lips, I., U. Lips & T. Liblik (2009) Consequences of coastal upwelling events on physical and chemical patterns in the central Gulf of Finland (Baltic Sea). *Continental Shelf Research,* 29**,** 1836–1847.

Lips, U., J. Laanemets, I. Lips, T. Liblik, I. Suhhova & Ü. Suursaar (2016) Wind-driven residual circulation and related oxygen and nutrient dynamics in the Gulf of Finland (Baltic Sea) in winter. *Estuarine, Coastal and Shelf Science*.

Lips, U. & I. Lips (2014) Bimodal distribution patterns of motile phytoplankton in relation to physical processes and stratification (Gulf of Finland, Baltic Sea). *Deep–Sea Research Part Ii–Topical Studies in Oceanography,* 101**,** 107–119.

Lips, U., I. Lips, V. Kikas, N. Kuvaldina (2008) Ferrybox Measurements: a Tool to Study Meso–Scale Processes in the Gulf of Finland (Baltic Sea). *2008 IEEE/OES US/EU–Baltic International Symposium***,** 334–339.

Lips, U., I. Lips, T. Liblik, V. Kikas, K. Altoja, N. Buhhalko & N. Rünk (2011) Vertical dynamics of summer phytoplankton in a stratified estuary (Gulf of Finland, Baltic Sea). *Ocean Dynamics,* 61**,** 903–915.

Martin, A. P. & P. Pondaven (2003) On estimates for the vertical nitrate flux due to eddy pumping. *Journal of Geophysical Research–Oceans,* 108**,** 10.

McGillicuddy, D. J., A. R. Robinson, D. A. Siegel, H. W. Jannasch, R. Johnson, T. Dickeys, J. McNeil, A. F. Michaels & A. H. Knap (1998) Influence of mesoscale eddies on new production in the Sargasso Sea. *Nature,* 394**,** 263–266.

Meier, H. E. M., E. Kjellstrom & L. P. Graham (2006) Estimating uncertainties of projected Baltic Sea salinity in the late 21st century. *Geophysical Research Letters,* 33**,** 4.

Myrberg, K. & O. Andrejev (2003) Main upwelling regions in the Baltic Sea – a statistical analysis based on three–dimensional modelling. *Boreal Environment Research,* 8**,** 97–112.

Myrberg, K., A. Lehmann, U. Raudsepp, M. Szymelfenig, I. Lips, U. Lips, M. Matciak, M. Konwalewski, A. Krezel, D. Burska, L. Szymanek, A. Ameryk, L. Bielecka, K. Bradtke, A. Galkowska, S. Gromisz, J. Jedrasik, M. Kaluzny, L. Kozlowski, A. Krajewska–Soltys, B. Oldakowski, M. Ostrowsk, M. Zalewski, O. Andrejev, I. Suomi, V. Zhurbas, O. K. Kauppinen, E. Soosaar, J. Laanemets, R. Uiboupin, L. Talpsepp, M. Golfnkos, N. Golenko & E. Vahtera (2008) Upwelling events, coastal offshore exchange, links to biogeochemical processes – Highlights from the Baltic Sea Science Congress at Rostock University, Germany, 19–22 March 2007. *Oceanologia,* 50**,** 95–113.

Männik, A. & M. Merilain (2007) Verification of different precipitation forecasts during extended winter–season in Estonia. *HIRLAM NewsletterHIRLAM Newsletter, 5*252**,** 65–70.

Nausch, M., G. Nausch, H. U. Lass, V. Mohrholz, K. Nagel, H. Siegel & N. Wasmund (2009) Phosphorus input by upwelling in the eastern Gotland Basin (Baltic Sea) in summer and its effects on filamentous cyanobacteria. *Estuarine Coastal and Shelf Science,* 83**,** 434–442.

Omstedt, A. & L. B. Axell (2003) Modeling the variations of salinity and temperature in the large Gulfs of the Baltic Sea. *Continental Shelf Research,* 23**,** 265–294.

Omstedt, A., J. Elken, A. Lehmann, M. Leppäranta, H. E. M. Meier, K. Myrberg & A. Rutgersson (2014) Progress in physical oceanography of the Baltic Sea during the 2003–2014 period. *Progress in Oceanography,* 128**,** 139–171.

Palmen, E. (1930) Untersuchungen über die Strömungen in den Finnland umgebenden Meeren [Investigations of currents in the seas surrounding Finland]. *Commentationes physico-mathematicae/Societas Scientiarium Fennica,* 12**,** 93.

Pavelson, J., J. Laanemets, K. Kononen & S. Nõmmann (1997) Quasi–permanent density front at the entrance to the Gulf of Finland: Response to wind forcing. *Continental Shelf Research,* 17**,** 253–265.

Petersen, W. (2014) FerryBox systems: State-of-the-art in Europe and future development. *Journal of Marine Systems,* 140**,** 4–12.

Petersen, W., F. Schroeder & F. D. Bockelmann (2011) FerryBox – Application of continuous water quality observations along transects in the North Sea. *Ocean Dynamics,* 61**,** 1541–1554.

Petersen, W., H. Wehde, H. Krasernann, F. Colijn & F. Schroeder (2008) FerryBox and MERIS – Assessment of coastal and shelf sea ecosystems by combining in situ and remotely sensed data. *Estuarine Coastal and Shelf Science,* 77**,** 296–307.

Pietri, A., P. Testor, V. Echevin, A. Chaigneau, L. Mortier, G. Eldin & C. Grados (2013) Finescale Vertical Structure of the Upwelling System off

Southern Peru as Observed from Glider Data. *Journal of Physical Oceanography,* 43**,** 631–646.

Rantajärvi, E. 2003. Alg@line in 2003: 10 Years of Innovative Plankton Monitoring and Research and Operational Information Service in the Baltic Sea. In *MERI – Report Series of the Finnish Institute of Marine Research*. Finnish Institute of Marine Research.

Reissmann, J. H. (2005) An algorithm to detect isolated anomalies in three–dimensional stratified data fields with an application to density fields from four deep basins of the Baltic Sea. *Journal of Geophysical Research–Oceans,* 110**,** 17.

Soomere, T., N. Delpeche, B. Viikmäe, E. Quak, H. E. M. Meier & K. Doos (2011) Patterns of current–induced transport in the surface layer of the Gulf of Finland. *Boreal Environment Research,* 16**,** 49–63.

Suursaar, U. & R. Aps (2007) Spatio–temporal variations in hydro-physical and -chemical parameters during a major upwelling event off the southern coast of the Gulf of Finland in summer 2006. *Oceanologia,* 49**,** 209–228.

Talpsepp, L., T. Noges, T. Raid & T. Kõuts (1994) Hydrophysical and hydrobiological processes in the Gulf of Finland in summer 1987: characterization and relationship. *Continental Shelf Research,* 14**,** 749–763.

Thomas, L. N. (2008) Formation of intrathermocline eddies at ocean fronts by wind–driven destruction of potential vorticity. *Dynamics of Atmospheres and Oceans,* 45**,** 252–273.

Tuomi, L., K. Myrberg & A. Lehmann (2012) The performance of the parameterisations of vertical turbulence in the 3D modelling of hydrodynamics in the Baltic Sea. *Continental Shelf Research,* 50–51**,** 64–79.

Uiboupin, R. & J. Laanemets (2009) Upwelling characteristics derived from satellite sea surface temperature data in the Gulf of Finland, Baltic Sea. *Boreal Environment Research,* 14**,** 297–304.

Uiboupin, R. & J. Laanemets (2015) Upwelling Parameters From Bias–Corrected Composite Satellite SST Maps in the Gulf of Finland (Baltic Sea). *Ieee Geoscience and Remote Sensing Letters,* 12**,** 592–596.

Uiboupin, R., J. Laanemets, L. Sipelgas, L. Raag, I. Lips & N. Buhhalko (2012) Monitoring the effect of upwelling on the chlorophyll a distribution in the Gulf of Finland (Baltic Sea) using remote sensing and in situ data. *Oceanologia,* 54**,** 395–419.

Vahtera, E., J. Laanemets, J. Pavelson, M. Huttunen & K. Kononen (2005) Effect of upwelling on the pelagic environment and bloom–forming cyanobacteria in the western Gulf of Finland, Baltic Sea. *Journal of Marine Systems,* 58**,** 67–82.

Väli, G., V. Zhurbas, J. Laanemets & J. Elken (2011) Simulation of nutrient transport from different depths during an upwelling event in the Gulf of Finland. *Oceanologia,* 53**,** 431–448.

Väli, G., V. Zhurbas, U. Lips & J. Laanemets (2016) Submesoscale structures related to upwelling events in the Gulf of Finland, Baltic Sea (numerical experiments). *Journal of Marine Systems*.

Zhurbas, V., J. Laanemets & E. Vahtera (2008) Modeling of the mesoscale structure of coupled upwelling/downwelling events and the related input of nutrients to the upper mixed layer in the Gulf of Finland, Baltic Sea. *Journal of Geophysical Research–Oceans,* 113**,** 8.

Zhurbas, V., I. S. Oh & T. Park (2006) Formation and decay of a longshore baroclinic jet associated with transient coastal upwelling and downwelling: A numerical study with applications to the Baltic Sea. *Journal of Geophysical Research–Oceans,* 111**,** 18.

PUBLICATIONS

Paper I

Kikas, V., Lips, U. (2016). Upwelling characteristics in the Gulf of Finland (Baltic Sea) as revealed by Ferrybox measurements in 2007–2013. *Ocean Science*, 12, 843–859, doi: 10.5194/os–12–843–2016.

Ocean Science

Open Access

EGU

Upwelling characteristics in the Gulf of Finland (Baltic Sea) as revealed by Ferrybox measurements in 2007–2013

Villu Kikas and Urmas Lips

Marine Systems Institute at Tallinn University of Technology, Akadeemia tee 15a, 12618 Tallinn, Estonia

Correspondence to: Villu Kikas (villu.kikas@msi.ttu.ee)

Abstract. Ferrybox measurements have been carried out between Tallinn and Helsinki in the Gulf of Finland (Baltic Sea) on a regular basis since 1997. The system measures autonomously water temperature, salinity, chlorophyll a fluorescence and turbidity and takes water samples for further analyses at a predefined time interval. We aimed to show how the Ferrybox technology could be used to study the coastal upwelling events in the Gulf of Finland. Based on the introduced upwelling index and related criteria, 33 coastal upwelling events were identified in May–September 2007–2013. The number of events, as well as the frequency of their occurrence and intensity expressed as a sum of daily average temperature deviations in the 20 km wide coastal area, were almost equal near the northern and southern coasts. Nevertheless, the wind impulse, which was needed to generate upwelling events of similar intensity, differed between the northern and southern coastal areas. It is suggested that the general thermohaline structure adapted to the prevailing forcing and the estuarine character of the basin weaken the upwelling created by the westerly to southwesterly (up-estuary) winds and strengthen the upwelling created by the easterly to northeasterly (down-estuary) winds. Two types of upwelling events were identified – one characterized by a strong temperature front and the other revealing gradual decrease in temperature from the open sea to the coastal area, with maximum temperature deviation close to the shore.

1 Introduction

Unattended monitoring of marine environments using ships of opportunity has been implemented in many regions of the world ocean (e.g., Paerl et al., 2009; Hardman-Mountford et al., 2008), including the Baltic Sea and the Gulf of Finland (Rantajärvi, 2003). The measurement systems installed on board commercial ferries or other ships are called "Ferryboxes", and they consist of various sensors, devices creating water flow through the sensors and software packages controlling the system and managing the data. The commonly used Ferryboxes measure temperature, salinity, and chlorophyll a fluorescence in the seawater pumped through the system from the surface layer along the ship track. First trials of using ships of opportunity for environmental monitoring in the Gulf of Finland were made by Estonian and Finnish scientists between Tallinn and Helsinki in 1990–1991 (Rantajärvi, 2003). Regular Ferrybox measurements along this route were started in 1997, while the longest data series of Ferrybox measurements (since 1993) is available along the Helsinki–Travemünde ferry route (Petersen, 2014).

The Gulf of Finland (GoF) lies in the northeastern part of the Baltic Sea (Fig. 1). It is an elongated basin with a length of about 400 km and a maximum width of 135 km (Alenius et al., 1998). The vertical stratification in the gulf is characterized by a quasi-permanent halocline at a depth of 60–80 m, and a seasonal thermocline, which forms in spring–summer at a depth of 10–20 m (e.g., Liblik and Lips, 2011). The long-term residual circulation in the surface layer of the gulf is characterized by a relatively low speed and by a cyclonic pattern. The saltier water of the northern Baltic proper flows into the gulf along the Estonian (southern) coast, and the gulf water, which is less saline due to the large freshwater inflow at the eastern end of the gulf (the Neva River), flows out along the Finnish (northern) coast. The circulation is more complex at timescales from days to weeks mainly due to the variable wind forcing. A variety of mesoscale processes/features (fronts, eddies, coastal upwelling/downwelling), which sig-
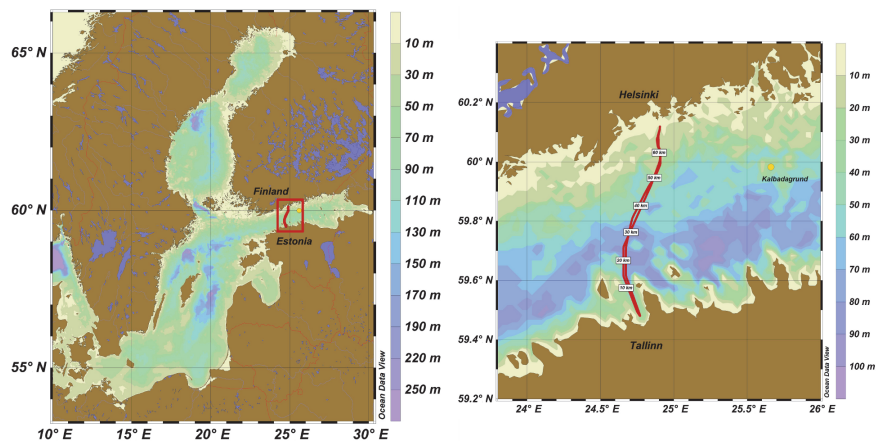
Figure 1. Map of the Baltic Sea (**a**) and the study area (**b**) with the Ferrybox transect and Kalbadagrund meteorological station. Maps are made using Ocean Data View software (Schlitzer, 2015).

nificantly affect the biological production, retention, and transport, have been observed in the Gulf of Finland (e.g., Talpsepp et al., 1994; Kononen et al., 1996; Pavelson et al., 1997; Vahtera et al., 2005; Lips et al., 2009).

Dynamics and characteristics of upwelling events have been studied in the Gulf of Finland based on in situ measurements (e.g., Haapala, 1994), remote sensing (e.g., Uiboupin and Laanemets, 2009) and modeling (e.g., Myrberg and Andrejev, 2003). Most prominent upwelling events that were captured by measurements are an event along the northern coast in July 1999 (Vahtera et al., 2005) and an event along the southern coast in August 2006 (Lips et al., 2009). The following characteristic features of upwelling events in the Gulf of Finland are suggested:

1. the Finnish coastal sea in the northwestern GoF is one of the main upwelling areas in the Baltic Sea (Myrberg and Andrejev, 2003), where upwelling frequency in May–September 1990–2009 has been up to 15 % (Lehmann et al., 2012); almost the same upwelling frequency is suggested by the latter authors for the central GoF along the Estonian (southern) coast;

2. mean upwelling area detected on the basis of 147 maps during the period of 2000–2009 was 5642 km^2 (19 % of the GoF surface area) along the northern coast and 3917 km^2 (13 % of the GoF surface area) along the southern coast (Uiboupin and Laanemets, 2015), while the largest area covered by the upwelling water was identified as 12140 km^2 (data from 2000 to 2006; Uiboupin and Laanemets, 2009); the authors' estimate of the mean cross-shore extent of the upwelling area was 20–30 km off the northern coast and varied between 7 and 20 km off the southern coast;

3. the intensity of upwelling events depends on the values of cumulative upwelling-favorable wind stress and strength of vertical stratification; Haapala (1994) suggested that an at least 60 h long wind event has to exist to create an upwelling event; based on the wind data analysis from 2000 to 2005 and taking the threshold value for cumulative wind stress of 0.1 N m^{-2} day, on average, about two upwelling events should appear off the southern coast and four events off the northern coast (Uiboupin and Laanemets, 2009);

4. it is suggested that the difference in topography off the southern and northern coasts of the GoF results in differing upwelling dynamics along the opposite coasts – in the case of similar wind stress (but in opposite directions) the transport of waters from deeper layers starts earlier and is larger along the southern coast (Väli et al., 2011).

The motivation of the present paper is to show how the Ferrybox technology can be used to study mesoscale processes, especially coastal upwelling events in the Gulf of Finland. We describe the approach, its advantages and limits, and present statistical characteristics of upwelling events on the basis of data collected in 2007–2013. The main aims are to relate the observed variability and dynamics of upwelling events to the atmospheric forcing, to reveal the differences in upwelling behavior in the northern and southern coastal areas, and to suggest an alternative physical explanation of the found differences by taking into account the prevailing forcing and estuarine character of the basin.

2 The measurement system and methods

2.1 Ferrybox system

Temperature (T), salinity (S), chlorophyll a fluorescence and turbidity data and water samples for nutrients and phytoplankton chlorophyll a (Chl a), species composition and biomass analyses have been collected unattended on passenger ferries traveling between Tallinn and Helsinki (Fig. 1) since 1997. Due to the internal arrangements of ferry company Tallink Silja and its predecessors, several ships were used as the platforms for Ferrybox measurements, which also differ regarding water intake features. A flow-through system from 4H-Jena, Germany, with the water intake attached to the sea chest of the ferry, has been in use since 2006. The water enters the sea chest through a grating with a total surface area of $0.84\,m^2$ located at about $4\,m$ depth below the waterline. The water flow from the sea chest into the system is forced by the hydrostatic pressure since the Ferrybox is located on the lower deck about 3 m below the waterline. To restrict larger particles from getting into the measurement system, a mud filter (pore size 1 mm) is used close to the water intake. Before the sensors, a debubbler is installed to avoid air bubbles to affect the measurements of conductivity, turbidity and Chl a fluorescence. The flow rate through the sensors is stabilized by an internal pump, which is controlled by a pressure sensor in the system. Water samples are taken by a sampling device (Hach Sigma 900 MAX), whereas the water is pumped from the debubbler into the bottles using an internal pump of the water sampler.

For temperature measurements, a PT100 temperature sensor is used that is installed close to the water intake to diminish the effect of warming of water while flowing through the tubes onboard. The sensor has a measuring range from -2 to $+40\,°C$ and an accuracy of $\pm0.1\,\%$ of the range, i.e., $0.04\,°C$. For salinity measurements an FSI Excell thermosalinograph (temperature and conductivity meter) and for Chl a fluorescence and turbidity measurements a SCUFA submersible fluorometer (Turner Designs) with a flow-through cap are used. The accuracy of the conductivity sensor is $0.0025\,S\,m^{-1}$. The system starts the measurements and data recording when the ferry is away from the harbor more than a predefined distance of 0.7 nautical miles (controlled by a GPS device in the system) and stops when it is closer than this distance to avoid sediments getting into the system. The data are recorded during every crossing (twice a day) every 20 s, which corresponds to a horizontal resolution of approximately 160 m.

2.2 Quality assurance and pre-processing of data

The sensors have been calibrated at the factory before the installation and if necessary sent for an additional laboratory calibration. Since the system contains two temperature sensors, the performance of them is routinely followed by a comparison of data acquired from the sensors. The quality of thermosalinograph data is guaranteed by taking a series of water samples (14–17 samples) and analyzing them using a high-precision salinometer (AUTOSAL) two to four times a year. The analyses have shown that a correction of 0.08 (units in Practical Salinity Scale; the value has been stable over the years) must be added to the recorded salinity. While the raw salinity is recorded in units according to the Practical Salinity Scale 1978, the results on salinity distribution and variability are given in the paper (Sects. 3 and 4) in $g\,kg^{-1}$ according to Feistel et al. (2010). Particular care is taken to calibrate the SCUFA fluorometer; however, since we do not use the fluorometer data in this study, the used routine is not described here.

The data acquired by the Ferrybox system recorded with a time step of 20 s are stored in an onboard terminal. To synchronize the measurements performed by the sensors with different sampling frequencies and GPS, the acquired data within every 19 s interval are averaged and recorded as measurements at every 20th second. The data are automatically delivered to the on-shore FTP server once a day when the ferry is in the harbor using a GSM connection. The performance of the system is validated by the control parameters, such as the flow rate and pressure in the system, and the data are checked for unrealistic values against the criteria set for every parameter on the basis of known natural variations of them in the Gulf of Finland.

One of the procedures, which has to be carried out when using the Ferrybox data, is the shifting of data points to the actual positions of the water intake. The problem arises since the coordinates attached to a data record correspond to the location of the ferry at the time of measurement, but the water is taken in earlier at a different position. Since various systems of water intake are applied, this procedure is unique for each combination of a Ferrybox and a ferry. As described above, in our design the seawater enters first a relatively large sea chest and the flushing through-time of it is unknown. While the water flows through the sea chest and into the tubes and debubbler with a flow rate of 12–$15\,L\,min^{-1}$, the ferry moves on at an average speed of 16 knots. We solved the problem of position correction taking into account the advantage of having two crossings a day.

Analysis of data from return journeys allowed us to introduce a position correction procedure – the best result is achieved by shifting the measured data points against the GPS time for 3–4 min, depending on the ferry and exact intake installation. This relatively long period is obviously related to the water exchange in the sea chest. Due to an almost constant cruising speed of the ferry outside the harbor areas, the applied procedure gives acceptable results. The comparison of data from Tallinn to Helsinki and back from Helsinki to Tallinn obtained on the same day is one of the used quality assurance procedures – the profiles containing unexpected deviations are marked by a quality flag indicating a possible quality problem.

2.3 Data and calculation methods

Temperature and salinity data collected along the Tallinn–Helsinki ferry line from May to September in 2007–2013 are used for analysis purposes. In 2008, the system on board the passenger ferry "Galaxy" was in use until 13 July and the measurements started again on 13 August when the system was installed on board the ferry "Baltic Princess". However, due to some technical problems, the regular measurements were only reliable from 2 September 2008. A failure of the system occurred late August 2012 and, therefore, the data are not available from 29 August until the end of September 2012. In early 2013, the next ferry ("Silja Europa") came to this line and the system was moved again, causing a break in the measurements until 15 July 2013. The number of crossings with the full data coverage is given in Table 1. Four years – 2007, 2009, 2010 and 2011 – were the years with almost complete data coverage, while most of the data were not available in the second half of July and August 2008, in September 2012 and in May, June and the first half of July 2013. Thus, the data from all months from May to September were analyzed at least from 6 years in 2007–2013.

Collected raw data were preliminarily processed, including shifting of measurements as described in Sect. 2.2, quality checked and stored in the database. This data set was used to draw the maps of temporal variations of horizontal distributions of T and S for all studied years (Fig. 2). A step (cell width) of 0.5 km along the south–north oriented line was used to transform the data set from the matrix with a constant time step into the matrix with a constant spatial resolution. The fixed south–north orientation was applied to eliminate the influence of differences in orientation of the ship track in the southern, central and northern parts of the route (see Fig. 1) and of possible deviations from the usual route. As a result, the extent of the upwelling area is presented below in the south–north direction, and a coefficient has to be applied to convert these values to the upwelling extent in the cross-shore direction (as the cosine of the angle between the south–north direction and a perpendicular line to the shore – approximately 20°).

An upwelling index was introduced in the coastal area off the southern coast (UI_S) and off the northern coast (UI_N). For each crossing, the average water temperature and horizontal profile of temperature deviations from the average were computed. The upwelling index was calculated as a sum of negative temperature deviations in the coastal areas (0–20 km offshore) as

$$UI_S = \sum_{\substack{i=1...40 \\ \Delta T_i < 0}} |\Delta T_i| \text{ and } UI_N = \sum_{\substack{i=101...140 \\ \Delta T_i < 0}} |\Delta T_i|, \quad (1)$$

where ΔT_i is the temperature deviation of 0.5 km cell i from the average temperature of the crossing. The width of 20 km was selected on the basis of the analysis of all available temperature data from the Tallinn–Helsinki ferry line in 2007–2013 (see Sect. 3.1 for details). The daily indexes were obtained by averaging the two upwelling indexes from a single day (from a return journey of the ferry). A cumulative upwelling index (CUI) can be calculated by summing up upwelling index values for certain periods. The obtained CUI values were divided by 40, which is the number of data cells in the 20 km wide coastal area, to keep the meaning of CUI as the sum of average negative temperature deviations, having a unit of °C day:

$$CUI_S(n1...n2) = \sum_{j=n1}^{j=n2} \left(\frac{1}{40} UI_{Sj} \right)$$

$$\text{and } CUI_N(n1...n2) = \sum_{j=n1}^{j=n2} \left(\frac{1}{40} UI_{Nj} \right), \quad (2)$$

where $n1$ and $n2$ are the start and end day numbers of the selected period, for which the cumulative upwelling index is calculated, and UI_{Sj} and UI_{Nj} are the upwelling indexes at day j off the southern and northern coasts, respectively. This approach of the CUI calculation is similar to that used previously in the studies of upwelling events and their influence on the phytoplankton dynamics in the Gulf of Finland (see, e.g., Lips and Lips, 2008; Myrberg et al., 2008).

An upwelling event can be characterized by the cumulative upwelling index calculated for the period when the upwelling index (UI_N or UI_S) exceeded a certain threshold value. We have defined this threshold value as 40 °C, which corresponds, e.g., to a 20 km wide upwelling with an average negative temperature deviation of 1 °C. This choice is explained in more detail in Sect. 3.2.

Wind data were obtained from the HIRLAM (High-Resolution Limited Area Model) version of the Estonian Meteorological and Hydrological Institute with the spatial resolution of 11 km and the time interval of 3 h (Väli, 2011; Männik and Merilain, 2007). The model data point close to Kalbådagrund, where a meteorological weather station is also located (Finnish Meteorological Institute), was chosen to represent the wind conditions in the study area. The data from Kalbådagrund weather station or the closest HIRLAM model point have also been used in the earlier studies of coastal upwellings in the Gulf of Finland (Lips et al., 2008a; Uiboupin and Laanemets, 2009). According to Keevallik and Soomere (2010), the HIRLAM output matches well with the observations at Kalbådagrund (the wind is measured at 32 m), although the modeled wind direction (at 10 m height) is turned 20° counter-clockwise from the measured wind direction.

Wind stress (in N m^{-2}) is calculated for the wind component along the axis of the Gulf of Finland, which corresponds to the direction turned by 70° clockwise from the northerly direction, as

$$\tau_{70} = C_D \rho_a |U| U_{70}, \quad (3)$$

Table 1. Periods of measurements along the Tallinn–Helsinki ferry route in 2007–2013, number of days with measurements and number of days with upwelling events off the northern coast (N) and off the southern coast (S).

Year	Ferry	Period	Number of days with data	Number of days with upwelling	
				N	S
2007	Galaxy	1 May–30 September	141	26	21
2008	Galaxy	1 May–13 July	90	8	11
	Baltic Princess	13 August–30 September			
2009	Baltic Princess	1 May–30 September	145	33	30
2010	Baltic Princess	1 May–30 September	140	5	32
2011	Baltic Princess	1 May–30 September	135	19	30
2012	Baltic Princess	1 May–28 August	113	22	0
2013	Silja Europa	15 July–30 September	74	37	16

where U is the wind speed (in $m\,s^{-1}$), U_{70} is its component in the along-gulf direction, C_D is the drag coefficient (a constant value of 1.2×10^{-3} was chosen in the present study; Large and Pond, 1981), and ρ_a is the air density ($1.2\,kg\,m^{-3}$). Accordingly, positive values of the wind stress should initiate southward Ekman transport in the surface layer and vice versa. The cumulative wind stress (in $N\,m^{-2}$ day) was calculated based on daily averages of wind stress. If the cumulative wind stress is large enough, upwelling events occur along the northern coast in the case of the positive wind stress and along the southern coast in the case of the negative wind stress.

3 Results

3.1 General variability and distribution patterns

The typical seasonal course of the surface layer temperature in the Gulf of Finland is characterized by temperatures of about 5 °C at the beginning of May, a maximum of > 20 °C in late July–early August and a drop below 15 °C in late September. Within the analyzed years 2007–2013, the surface layer temperature was highest in summer 2010 (Fig. 2) when the period with the average along-transect temperature of > 20 °C was 35 days. Against the background of seasonal course and simultaneous shorter-term increases or decreases in temperature over the whole study transect, periods with distinctly lower temperature were observed off the northern or southern shore. Such situations are related to the coastal upwelling events – their characteristic timescale was several days to 1–2 weeks, and they extended towards the open sea by 15–20 km (Fig. 2).

Interannual variations of the surface layer salinity in 2007–2013 were high, with the highest salinity in 2011 and the lowest in 2009. The surface layer salinity exceeded $6.5\,g\,kg^{-1}$ for a longer period only in 2011 in the southern half of the study transect (Fig. 2j) and for shorter periods of several days in the case of coastal upwelling events off the southern shore

(e.g., Fig. 2b and d). Note that in the case of coastal upwelling events seen in the temperature distributions off the northern coast, a simultaneous increase in salinity was not very visible. As a rule, the surface layer salinity was higher near the southern coast than that near the northern coast. However, often the lowest salinity was measured in the middle of the transect – that is, in the open sea areas (e.g., Fig. 2f and h). The seasonal course of salinity differed remarkably between the years. While usually the lowest surface layer salinity was observed in June–July, in 2008 the salinity was lowest in May, and in 2010 and 2011 it was lowest in August.

The average temperature and salinity deviations in May–September each year and for the entire study period, as well as their root mean square errors (RMSEs), were calculated in each 0.5 km cell. On average, the temperature deviations were close to zero along the entire study transect (Fig. 3a) – the absolute values of average deviation were 6 times less than the estimated RMSE of temperature. Nevertheless, the surface layer temperature was slightly warmer in the open Gulf of Finland than in approximately 20 km wide coastal areas (Fig. 3a). We relate this finding to the occurrence of coastal upwelling events. For instance, in 2009, when coastal upwelling events were observed off both coasts, the average temperature deviations were negative near both coasts (Fig. 3c). In 2010, when upwelling events occurred mostly off the southern coast, the negative values of average temperature deviations were detected only in the southern part of the transect (Fig. 3e).

It is remarkable that, on average, the variability of temperature deviations was much higher near the coasts than in the central part of the study transect (Fig. 3a). In the case of upwelling events off the southern coast and their absence off the northern coast (in 2010), this high variability of temperature was concentrated only in the 20 km wide coastal area off the southern shore (Fig. 3e). We suggest that this high variability of temperature in the coastal areas is mostly related to the upwelling activity and, therefore, we estimated the intensity of
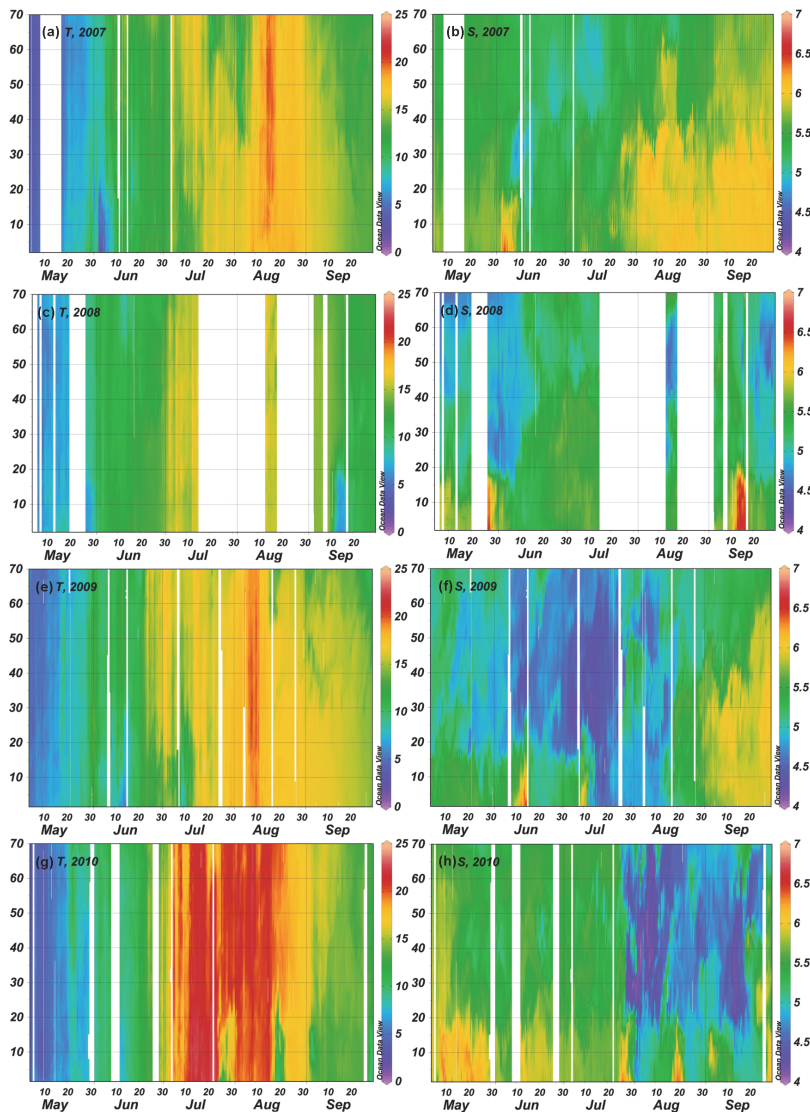
Figure 2.

upwelling events based on data from the 20 km wide coastal zones.

The average distribution of the surface layer salinity along the transect was characterized by higher salinity values in the southern gulf and lower values in the northern gulf (Fig. 3b). The salinity deviations were positive in the 28 km wide area off the southern coast (with clearly higher salinity in the first 10 km) and negative along the rest of the study transect. How-

ever, the minimum of the surface layer salinity was observed at about 20 km from the northern shore (or at a distance of 50 km from the southern end of the study transect) in almost every year (Fig. 3b, d, and f). The only exception was the year 2007 when the lowest salinity was observed on average in the cell closest to the northern shore. The low salinity water at the distance of 50 km indicates that, in summer, the outflow of the less saline Gulf of Finland surface waters oc-
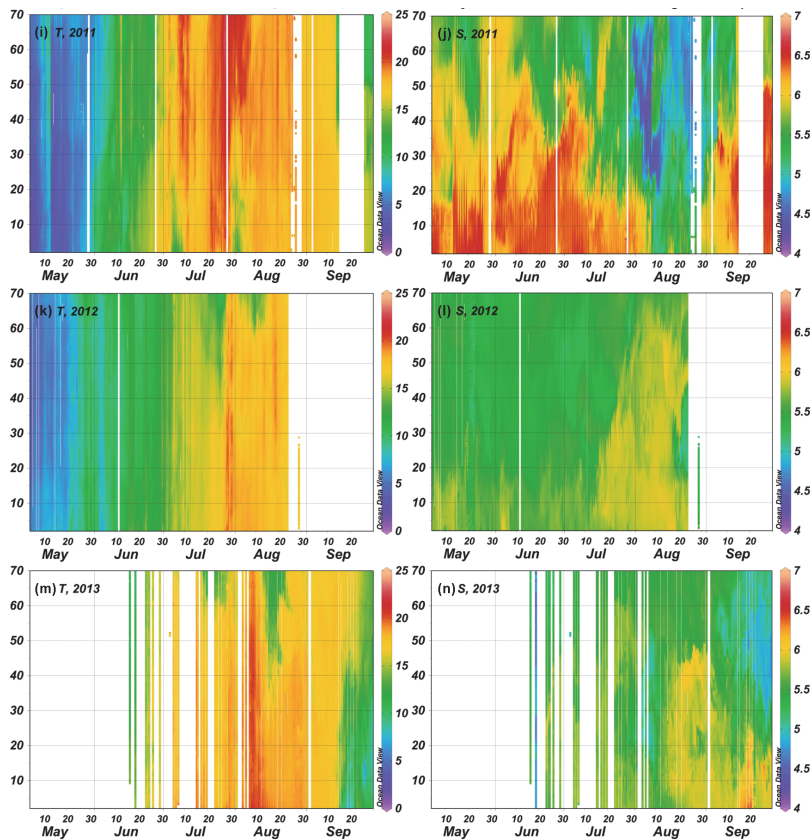
Figure 2. Temporal changes in temperature (in °C) and salinity (in g kg^{-1}) distributions between Tallinn and Helsinki from 1 May to 30 September in 2007 **(a, b)**, 2008 **(c, d)**, 2009, **(e, f)**, 2010 **(g, h)**, 2011 **(i, j)**, 2012 **(k, l)** and 2013 **(m, n)**; y axis shows the distance from Tallinn Bay (latitude 59.48 N) in km along the meridional transect. Maps are made using Ocean Data View software (Schlitzer, 2015).

curs mostly in the northern part of the open gulf. The variability of the surface layer salinity did not differ between the coastal and open sea areas as much as the variability of the surface layer temperature. One can recognize slightly higher variability (RMSE) of the surface layer salinity in the coastal areas and the southern part of the open gulf at a distance of 20–30 km.

3.2   Upwelling characteristics

As is seen on the maps of temperature deviations (Fig. 4), the years 2007 and 2009 had a similar pattern – the upwelling events occurred off the southern coast in the first half of the season and off the northern coast in the second half. In 2008, upwelling events were observed near the southern coast in May and September, and they appeared near the northern coast in June. The year 2010 was an exceptional

year when the upwelling events occurred mostly along the southern coast. It was exceptional also because the sea surface temperature outside the upwelling waters was the highest among the studied summers. A sequence of consecutive upwelling events near the northern and southern coasts was observed in 2011. Upwelling events occurred mostly off the northern coast in 2012 and 2013.

We selected a criterion to detect whether an upwelling event occurs or not as the value of the upwelling index (UI) exceeded 40 °C (in absolute values, while UI is by definition a negative number). The upwelling events found using the selected criterion were also the occasions when the maximum negative temperature deviation from the transect mean value was at least −2 °C (except one event on 10–17 September 2007 when the maximum deviation was −1.97 °C). Furthermore, no other cases with negative temperature deviations exceeding −2 °C were detected. Thus, the criterion UI
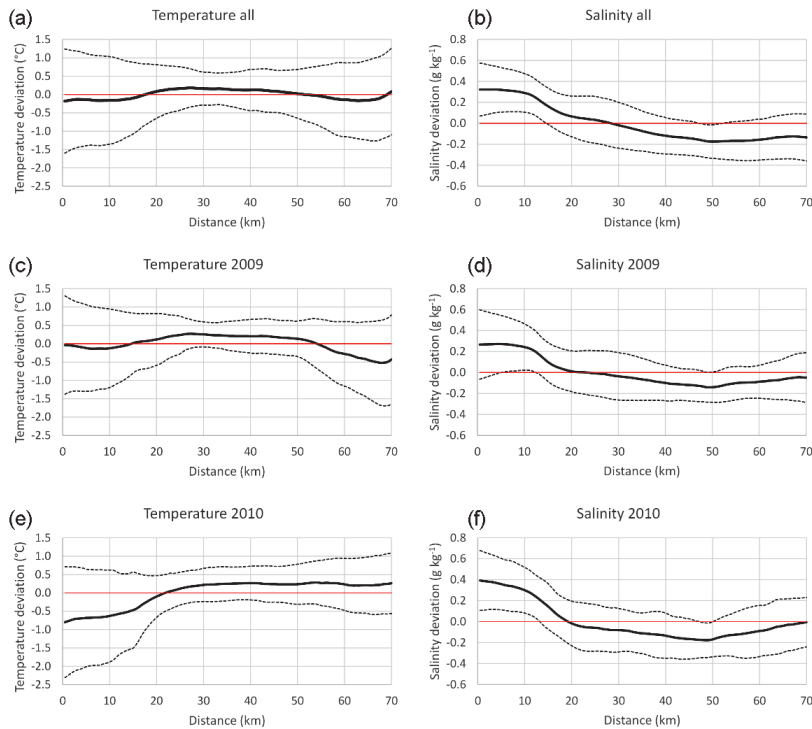
Figure 3. Distributions of temperature (in °C) and salinity (in g kg^{-1}) deviations from the transect mean value along the Tallinn–Helsinki ferry route for all measurements in May–September 2007–2013 (**a, b**), 2009 (**c, d**) and 2010 (**e, f**). Mean values for each 0.5 km cell (solid curves) and plus/minus RMSE (dashed curves) are shown; x axis indicates the distance from Tallinn Bay (latitude 59.48 N) in km along the meridional transect.

< -40 °C gives quite similar results to the criterion based on the maximum negative temperature deviation of -2 °C.

We identified in May–September 2007–2013 altogether 33 upwelling events, approximately half of them (17) near the northern coast and half (16) near the southern coast (Table 2). The number of days with the upwelling near the northern coast was 150 and, near the southern coast, 140. As the total number of days with measurements was 838, the upwelling occurred in 18 and 17 % of days off the northern and southern coasts, respectively. The maximum negative temperature deviation from the transect mean value was detected in August 2010 near the southern coast, when it reached -7.78 °C. While the maximum temperature deviation characterizes the peak of the upwelling, the introduced cumulative upwelling index also takes into account the extent of the upwelling in space and time. As based on CUI, the largest upwelling events were observed in 2013 – on 15–30 September 2013 off the southern coast (CUI $= -40.2$ °C day) and on 11–31 August 2013 off the northern coast (CUI $= -39.7$ °C day). The average CUI value of all upwelling events off the northern coast was -14.5 °C day and, off the southern coast,

-16.2 °C day. The sum of CUI values of all detected upwelling events off the northern coast was -247.0 °C day and, off the southern coast, -258.4 °C day.

The total CUI for all measurement days in 2007–2013 was -405.3 °C day for the northern coastal area and -356.6 °C day for the southern coastal area. Thus, the negative temperature deviations from the transect mean were more common for the northern coastal sea area, while the upwelling events were more intense in the southern coastal sea area.

The highest number of upwelling events was observed in July – 10 events, 5 off the northern coast and 5 off the southern coast – and the lowest in May – 4 events. The sums of CUI values of all events in July and August were -185.3 °C day and -187.9 °C day, respectively, while it was only -28.6 °C day in May. Obviously, the revealed seasonal trend was partly related to the temperature difference between the surface layer and the cold layer beneath the seasonal thermocline, which has its maximum in the Gulf of Finland in July–August (Liblik and Lips, 2011).
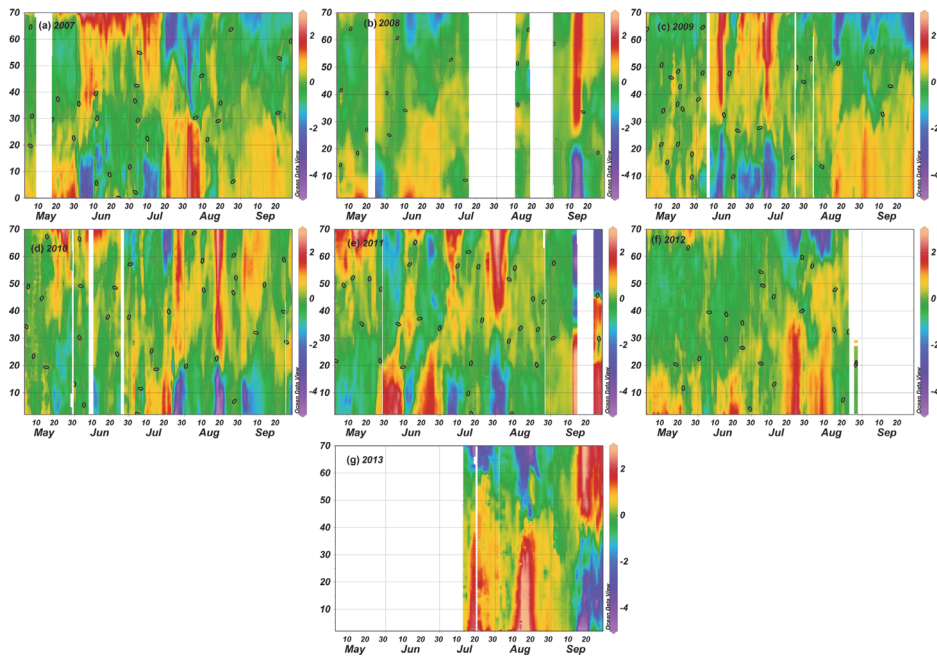
Figure 4. Temporal changes in spatial distributions of temperature deviations (in °C) from the daily transect mean value between Tallinn and Helsinki from 1 May to 30 September in 2007 **(a)**, 2008 **(b)**, 2009 **(c)**, 2010 **(e)**, 2011 **(f)**, 2012 **(g)** and 2013 **(h)**; y axis shows the distance from Tallinn Bay (latitude 59.48 N) in kilometers along the meridional transect. Maps are made using Ocean Data View software (Schlitzer, 2015).

3.3 Upwelling characteristics in relation to wind forcing

The occurrence of coastal upwelling events in the Gulf of Finland can be related quite well to the variations of the along-gulf wind stress (Fig. 5). The upwelling events appeared after a certain favorable wind pulses with long enough duration and magnitude. In the case of upwelling events off the northern coast, the positive along-gulf wind stress was usually observed a few days before the event and, in the case of upwelling events off the southern coast, the wind stress was negative for a few days (Fig. 5).

The estimated cumulative wind stress for the detected up-welling events varied between 0.31 and 1.37 N m^{-2} day for westerly winds and between -0.09 and -1.08 N m^{-2} day for easterly winds (Table 2). The cumulative wind stress associated with each upwelling event was calculated based on daily average wind stress values by summing them up from the first day with favorable wind stress (within a period of 1 week before the event) to the last day with favorable wind stress before the end of the event. If only 1 day with opposite wind stress appeared in a sequence in the favorable wind stress series, then the calculation period was not broken. The

average value of the cumulative wind stress for an upwelling event off the northern coast was 0.71 N m^{-2} day and, off the southern coast, -0.44 N m^{-2} day. It suggests that to produce a coastal upwelling event of an equal magnitude the required favorable along-gulf wind stress has to be larger for the up-welling events off the northern coast than for the events off the southern coast. This conclusion is drawn by taking into account the above result that the average upwelling intensity (estimated as CUI) was similar for both coastal areas, with slightly higher values of CUI for the upwelling events off the southern coast. This suggestion is also supported by comparison of relationships between the CUI and cumulative wind stress (CWS) related to the upwelling events near the opposite coasts (Fig. 6). The linear regression lines between CUI and CWS indicate that at the same CWS values, the up-welling events had higher intensities off the southern coast than off the northern coast. Nevertheless, the results are quite scattered, and the coefficient of determination (r^2) between the CUI and CWS is 0.30 for the southern and 0.19 for the northern upwelling events.

The average along-gulf wind stress for the entire study period from May to September in 2007–2013 was 0.016 N m^{-2}. The seasonal averages had positive values in all studied
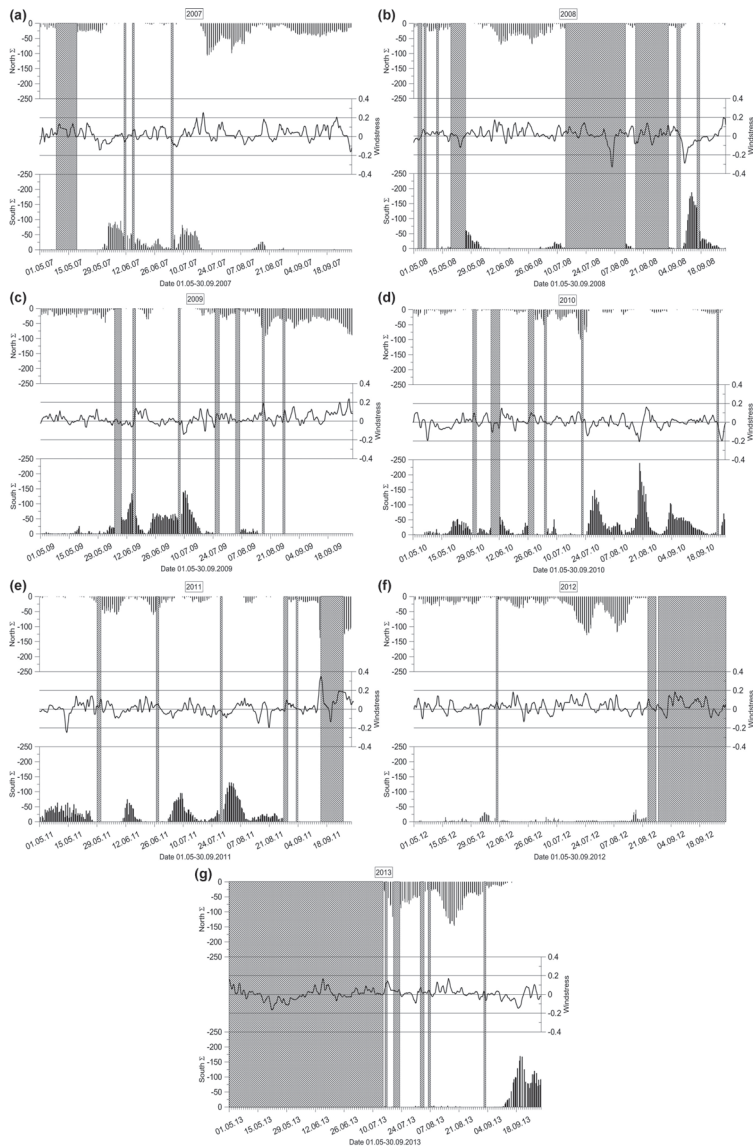
Figure 5. Temporal changes in upwelling index off the northern coast (at the top of each subplot; °C) and off the southern coast (at the bottom of each subplot; °C) and along-gulf wind stress (black curve in the middle; N m^{-2}) in May–September 2007 (**a**), 2008 (**b**), 2009 (**c**), 2010 (**d**), 2011 (**e**), 2012 (**f**) and 2013 (**g**).

years, indicating that the westerly to southwesterly winds prevailed in the region. The average values of wind stress varied between 0.001 N m^{-2} in 2010 and 0.029 N m^{-2} in 2007, 2009 and 2012. In May–September 2010, when five upwelling events occurred off the southern coast and only

one event off the northern coast, the average along-gulf wind stress was close to zero, indicating that the cumulative wind forcing was almost equal from both directions. Furthermore, the wind stress averaged over all observed upwelling events in 2007–2013 was 0.015 N m^{-2}, which is very close to the

Table 2. Characteristics of detected upwelling events; dates, coastal area (N – off northern coast; S – off southern coast), type (UF – with strong upwelling front; GD – with gradual decrease in temperature), maximum temperature deviation from the transect mean value, cumulative upwelling index calculated for each event and cumulative along-gulf wind stress calculated for upwelling favorable winds before and during the upwelling event.

No.	Dates	Coast	Type	Maximum temperature deviation (°C)	Cumulative upwelling intensity (°C day)	Cumulative wind stress (N m^{-2} day)
1.	3–14 June 2007	S	UF	−4.12	−19.8	−0.49
2.	8–16 July 2007	S	GD	−3.02	−12.6	−0.34
3.	21–27 July 2007	N	UF	−4.02	−13.9	0.93
4.	29 July–8 August 2007	N	GD	−3.64	−16.5	0.38
5.	10–17 September 2007[1]	N	GD	−1.97	−7.5	0.75
6.	26-28 May 2008[2]	S	UF	−2.52	−3.9	−0.20
7.	11–15 June 2008	N	UF	−2.73	−7.2	0.62
8.	27–29 June 2008	N	UF	−2.27	−6.2	0.53
9.	10–17 September 2008	S	UF	−5.42	−23.0	−1.08
10.	9–16 June 2009	S	UF	−4.77	−14.8	−0.27
11.	24 June–14 July 2009	S	GD	−5.78	−36.1	−0.42
12.	16–22 August 2009	N	UF	−3.20	−10.7	0.54
13.	28 August–9 September 2009	N	UF	−2.74	−14.1	0.56
14.	17–30 September 2009[3]	N	UF	−3.09	−19.3	1.28
15.	20–24 May 2010	S	GD	−2.21	−5.1	−0.56
16.	12–13 June 2010[4]	S	UF	−2.60	−2.3	−0.19
17.	20–24 July 2010	N	UF	−4.70	−9.3	0.31
18.	26 July–1 August 2010	S	UF	−6.19	−15.7	−0.34
19.	17–23 August 2010	S	UF	−7.78	−20.8	−0.66
20.	2–12 September 2010	S	GD	−5.27	−16.0	−0.25
21.	4–12 May 2011[5]	S	GD	−2.22	−9.3	−0.09
22.	31 May–8 June 2011	N	UF	−2.32	−10.3	0.60
23.	11–15 June 2011	S	UF	−3.12	−6.0	−0.38
24.	24–27 June 2011	N	UF	−2.40	−4.8	0.41
25.	5–10 July 2011	S	GD	−5.05	−10.6	−0.38
26.	29 July–7 August 2011	S	GD	−4.69	−22.2	−0.62
27.	14 September 2011[6]	N	UF	−4.90	−3.1	0.47
28.	26–30 September 2011[7]	N	UF	−3.27	−13.8	1.26
29.	18–27 July 2012[8]	N	GD	−4.55	−22.4	1.37
30.	2–13 August 2012	N	UF	−4.17	−22.2	0.58
31.	17 July–1 August 2013[9]	N	UF	−6.15	−26.0	0.63
32.	11–31 August 2013	N	GD	−5.03	−39.7	0.92
33.	15–30 September 2013	S	UF	−7.34	−40.2	−0.71

[1] Temperature deviation was less than −2 °C during the event on 10–17 September 2007; [2] data absent before 26 May 2008 for more than 1 day; [3] data analyzed until 30 September 2009 (upwelling event continued); [4] data absent before 12 June 2010 for more than 1 day; [5] early spring with possible contribution of difference in surface water warming; [6] no data available after 14 September 2011; [7] no data available before 26 September 2011, wind data missing on 24–26 September 2011; [8] wind data on 14–15 July 2012 not available; [9] ferrybox data on 20–21 July 2013 not available.

average wind stress over the entire study period. This estimate was obtained based on the mean length of upwelling events of 8.8 days and mean cumulative wind stress values of 0.71 and −0.44 N m^{-2} day off the northern and southern coasts, respectively. It can be concluded that the difference between the wind impulses needed for the generation of upwelling events with similar intensity near the opposite coasts

is comparable to the average along-gulf wind stress in the region.

Usually, the upwelling events occurred 1 or a few days after the start of the favorable wind pulse, and the maximum of upwelling intensity was reached 1 or a few days after the maximum wind stress (Fig. 5). We made an attempt to identify characteristic spatial temperature and salinity distributions in the surface layer from coast to coast at times
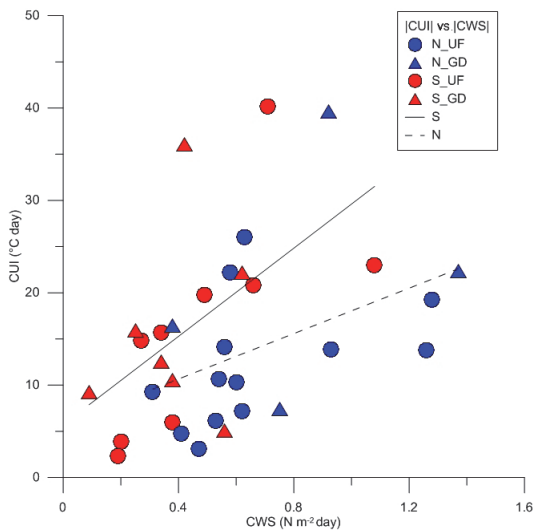
Figure 6. The relationship between the cumulative upwelling index (CUI) and cumulative along-gulf wind stress (CWS) based on 33 detected upwelling events in May–September 2007–2013. Red symbols indicate the events off the southern coast and blue symbols the events off the northern coast; circles correspond to the events with a pronounced upwelling front (N_UF and C_UF) and triangles the events with a gradual decrease in temperature towards the coast (N_GD and S_GD). The linear regression lines for southern (solid line) and northern upwelling events (dashed line) are shown.

of the maximum intensity of upwelling events. Surprisingly, the results did not differ significantly between the northern and southern coasts – two characteristic shapes of upwelling events in the temperature distribution were identified for both coastal areas.

Mostly the upwelling events were characterized by a sharp and very intense temperature front between the upwelling waters and the rest of the transect (red curves in Fig. 7a and c). The sharp upwelling fronts are usually associated with strong along-front jet currents, for instance, as measured by Suursaar and Aps (2007) in the Gulf of Finland in summer 2006. Typical for such events were an almost uniform temperature outside the upwelling area and the temperature minimum (maximum temperature deviation) close to the upwelling front. The other distribution pattern (dark blue curves in Fig. 7a and c) exposed a gradual decrease in temperature towards the upwelling waters. Typical for the latter events were the irregularities in temperature distribution with a characteristic scale of a few kilometers and the temperature minimum (maximum temperature deviation) in the cell closest to the shore. In some cases, e.g., the event near the northern coast with maximum intensity on 18 August 2013 (dark blue solid curve in Fig. 7a), the observed temperature deviations

were as large as during the upwelling events with strong temperature fronts. There was also a third type of temperature distribution when the upwelling waters were not attached to the shore (red dotted curve in Fig. 7a), at least according to the measurements along the ferry route. All these types of upwelling events are well recognized on the maps of temporal changes in temperature and temperature deviation along the Tallinn–Helsinki ferry route (Figs. 2 and 4).

The spatial distribution of salinity in the surface layer from coast to coast drastically differed between the upwelling events near the northern coast and the events near the southern coast (Fig. 7b and d). In the latter case, both the salinity difference across the gulf and the spatial variability at scales of a few kilometers to 10 km were much larger than in the former case. It is also interesting that in the case of southern upwelling events, the salinity minimum along the transect can be situated either very close to the upwelling front (e.g., on 28 July 2010) or near the northern coast (e.g., 8 July 2011). Although such diverse patterns are partly related to the history of water movements in the gulf, the salinity minimum (at least local minimum) close to the upwelling front might be caused by the westward current jet along the front as also revealed by model experiments (Laanemets et al., 2011). The salinity distribution across the gulf associated with the northern upwelling events is very uniform, with some variability at scales of a few kilometers to 10 km, which have the amplitude several times less than spatial salinity variations associated with the southern upwelling events.

4 Discussion

Several studies have shown how the Ferrybox measurements are successfully used for different applications, such as for monitoring of coastal waters in combination with remote sensing (Petersen et al., 2008), estimating carbon fluxes and primary productivity (Schneider et al., 2014) and detecting cyanobacterial blooms (Seppälä et al., 2007). However, not enough attention is paid to the Ferrybox systems, especially to the question of how the results are affected by the used technical solutions (like water intake depth and construction, piping). Furthermore, the particularities of geographical location as well as the ferry route and schedule often determine the most suitable applications and requirements for the data treatment. A good example of taking advantage of the geographical location and ferry route is demonstrated by Buijsman and Ridderinkhof (2007), who estimated the water and suspended matter exchange between the Wadden Sea and the North Sea using data collected along the Den Helder–Texel ferry route.

The ferry route between Tallinn and Helsinki across the elongated Gulf of Finland and the schedule consisting of two cruises a day and a short 1.5 h stay in Helsinki made it possible to introduce a procedure for correction of coordinates of measurement points and an additional quality check
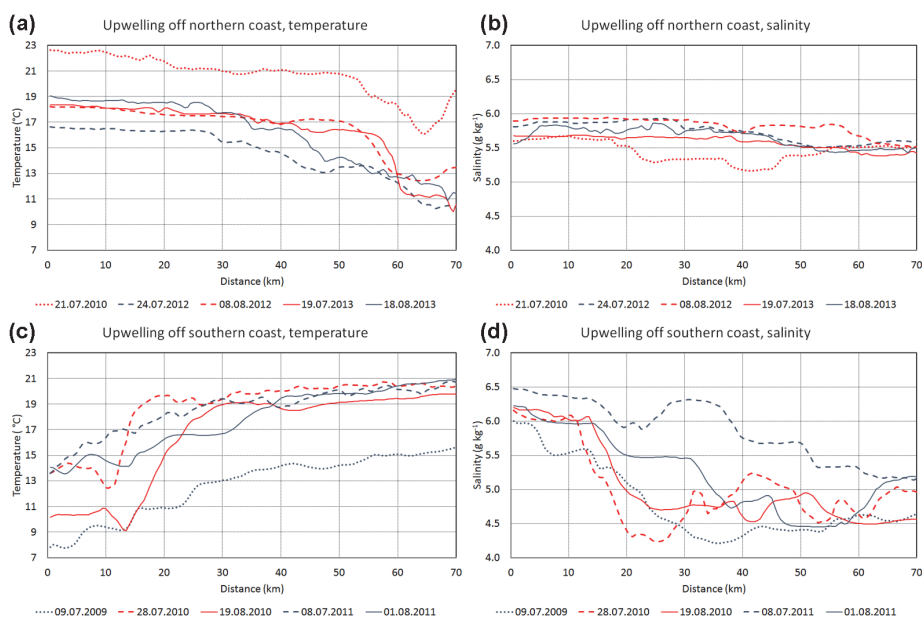
Figure 7. Characteristic distributions of temperature and salinity along the Tallinn–Helsinki ferry route with coastal upwelling events off the northern coast **(a, b)** and off the southern coast **(c, d)**; *x* axis shows the distance from Tallinn Bay (latitude 59.48 N) in km along the meridional transect.

routine for the collected data. The correlation between the data from the two crossings on the same day must be sufficiently high; if not, the data are marked as suspicious. We found that the highest correlation between the two data sets is achieved when the data points are shifted by 3–4 min, depending on the intake installation and the ferry. This analysis also demonstrates the confidence of the applied Ferrybox system even though the water is taken in through a relatively large sea chest. Furthermore, the ferry route across the relatively narrow gulf from coast to coast is very convenient to collect data on the offshore extension and intensity of coastal upwelling events.

Various methods have been applied to reveal characteristic features of coastal upwelling events in the Baltic Sea based on data mainly from remote sensing and numerical models. Data of high-resolution long-term Ferrybox measurements have not been analyzed with this aim until now. A certain temperature isoline as the boundary of the upwelling area was used by Uiboupin and Laanemets (2009) and a temperature deviation (2 °C) from the mean temperature along zonal transects was employed by Lehmann et al. (2012). The latter method is similar to the approach applied in the present study, but we argue that the analysis of temperature deviations along meridional transects is more appropriate in the Gulf of Finland. This conclusion is justified by the fact that, on average, the north–south temperature gradient is negligi-

ble in the gulf (see Fig. 3a), while the west–east temperature gradient could exist between the shallower and narrower Gulf of Finland and the deeper and wider northern Baltic proper due to differential warming and cooling.

Nevertheless, it is interesting that our results on upwelling frequencies of about 17–18 % near the northern and southern coasts are very close to the results of Lehmann et al. (2012) if their results based on remote sensing data were considered. They concluded that upwelling events were present more than 15 % of the time near the northern coast and about 15 % of the time near the southern coast. At the same time, the estimates of corresponding upwelling frequencies based on numerical experiments differ from the values obtained from the remote sensing data and the results of the present study. Based on model results, the northern coastal area has been suggested as the main upwelling area in the Gulf of Finland, with the upwelling occurrence up to 30 % of the time (Lehmann et al., 2012; Myrberg and Andrejev, 2003), while near the southern coast downwelling should prevail (Myrberg and Andrejev, 2003).

Analysis of wind data has also suggested that the coastal upwelling events should occur more often along the northern coast than along the southern coast of the Gulf of Finland (Lehmann et al., 2012; Uiboupin and Laanemets, 2009). The data set consisting of 838 days of measurements from coast to coast used in the present analysis has revealed that, on
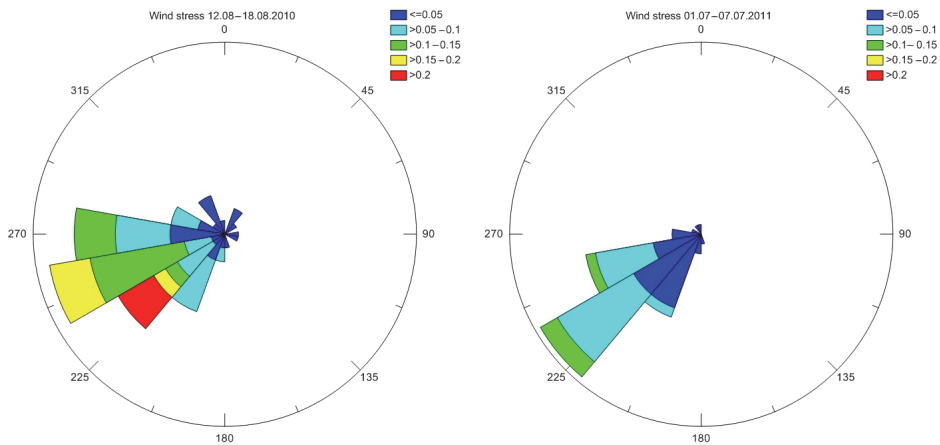
Figure 8. Polar histogram of wind stress vectors ($N\,m^{-2}$) based on the wind data from a weekly period before the peak of upwelling events off the Estonian coast on 17–23 August 2010 (left panel) and 5–11 July 2011 (right panel).

average, the frequency of upwelling events and their intensity are similar near the northern and southern coasts of the gulf, although the wind data from the same period suggest prevalence of upwelling events off the northern coast. Partly, this outcome can be explained by the higher position of the thermocline, steeper bottom slope and greater depths in the southern part of the gulf as suggested by some earlier studies (e.g., Väli et al., 2011; Laanemets et al. 2009). Based on a simple theory of upwelling dynamics linking the position of the onshore return flow with the bottom slope and stratification (Lentz and Chapman, 2004), Laanemets et al. (2009) estimated that the onshore return flow should occur in the near-bottom layer for both northern and southern upwelling events in the Gulf of Finland. Due to the steeper slope and greater depths, the upwelling outcome in the vertical transport of cold and nutrient rich waters could be more intense in the southern gulf (Väli et al., 2011; Laanemets et al., 2009).

An additional explanation could be suggested when taking into account the estuarine character of the Gulf of Finland – the basin has free water exchange with the Baltic proper in the west, while it is closed in the east where the main freshwater source is located. First, this basin configuration and the prevalence of southwesterly winds together with the Coriolis force cause a general cyclonic circulation in the surface layer of the gulf (Alenius et al., 1998). Such circulation, in accordance with the geostrophic balance, results in a higher sea level and deeper thermocline in the northern part of the gulf (e.g., see Andrejev et al., 2004). A similar transverse thermohaline and residual flow structure has been noted by Thomson et al. (2007) in the Juan de Fuca Strait. Liblik and Lips (2016) also concluded that the thermocline is on average at a deeper depth in the northern Gulf of Finland based on their analysis of the data from 35 cross-gulf CTD (conductiv-

ity, temperature and depth) surveys conducted in 2006–2013. Thus, the wind impulse needed for the initiation of a coastal upwelling event near the southern coast can have a smaller magnitude. This suggestion is supported by the comparison of the lowest cumulative wind stress values, which have initiated upwelling events in 2007–2013 near the two coasts. The lowest CWS value related to an upwelling event along the northern coast is larger than the CWS values for five upwelling events along the southern coast (see Fig. 6).

Secondly, we suggest that for a stronger wind impulse during a longer period, the estuarine character of the basin has a significant influence on the outcome. The strong southwesterly (up-estuary) winds counteract the estuarine circulation and cause an inflow (convergence) in the surface layer (Elken et al., 2003; Lips et al., 2008b), and thus, a downward movement of the thermocline in the gulf as a whole. In contrast, the down-estuary winds intensify the outflow (cause divergence) in the surface layer, and thus, a general upward movement of the thermocline in the gulf. Consequently, the up-estuary southwesterly winds, on the one hand, cause upwelling along the northern coast, but on the other hand downwelling in the gulf as a whole that could weaken the outcome. In the case of the down-estuary easterly to northeasterly winds, a general upward movement of the thermocline in the gulf supports the coastal upwelling along the southern coast. Such a response of the water movements to the forcing could be an explanation why, in general, the cumulative upwelling indices (presented in Fig. 6) increase faster with the strengthening of the favorable wind stress (CWS in Fig. 6) for the southern upwelling events than for the northern upwelling events.

The average cross-gulf distributions of temperature and salinity were described based on the 7-year data set of horizontal profiles. On average, the surface layer temperature

did not have any horizontal gradient, while the surface layer salinity was higher in the southern part than in the northern part of the gulf. The result that the surface water with the lowest salinity was on average at about 20 km from the northern coast supports the suggested general circulation scheme in the Gulf of Finland (e.g., Andrejev et al., 2004). At the same time, if the wind forcing favorable for upwelling events near the southern coast prevailed (as was observed in summer 2010), the low salinity water appeared in the southern part of the open gulf, close to the upwelling front. This phenomenon was also observed during an intense upwelling event in August 2006 (Lips et al., 2009); it was modeled by Laanemets et al. (2011) and noted by Liblik and Lips (2016) based on an analysis of CTD data from surveys across the gulf in 2006–2013.

The most intense upwelling events regarding temperature deviations were observed near the southern coast, as was also found by Uiboupin and Laanemets (2009, 2015). However, we did not identify clear differences in the temperature distribution patterns between the upwelling events off the two coasts. Instead, near both coasts, the classical distributions with a sharp temperature front as well as the distribution characterized by a gradual decrease in temperature towards the coast have been observed. We suggest that the upwelling events with the gradual temperature decrease could be associated with the development of upwelling filaments, which occurred under certain conditions and stayed in our measurement window.

In the case of the upwelling events along the southern coast, the wind speed was on average higher before the events with the sharp temperature front (see Fig. 6 and Table 2). For instance, the polar histograms of wind stress vectors shown in Fig. 8 are very similar except for the distribution of wind stress magnitudes. The period before the culmination of the upwelling event with the sharp temperature front observed on 19 August 2010 had a large share of wind stress values $> 0.15\,\mathrm{N\,m^{-2}}$. Nevertheless, the two prominent upwelling events along the northern coast – the most intense event (on 11–31 August 2013) and the event corresponding to the largest cumulative wind stress (on 18–27 July 2012) – were both characterized by the gradual decrease in temperature towards the coast (Fig. 6).

The filaments of upwelled waters are characteristic features of the upwelling events in the Gulf of Finland (Uiboupin and Laanemets, 2009). Zhurbas et al. (2008) have shown based on a numerical experiment that the cold/warm water squirts and filaments could develop after the weakening of the upwelling favorable winds. Similarly, the squirts and filaments could develop if the wind forcing is strong enough to initiate an upwelling event but not as strong as needed to retain the mesoscale frontal dynamics. In the case of the southern upwelling events, it explains why upwelling events with the gradual decrease in temperature mostly occurred when the wind forcing was on average weaker.

As shown by Zhurbas et al. (2006), the baroclinic instability of the upwelling jet is expected to occur when the bottom slope is smaller than the isopycnal slope. Thus, for the strong upwelling events, the filaments might appear with a higher probability in the case of northern upwelling events since the bottom slope is about 2 times shallower in the northern gulf than in the southern gulf (Uiboupin and Laanemets, 2009). The prevailing westerly to southwesterly winds, which cause an inflow in the upper layer and a compensating outflow in the deeper layers (Elken et al., 2003; Liblik and Lips, 2012), could lead to the deepening of the seasonal thermocline in the gulf in 2012 and 2013. The two very intense upwelling events with the gradual temperature decrease were observed in these summers along the northern coast. Since the upwelling dynamics is dependent on the vertical structure of the water column before the event (e.g., Lentz and Chapman, 2004), these suggestions have to be studied further in the future by combining Ferrybox data (restricted to the surface layer and single transect) with the remote sensing and water column data.

5 Conclusions

We showed that Ferrybox data from the Tallinn–Helsinki ferry route could be successfully employed to describe the characteristics of coastal upwelling events in the Gulf of Finland. An advantage of the geographical location of the ferry route across the relatively narrow gulf and the schedule consisting of two crossings a day allowed one to control the quality of the data and introduce the upwelling index based on the data from a single crossing and the cumulative upwelling index. In total, 33 coastal upwelling events were identified in May–September 2007–2013. It is shown that the upwelling occurrences of 18 and 17 % of days, as well as intensities of upwelling events, are similar near the northern and southern coasts. The most intense events occur in July–August, most probably because of the warmest surface layer (strongest thermocline) during those months. It is shown that the wind impulse needed to generate upwelling events of similar intensity differs between the two coastal areas. We suggest that the general thermohaline structure (adapted to the prevailing forcing) and the estuarine character of the basin are reasons for the found different outcome. The thermohaline structure of the Gulf of Finland is characterized by a deeper position of the thermocline in the northern gulf; thus, the upwelling initiation requires a stronger southwesterly wind impulse to cause upwelling along the northern coast as compared to a weaker northeasterly impulse to cause upwelling along the southern coast. Furthermore, the estuarine character of the basin leads to the weakening of the upwelling created by the westerly (up-estuary) winds and strengthening of the upwelling created by the easterly (down-estuary) winds. Two types of upwelling events were identified – one characterized by a strong temperature (upwelling) front and the other revealing grad-

ual decrease in temperature from the open sea to the coastal area, with maximum temperature deviation very close to the shore. We suggest that the spatial variations in temperature with scales of a few kilometers, which were characteristic of the upwelling events with the gradual temperature decrease, could be signs of the meso- and sub-mesoscale features (filaments and squirts) associated with the upwelling dynamics.

6 Data availability

Underlying data (as raw data which have passed automatic quality check) are available via EMODnet Physics portal   http://www.emodnet-physics.eu/Map/platinfo/PIROOSDownload.aspx?PlatformID=8440.

References

Alenius, P., Myrberg, K., and Nekrasov, A.: The physical oceanography of the Gulf of Finland: a review, Boreal Environ. Res., 3, 97–125 1998.

Andrejev, O., Myrberg, K., Alenius, P., and Lundberg, P. A.: Mean circulation and water exchange in the Gulf of Finland – a study based on three-dimensional modeling, Boreal Environ. Res., 9, 1–16, 2004.

Buijsman, M. C. and Ridderinkhof, H.: Long-term ferry-ADCP observations of tidal currents in the Marsdiep inlet, J. Sea Res., 57, 237–256, 2007.

Elken, J., Raudsepp, U., and Lips, U.: On the estuarine transport reversal in deep layers of the Gulf of Finland, J. Sea Res. 49, 267–274, 2003.

Feistel, R., Weinreben, S., Wolf, H., Seitz, S., Spitzer, P., Adel, B., Nausch, G., Schneider, B., and Wright, D. G.: Density and Absolute Salinity of the Baltic Sea 2006–2009, Ocean Sci., 6, 3–24, doi:10.5194/os-6-3-2010, 2010.

Haapala, J.: Upwelling and its influence on nutrient concentration in the coastal area of the Hanko Peninsula, entrance of the Gulf of Finland, Est. Coast. Shelf Sci., 38, 507–521, 1994.

Hardman-Mountford, N. J., Moore, G., Bakker, D. C. E., Watson, A. J., Schuster, U., Barciela, R., Hines, A., Moncoiffé, G., Brown, J., Dye, S., Blackford, J., Somerfield, P. J., Holt, J., Hydes, D. J., and Aiken, J.: An operational monitoring system to provide indicators of CO_2-related variables in the ocean, ICES J. Mar. Sci., 65, 1498–1503 2008.

Keevallik, S. and Soomere, T.: Towards quantifying variations in wind parameters across the Gulf of Finland, Est. J. Earth Sci., 59, 288–297, 2010.

Kononen, K., Kuparinen, J., Mäkela, K., Laanemets, J., Pavelson, J., and Nõmmann, S.: Initiation of cyanobacterial blooms in a frontal region at the entrance to the Gulf of Finland, Baltic Sea, Limnol. Oceanogr., 41, 98–112, 1996.

Laanemets, J., Zhurbas, V., Elken, J., and Vahtera, E.: Dependence of upwelling-mediated nutrient transport on wind forcing, bottom topography and stratification in the Gulf of Finland: model experiments, Boreal Environ. Res., 14, 213–225, 2009.

Laanemets, J., Väli, G., Zhurbas, V., Elken, J., Lips, I., and Lips, U.: Simulation of mesoscale structures and nutrient transport during summer upwelling events in the Gulf of Finland in 2006, Boreal Environ. Res., 16, 15–26, 2011.

Large, W. G. and Pond, S.: Open ocean momentum flux measurements in moderate to strong winds, J. Phys. Oceanogr., 11, 324–336, 1981.

Lehmann, A., Myrberg, K., and Höflich, K.: A statistical approach to coastal upwelling based on the analysis of satellite data for 1990–2009, Oceanologia, 54, 369–393, 2012.

Lentz, S. J. and Chapman, D. C.: The importance of nonlinear cross-shelf momentum flux during wind-driven coastal upwelling, J. Phys. Oceanogr., 34, 2444–2457, 2004.

Liblik, T. and Lips, U.: Characteristics and variability of the vertical thermohaline structure in the Gulf of Finland in summer, Boreal Environ. Res., 16, 73–83, 2011.

Liblik, T. and Lips, U.: Variability of synoptic-scale quasi-stationary thermohaline stratification patterns in the Gulf of Finland in summer 2009, Ocean Sci., 8, 603–614, doi:10.5194/os-8-603-2012, 2012.

Liblik, T. and Lips, U.: Variability of pycnoclines in a three-layer, large estuary: the Gulf of Finland, Boreal Environ. Res., in press, 2016.

Lips, I. and Lips, U.: Abiotic factors influencing cyanobacterial bloom development in the Gulf of Finland (Baltic Sea), Hydrobiologia, 614, 133–140, 2008.

Lips, U., Lips, I., Kikas, V., and Kuvaldina, N.: Ferrybox measurements: a tool to study meso-scale processes in the Gulf of Finland (Baltic Sea), US/EU-Baltic Symposium, Tallinn, 27–29 May 2008, IEEE Conference Proceedings, 1–6, 2008a.

Lips, U., Lips, I., Liblik, T., and Elken, J.: Estuarine transport versus vertical movement and mixing of water masses in the Gulf of Finland (Baltic Sea), US/EU-Baltic Symposium, Tallinn, 27–29 May 2008, IEEE Conference Proceedings, 1–8, 2008b.

Lips, I., Lips, U., and Liblik, T.: Consequences of coastal upwelling events on physical and chemical patterns in the central Gulf of Finland (Baltic Sea), Cont. Shelf Res. 29, 1836–1847 2009.

Männik, A. and Merilain, M.: Verification of different precipitation forecasts during extended winter-season in Estonia, HIRLAM Newsletter, 52, 65–70, 2007.

Myrberg, K., Lehmann, A., Raudsepp, U., Szymelfenig, M., Lips, I., Lips, U., Matciak, M., Kowalewski, M., Krezel, A., Burska, D., Szymanek, L., Ameryk, A., Bielecka, L., Bradtke, K., Galkowska, A., Gromisz, S., Jedrasik, J., Kaluzny, M., Kozlowski, L., Krajewska-Soltys, A., Oldakowski, B., Ostrowski, M., Zalewski, M., Andrejev, O., Suomi, I., Zhurbas, V., Kauppinen, O.-K., Soosaar, E., Laanemets, J., Uiboupin, R., Talpsepp, L., Golenko, M., Golenko, N., and Vahtera, E.: Upwelling events,

coastal offshore exchange, links to biogeochemical processes – Highlights from the Baltic Sea Science Congress at Rostock University, Germany, 19–22 March 2007, Oceanologia, 50, 95–113, 2008.

Myrberg, K. and Andrejev, O.: Main upwelling regions in the Baltic Sea – a statistical analysis based on three-dimensional modeling, Boreal Environ. Res., 8, 97–112, 2003.

Paerl, H. W., Rossignol, K. L., Guajardo, R., Hall, N. S., Joyner, A., Peierls, B. L., and Ramus, J. S.: FerryMon: Ferry-Based Monitoring and Assessment of Human and Climatically Driven Environmental Change in the Albemarle-Pamlico Sound System, Environ. Sci. Technol., 43, 7609–7613, 2009.

Pavelson, J., Laanemets, J., Kononen, K., and Nõmman, S.: Quasi-permanent density front at the entrance to the Gulf of Finland: Response to wind forcing, Cont. Shelf Res., 17, 253–265, 1997.

Petersen, W.: FerryBox systems: State-of-the-art in Europe and future development, J. Marine Syst., 140, 4–12, 2014.

Petersen W., Wehde, H., Krasemann, H., Colijn, F., and Schroeder, F.: FerryBox and MERIS – Assessment of coastal and shelf sea ecosystems by combining in situ and remotely sensed data, Est. Coast. Shelf Sci., 77, 296–307, 2008.

Rantajärvi, E. (Ed.): Alg@line in 2003: 10 years of innovative plankton monitoring and research and operational information service in the Baltic Sea, MERI – Report Series of the Finnish Institute of Marine Research, No. 48, 1–36, 2003.

Schlitzer, R.: Ocean Data View, https://odv.awi.de/, 2015.

Schneider, B., Gülzow, W., Sadkowiak, B., and Rehder, G.: Detecting sinks and sources of CO_2 and CH_4 by ferrybox-based measurements in the Baltic Sea: Three case studies, J. Marine Syst., 140, 13–25, 2014.

Seppälä, J., Ylöstalo, P., Kaitala, S., Hällfors, S., Raateoja, P., and Maunula, P.: Ship-of-opportunity based phycocyanin fluorescence monitoring of the filamentous cyanobacteria bloom dynamics in the Baltic Sea, Est. Coast. Shelf Sci., 73, 489–500, 2007.

Suursaar, Ü. and Aps, R.: Spatio-temporal variations in hydrophysical and -chemical parameters during a major upwelling event off the southern coast of the Gulf of Finland in summer 2006, Oceanologia, 49, 209–228, 2007.

Talpsepp, L., Nõges, T., Raid, T., and Kõuts, T.: Hydrophysical and hydrobiological processes in the Gulf of Finland in summer 1987 – characterization and relationship, Cont. Shelf Res., 14, 749–763, 1994.

Thomson, R. E., Mihaly, S. F., and Kulikov E. A.: Estuarine versus transient flow regimes in Juan de Fuca Strait, J. Geophys. Res., 112, C09022, doi:10.1029/2006JC003925, 2007.

Uiboupin, R. and Laanemets, J.: Upwelling characteristics derived from satellite sea surface temperature data in the Gulf of Finland, Baltic Sea, Boreal Environ. Res., 14, 297–304, 2009.

Uiboupin, R. and Laanemets, J.: Upwelling parameters from bias-corrected composite satellite SST maps in the Gulf of Finland (Baltic Sea), IEEE Geosci. Remote Sens. Lett., 12, 592–596, 2015.

Vahtera, E., Laanemets, J., Pavelson, J., Huttunen, M., and Kononen, K.: Effect of upwelling on the pelagic environment and bloom-forming cyanobacteria in the Western Gulf of Finland, Baltic Sea, J. Marine Syst., 58, 67–82, 2005.

Väli, G.: Numerical experiments on matter transport in the Baltic Sea. PhD thesis, Tallinn Technical University Press, 2011.

Väli, G., Zhurbas, V., Laanemets, J., and Elken, J.: Simulation of nutrient transport from different depths during an upwelling event in the Gulf of Finland, Oceanologia, 53, 431–448, 2011.

Zhurbas, V., Laanemets, J., and Vahtera, E.: Modeling of the mesoscale structure of coupled upwelling/downwelling events and the related inputs of nutrients to the upper mixed layer in the Gulf of Finland, Baltic Sea, J. Geophys. Res., 113, C05004, doi:10.1029/2007JC004280, 2008.

Zhurbas, V. M., Oh, I. S., and Park, T.: Formation and decay of a longshore baroclinic jet associated with transient coastal upwelling and downwelling: a numerical study with application to the Baltic Sea, J. Geophys. Res., 111, C04014, doi:10.1029/2005JC003079, 2006.

Paper II

Kikas, V., Norit, N., Meerits, A., Kuvaldina, N., Lips, I., Lips, U. (2010). High-resolution monitoring of environmental state variables in the surface layer of the Gulf of Finland (during a dynamic spring bloom in March–May 2010). *IEEE Conference Publications: Baltic International Symposium (BALTIC), 2010 IEEE/OES US/EU, Riga, 24–27 August 2010*, 1–9, doi: 10–1109/BALTIC.2010.5621627.
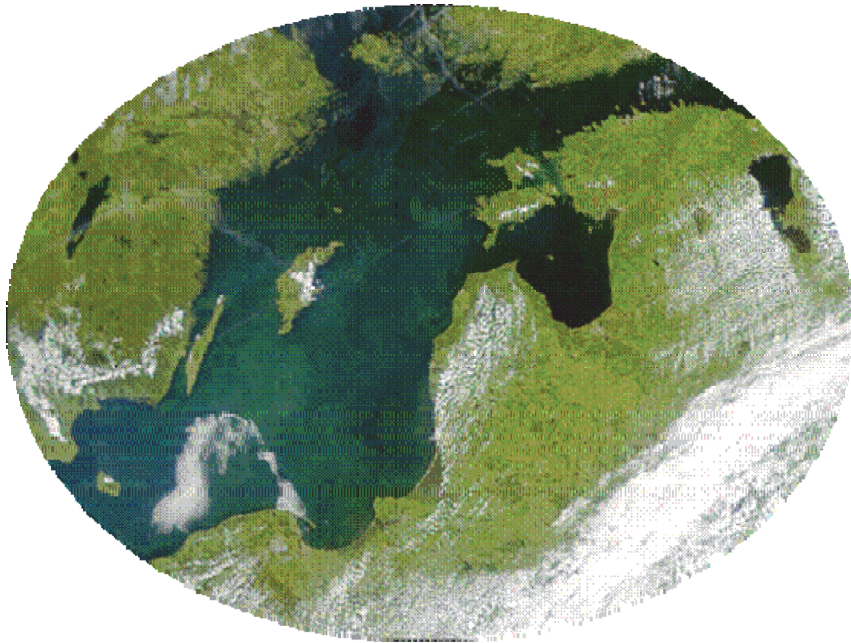
2010 IEEE/OES US/EU Baltic International Symposium (BALTIC)

August 25, 26, 27 2010 - Riga, Latvia

High-resolution monitoring of environmental state variables in the surface layer of the Gulf of Finland (during a dynamic spring bloom in March-May 2010)

Villu Kikas, Nelli Norit, Aet Meerits, Natalja Kuvaldina, Inga Lips, Urmas Lips

Marine Systems Institute, Tallinn University of Technology (Akadeemia Rd 21, 12618 Tallinn, Estonia, e-mail: villu.kikas@phys.sea.ee)

ABSTRACT

The flow-through system (Ferrybox) installed onboard a ferry cruising between Tallinn and Helsinki in the Gulf of Finland (Baltic Sea) measures temperature, salinity, chlorophyll a fluorescence, turbidity and since January 2010 also pCO_2. In March-May 2010, the water sampling was conducted on a weekly basis at 17 locations along the ferry route to measure nutrient concentrations (NO_2+NO_3 and PO_4), chlorophyll a content and phytoplankton species composition and biomass. Our aim was to show that the Ferrybox technology can be successfully applied to follow the rapid changes of state variables during a very dynamic season of the year – phytoplankton spring bloom. High variability of environmental parameters has been observed both in space and time in the Gulf of Finland in spring 2010. It is suggested that both the general circulation in the surface layer and mesoscale hydrodynamic processes are influencing the bloom evolution and spatio-temporal variability. The observed coincidence of Chl a peaks with the periods of relatively fast temperature increase indirectly shows the importance of positive buoyancy fluxes (vertical stratification) for phytoplankton growth in spring. Spatio-temporal distribution of pCO_2 was in a good accordance with the Chl a dynamics confirming that the pCO_2 measurements can be used for the estimates of phytoplankton productivity. Our data confirm that the regular late evening fluorescence measurements can be successfully applied to determine the Chl a content in the surface waters in spring. It is concluded that autonomous high-resolution *in-situ* monitoring in combination with adaptive water sampling and remote sensing could give a full enough data set to assess the environmental state of the Gulf of Finland during this highly dynamic season of the year.

I. INTRODUCTION

Unattended monitoring of marine environment using ships of opportunity, where autonomous measurement systems (so called "Ferryboxes") are installed, has been implemented in many regions of the World Ocean (e.g. [1]). First trials of using ships of opportunity for the environmental monitoring in the Baltic Sea were made by Estonian and Finnish scientists in the Gulf of Finland between Tallinn and Helsinki in 1990-1991 [2]. Regular measurements of temperature, salinity and chlorophyll a fluorescence along this route were started in 1997 while the longest data series in the Baltic (since 1993) is available along the ferry route Helsinki-Travemünde.

The Gulf of Finland is an elongated basin in the northeastern part of the Baltic Sea (Fig. 1) with a length of about 400 km and a maximum width of 135 km [3]. The long-term residual circulation in the surface layer of the Gulf is characterized by an inflow of the saltier water of the northern Baltic Proper along the southern coast and the seaward flow of gulf water along the northern coast. The circulation is more complex at time scales from days to weeks mainly due to the variable wind forcing. A variety of mesoscale processes/features (fronts, eddies, upwelling/downwelling), which significantly affect the biological production, retention and transport, have been observed in the Gulf of Finland (e.g. [4,5,6]).
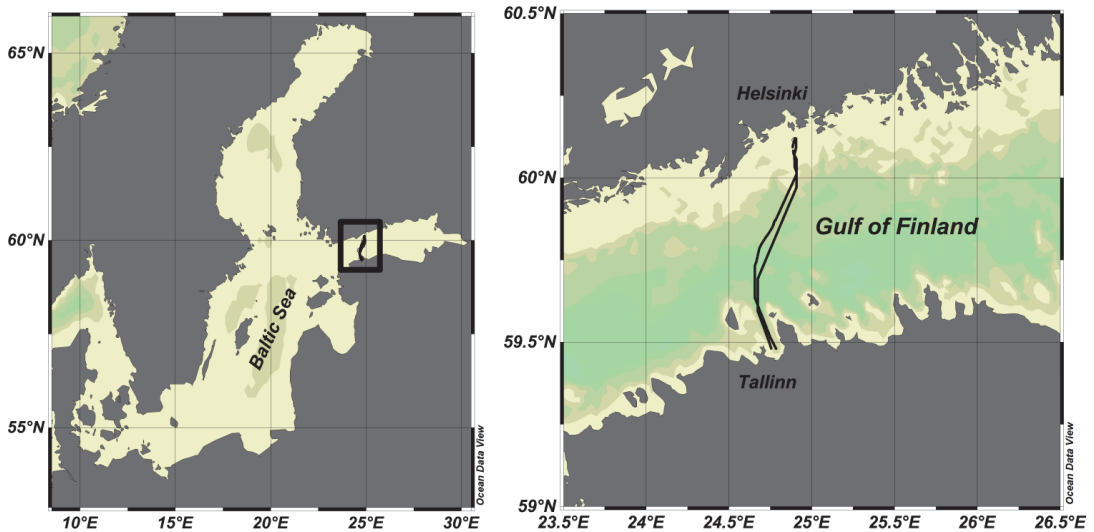
Figure 1. Map of the Baltic Sea and the ferry route between Tallinn and Helsinki in the Gulf of Finland (maps were prepared using ODV software [7]).

A seasonal thermocline forms in the Gulf in spring-summer at the depths of 10-20 m. While high concentrations of dissolved inorganic nitrogen (DIN) and phosphorus (DIP) are observed in winter, the DIN and DIP concentrations decline fast in April-May and are usually below the detection limit in summer in the upper mixed layer. The seasonal dynamics of phytoplankton is characterized by the spring bloom in April-May dominated by dinoflagellates/diatoms and the late summer bloom in July-August dominated by cyanobacteria [8].

Ferrybox technology is successfully applied in the Baltic Sea to monitor the late summer cyanobacteria blooms and the environmental factors influencing the bloom intensities [9,10,11]. Less attention is paid to the studies of the dynamics of spring bloom using unattended measurements, although a spring bloom intensity index is developed and applied [12]. It was shown in the latter study that the spring bloom has been very variable in the Gulf of Finland in 1997-2004. The winter nutrient levels were suggested as the main factor influencing the bloom intensity. It is well known that also other factors, such as vertical stratification, could influence the onset and intensity of the vernal bloom [13,14]. In addition, it has been shown on the basis of data of an intensive measurement campaign in the open Baltic Sea that the spatio-temporal variability of spring bloom could heavily be influenced by mesoscale hydrodynamic features [15].

The main aim of the present paper is to demonstrate that the Ferrybox measurements provide a suitable monitoring method to follow the rapid changes of state variables during a very dynamic season of the year – phytoplankton spring bloom. We describe the spring bloom dynamics in the Gulf of Finland in 2010 and analyze the advantages and limits of the applied monitoring method.

II.   MATERIAL AND METHODS

Ferrybox system (4H-Jena, Germany) installed on a ferry (since 2008 "Baltic Princess", AS Tallink Grupp) making daily trips between Tallinn and Helsinki (see route in Fig. 1) measures temperature (T), salinity (S), chlorophyll a (Chl a) fluorescence and turbidity. In January 2010 a pCO_2 sensor was added into the system. Water taken in from the surface layer (water intake is located at about 4 m depth) is pumped through the system with a flow rate of 6-7 l s^{-1}. Data are recorded while the ferry is on route with a time step of 20 seconds that corresponds to a horizontal resolution of approximately 150 m. In March-May 2010 water sampling was conducted on a weekly basis at 17 locations along the ferry route from Helsinki to Tallinn. The water samples with a volume of 1 l were kept in dark, at temperature of 4 °C for about 10 hours after the sampling and transported to the on-shore laboratory where divided into three sub-samples to measure nutrient concentrations ($NO_2 + NO_3$ and PO_4), Chl a content and phytoplankton species composition and biomass.

Nutrient analyses were performed using Lachat Instruments QuikChem® 8500 Series 2 Flow Injection Analysis System. NO_3+NO_2 detection limit was 0.014 µmol l^{-1} (µM) and $PO_4 < 0.01$ µM. Chl a content in the water samples was measured using a spectrophotometer Thermo Helios γ. The concentration of Chl a was determined by filtering the water samples through Millipore APFF glassfibre filters, extracting the pigments 24 hours at room temperature with ethanol (96%) and measuring the absorption at the wavelength of 665 nm. Phytoplankton samples were preserved with acid Lugol solution and stored for further analyses (data not shown here).

Altogether data of 112 crossings from 23 March to 29 May were analyzed in the present paper. In total 139 water samples were taken for nutrient analyses from 25 March until 17 May and 177 water samples for Chl a analyses from 25 March until 31 May. Satellite images (only a few were available without cloud cover) allowed to see the horizontal distribution of the sea surface temperature and Chl a in a wider area adjacent to the ferry route.

III.   RESULTS

The Gulf of Finland was partly ice-covered and the presence of ice created some difficulties for flow-through measurements in February-March 2010. Ice started to disappear in late March when the surface layer water temperature was close to or still below 0 °C (Fig. 2, left panel). In early April the water temperature rose faster near the southern coast than in the central part and near the northern coast. The temperature of maximum density (2.5 °C) was reached almost along the whole transect on 12-13 April. Fast warming up of the surface layer (or transport of a warmer water mass into the study area) was observed in the northern part of the Gulf in the second half of May.

The surface layer salinity varied in a range of 5.6-6.2 in the southern and central parts of the Gulf and was remarkably lower off northern coast in late March and April (Fig. 2, right panel). The lowest salinity was observed off Helsinki in mid April. In the beginning of May saltier surface waters occupied almost the entire study transect and a more saline water mass appeared in the southernmost part of the transect in the second week of May (accompanied with a slight temperature decrease). In mid May salinity decreased to the previous values at the northernmost end of the transect while a low salinity water mass appeared also in the central Gulf of Finland.

In order to convert Chl a fluorescence readings to Chl a values a linear regression between fluorescence and Chl a content detected spectrophotometrically was found. Our results obtained in March-May 2010 revealed a good consistency of fluorescence and Chl a data (Fig. 3, left panel) indicating that a single regression line ($Chl = 0.82 \cdot Fluor + 1.41$, where Chl is Chl a value in mg m^{-3} and $Fluor$ is measured Chl a fluorescence in arbitrary units) can be used during the spring bloom period ($r^2 = 0.97$, $p < 0.0001$). It is known that Chl a fluorescence measurements are biased due to the quenching effect in case of daytime high irradiances (e.g. [16]). In order to exclude the quenching effect, only fluorescence data collected when ferry was travelling from Helsinki to Tallinn (measurements after 6:30 p.m.) were taken into account in the analysis. Examples of differences in fluorescence signal between two consecutive crossings in a day are shown and discussed later (Section IV. Discussion and Conclusions).
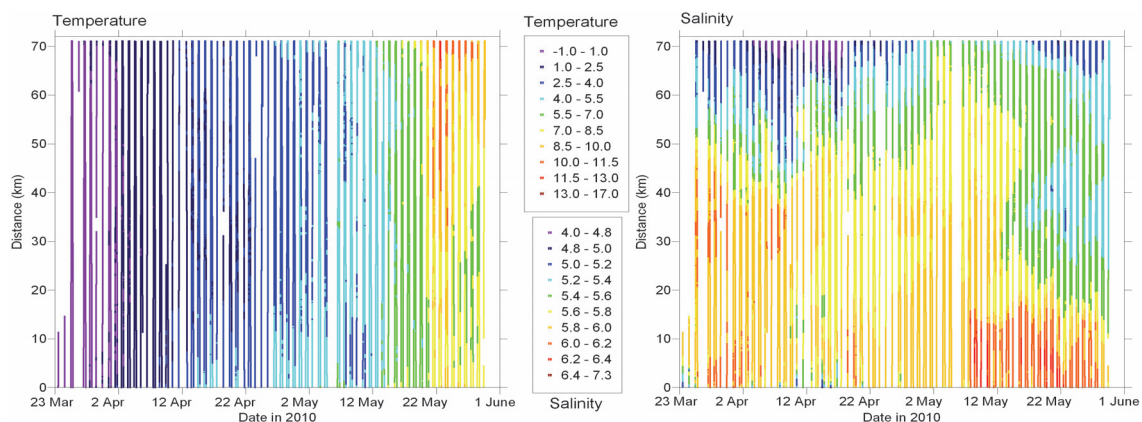
Figure 2. Temporal variations of temperature (°C) and salinity distributions along the ferry route between Tallinn and Helsinki in the Gulf of Finland in March-May 2010. Distance in km from the starting point of the transect in the Tallinn Bay (at Latitude 59.48 N) is shown on y-axis.
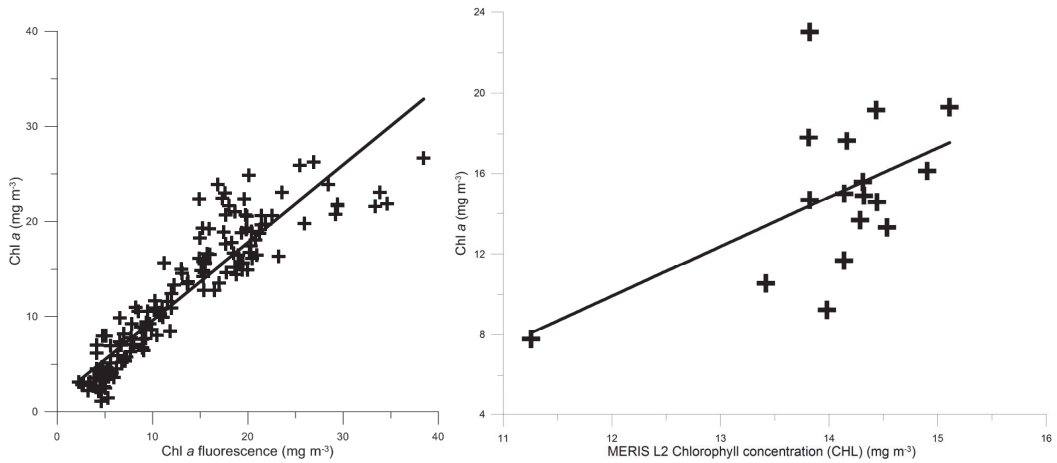
Figure 3. Scatter plot of Chl a fluorescence and Chl a detected from the water samples collected along the ferry route Tallinn-Helsinki in March–May 2010 (left panel) and scatter plot of MERIS L2 Chl a concentration and Chl a detected from the water samples on 12 April 2010. Best linear fits are shown as solid lines.

The spring bloom dynamics is described using spatio-temporal variations of Chl a and pCO_2 (Fig. 4) and temporal changes of average Chl a content along the entire transect (as recorded by the autonomous system and measured from the water samples at the laboratory; Fig. 5). The bloom started in the first decade of April with a very fast growth after 10 April and the maximum was reached on 16 April. After several days of somewhat lower Chl a content, the second maximum was observed on 26 April. Sampling with a weekly interval did not reveal these changes within the bloom peak period – similar Chl a values were measured on 19 and 27 April and 3 May (see Fig. 5).
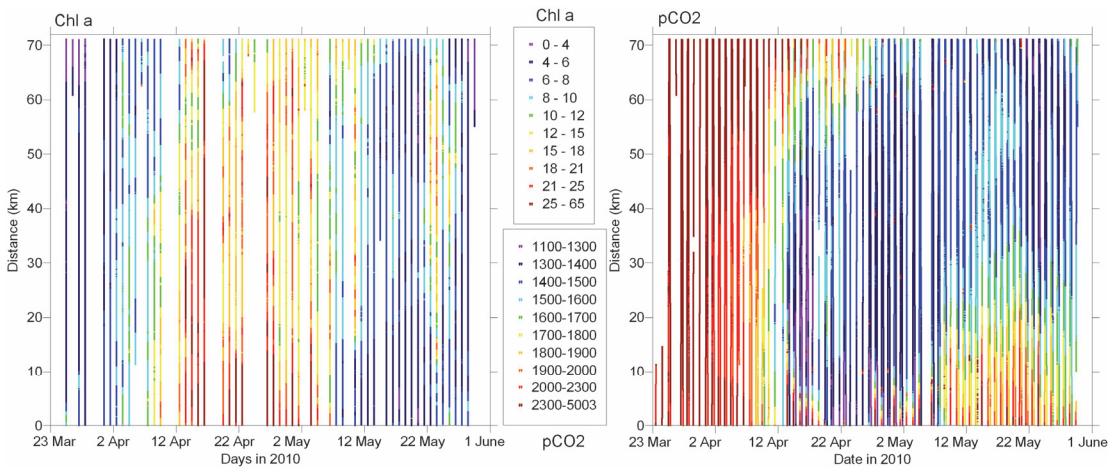
Figure 4. Temporal variations of Chl a content (mg m^{-3}) and pCO$_2$ (arbitrary units) distributions along the ferry route between Tallinn and Helsinki in the Gulf of Finland in March–May 2010. Distance in km from the starting point of the transect in the Tallinn Bay (at Latitude 59.48 N) is shown on y-axis.
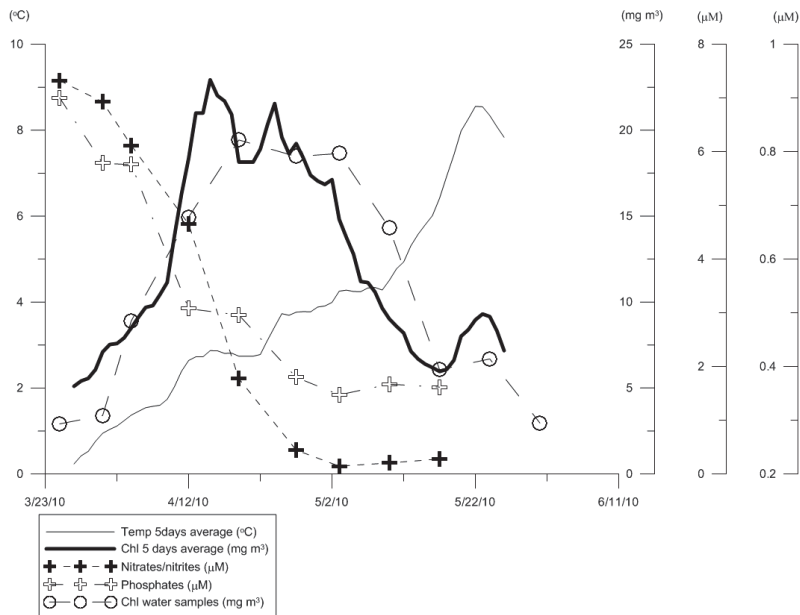
Figure 5. Temporal variations of environmental parameters in the Gulf of Finland in March-May 2010 presented as along transect daily averages for water sample analyses and as 5-day running mean values of along transect daily averages for flow-through data: Ferrybox water temperature (left y-axis), Ferrybox Chl a content and Chl a content from water samples (first y-axis on right side), NO_3+NO_2 concentration (second y-axis on right side) and PO_4 concentration (third y-axis on right side).

The bloom started about 4-5 days earlier in the southern half of the study transect and generally higher Chl *a* values were recorded there during the bloom peak period (Fig. 4, left panel). Fast decay of the bloom was observed after 3 May in the southern part of the study transect while the bloom lasted about 5-7 days longer in the central and northern part. For instance, Chl *a* content of 4.4-7.6 mg m^{-3} was measured in the water samples collected at the four southernmost sampling points and up to 20 mg m^{-3} at some points in the central and northern Gulf. In addition, an increase of Chl *a* content in this area (central and northern part) was observed on 20-25 May. This increase was captured also by the water sampling on 24 May.

A comparison of the bloom development with the changes in water temperature (Fig. 5) showed that the observed growth and Chl *a* peaks were all accompanied with more pronounced temperature increase than an average during the spring period. Nutrient concentrations started to decrease from the winter levels together with the phytoplankton growth. The decay of the bloom occurred when nitrates/nitrites were almost consumed from the surface layer (concentrations < 0.16 µM were measured at all sampling points) although the phosphates were still available at relatively high concentrations of (on average 0.35 µM) in the surface layer. Nevertheless, it has to be noted that the low nitrates/nitrites level was measured already on 3 May but still relatively high Chl *a* content was observed a week later on 10 May in the central and northern parts of the study transect. The weekly sampling did not reveal an increase of nitrates/nitrites concentration before the temporal Chl *a* content maximum in late May.

Spatio-temporal variations in pCO$_2$ content (the results are presented in arbitrary units, only factory calibration of the sensor was made) were in a good accordance with the described changes in Chl *a* concentration – low pCO$_2$ values (or decrease of pCO$_2$) corresponded to high Chl *a* content indicating high primary production in those regions/periods. However, some discrepancies could be recognized in April in the very coastal areas, where also higher turbidity was measured (data not shown here). At the same time, the higher pCO$_2$ values observed in the more saline water mass occupying a 20 km wide coastal area off southern coast in mid May were associated with low turbidity.
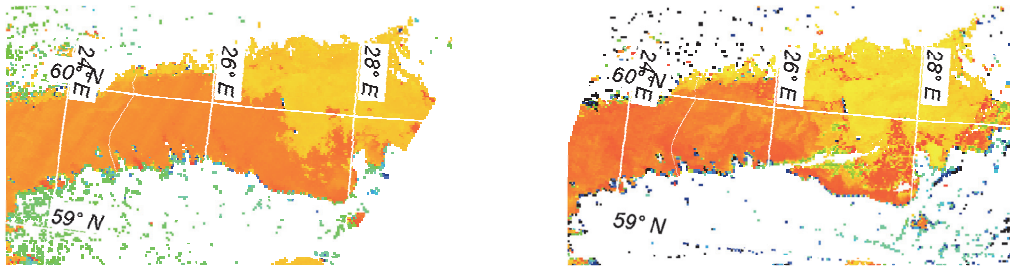
Figure 6. MERIS Level 2 processed images on 12 April 2010 (left panel) and on 14 April 2010 (right panel), ferry route Tallinn-Helsinki is shown as white line.

We tried to describe the spatial differences in bloom development using satellite images. Two images, presented here as reduced resolution MERIS L2 products, were available from the bloom development period on 12 and 14 April (Fig. 6). It has to be noted that there was still floating ice in the north-eastern Gulf of Finland and the images are biased for that region. The following characteristic features could be brought up in the region along and adjacent to our study transect: 1) the Chl *a* levels were higher on 14 April than those on 12 April pointing to the phytoplankton growth (bloom development); 2) the Chl *a* levels were higher in the central and southern parts than those close to the northern shore; 3) clearer spatial variability in mesoscale was detected on 14 April.

To compare quantitatively the remote sensing and Ferrybox data we extracted MERIS L2 product data along the ferry route. Both data sets were calibrated against Chl *a* content measured from the water samples. To convert MERIS data, the equation $Chl = 2.45 \cdot CHL - 19.46$ (where *Chl* is Chl *a* value detected from water samples in mg m^{-3} and *CHL* is MERIS L2 Chl *a* in mg m^{-3}), which corresponds to the regression line shown in Fig. 3 (right panel; $r^2 = 0.28$, $p < 0.03$), was used.
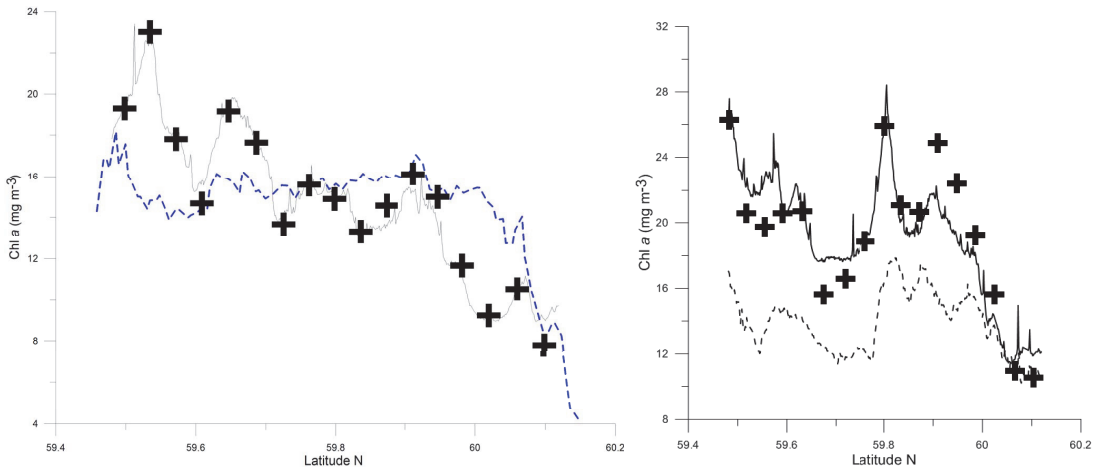
Figure 7. Comparison between Chl a data – MERIS L2 product (dashed blue line), Ferrybox data (grey solid line) and water samples analysis results (crosses) obtained along the ferry route on 12 April 2010 (left panel). Comparison between Ferrybox Chl a data acquired on 19 April 2010 when ferry was travelling from Tallinn to Helsinki (dashed line) and from Helsinki to Tallinn (solid line) and water samples analysis results (crosses) collected from Helsinki to Tallinn.

The results showed that the remote sensing data qualitatively agree with the Ferrybox and water sample analysis data – a tendency of decrease of Chl *a* close to the northern coast and a similar (compared with the Ferrybox data) sequence of areas of relatively high and low Chl *a* in the southern part of the study transect were observed (Fig. 7, left panel). A characteristic spatial scale of these areas of contrasting Chl *a* content was about 10 km. Quantitative comparison revealed that the correlation between MERIS data and water samples analysis results was low (although significant). One reason for the latter could be the time lag between the

satellite image and ground measurements – more than 10 hours, which might lead to some shifts of borders between the water masses with high and low Chl *a* content. However, the satellite images showed clearly that the bloom was developing earlier in the southern and western Gulf and the spatial distribution of phytoplankton was influenced by mesoscale processes – water masses containing phytoplankton at different stages of bloom development were redistributed by water movements in mesoscale. Similar mesoscale variability but with opposite general Chl *a* gradient (increase from south-west to north-east) was observed in late May after the spring bloom decay in our study area.

IV. DISCUSSION AND CONCLUSIONS

The analysis of spatio-temporal variability of environmental parameters in the Gulf of Finland in spring 2010 enabled us to point out some relationships between the spring bloom development and influencing abiotic factors. In general the start of the spring bloom was depending on the presence of the ice and, since it disappeared later in the northern part of the Gulf, a later development of the bloom was observed there. On the other hand, since this situation with a later bloom development in the northern part was retained during the entire bloom period (most probably due to the prevailing circulation in the surface layer of the Gulf), the decay of bloom was observed also later in the northern part. This general pattern was superimposed by the spatial variability of Chl *a* distribution with a characteristic scale of 10 km, which was revealed both by Ferrybox measurements and satellite images, supporting the earlier results of the importance of mesoscale hydrodynamic processes [15].

It was obvious that the bloom started when the water temperature was still below the temperature of maximum density but the first peak was reached 3-4 days after the surface layer became warmer than 2.5 °C. Moreover the growth and following bloom peaks were observed in periods of relatively fast increase of surface layer temperature. We suggest that it could indicate the importance of the vertical stratification for the bloom development since warming of the surface layer is associated with the positive buoyancy flux and the development of vertical stratification. However to confirm this, vertical profiles of temperature, salinity and Chl *a* must be acquired at least with the same temporal resolution than Ferrybox measurements.

A temporal increase of Chl *a* content was detected in the northern half of the Gulf in late May. A simultaneous increase of surface layer temperature up to 8-10 °C and decrease of salinity suggests that a water mass from the adjacent region, where the bloom was not completely decayed yet, was transported into the study area. On the other hand, the pCO_2 data suggest that phytoplankton productivity was still high in this water mass. Thus, the total productivity in a sea area is determined not only by the nutrient pool available prior to the vernal bloom but also by the redistribution of productive phytoplankton biomass by the general circulation and mesoscale processes. Very fast decrease of Chl *a* content and an increase in salinity and pCO_2 (and a slight drop of temperature) off the southern coast in the first decade of May clearly indicate that these changes were caused by an upwelling event occurred there. The described examples show that the pCO_2 measurements give very valuable information that can be used for productivity estimates (as shown e.g. in [17]) and as supporting parameter also for studying vertical transport of water and substances.

Several studies have shown how the Ferrybox technology is successfully used for different applications (e.g. [18,19]). The main advantages of this method are the low cost and high resolution of measurements whereas a variety of sensors can be used in the system. We showed that the autonomously collected data and water sampling ensuring *in-situ* calibration of sensors and measurement of additional environmental parameters (e.g. nutrient concentrations) can be applied to describe in detail the dynamics of spring bloom. The main limitation of this technology is also known – the water is analyzed only from one depth (about 4 m in our case) and only along route spatial distribution of parameters is recorded. The former problem can be solved by deploying an autonomous profiler in the area and the latter problem by making use of satellite images if those are available.

It has been argued that the Chl *a* fluorescence measurements alone are not applicable to monitor the Chl *a* content in a sea are in summer [20]. We demonstrated that in spring the correlation between the Chl *a* fluorescence and Chl *a* detected spectrophotometrically from the water samples is almost perfect. The main problem is related to the fluorescence quenching in daytime high irradiances. To characterize the extent of the problem a comparison between two successive Chl *a* fluorescence profiles (and water sample analyses) is presented in Fig. 7 (right panel). As it is seen, the difference between two profiles in the southern half of the transect, where the time lag between measurements was substantial (the measurements were carried out 1:30-5:00 p.m. and 6:30-10:00 p.m. resulting in a time lag up to 8.5 hours), was about 30 %. This result is similar to the findings in [16]. However, due to the unchangeable ferry schedule the fluorescence measurements from Helsinki to Tallinn performed late evening can be successfully applied to follow the spring bloom in the area under consideration.

In conclusion, high variability of environmental parameters has been observed both in space and time in the Gulf of Finland in spring 2010. Both the general circulation in the surface layer and mesoscale hydrodynamic processes has been employed to explain the observed bloom evolution and spatio-temporal variability. The observed coincidence of Chl *a* peaks with the periods

of relatively fast temperature increase indirectly shows the importance of positive buoyancy fluxes (vertical stratification) for phytoplankton growth in spring. Spatio-temporal distribution of pCO_2 was in a good accordance with the Chl a dynamics confirming that the pCO_2 measurements can be used for the estimates of phytoplankton productivity. Our data confirm that the regular late evening fluorescence measurements can be successfully applied to determine the Chl a content in the surface waters in spring. It is concluded that autonomous high-resolution *in-situ* monitoring in combination with adaptive water sampling and remote sensing could give a full enough data set to assess the environmental state of the Gulf of Finland during this highly dynamic season of the year.

REFERENCES

[1] Kahru, M., Brown C.W. (Eds). Monitoring algal blooms: New techniques for detecting large-scale environmental change. Springer Verlag, Berlin-Heidelberg-New York, 178 pp, 1997.
[2] Rantajärvi, E. (Ed). Alg@line in 2003: 10 years of innovative plankton monitoring and research and operational information service in the Baltic Sea. *MERI – Report Series of the Finnish Institute of Marine Research*, No. 48, pp. 7-36, 2003.
[3] Alenius, P., Myrberg, K., Nekrasov, A. The physical oceanography of the Gulf of Finland: a review. *Boreal Env. Res.*, 3, pp. 97-125, 1998.
[4] Talpsepp, L., Nõges, T., Raid, T., Kõuts, T. Hydrophysical and hydrobiological processes in the Gulf of Finland in summer 1987: Characterization and relationship. *Cont. Shelf Res*. 14, pp. 749-763, 1994.
[5] J. Pavelson, J. Laanemets, K. Kononen and S. Nõmman. Quasipermanent density front at the entrance to the Gulf of Finland: Response to wind forcing, *Cont. Shelf Res.,* 17, pp. 253-265, 1997.
[6] Lips, I., Lips, U. and Liblik, T. Consequences of coastal upwelling events on physical and chemical patterns in the central Gulf of Finland (Baltic Sea). *Cont. Shelf Res*., 29, pp. 1836–1847, 2009.
[7] Shlitzer, R. Ocean Data View, http://odv.awi.de, 2010.
[8] Helsinki Commission, Environment of the Baltic Sea area 1994-1998. *Baltic Sea Environment Proceedings*, No. 82B, pp. 215, 2002.
[9] Leppänen, J.-M., Rantajärvi, E., Hällfors, S., Kruskopf, M., Laine, V. Unattended monitoring of potentially toxic phytoplankton species in the Baltic Sea in 1993. *J. Plankton Res.* 17, pp. 891–902, 1995.
[10] Kanoshina, I., Lips, U. and Leppänen, J.-M. (2003) The influence of weather conditions (temperature and wind) on cyanobacterial bloom development in the Gulf of Finland (Baltic Sea). *Harmful Algae*, **2**, 29–41.
[11] Lips, I., Lips, U., 2008. Abiotic factors influencing cyanobacterial bloom development in the Gulf of Finland (Baltic Sea). *Hydrobiologia*, 614, pp. 133–140, 2008.
[12] Fleming, V., Kaitala, S. Phytoplankton spring bloom intensity index for the Baltic Sea estimated for the years 1992 to 2004 *Hydrobiologia*, 554, pp. 57–65, 2006.
[13] Kahru, M., Nõmmann, S. The phytoplankton spring bloom in the Baltic Sea in 1985, 1986: multitude of spatio-temporal scales. *Cont. Shelf Res.*, Vol. 10, No. 4, pp. 329-354, 1990.
[14] Wassmund, N., Nausch, G., Matthäus, W. Phytoplankton spring blooms in the southern Baltic Sea – spatiotemporal development and long-term trends. *J. Plankton Res.* 20, pp. 1099–1117, 1998.
[15] Kahru, M., Leppänen, J.-M., Nõmmann, S., Passow, U., Postel, L., Schulz, S. Spatio-temporal mosaic of the phytoplankton spring bloom in the open Baltic Sea in 1986. *Mar. Ecol. Progr. Series*, 66, pp. 301-309, 1990.
[16] Sackmann, B.C., Perry, M.J., Eriksen, C.C. Seaglider observations of variability in daytime fluorescence quenching of chlorophyll-*a* in Northeastern Pacific coastal waters. *Biogeosciences Discuss.*, 5, pp. 2839–2865, 2008.
[17] Schneider, B., Kaitala, M., Maunula, P. Identification and quantification of plankton bloom events in the Baltic Sea by continuous *p*CO_2 and chlorophyll *a* measurements on a cargo ship. *J. Mar. Res.*, 59, pp. 238-248, 2006.
[18] Buijsman, M.C., Ridderinkhof, H. Long-term ferry-ADCP observations of tidal currents in the Marsdiep inlet. *J. Sea Res.*, 57, pp. 237-256, 2007.
[19] Petersen, W., Wehde, H., Krasemann, H., Colijn, F., Schroeder, F. *Ferrybox* and MERIS – Assessment of coastal and shelf sea ecosystems by combining *in situ* and remotely sensed data. *Est. Coast. Shelf Sci.*, 77, pp. 296-307, 2008.
[20] Seppälä, J., Ylöstalo, P., Kaitala, S., Hällfors, S., Raateoja, M., Maunula, P. Ship-of-opportunity based phycocyanin fluorescence monitoring of the filamentous cyanobacteria bloom dynamics in the Baltic Sea. *Est. Coast. Shelf Sci.*, 73, pp. 489-500, 2007.

Paper III

Lips, U., Kikas, V., Liblik, T., Lips, I. (2016). Multi-sensor in situ observations to resolve the sub-mesoscale features in the stratified Gulf of Finland, Baltic Sea. *Ocean Science*, 12, 715–732, doi:10.5194/os–12–715–2016.

Ocean Science

Multi-sensor in situ observations to resolve the sub-mesoscale features in the stratified Gulf of Finland, Baltic Sea

Urmas Lips, Villu Kikas, Taavi Liblik, and Inga Lips

Marine Systems Institute at Tallinn University of Technology, Akadeemia Road 15a, 12618 Tallinn, Estonia

Correspondence to: Urmas Lips (urmas.lips@msi.ttu.ee)

Abstract. High-resolution numerical modeling, remote sensing, and in situ data have revealed significant role of sub-mesoscale features in shaping the distribution pattern of tracers in the ocean's upper layer. However, in situ measurements are difficult to conduct with the required resolution and coverage in time and space to resolve the sub-mesoscale, especially in such relatively shallow basins as the Gulf of Finland, where the typical baroclinic Rossby radius is 2–5 km. To map the multi-scale spatiotemporal variability in the gulf, we initiated continuous measurements with autonomous devices, including a moored profiler and Ferrybox system, which were complemented by dedicated research-vessel-based surveys. The analysis of collected high-resolution data in the summers of 2009–2012 revealed pronounced variability at the sub-mesoscale in the presence of mesoscale upwelling/downwelling, fronts, and eddies. The horizontal wavenumber spectra of temperature variance in the surface layer had slopes close to -2 between the lateral scales from 10 to 0.5 km. Similar tendency towards the -2 slopes of horizontal wavenumber spectra of temperature variance was found in the seasonal thermocline between the lateral scales from 10 to 1 km. It suggests that the ageostrophic sub-mesoscale processes could contribute considerably to the energy cascade in such a stratified sea basin. We showed that the intrusions of water with different salinity, which indicate the occurrence of a layered flow structure, could appear in the process of upwelling/downwelling development and relaxation in response to variable wind forcing. We suggest that the sub-mesoscale processes play a major role in feeding surface blooms in the conditions of coupled coastal upwelling and downwelling events in the Gulf of Finland.

1 Introduction

Essential contribution of mesoscale processes to the vertical exchanges of nutrients in the open ocean has been suggested and proved by a number of studies in the last 2 decades (e.g., McGillicuddy et al., 1998; Martin and Pondaven, 2003). These studies were motivated by the discrepancies between the direct measurements of vertical turbulent exchanges and indirect estimates of nutrient fluxes to support net primary production (Jenkins, 1988). Two conceptual views of additional nutrient supplies related to mesoscale eddies exist: (1) vertical exchanges due to the time evolution of eddies and (2) vertical pumping at small scales, i.e., within the sub-mesoscale structures (Klein and Lapeyre, 2009). The latter hypothesis is supported by recent observations and modeling with increased spatial resolution suggesting that the sub-mesoscale processes significantly contribute to the vertical exchange of water mass properties between the upper and deep ocean (Bouffard et al., 2012). Sub-mesoscale processes are characterized by order-one (O(1)) Rossby and Richardson numbers (Thomas, 2008), large vertical velocity and vorticity fluctuations and large vertical buoyancy flux, resulting in considerable intermittency of oceanographic properties in the upper ocean (Capet et al., 2008).

Main physical forcing components for the non-tidal Baltic Sea system are the atmospheric forcing, exchange of heat energy and fresh water through the sea surface, and input of freshwater from rivers and the saltier North Sea water through the Danish Straits (Omstedt et al., 2004). It was identified already in the 1980s that the Baltic Sea has rich mesoscale variability with spatial scales O(10) km through the whole water column (Aitsam et al., 1984) and evidence is increasing that remarkable changes occur in the system due to meso- and sub-mesoscale processes (e.g., Nausch et

al., 2009; Lips et al., 2009). Recent results based on analysis of high-resolution in situ (Lips et al., 2011), numerical modeling (Laanemets et al., 2011) and remote sensing (Uiboupin et al., 2012) data from the Gulf of Finland showed that the sub-mesoscale features significantly shape the distribution pattern of tracers in this stratified basin. Among such features, the upwelling filaments and intra-thermocline intrusions with lateral scales less than the internal Rossby radius of deformation, which is about 2–5 km in the Gulf of Finland (Alenius et al., 2003), are named.

The layered structure of the major basins of the Baltic Sea, with the seasonal thermocline and the halocline situated at different depths – about 10–30 and 60–80 m, respectively, is a challenge to be accurately described by numerical models (Tuomi et al., 2012). In many cases, a proper validation of model results is difficult due to the absence of observational data with the required resolution and coverage in time and space. In order to fill this gap a number of autonomous devices, including moored profilers and Ferryboxes, and towed instruments are applied in the Gulf of Finland. According to high-resolution profiling at a fixed position in the Gulf of Finland, quasi-stationary stratification patterns of the thermocline occurred there at timescales of 4–15 days (Liblik and Lips, 2012) and the vertical dynamics of phytoplankton were largely defined by these patterns (Lips et al., 2011). Furthermore, temperature–salinity variability at the sub-mesoscale was significant during the transition periods between the quasi-stationary patterns (Liblik and Lips, 2012).

Coastal upwelling events are prominent mesoscale features in the Gulf of Finland (Uiboupin and Laanemets, 2009) leading to considerable vertical transport of nutrients into the euphotic layer (Laanemets et al., 2011; Lips et al., 2009) and influencing the phytoplankton growth and species composition (e.g., Lips and Lips, 2010). Analysis of Ferrybox data collected along the ferry line Tallinn–Helsinki in the central part of the Gulf of Finland revealed the occurrence of the two types of upwelling events (Kikas and Lips, 2015). In addition to the classical coastal upwelling with a strong upwelling front, the second type of upwelling event existed where a gradual decrease of surface layer temperature from the open sea towards the coast was observed. The latter type was characterized by a relatively high spatial variability at scales of a few to 10 km, which as suggested by Kikas and Lips (2015) could be a sign of sub-mesoscale dynamics in the case of wind forcing not strong enough to produce an Ekman transport in the entire surface layer. This suggestion of higher sub-mesoscale activity associated with some types or phases of coastal upwelling has to be analyzed further. Such analysis based on combined Ferrybox, buoy profiler, and ScanFish data was one of the tasks of the present study.

According to the theory of quasi-geostrophic turbulence, the shape of the energy spectrum should follow the −3 slope in the logarithmic scale at the spatial scales below the mesoscale (Charney, 1971). It has been shown that if the spatial resolution of numerical models was increased the spectral slope converted to −2 rather than −3 (Capet et al., 2008) suggesting that sub-mesoscale processes play an important role in the energy cascade from larger to smaller scales. Still, it is a major challenge to map sub-mesoscale processes and phenomena by in situ observations. Due to the temporal and spatial scales to be resolved, the distinction between the temporal and spatial variability is difficult based on the high-resolution 3-D surveys by a single technique, platform or device. We have applied in situ observations, using both autonomous devices and a research vessel, for mapping temporal variability in temperature, salinity and chlorophyll a distribution patterns in the Gulf of Finland. Close to the Ferrybox line Tallinn–Helsinki, an autonomous profiler was deployed in the summers of 2009–2012. This data set allows us to estimate the temporal changes in the horizontal distribution patterns in the surface layer and vertical stratification (vertical temperature and salinity distribution) at a station close to the Ferrybox line simultaneously. In addition, ScanFish surveys were conducted in the area to reveal the spatial variability in the sub-surface layer.

The main aim of the present paper is to describe spatial and temporal variability at the mesoscale and sub-mesoscale, indicate the main sub-mesoscale features and their effects on the vertical stratification as well as chlorophyll a dynamics under different forcing conditions by combining high-resolution observational data (Ferrybox, buoy profiler, and ScanFish). We would like to demonstrate that multi-sensor in situ observations, initiated to meet the data needs in operational oceanography, are able to resolve the sub-mesoscale features and are a good basis for descriptive and statistical analysis of mesoscale and sub-mesoscale variability/features in the Gulf of Finland. The hypothesis that under certain mesoscale conditions, such as development and relaxation of coastal upwelling events in a stratified estuary, the sub-mesoscale processes are more energetic than predicted by the theory of quasi-geostrophic turbulence in the ocean interior is tested.

2 Material and methods

2.1 Measurement systems and data

The data set analyzed in the present study was gathered using an observational network applied by the Marine Systems Institute at Tallinn University of Technology in the Gulf of Finland, Baltic Sea. It includes autonomous measurements and sampling on board a ferry traveling between Tallinn and Helsinki and autonomous measurements at a profiling buoy station close to the ferry route. Additionally, research-vessel-based measurements and sampling, as well as surveys using a towed undulating vehicle (ScanFish), are employed (Fig. 1).

The Ferrybox system records temperature (T), salinity (S), and chlorophyll a (Chl a) fluorescence in the surface
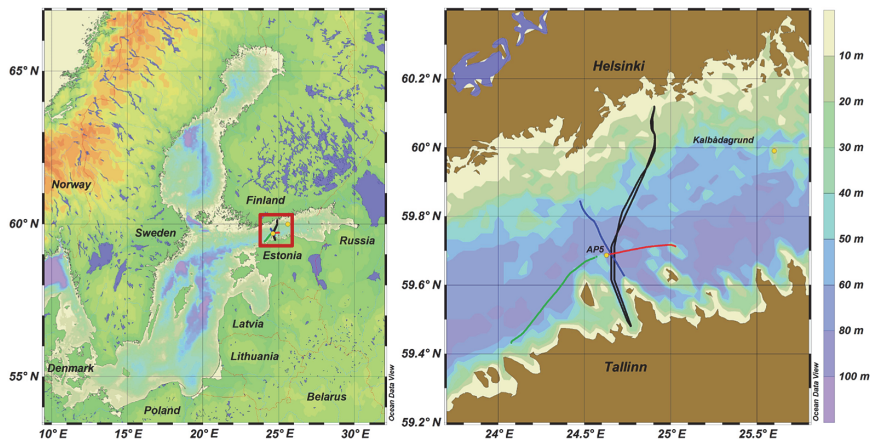
Figure 1. Map of the Baltic Sea (left panel) and the study area (right panel). Black lines indicate the Ferrybox route between Tallinn and Helsinki, blue line the ScanFish track on 22 July 2010, 2 August 2010, 4 July 2012, and 20 July 2012, green line the ScanFish track on 27 July 2010, and red line the ScanFish track on 31 July 2012. Yellow dots indicate the location of the buoy station AP5 and the Kalbadagrund meteorological station.

layer (water intake is approximately at 4 m depth) twice a day along the ferry route Tallinn–Helsinki (the system is described in detail by Kikas and Lips, 2015). The time resolution of measurements of 20 s corresponds to an average spatial resolution of 160 m. For temperature measurements, a PT100 temperature sensor with a measuring range from -2 to $+40\,°C$ with an accuracy of $\pm 0.1\,\%$ is used. The sensor is installed close to the water intake to diminish the effect of warming of water while flowing through the tubes onboard. For salinity measurements a FSI Excell thermosalinograph (temperature and conductivity meter) is used, and the data quality is checked by water sampling and analysis of samples by a high-precision salinometer Portasal 8410A (Guildline Instruments) 2–4 times a year. For Chl a fluorescence and turbidity (turbidity data not presented here) measurements, a SCUFA (Self-Contained Underwater Fluorescence Apparatus) submersible fluorimeter (Turner Designs) with a flow-through cap is used. An acid-washing cleaning system is applied to prevent biofouling and 11–17 water samples along the ferry route are collected once a week for laboratory analysis of Chl a content to calibrate the fluorimeter data.

The autonomous profiler deployed in the summers of 2009–2012 at station AP5 (Fig. 1) recorded vertical profiles of temperature, salinity, and Chl a fluorescence in the water layer from 2 to 50 m with a time resolution of 3 h and a vertical resolution of 10 cm. The sensor set at the buoy profiler consisted of an OS316*plus* CTD probe (Idronaut S.r.l.) equipped with a Seapoint Chl a fluorimeter. To avoid biofouling of sensors, the parking depth well below the euphotic layer depth and electrochemical antifouling system were applied. Ship-borne measurements and sampling close to the

buoy profiler were arranged bi-weekly to check the quality of data (compare the vertical profiles from the buoy with those from the research vessel) and to calibrate the Chl a fluorimeter by laboratory analyses of Chl a content from the water samples.

The data set used also includes ScanFish surveys of temperature, salinity, and Chl a fluorescence conducted to map the horizontal distribution of T, S, and Chl a in the water column from 2 to 45 m (see location of sections in Fig. 1). The average distance between the consecutive ScanFish cycles, including down- and upcast while the vessel was moving with a speed of 7 knots, was 600 m. Data were recorded continuously (both down- and upcast are used) and the processed data were stored with a vertical resolution of 0.5 m. The ScanFish sensor set consisted of a Neil Brown Mark III CTD probe and TriOS microFlu-chl-A fluorimeter. Shipborne CTD measurements and water sampling was conducted before and after the ScanFish surveys to control the quality of ScanFish data and calibrate the fluorimeter.

To calibrate the used (different) Chl a sensors, the Chl a concentration in the water samples was determined in the laboratory. Whatman GF/F glass fiber filters and extraction at room temperature in the dark with 96 % ethanol for 24 h were used. The Chl a content from the extract was measured spectrophotometrically (HELCOM, 1988) by Thermo Helios γ.

The data set from July-August 2009-2012 analyzed in the present study consists of 461 ferry crossings (Tallinn-Helsinki), 968 CTD and Chl a profiles collected at station AP5, and 6 ScanFish surveys.

2.2   Calculations

The results in the following sections are presented as graphs of pre-processed observational data and horizontal wavenumber spectra of temperature variance calculated from the Ferrybox and ScanFish measurements as well as the estimated characteristics of vertical stratification at station AP5. The use of spatial spectra of temperature (instead of density) was based on the assumptions that in summer in the surface and thermocline layer of the Gulf of Finland (GoF), the water density is mainly controlled by temperature and it is measured by one sensor while density has to be estimated from the readings of two separate sensors. The following approaches are used in the calculations.

Horizontal wavenumber spectra of temperature variance were calculated for each ferry crossing between Tallinn and Helsinki assuming that the distance between the data points along the ferry route was constantly 160 m. The areas close to the harbors, where the ferry speed varied, were excluded, and only the data along the ferry route between the latitudes 59.48 and 60.12° N were used. The mean spectra for a certain period with quasi-stationary variability were obtained by averaging of single spectra over this period. The spectral slopes between the spatial scales of 10 and 0.5 km were estimated. The overall variability was characterized by daily standard deviations of temperature along the ferry route.

Horizontal wavenumber spectra of temperature variance in the sub-surface layer were calculated using the data of Scan-Fish surveys. Since the distance between the consecutive profiles varies depending on the depth, the ScanFish data were first interpolated to the grid with a constant horizontal step of 300 m, which corresponds to the average distance between the up- and downward casts. Then the individual spectra for every depth (with 0.5 m step) were calculated, and the mean spectra in 10 m thick water layers were obtained by averaging all spectra in those layers containing 21 individual spectra. The spectral slopes between the spatial scales of 10 and 1 km were estimated.

Vertical stratification was described by estimating the potential energy anomaly P (Simpson and Bowers, 1981; Simpson et al., 1990) as

$$P = \frac{1}{h} \int\limits_{-h}^{0} (\rho_A - \rho) g z \, \mathrm{d}z, \quad \rho_A = \frac{1}{h} \int\limits_{-h}^{0} \rho \, \mathrm{d}z; , \qquad (1)$$

where $\rho(z)$ is the density profile over the water column of depth h. The stratification parameter $P(\mathrm{J\,m^{-3}})$ is the work required to bring about the complete mixing of the water column under consideration. Similarly to Liblik and Lips (2012), the integration was conducted from the sea surface until 40 m depth. If the surface data were missing (upper 2 m where the buoy profiler did not measure), the uppermost available density value was extrapolated to the surface.

The intrusion index was calculated as a sum of negative salinity gradients ($\mathrm{g\,kg^{-1}\,m^{-1}}$) in the water layer from the sea surface to 40 m depth. Before calculations, the salinity profiles were smoothed by 2.5 m window. The idea behind the method comes from the fact that on the background of vertical salinity gradient with a fresher surface layer and more saline deep layer, lateral salinity gradients exist in the study area. In general, fresher water originates from the east (the Neva River and other larger rivers in the GoF) while more saline water originates from the Baltic proper. This general lateral salinity gradient could be enhanced locally as a result of meso- and sub-mesoscale dynamics. If the water layers with a thickness of a few to 10 m move in different directions, vertical salinity inversions could be generated in the water column where the vertical density gradient is mostly maintained by the temperature distribution. Thus, high values of intrusion index indicate the occurrence of layered flow structures.

The Chl a fluorescence data acquired with different sensors attached to the Ferrybox system, buoy profiler, and ScanFish were converted into Chl a content values using equations of linear regression between the fluorescence readings and results of laboratory analyses of water samples. The conversation equation of Chl $a = 2.47 \times F$ ($r^2 = 0.41$, $p < 0.05$) was used for the buoy profiler fluorescence data analyzed in this paper to convert fluorescence (F; in arbitrary units) into Chl a content in $\mathrm{mg\,m^{-3}}$. Interpretation of Ferrybox fluorescence data was sometimes difficult due to some problems with biofouling. In the present study, we used only data from July 2010 when the found regression line had the following parameters: Chl $a = 2.34 \times F - 2.41$ ($r^2 = 0.77$, $p < 0.05$) and from summer 2012 by applying the following regression line equation: Chl $a = 1.06 \times F - 4.11$ ($r^2 = 0.80$, $p < 0.05$). Data only from evening crossings were used to diminish the fluorescence quenching effect.

3   Results

3.1   Forcing and general features

The study period in July–August of 2009–2012 was characterized by distinct inter-annual differences in wind conditions and distribution patterns of temperature and salinity in the central part of the Gulf of Finland. Based on HIRLAM (High-Resolution Limited Area Model) wind data, the average wind speed in July–August 2009–2012 in the GoF area was $6.0\,\mathrm{m\,s^{-1}}$, and the prevailing wind direction was from the south-southeast with an average velocity of the airflow of $1.4\,\mathrm{m\,s^{-1}}$. While the winds from the southwest prevailed in July–August 2009 and 2012 (average direction from 217 and 214°, respectively), the dominating wind direction was from the southeast in 2010 and 2011 (average direction from 160 and 122°, respectively). Both in 2010 and in 2011 the monthly average wind direction differed between the 2 analyzed months being from 192° in July to 115° in August 2010 and from 73° in July to 177° in August 2011.
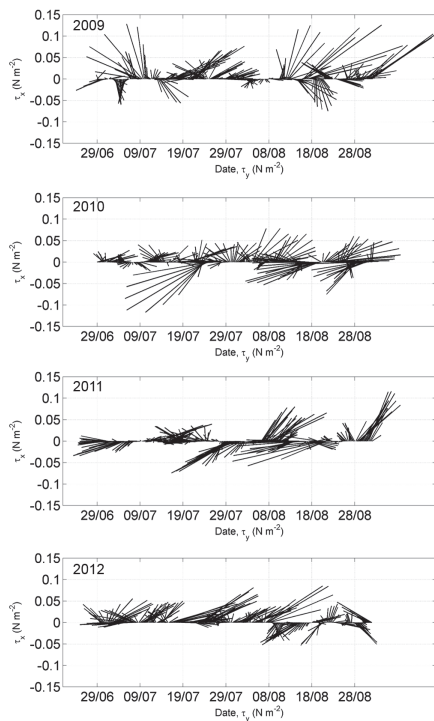
Figure 2. Temporal changes in wind stress during the study period of 29 June–31 August in 2009–2012 based on 3 h average wind measured at the Kalbadagrund meteorological station (Finnish Meteorological Institute) and shown as series of wind stress vectors with a time step of 6 h smoothed using 24 h moving average.

On the synoptic scale (several days – a couple of weeks), mostly westerly wind pulses occurred in 2009 except for a period in the first half of July with a relatively strong wind pulse from the south-southeast (see time series of wind stress vectors in Fig. 2). In 2010, moderate winds from the southwest were prevailing in the first half of July while several wind pulses from the east, northeast and south occurred during the rest of the study period. Typical for 2011 was a consecutive appearance of relatively strong wind pulses from southwest and east-northeast. In 2012, westerly winds clearly prevailed with only two short periods when the wind pulses from the east (early July) and northeast (second half of August) occurred.

In general, as described by Kikas and Lips (2015) based on Ferrybox data, the surface layer temperature was clearly higher in 2010 and 2011 than in 2009 and 2012. The surface layer salinity was the highest at the beginning of the study period in 2011; the less saline water occupied the central gulf in 2009 and the second half of summer in 2010 and 2011

while the surface layer salinity stayed relatively high in July–August 2012.

Based on the combined figures of horizontal and vertical distributions of temperature and salinity in July–August 2009 (Fig. 3a and b), the following characteristic features could be identified. In the first half of July, an upwelling event developed near the southern coast resulting in large variations of temperature (7.8–17.8 °C) and salinity (4.2–6.1 g kg^{-1}) across the gulf. Deepening of the thermocline occurred after the upwelling relaxation in the southern part of the gulf. A shallow and warm upper layer (temperature between 17.3 and 20.4 °C) with very low variations of salinity across the gulf (between 4.6 and 5.0 g kg^{-1}) appeared in the study area due to a period of weak winds in the first half of August. Upwelling near the southern coast occurred in the second half of August with increased across-gulf variability of temperature (from 12.9 to 17.7 °C) and salinity (4.7–5.6 g kg^{-1}).

At the beginning of the study period in 2010, when mainly weak or variable moderate winds prevailed, the variations of temperature (mostly being between 20 and 22 °C) and salinity in the surface layer were very low across the gulf (Fig. 3c and d). This calm period was followed by a relatively weak upwelling event off the northern coast and deepening of the thermocline from 10 m to 15 m in the southern part. A strong upwelling event near the southern coast with the high spatial variability of temperature (varying between 11.1 and 21.6 °C) and salinity (varying between 4.0 and 6.3 g kg^{-1}) across the gulf occurred in late July. The seasonal thermocline had a much shallower position in 2010 (for the period with available data until early August) than in 2009.

Study period in July–August 2011 started with an upwelling event near the southern coast with the surface layer temperature varying across the gulf from 12.8 to 20.6 °C and salinity varying from 5.1 to 6.5 g kg^{-1} (Fig. 3e and f). During the next extensive upwelling event in late July–early August off the southern coast, high variability of the surface layer temperature (varying between 13.5 and 21.4 °C), and salinity (varying between 4.4 and 6.4 g kg^{-1}) across the gulf was observed. Relaxation of the latter event was accompanied by a moderate deepening of the thermocline in the southern part of the gulf. Strong winds from variable directions in the second half of August caused strong vertical mixing and downwelling with a drastic deepening of the seasonal thermocline to 45 m depth in the southern part of the gulf.

The first half of July 2012 was characterized by relatively low spatial variability of temperature and salinity in the surface layer of the study area (Fig. 3g and h). An upwelling event occurred near the northern coast at the end of July, creating a temperature difference across the gulf from 10.3 to 17.2 °C, and accompanied by the deepening of the seasonal thermocline in the southern part (to 45 m). After a short period with low variability, the second upwelling event appeared near the northern coast while the surface layer temperature stayed quite high in the rest of the study transect (up to 20 °C). In the period between the two upwelling events,
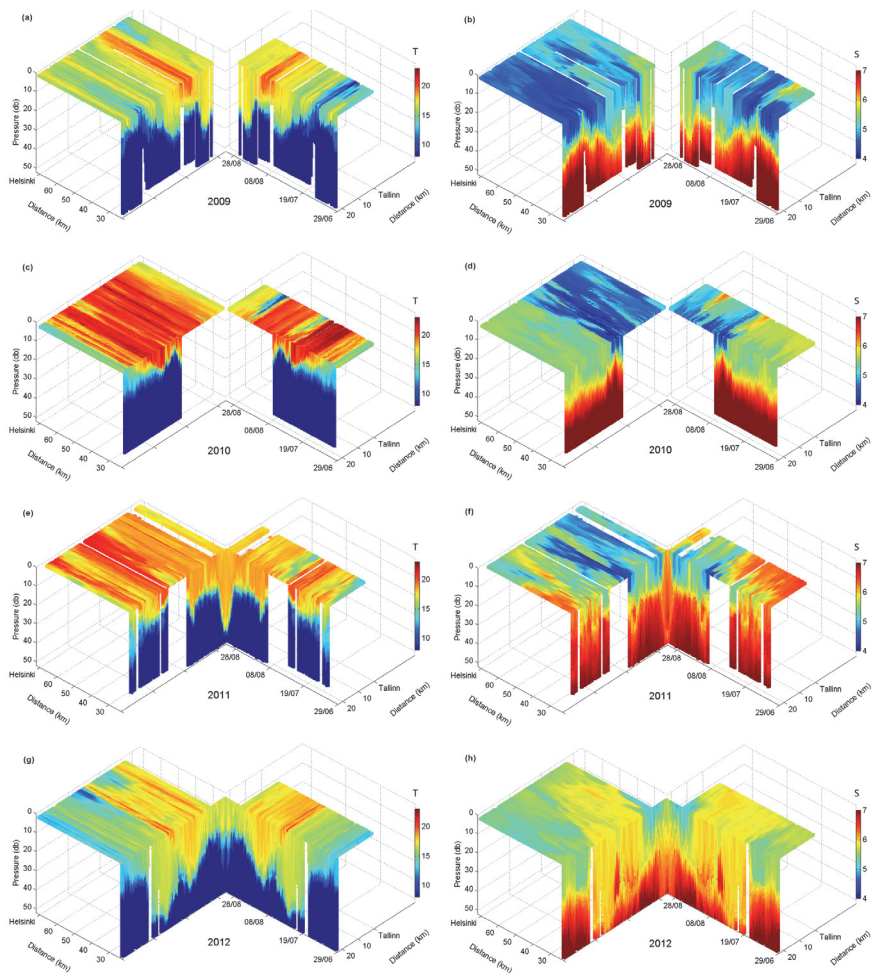
Figure 3. Temporal changes in horizontal and vertical distributions of temperature (°C) and salinity (g kg^{-1}) in the Gulf of Finland measured by the Ferrybox system between Tallinn and Helsinki and the autonomous buoy profiler at station AP5 from 29 June to 31 August in 2009 (**a, b**, respectively), 2010 (**c, d**), 2011 (**e, f**), and 2012 (**g, h**). The Ferrybox data are split into two parts at the position of the buoy profiler AP5. The *x* axis shows the distance along the ferry route from a starting point off Tallinn harbor at the latitude of 59.48° N.

strong intrusions of more saline water were observed in the subsurface layer at the buoy station. The position of the seasonal thermocline in the southern part of the gulf was the deepest in 2012 among the analyzed years.

3.2 Lateral variability of temperature in the surface layer

Overall horizontal variability of temperature characterized as the standard deviation of temperature along the ferry route varied in quite large ranges in time, from 0.2 to 3.7 °C

(Fig. 4). High values of standard deviation of temperature in the surface layer were related to the observed coastal upwelling events and, as a rule, the upwelling events near the southern coast resulted in larger spatial variations of temperature than those near the northern coast. During the upwelling event in August 2010, the standard deviation of temperature was as high as 3.7 °C while during the other upwelling events within the study period in July–August 2009–2012, the values of standard deviation of temperature did not exceed 2.5 °C. Despite the high temporal variability of standard deviations of temperature calculated based on data from
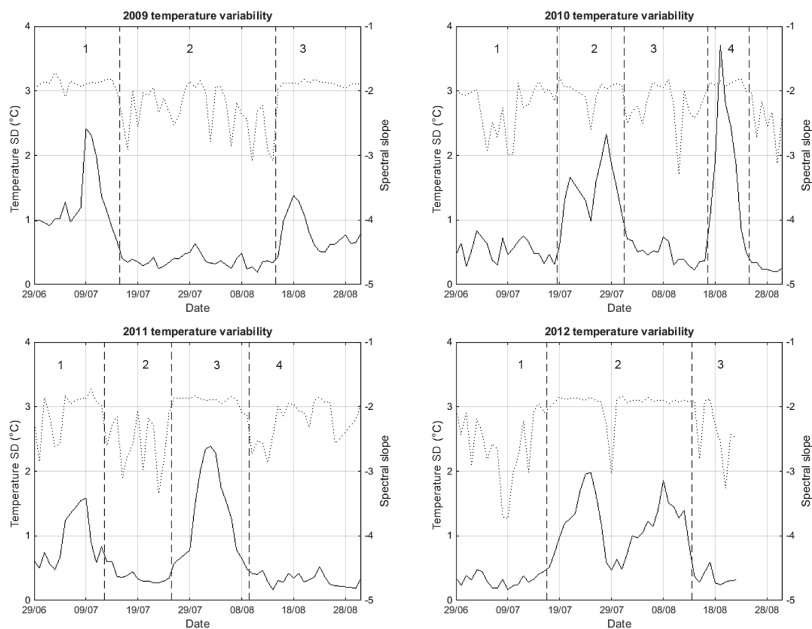
Figure 4. Statistical characteristics of the temperature variability in the surface layer of the Gulf of Finland along the ferry route Tallinn–Helsinki from 29 June to 31 August in 2009, 2010, 2011, and 2012. Standard deviations of temperature are shown as solid lines and spectral slopes of temperature variance between the horizontal scales of 10 and 0.5 km as dotted lines. The vertical dashed lines denote the borders between the selected characteristic periods with similar variability patterns (numbers of periods are shown in the upper part of the panels).

single crossings, the average values of standard deviations for the studied 4 years did not differ much; a minimum of 0.71 °C was found in 2009 and a maximum of 0.83 °C in 2010 (Table 1).

The calculated horizontal wavenumber spectra of temperature variance had also relatively large variability if to compare the spectra estimated based on data from single crossings. The spectral slope between the lateral scales of 10 and 0.5 km varied between −1.8 and −3.7 (in logarithmic scales). Note that the spectral curves were approximately linear (Fig. 5) between the scales of 15–20 km (the latter corresponds to a horizontal wavenumber of 0.05 km^{-1} or in a logarithmic scale −1.3 in Fig. 5) and 0.5 km (corresponds to wavenumber of 2 km^{-1} or in logarithmic scale 0.3 in Fig. 5); thus, linear approximation of their slopes is feasible. Within the periods of the high spatial variability of temperature, mostly related to upwelling events affecting the distribution of temperature in the surface layer of the Gulf of Finland, the estimated slopes were between −1.8 and −2. When the spatial variability of temperature was low in the surface layer, the slopes varied mostly between −2 and −3 (Fig. 4). At the same time, the average spectra for the entire period under consideration in the studied years were quite close to each

other (Fig. 5, bold lines) and the spectral slopes on average were close to −2 (from −2.1 to −2.2; see also Table 1).

Based on the presented lateral variability of temperature, some distinct periods when the standard deviation of temperature was high and spectral slope was close to −2 can be distinguished. We selected 3–4 periods with the almost quasi-stationary character of variability in each year to quantitatively describe the character of variability within these periods; the periods are marked in the Fig. 4 by dashed lines.

In 2009, two periods of high spatial variability caused by coastal upwelling events existed (periods 1 and 3 marked in Fig. 4). During both periods, the spectral lines had a higher position, and their slopes were shallower than the average for the entire study period in 2009 (see Fig. 5 and Table 1). In 2010, two periods, which were also associated with the upwelling events (periods 2 and 4; see Fig. 4), had much higher spatial variability, and the spectral slopes were shallower than the average in 2010. All time intervals comprising upwelling events in 2011 (periods 1 and 3; see Fig. 4) and 2012 (period 2; see Fig. 4) were also characterized by a higher position and shallower slope of spectral lines than the lines representing the average for July–August 2011 and 2012. The noticed divergence of spectral slopes from the high-variability and low-variability periods resulted in a
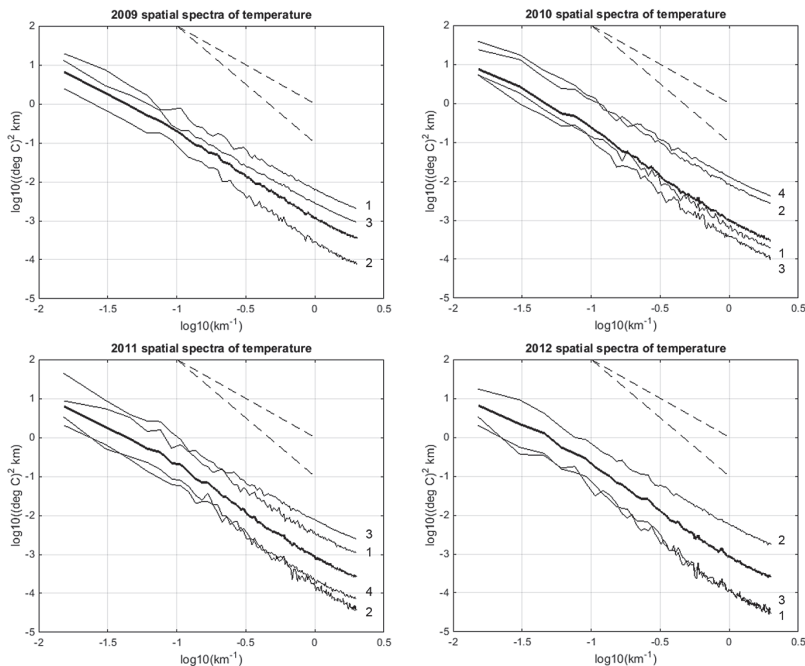
Figure 5. Horizontal wavenumber spectra of temperature variance in the surface layer of the Gulf of Finland calculated using Ferrybox data from the Tallinn–Helsinki ferry line in the summers of 2009–2012. The bold lines show the average spectral curve for the entire study period from 29 June to 31 August in each year, and the thin lines represent the average spectral curves in the selected periods. The numbers of the periods, corresponding to those marked in Fig. 4 and listed in Table 1, are shown close to each respective spectral curve. The dashed lines correspond to −2 and −3 slopes.

clearly larger separation between the spectral curves at the sub-mesoscale than at the mesoscale. While the spectral density of spatial variations of temperature at the spatial scale of 1 km varied more than 1.5 in magnitude, it varied in ranges of 1 magnitude at the spatial scale of 10 km (Fig. 5).

3.3 Temporal variability of the vertical stratification

The vertical distributions of temperature and salinity at the buoy station varied considerably in time similarly to the horizontal distributions of temperature and salinity along the ferry route. The variations were revealed as changes in the magnitude of vertical gradients, depth of the upper mixed layer and seasonal thermocline, fast deepening or surfacing of the thermocline, and occurrence of intrusions leading in certain cases to local inversions in vertical salinity distribution (Fig. 3).

Temporal changes in vertical stratification in the Gulf of Finland could be related to the differences in the heat flux through the sea surface and to the prevailing wind forcing that influences both the estuarine circulation alterations and the intensity of vertical mixing (see e.g., Liblik and Lips,

2012). Note that the autonomous buoy station in the present study was located in the southern part of the open Gulf of Finland. Thus, in addition to the seasonal course of stratification and its dependence on the estuarine circulation, the vertical stratification at this location could be significantly influenced both by the upwelling and by the downwelling along the southern coast.

Stratification parameter (P) calculated for the water layer between the sea surface and 40 m depth increased in July 2010 and 2011 in accordance with the strengthening of the seasonal thermocline (Fig. 6). In July–August of these years, the winds from the southeast prevailed supporting the estuarine circulation and, in turn, keeping up the strong vertical stratification; the maximum of $P = 370\,\mathrm{J\,m^{-3}}$ was observed at the beginning of August 2010. This continuous increase of P in both years was disrupted only due to the coastal upwelling events (in 2010 also due to a weak downwelling event) leading to rapid changes in the stratification parameter mostly because of vertical movements of the thermocline. In contrast to 2010 and 2011, the stratification parameter did not increase much during the study window in 2009 and 2012 in accordance with the prevailing southwest-
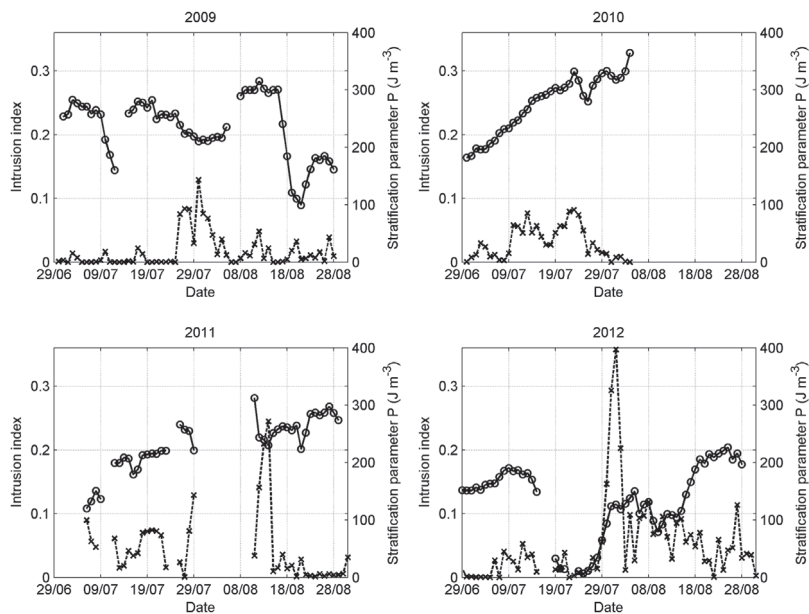
Figure 6. Daily average stratification parameter (solid line with open circles) and intrusion index (dashed line with crests) estimated for the water column from the sea surface to 40 m depth at the buoy station AP5 in the central Gulf of Finland from 29 June to 31 August in 2009–2012. Location of the buoy station is shown in Fig. 1.

erly winds. In 2009, the stratification parameter being relatively high due to the vertical salinity stratification had the maximum in the first half of August ($P = 300\,\mathrm{J\,m^{-3}}$) and decreased rapidly afterwards when the downwelling influence reached the buoy station. In 2012, the vertical stratification in the water layer from the surface to 40 m depth almost vanished at the measurement site AP5 by 20 July due to a very strong downwelling event, which appeared along the southern coast of the Gulf of Finland. Later on, the stratification at the buoy station strengthened, but the stratification parameter was clearly the lowest in 2012 if compared to the other years due to the deepest position of the seasonal thermocline.

Vertical profiles of temperature and salinity collected at the buoy station often exposed variability with vertical scales of a few to 10 m, which could be interpreted as intrusions related to the sub-mesoscale dynamics. Since the temperature was the main contributor to the vertical density distribution in the seasonal thermocline, such intrusions could create local inversions in the vertical distribution of salinity as mentioned above and seen in Fig. 3. The calculated intrusion index showing how much the vertical stratification is weakened due to local salinity inversions varied mostly between 0 and 0.05. However, every year one or a few periods were detected when the index exceeded 0.05, whereas the maximum index value obtained on 1–2 August 2012 reached 0.36.

In 2009, the only period with relatively high intrusion index values was detected during and just after the period of estuarine circulation reversal (Liblik and Lips, 2012). The maximum of the intrusion index coincided with the last day of the upwelling event near the northern coast that was followed by the event near the southern coast and rapid decrease of the intrusion index. In 2011, the index values > 0.05 were detected a few times in July, whereas the highest values on 12–14 August (exceeding 0.24 on 14 August) were related to the relaxation of an intense upwelling event near the southern coast and short-term deepening of the thermocline at the buoy station during a weak upwelling event near the northern coast. The mentioned highest intrusion index value on 1–2 August 2012 was detected within the period when two consecutive major upwelling events occurred near the northern coast, whereas this maximum emerged between the upwelling events just before the second one.

Thus, the intrusions were most intense (in the sense of salinity inversions) at the buoy station AP5 in connection with the relaxation of upwelling events near the southern coast, development of upwelling events near the northern coast and estuarine circulation reversals. All these situations correspond to the periods when the thermocline was deepening or was already at a deep position at the buoy station in the southern part of the open Gulf of Finland. In addition, the stratification parameter values were low or decreas-
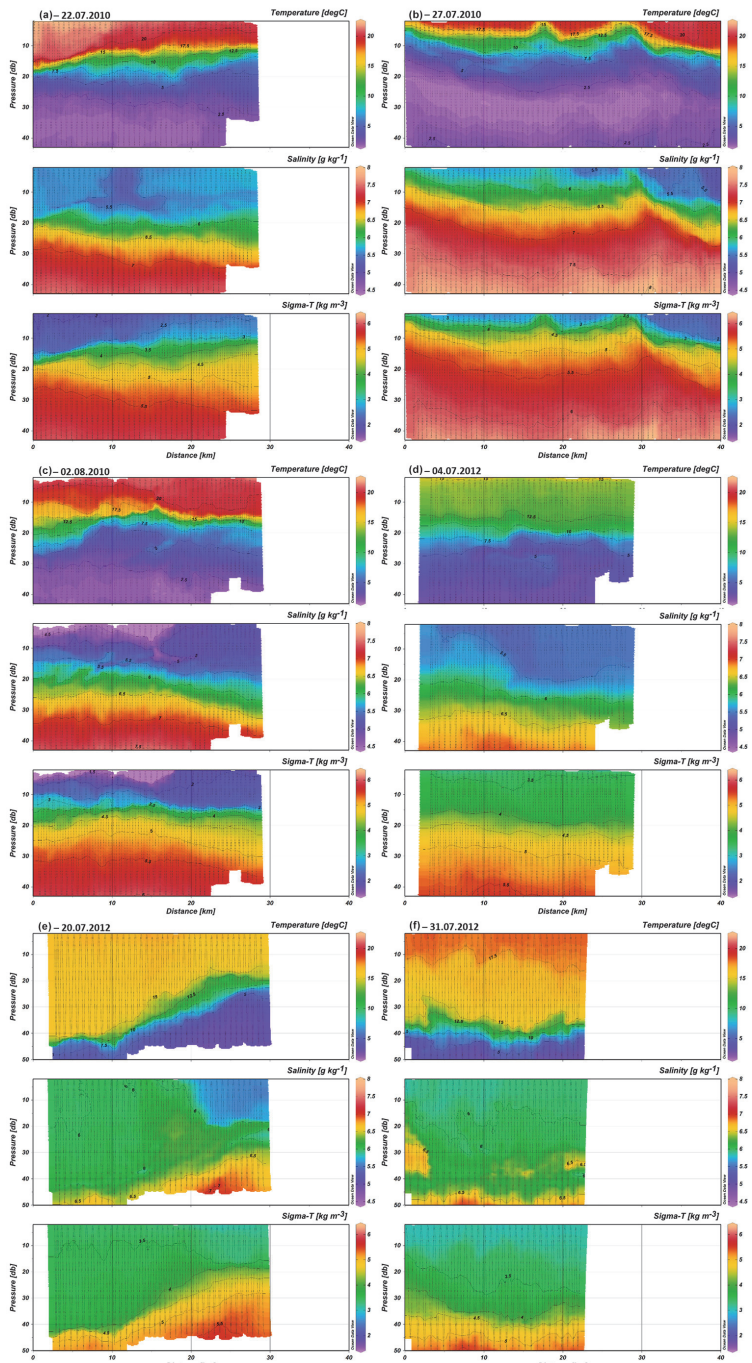
Figure 7. Vertical sections of temperature, salinity, and density anomaly measured using the ScanFish on 22 July 2010 (**a**), 27 July 2010 (**b**), 2 August 2010 (**c**), 4 July 2012 (**d**), 20 July 2012 (**e**), and 31 July 2012 (**f**). The corresponding ScanFish tracks are shown in Fig. 1.
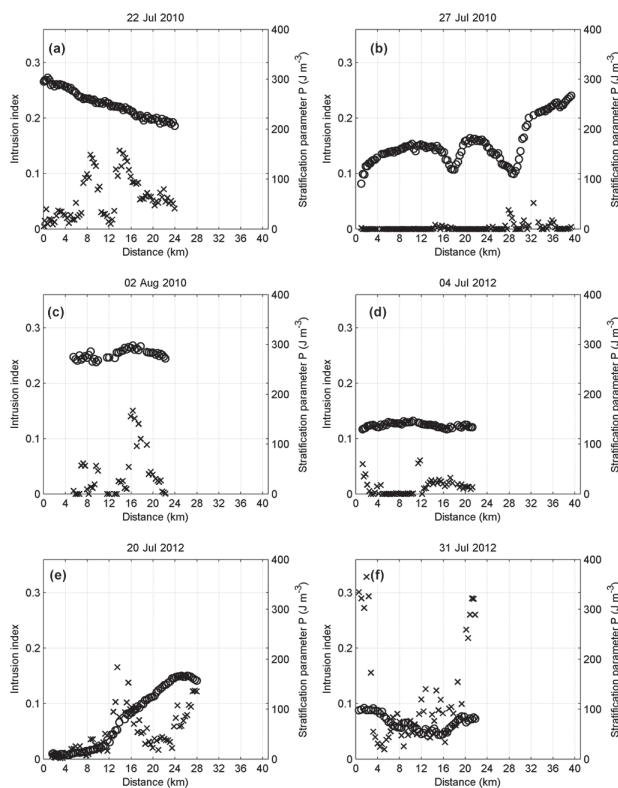
Figure 8. Stratification parameter (open circles) and intrusion index (crests) estimated for the water column from the sea surface to 40 m depth along the ScanFish tracks on 22 July 2010 (**a**), 27 July 2010 (**b**), 2 August 2010 (**c**), 4 July 2012 (**d**), 20 July 2012 (**e**), and 31 July 2012 (**f**). The corresponding ScanFish tracks are shown in Fig. 1.

ing when the temporal maximum of intrusion index was detected. When relating intrusion index values with the lateral variability in the surface layer one could conclude that the found temporal maxima of intrusion index corresponded to the periods of moderate lateral variability in the surface layer. Nevertheless, during such periods, the slopes of horizontal wavenumber spectra of temperature variance were close to -2 as during the periods of high lateral variability, and approximately a week before the highest intrusion index values, the lateral variability in the surface layer was also high (Figs. 4 and 6).

3.4 Spatial variability in the thermocline

We analyzed the data of ScanFish surveys in the Gulf of Finland conducted across the gulf in the open, deeper part and along the southern coast in the summers of 2010 and 2012. The hydrographic background of surveys in 2010 is characterized by the development of a weak upwelling along

the northern coast of the gulf on 22 July 2010, a strong upwelling event along the southern coast on 27 July 2010 and relaxation of it by 2 August 2010 when the last survey was conducted (see Fig. 3c, d). In summer 2012, when the upwelling events along the northern coast dominated, the survey on 4 July 2012 characterizes the situation before those upwelling events, on 20 July 2012 the development of upwelling and on 31 July 2012, which was conducted along the gulf, the situation related to a temporal relaxation of upwelling (see Fig. 3g, h).

A clear cross-gulf inclination of the thermocline was revealed on 22 July 2010 (Fig. 7a), although the ScanFish section did not reach the upwelling area near the northern coast. At the same time, the isopycnals had opposite inclination below the 20 m depth resulting in a weakening of the vertical stratification from south to north (Fig. 8). A well-pronounced, less saline water zone with a width of less than 5 km was observed in the surface layer. The extension of an associated intrusion of lower salinity in the thermocline was
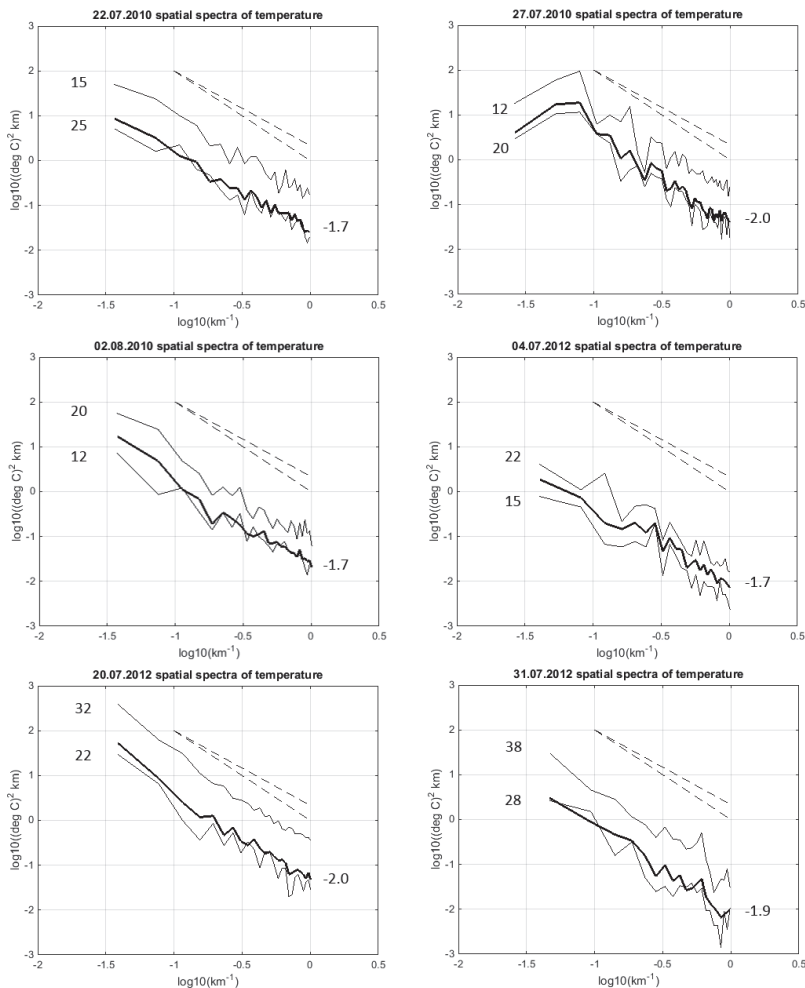
Figure 9. Horizontal wavenumber spectra of temperature variance in the sub-surface layer of the Gulf of Finland calculated using ScanFish data from 22 July 2010, 27 July 2010, 2 August 2010, 4 July 2012, 20 July 2012, and 31 July 2012. The bold lines show the average spectral curve for each survey and the thin lines represent the spectral curves in the selected layers with the thickness of 10 m. The central depth values of the selected layers are indicated at the left side of panels and the estimated spectral slopes for the average spectral curve at the right of panels. The dashed lines correspond to −5/3 and −2 slopes.

wider in the horizontal dimension and its thickness, decreasing from north to south in accordance with the strength of the vertical stratification, was less than 5 m.

The along-gulf ScanFish section on 27 July 2010 from the buoy station AP5 to the southwest crossed the meandering upwelling front (Fig. 7b). The observed variability is characterized by clear mesoscale meanders of the front with spatial scales of 10–15 km, strong stratification at the warm, less saline side of the front and much weaker stratification at the

cold, more saline side of it, and very low intrusion index almost along the entire section (Fig. 8b). A remarkable variability at the sub-mesoscale, also resulting in intrusions of water with different salinity seen in Fig. 7c and expressed in high values of intrusion index (Fig. 8c), was observed on 2 August 2010. A less saline water zone was well visible almost at the same location as on 22 July 2010, but the surface layer salinity in it was much lower, less than 4.5 g kg^{-1} (Fig. 7c).
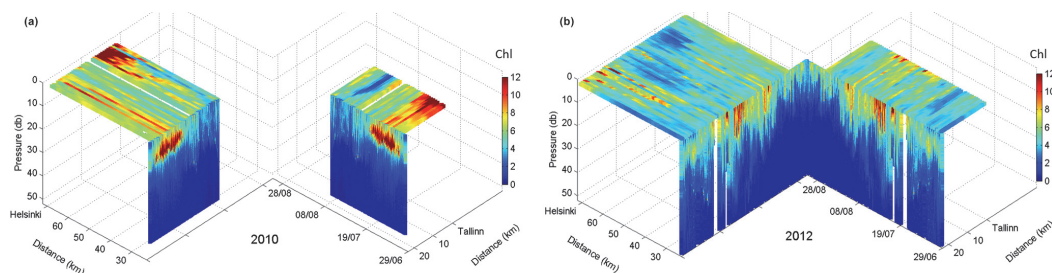
Figure 10. Temporal changes in horizontal and vertical distribution of chlorophyll *a* (mg m^{-3}) in the Gulf of Finland measured by the Ferrybox system between Tallinn and Helsinki and the autonomous buoy profiler at station AP5 from 29 June to 31 August in 2010 (**a**) and 2012 (**b**). The Ferrybox route and the location of station AP5 are shown in Fig. 1.

Table 1. Standard deviations of temperature and slopes of wavenumber spectra of temperature variance based on the data collected in the surface layer along the ferry route between Tallinn and Helsinki. Average values for each year over the study period from 29 June to 31 August (to 22 August in 2012) and within the selected periods with similar spatial variability are given. Numbers of the periods correspond to the periods marked in Fig. 4.

Year no.	Dates	Standard deviation (°C)	Spectral slope (10–0.5 km)
2009	29 June–31 August	0.71	−2.1
1	29 June–15 July	1.26	−1.9
2	16 July–14 August	0.37	−2.3
3	15 August–31 August	0.78	−1.9
2010	29 June–31 August	0.83	−2.2
1	29 June–18 July	0.52	−2.3
2	19 July–31 July	1.46	−2.0
3	1 August–16 August	0.48	−2.2
4	17 August–24 August	1.89	−1.9
2011	29 June–31 August	0.73	−2.2
1	29 June–12 July	0.93	−2.1
2	13 July–25 July	0.38	−2.6
3	26 July–9 August	1.43	−1.9
4	10 August–31 August	0.34	−2.2
2012	29 June–22 August	0.76	−2.2
1	29 June–16 July	0.32	−2.6
2	17 July–13 August	1.16	−2.0
3	14 August–22 August	0.35	−2.4

The average vertical gradients of all parameters – temperature, salinity, and density – in the upper 40 m water layer were clearly lower in summer 2012 (Fig. 7d–f) than in summer 2010 (Fig. 7a–c). A less saline water zone in the central part and slightly stronger vertical stratification in the southern part of the section were observed on 4 July 2012 (Figs. 7d and 8d). Development of the upwelling along the northern coast and downwelling in the southern part caused strong inclination of the thermocline across the gulf and a clear strengthening of vertical stratification from south to north on 20 July 2012 (Figs. 7e and 8e). In the area of strong inclination of the thermocline, relatively large horizontal gradients of salinity and intense sub-mesoscale variability, also seen as intrusions of water with different salinity (Fig. 7e), were observed. On 31 July 2012, the ScanFish survey revealed a mesoscale eddy-like feature (Fig. 7f), which could be formed in the process of downwelling relaxation as also observed earlier along the southern coast of the gulf (in its mouth area; see Lips et al., 2005). This mesoscale feature was characterized by relatively weak vertical stratification in its central part and high intrusion index values, especially at its periphery (Fig. 8f). Note that the pronounced intrusion of more saline water detected at the western end of the section was also registered at the buoy station during several days (Fig. 3h).

The horizontal wavenumber spectra of temperature variance shown in Fig. 9 vary considerably between the analyzed six surveys, both in the spectral level and the shape of the curves. The highest variability at the meso- and sub-mesoscale was related to the surveys, which were conducted when pronounced upwelling events dominated in the study area, on 27 July 2010 and 20 July 2012. The former survey crossed the meandering upwelling front, and the peak of the spectral density was found at the lateral scale of about 15 km. The latter survey was conducted when an upwelling event along the northern coast was developing, and the Scan-Fish section crossed the inclined thermocline. A similar situation with a weaker upwelling development and slightly lower spectral densities was mapped on 22 July 2010.

The spectral slopes between the horizontal scales of 10 and 1 km for spectra averaged over depth intervals with the thickness of 10 m were mostly shallower than −2; the average values of spectral slopes for each survey (shown in Fig. 9) varied between −1.7 and −2.0. The slopes close to −2 were obtained for the surveys with the most pronounced mesoscale features. Local vanishing of the spectral slope
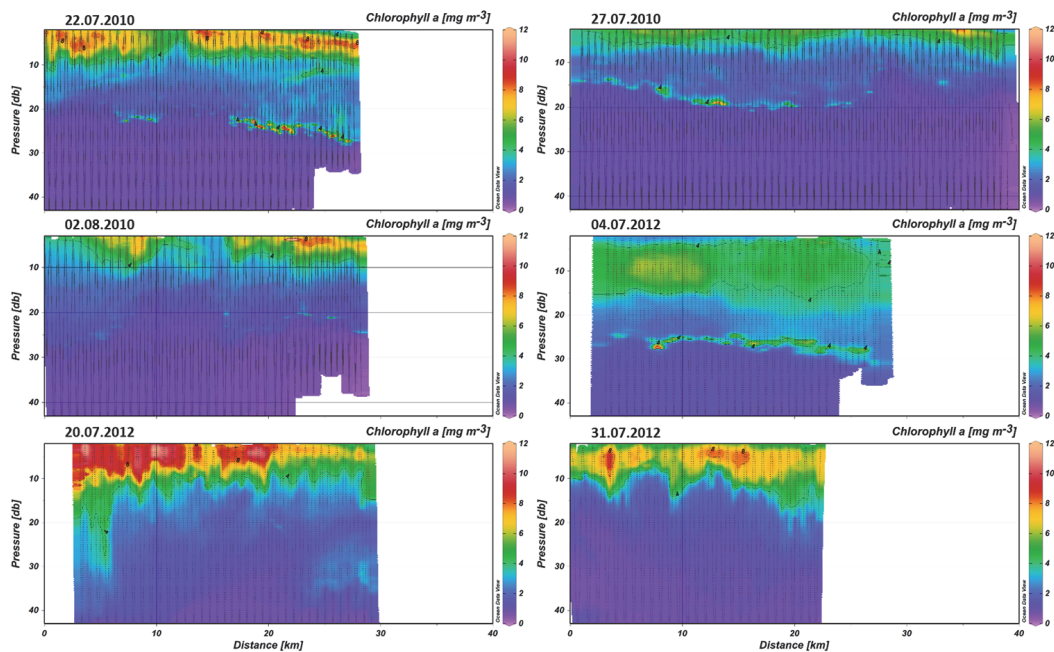
Figure 11. Vertical sections of chlorophyll *a* content measured using the ScanFish on 22 July 2010, 27 July 2010, 2 August 2010, 4 July 2012, 20 July 2012, and 31 July 2012. The corresponding ScanFish tracks are shown in Fig. 1.

could be detected between the horizontal scales from 3 to 1 km on 2 August 2010 and at scales from 3 to 2 km on 31 July 2012. High intrusion index values were characteristic for the both mentioned surveys, especially for the survey on 31 July 2012 (Fig. 8c, f), which is in accordance with the index estimates based on the buoy profiler data (Fig. 6d). High intrusion index values were also found for the survey on 20 July 2012 when a patch of more saline water appeared in the sub-surface layer at the warm side of the upwelling front (Figs. 7d and 8d).

3.5 Consequences to chlorophyll *a* dynamics

Temporal variability of chlorophyll *a* at the scales of days is usually much higher than that of temperature and salinity since in addition to the advection and mixing, the phytoplankton growth (and decay) could increase (decrease) the biomass and consequently chlorophyll *a* content rapidly. Despite such high variability and other factors that could influence the comparability of acquired chlorophyll *a* fluorescence data, e.g., fluorescence quenching, the presented combined plots of changes in horizontal and vertical distributions agree reasonably well (Fig. 10).

In the first half of July 2010, a sub-surface bloom developed in the southern part of the Gulf of Finland, which

occasionally was also seen in the surface layer with higher chlorophyll *a* values off the southern coast (Fig. 10a). When an upwelling event along the southern coast started to dominate (see Fig. 3c), the chlorophyll *a* content decreased in the southern part and increased in the northern part of the study area. Before the bloom near the northern coast, relatively deep chlorophyll *a* maxima were detected at the buoy station at depths below 20 m (since the maxima layers were thin they are not well seen in Fig. 10) and at the ScanFish section on 22 July 2010, especially at its northern part (Fig. 11). When the upwelling developed along the southern coast of the gulf, the sub-surface chlorophyll *a* maxima were situated at a shallower position in the warmer side of the front, but they almost disappeared by 2 August 2010 after relaxation of the upwelling event. In between the two surveys, the bloom developed near the northern coast in the convergence/downwelling area. It was suggested that this bloom could be related to the observed sub-surface maxima of chlorophyll *a*, which contained the dinoflagellate *Heterocapsa triquetra* in very high numbers (Lips and Lips, 2014).

In 2012, the chlorophyll *a* content was higher in the northern half of the study area than in its southern part in the first half of July. Later, when the two consecutive upwelling events appeared along the northern coast, the highest chlorophyll *a* values were observed close to the southern coast. At

the buoy station, where the downwelling influence was visible (see Fig. 3g), the chlorophyll *a* content also increased in the sub-surface layer. Occasionally, high chlorophyll *a* values were detected close to the upwelling front in the northern part of the study area. While the sub-surface maxima of chlorophyll *a* were observed at the buoy station and the ScanFish transect at the beginning of July 2012 (Fig. 11), they disappeared when the upwelling events occurred near the northern coast. During the upwelling development, both the chlorophyll *a* content in the surface layer and the thickness of the surface layer with elevated chlorophyll *a* increased from north to south. However, those tendencies had pronounced intermittency at lateral scales of 1 to a few kilometers. A similar distribution pattern was registered in the phase of the upwelling/downwelling relaxation on 31 July 2012.

4 Discussion and conclusions

Many earlier studies have noticed that proper in situ measurements to reveal sub-mesoscale features are difficult to organize since the variability both in space and in time has to be tackled simultaneously (e.g., Hosegood et al., 2008, Niewiadomska et al., 2008, Pietri et al., 2013). Especially challenging are the investigations of sub-mesoscale processes in the coastal, relatively shallow but vertically stratified sea areas where the characteristic baroclinic Rossby radius is on the order of a few kilometers, as in the Gulf of Finland – 2–5 km (Alenius et al., 2003). We suggest that the most promising approach to solve the problem is to apply a combination of autonomous and research-vessel-based devices, such as Ferryboxes, moored profilers, underwater autonomous vehicles (gliders) and towed undulating instruments (ScanFish).

Simultaneous temporal changes that could be related to mesoscale processes are clearly seen in horizontal and vertical distributions of temperature and salinity presented in Fig. 3. The sub-mesoscale features such as upwelling filaments were also registered simultaneously by both systems, for instance in the first half of July 2009 and on 24 July 2010. Furthermore, the buoy profiler and ScanFish simultaneously detected intrusions of water with different salinity in the thermocline layer. Thus, the application of high-resolution autonomous and towed devices, which measure horizontal and vertical distributions of environmental parameters, makes it possible to detect meso- and sub-mesoscale features and quantitatively estimate their properties. In the present study, the underwater gliders were not applied, but they have been successfully tested in the Baltic Sea (e.g., Karstensen et al., 2014).

If the high-resolution measurements have a large enough coverage in space and time, one is able to reveal statistical parameters of sub-mesoscale variability. In turn, this would lead to an improved parameterization of sub-grid processes in the numerical models that has been considered as a prob-

lem in the modeling of the relatively shallow, but stratified Baltic Sea sub-basins (Tuomi et al., 2012; Omstedt et al., 2014). It also allowed us to display some general features of spatiotemporal variability of temperature and salinity in the study region – the central Gulf of Finland. The upwelling events along the southern coast were associated with higher horizontal variability of temperature in the surface layer than those along the northern coast (Kikas and Lips, 2015; Liblik and Lips, 2016). In the case of prevailing westerly winds, the seasonal thermocline has a deeper position and the vertical gradient of salinity is weaker than in the case of easterly winds (Liblik and Lips, 2012).

One of the questions addressed in the present study was whether the wavenumber spectra of temperature variance convert to -3 slope predicted by the theory of quasi-geostrophic turbulence in the ocean interior (Charney, 1971) or rather to $-5/3$ slope predicted by the theory of surface quasi-geostrophic turbulence (Held et al., 1995). We found that the wavenumber spectra of temperature variance in the surface layer had slopes varying mostly between -1.8 and -3.7 estimated for the lateral scales from 10 to 0.5 km. Nevertheless, when high variability at the mesoscale, i.e., pronounced mesoscale features, were observed, the spectral slopes were shallower than -2. Similar tendency towards -2 slope was obtained for the wavenumber spectra of temperature variance in the thermocline layer between the spatial scales of 10 and 1 km. These estimates were very stable over the 4 years of Ferrybox measurements and all ScanFish surveys analyzed in the present study.

Such conversion of wavenumber spectra of temperature variance to -2 slope has been identified earlier in other sea areas by high-resolution modeling (e.g., Capet et al., 2008) and in situ measurements (e.g., Hodges and Rudnick, 2006). Based on remote sensing altimeter data, it is shown that sea level wavenumber spectra also correspond well to the surface quasi-geostrophic theory (Le Traon et al., 2008). In a recent study, Kolodziejczyk et al. (2015) showed that if the surface density is analyzed then the -2 spectral slope is obtained in summer conditions when the salinity and temperature variations do not compensate each other (in north-eastern subtropical Atlantic Ocean). We have used temperature data to estimate potential energy wavenumber spectra assuming that mostly temperature determines the density in the upper layer (including the seasonal thermocline) in the Gulf of Finland in summer. It has to be noted that the wavenumber spectra of density variance corresponded to -2 slope as well when the spatial variability was dominated by coastal upwelling events. According to these findings, the sub-mesoscale processes have to be more energetic than suggested by the quasi-geostrophic theory of turbulence in the ocean interior. Thus, the observed high lateral variability of temperature in the surface layer and associated -2 spectral slopes suggest a significant role of sub-mesoscale processes in vertical exchanges in the stratified Gulf of Finland and similar sea areas.

The lateral variability of temperature in the sub-surface layer was the highest during the surveys when the upwelling events either off the southern or off the northern coast occurred (ScanFish sections on 27 July 2010 and 20 July 2012). Higher intrusion index values in the sub-surface layer were also found at the ScanFish sections in relation to the development and relaxation of coupled upwelling/downwelling events, except at the section crossing the meandering upwelling front on 27 July 2010. One could suggest that the intrusion index (counted as a sum of salinity inversions) indicates the presence of the layered flow structure and thus, the intensity of lateral mixing. When analyzing the characteristics of coastal upwelling, Kikas and Lips (2015) suggested that two types of upwelling events could be identified. During the event on 18–27 July 2012, no pronounced upwelling front was detected, rather a gradual decrease of the surface temperature from the open sea towards the coast with remarkable variability at the sub-mesoscale was observed. It was suggested that such upwelling events could develop when the wind forcing is weaker than required to generate an Ekman drift in the entire upper layer and consecutive surfacing of the thermocline.

The observed salinity intrusions at the ScanFish section on 20 July 2012 support the above suggestion by Kikas and Lips (2015). The seasonal thermocline was relatively deep in July 2012 and most probably, the observed salinity intrusions were formed as a response to the winds favorable for the upwelling near the northern coast. Consequently, in such conditions, the lateral mixing is enhanced as the transport of water with different characteristics upward and downward along the inclined isopycnals. In turn, it could result in enhanced vertical (diapycnal) mixing of water at laterally distant places from their origin. We suggest that sub-mesoscale dynamics and layered flow structure contribute significantly to the lateral and vertical mixing in the stratified sea areas under variable wind forcing.

The highest values of intrusion index were registered at the buoy station in late July – early August 2012 and at the ScanFish section on 31 July 2012 during the relaxation of the downwelling near the southern coast. Apart of this major sub-mesoscale structure, similar intrusions visible in the vertical salinity distribution at the buoy station were quite frequent in the summers of 2009–2012 in the seasonal thermocline layer, e.g., in late July–early August 2009, in mid-August 2011 and in July and August 2012 (Fig. 3). In addition, water with slightly lower salinity was occasionally seen at the buoy station in July 2010 and clear evidence is provided by the ScanFish surveys on 22 July 2010 and 2 August 2010 that such intrusions of low salinity water in the upper part of the seasonal thermocline originated from patches of lower surface salinity in the central gulf. At least on two occasions could we detect clear inclination of salinity intrusions in relation to the isopycnals – on 2 August 2010 in the southern part of the section and on 20 July 2012 in the central part of it. This finding is similar to the observations by Pietri

et al. (2013) in the upwelling system off southern Peru, where they suggested that observed sub-mesoscale features could be the result of the stirring by the mesoscale circulation. Note that the sub-surface chlorophyll a maxima registered in the northern part of the ScanFish section on 22 July 2010 were also inclined in relation to the isopycnals (see Fig. 11).

Two examples of bloom development in the near-coastal convergence zone were shown in the present study – in late July 2010 near the northern coast and in July and August 2012 near the southern coast (Fig. 10). Lips and Lips (2014) suggested that the bloom near the northern coast in 2010 could be related to the sub-surface maxima of chlorophyll a, which contained the vertically migrating dinoflagellate *Heterocapsa triquetra* in very high numbers. Similar development of the biomass peak with a relatively high share of this vertically migrating species in the surface layer was observed in the same area also in August 2006 (Lips and Lips, 2010). The highest biomass and chlorophyll a content in that convergence zone was associated with the locally higher location of isopycnals, thus, with the stratified conditions in the surface layer, although in the downwelling area.

The ScanFish surveys conducted during the downwelling event and its relaxation at the end of July 2012 did not show high chlorophyll a content in the sub-surface layer. However, the data both from the buoy station and from the ScanFish surveys registered clearly enhanced chlorophyll a content in the surface layer with quite a large intermittency in the chlorophyll a content and layer thickness with enhanced chlorophyll a content (Figs. 10 and 11). Note that the blooms lasted relatively long time (about 10 days), and the highest biomass (chlorophyll a content) was not observed near the mesoscale upwelling front where the largest vertical velocities could be expected (e.g., Thomas and Lee, 2005). Levy et al. (2012) showed that the sub-mesoscale processes have large-scale effect on phytoplankton growth in the ocean, which could be seen at larger scales and distant places. An improvement in the resolution of ocean circulation models has resulted in more energetic motions not only close to the large scale (or mesoscale) fronts but rather in the surface layer of the whole modeling domain (Capet et al., 2008; Levy et al., 2010).

We suggest that the maintenance of the bloom, which could not be explained by pure convergence due to the Ekman drift in the surface layer, must benefit from other processes feeding the surface layer with nutrients and/or biomass. The ageostrophic sub-mesoscale processes could be responsible for re-stratification of the surface layer, vertical transport and thus, also for growth enhancement (Levy et al., 2012). This conclusion supports the concept that the vertical exchanges related to the mesoscale processes (eddies) are enhanced due to the sub-mesoscale activity and not only in the vicinity but also far off the mesoscale features (Klein and Lapeyre, 2009).

The results of the present study can be concluded as follows. The analysis of high-resolution data from summers

2009–2012 revealed pronounced sub-mesoscale features in the surface and subsurface layer, e.g., upwelling and downwelling filaments and intra-thermocline intrusions with spatial scales of a few kilometers (typical baroclinic Rossby radius in the Gulf of Finland is 2–5 km). The horizontal wavenumber spectra of temperature variance estimated between the lateral scales of 10 and (1)0.5 km had the slopes close to −2 both in the surface layer and in the seasonal thermocline. It shows that the ageostrophic sub-mesoscale processes contribute considerably to the energy cascade in this stratified sea basin. We showed that the role of sub-mesoscale processes was significant especially in the conditions of changing wind forcing, e.g., during the development and relaxation of coastal upwelling and downwelling events. We suggest that the sub-mesoscale processes play a major role in feeding surface blooms in the conditions of coupled coastal upwelling and downwelling events in the Gulf of Finland.

References

Aitsam, A., Hansen, H.-P., Elken, J., Kahru, M., Laanemets, J., Pajuste, M., Pavelson, J., and Talpsepp, L.: Physical and chemical variability of the Baltic Sea: a joint experiment in the Gotland basin, Cont. Shelf Res., 3, 291–310, 1984.

Alenius, P., Nekrasov, A., and Myrberg, K.: Variability of the baroclinic Rossby radius in the Gulf of Finland, Cont. Shelf Res., 23, 563–573, 2003.

Bouffard, J., Renault, L., Ruiz, S. Pascual, A., Dufau, C., and Tintoré, J.: Sub-surface small-scale eddy dynamics from multi-sensor observations and modeling, Progr. Oceanogr., 106, 62–79, 2012.

Capet, X., Mcwilliams, J. C., Molemaker, M. J., and Shchepetkin, A. F.: Mesoscale to submesoscale transition in the California current system, Part I: Flow structure, eddy flux, and observational tests, J. Phys. Oceanogr., 38, 29–43, 2008.

Charney, J.: Geostrophic turbulence, J. Atmos. Sci., 28, 1087–1095, 1971.

HELCOM: Guidelines for the Baltic monitoring programme for the third stage, Part D: Biological determinants, Baltic Sea Environmental Proceedings, 27, 1–161, 1988.

Held, I. M., Pierrehumbert, R. T., Garner, S. T., and Swanson, K. L.: Surface quasi-geostrophic dynamics, J. Fluid Mech., 282, 1–20, 1995.

Hodges, B. A. and Rudnick, D. L.: Horizontal variability in chlorophyll flyuorescence and potential temperature, Deep-Sea Res. Pt. I, 53, 1460–1482, 2006.

Hosegood, P. J., Gregg, M. C., and Alford, M. H.: Restratification of the surface mixed layer with submesoscale lateral density gradients: diagnosing the importance of the horizontal dimension, J. Phys. Oceanogr., 38, 2438–2460, 2008.

Jenkins, W. J.: Nitrate flux into the euphotic zone near Bermuda, Nature, 331, 521–523, 1988.

Karstensen, J., Liblik, T., Fischer, J., Bumke, K., and Krahmann, G.: Summer upwelling at the Boknis Eck time-series station (1982 to 2012) – a combined glider and wind data analysis, Biogeosciences, 11, 3603–3617, doi:10.5194/bg-11-3603-2014, 2014.

Kikas, V. and Lips, U.: Upwelling characteristics in the Gulf of Finland (Baltic Sea) as revealed by Ferrybox measurements in 2007–2013, Ocean Sci. Discuss., 12, 2863–2898, doi:10.5194/osd-12-2863-2015, 2015.

Klein, P. and Lapeyre, G.: The oceanic vertical pump induced by mesoscale and submesoscale turbulence, Annu. Rev. Mar. Sci., 1, 351–75, 2009.

Kolodziejczyk, N., Reverdin, G., Boutin, J., and Hernandez, O.: Observation of the surface horizontal thermohaline variability at mesoscale to submesoscale in the north-eastern subtropical Atlantic Ocean, J. Geophys. Res. Oceans, 120, 2588–2600, 2015.

Laanemets, J., Väli, G., Zhurbas, V., Elken, J., Lips, I., and Lips, U.: Simulation of mesoscale structures and nutrient transport during summer upwelling events in the Gulf of Finland in 2006, Boreal Environ. Res., 16, 15–26, 2011.

Le Traon, P. Y., Klein, P., Hua, B. L., and Dibarboure, G.: Do altimeter wavenumber spectra agree with the interior or surface quasi-geostrophic theory?, J. Phys. Oceanogr., 38, 1137–1142, 2008.

Levy, M., Klein, P., Trequier, A. M., Iovino, D., Madec, G., Masson, S., and Takahashi, K.: Modifications of gyre circulation by sub-mesoscale physics, Ocean Model., 34, 1–15, 2010.

Levy, M., Ferrari, R., Franks, P. J., Martin, A. P., and Riviere, P.: Bringing physics to life at the submesoscale, Geophys. Res. Lett., 39, L14602, doi:10.1029/2012GL052756, 2012.

Liblik, T. and Lips, U.: Variability of synoptic-scale quasi-stationary thermohaline stratification patterns in the Gulf of Finland in summer 2009, Ocean Sci., 8, 603–614, doi:10.5194/os-8-603-2012, 2012.

Liblik, T. and Lips, U.: Variability of pycnoclines in a three-layer, large estuary: the Gulf of Finland, Est. Boreal Environ. Res., in press, 2016.

Lips, I. and Lips, U.: Phytoplankton dynamics affected by the coastal upwelling events in the Gulf of Finland in July–August 2006, J. Plankton Res., 32, 1269–1282, 2010.

Lips, I., Lips, U., Jaanus, A., and Kononen, K.: The effect of hydrodynamics on the phytoplankton primary production and species composition at the entrance to the Gulf of Finland (Baltic Sea) in July 1996, Proc. Est. Acad. Sci. Biol. Ecol., 54, 210–229, 2005.

Lips, I., Lips, U., and Liblik, T.: Consequences of coastal upwelling events on physical and chemical patterns in the central Gulf of Finland (Baltic Sea), Cont. Shelf Res., 29, 1836–1847, 2009.

Lips, U. and Lips, I.: Bimodal distribution patterns of motile phytoplankton in relation to physical processes and stratification (Gulf of Finland, Baltic Sea), Deep-Sea Res. Pt. II, 101, 107–119, 2014.

Lips, U., Lips, I., Liblik, T., Kikas, V., Altoja, K., Buhhalko, N., and Rünk, N.: Vertical dynamics of summer phytoplankton in a stratified estuary (Gulf of Finland, Baltic Sea), Ocean Dyn., 61, 903–915, 2011.

Martin, A. P. and Pondaven, P.: On estimates for the vertical nitrate flux due to eddy pumping, J. Geophys. Res., 108, 3359, doi:10.1029/2003JC001841, 2003.

McGillicuddy, D. J., Robinson, A. R., Siegel, D. A., Jannasch, H. W., Johnson, R., Dickey, T. D., McNeil, J., Michaels, A. F., and Knap, A. H.: Influence of mesoscale eddies on new production in the Sargasso Sea, Nature, 394, 263–266, 1998.

Nausch, M., Nausch, G., Lass, H. U., Mohrholz, V., Nagel, K., Siegel, H., and Wasmund, N.: Phosphorus input by upwelling in the eastern Gotland Basin (Baltic Sea) in summer and its effects on filamentous cyanobacteria, Estuar. Coast. Shelf Sci., 83, 434–442, 2009.

Niewiadomska, K., Claustre, H., Prieur, L., and d'Ortenzio, F.: Sub-mesoscale physical-biogeochemical coupling across the Ligurian Current (northwestern Mediterranean) using a bio-optical glider, Limnol. Oceanogr., 53, 2210–2225, 2008.

Omstedt, A., Elken, J., Lehmann, A., and Piechura, J.: Knowledge of the Baltic Sea physics gained during the BALTEX and related programmes, Progr. Oceanogr., 63, 1–28, 2004.

Omstedt, A., Elken, J., Lehmann, A., Leppäranta, M., Meier H. E. M., Myrberg, K., and Rutgersson, A.: Progress in physical oceanography of the Baltic Sea during the 2003–2014 period, Progr. Oceanogr., 128, 139–171, 2014.

Pietri, A., Testor, P., Echevin, V., Chaigneau, A., Mortier, L., Eldin, G., and Grados, C.: Fine scale vertical structure of the upwelling system of Southern Peru as observed from glider data, J. Phys. Oceanogr., 43, 631–646, 2013.

Simpson, J. H. and Bowers D. G.: Models of stratification and frontal movements in shelf seas, Deep-Sea Res., 28, 727–738, 1981.

Simpson, J. H., Brown, J., Matthews, J., and Allen, G.: Tidal straining, density currents and mixing in the control of estuarine stratification, Estuar. Coast., 13, 125–132, 1990.

Thomas, L. N.: Formation of intrathermocline eddies at ocean fronts by wind-driven destruction of potential vorticity, Dynam. Atmos. Oceans, 45, 252–273, 2008.

Thomas, L. N. and Lee, C. M.: Intensification of ocean fronts by down-front winds, J. Phys. Oceanogr., 35, 1086–1102, 2005.

Tuomi, L., Myrberg, K., and Lehmann, A.: The performance of the parameterisations of vertical turbulence in the 3D modelling of hydrodynamics in the Baltic Sea, Cont. Shelf Res., 50/51, 64–79, 2012.

Uiboupin R. and Laanemets J.: Upwelling characteristics derived from satellite sea surface temperature data in the Gulf of Finland, Baltic Sea, Boreal Environ. Res., 14, 297–304, 2009.

Uiboupin, R., Laanemets, J., Sipelgas, L., Raag, L., Lips, I., and Buhhalko, N.: Monitoring the effect of upwelling on the chlorophyll a distribution in the Gulf of Finland (Baltic Sea) using remote sensing and in situ data, Oceanologia, 54, 395–419, 2012.

Paper IV

Lips, I., Rünk, N., Kikas, V., Meerits, A., Lips, U. (2014). High-resolution dynamics of spring bloom in the Gulf of Finland, Baltic Sea. *Journal of Marine Systems*, 129, 135–149, doi: 10.1016/j.jmarsys.2013.06.002.

High-resolution dynamics of the spring bloom in the Gulf of Finland of the Baltic Sea

Inga Lips *, Nelli Rünk, Villu Kikas, Aet Meerits, Urmas Lips

Marine Systems Institute, Tallinn University of Technology, Akadeemia Rd. 15A, 12618 Tallinn, Estonia

ARTICLE INFO

ABSTRACT

During the period from March to the end of May in 2009 and 2010, intensive measurements and sampling were undertaken in the Gulf of Finland. The compiled results indicate a high variability of the phytoplankton distribution both temporally and spatially. The spring bloom dynamics and heterogeneity was influenced by physical forcing, such as prevailing circulation in the surface layer and the development of stratification, including the upward and downward movement of the seasonal thermocline. The estimated ratio of nitrogen to phosphorus consumption during the growth phase of the spring bloom was close to the Redfield ratio during both springs. The maximum phytoplankton carbon biomass was observed after the depletion of inorganic nitrogen from the surface layer, which coincides with the transition in the community dominance from diatoms to dinoflagellates. Diatoms exhibited a short, well-defined period of high biomass, and we argue that measurements with low temporal resolution can overlook this period of diatom dominance in the Gulf of Finland. The observed dominance of dinoflagellates (*Peridiniella catenata* and the *Scrippsiella/Biecheleria* complex) and the ciliate *Myrionecta rubra* might have a substantial biogeochemical impact because these species increase the retention time of newly produced material in the nutrient-limited surface layer in late spring.

© 2013 Elsevier B.V. All rights reserved.

1. Introduction

According to the European Water Framework Directive (WFD, 2000/60/EC) and the Marine Strategy Framework Directive (MSFD, 2008/56/EC), the phytoplankton community composition, abundance and biomass are one of the biological quality elements that are used in the assessment of the ecological/environmental status of coastal and marine waters. During the last decade, climate change and global warming have received much attention in the context of changes to the marine ecosystem. Thus, the spring bloom, which is a typical feature in temperate aquatic ecosystems, has also received extensive attention in the assessment of the impact of anthropogenic pressure and climate change. The wintertime accumulation of inorganic nutrients in the whole water body and the physical conditions in the surface layer determine the spring bloom in the Baltic Sea (Kahru and Nõmmann, 1990; Stipa, 2004; Sverdrup, 1953). Nitrogen is considered the limiting nutrient in the Baltic Sea, and nitrate is the main form of inorganic nitrogen present at the commencement of the spring bloom. In the Gulf of Finland, nitrate depletion during the bloom is obviously a major cause of the rapid decline in the phytoplankton biomass, especially under the recently observed nutrient conditions, which usually include detectable residual amounts of

phosphates and silicates in the surface layer after the spring bloom (e.g., Hällfors et al., 1981; Tamelander and Heiskanen, 2004).

In the Baltic Sea, a major part of the spring bloom phytoplankton biomass is lost by sedimentation due to the slow development of mesozooplankton. Johansson et al. (2004) showed that 85% of the spring heterotrophic biomass (micro- and mesozooplankton) in the Baltic Sea is composed of ciliates. The mesozooplankton species are mostly in the nauplii stage during the vernal bloom. Because nauplii feed on smaller particles, these organisms cannot control the spring bloom biomass, which mostly consists of large chain-forming diatoms and dinoflagellates (Lignell et al., 1993). Ciliates are known to reach their peak biomass shortly after the spring bloom, and, according to carbon consumption estimates (Johansson et al., 2004), up to 15% and 4% of the spring net primary production are potentially consumed by ciliates and mesozooplankton, respectively. The marine photosynthetic ciliate *Myrionecta rubra* (Lohmann, 1908) Jankowski 1976 is an important protist in the stratified Baltic Sea, where it can exploit the available resources through diurnal vertical migration (Crawford and Lindholm, 1997; Lindholm and Mörk, 1990; Thamm et al., 2004). This ciliate can attain high biomasses during spring bloom (e.g., Wasmund et al., 2013) and inhabits different depths in the summer (e.g., Rychert, 2004).

Studies in the 1970s demonstrated the dominance of cold-water diatoms in the Baltic Sea during the spring bloom (Hällfors et al., 1981 and references therein). Several recent analyses have shown long-term changes in the phytoplankton community composition,

* Corresponding author. Tel.: +372 6204303; fax: +372 6204301.
E-mail address: inga.lips@msi.ttu.ee (I. Lips).

abundance, and annual succession. The observed changes in phytoplankton include a higher overall spring bloom biomass throughout the Baltic Sea (Alheit et al., 2005), an increased dinoflagellate contribution to the spring bloom biomass (Wasmund and Uhlig, 2003), and an earlier onset of the spring bloom (Fleming and Kaitala, 2006). In the latest reports of the periodic assessment of the state of the marine environment in the Baltic Sea published by the Helsinki Commission (HELCOM), the spring bloom was not thoroughly described due to a clear focus shift toward summer cyanobacterial blooms. However, five dominant vernal bloom species in the Baltic Sea basins during three periods (1979–83, 1984–88, and 1989–93) were reported in the third periodic assessment (HELCOM, 1996) and allow us to determine whether there have been clear changes in the species dominance in the Gulf of Finland during the spring bloom since that time.

There are few data available on the phytoplankton community composition due to the costs associated with traditional marine environment monitoring using research vessels and manpower for the quantitative counting of samples. This lack of data results in a reduction in the spatial coverage and temporal resolution that is required to study phytoplankton dynamics and the correlations between phytoplankton and physical, chemical, and other biological parameters. This is especially true during the spring bloom period due to the high variability in the phytoplankton community, i.e., if the aim is to follow the seasonal dynamics in detail or to study the long-term trends in the composition of the spring bloom community. To fill the gaps and increase the knowledge and understanding of the dynamics in a marine environment, the use of different autonomous platforms in marine research and monitoring in the Baltic Sea area is increasing (Fleming and Kaitala, 2006; Jaanus et al., 2009; Lips and Lips, 2008; Lips et al., 2011; Rantajärvi et al., 1998; Schneider et al., 2006; Vepsäläinen et al., 2005). In addition, autonomous platforms have been used to improve the prognostic capabilities of circulation, especially in areas with complex hydrography (e.g., Grayek et al., 2011), and biogeochemical models (Roiha et al., 2010).

Several recent studies have analysed conventional phytoplankton monitoring data with the aim of showing the trends or shifts in the Baltic Sea ecosystem, including the characteristics of the spring bloom (e.g., Klais et al., 2011; Wasmund et al., 2011). A more detailed temporal evolution of the spring bloom can be obtained using the ships-of-opportunity/Ferrybox technique, but most of these studies have focused on chlorophyll *a* (Chl *a*) or fluorescence data (Fleming and Kaitala, 2006). High-resolution data (in both space and time) on the phytoplankton species composition and biomass that cover the full spring bloom period have not been available until now.

Attempts have been made to model the long-term and seasonal dynamics of nutrients and the Chl *a* content or phytoplankton/cyanobacteria biomass in the Baltic Sea and its sub-basins (e.g., Eilola et al., 2009; Maar et al., 2011; Müller-Karulis and Aigars, 2011). Mostly constant values have been used for the conversion factors that link carbon (C) to the nitrogen (N) and phosphorus (P) contents in accordance with the Redfield ratio (molar ratio 106:16:1) and the nutrient contents to the Chl *a* content, e.g., carbon to chlorophyll as 50 μg C to 1 μg Chl *a* (Eilola et al., 2009) and nitrogen to chlorophyll as 0.63 μM N to 1 μg Chl *a* l^{-1} (Eilola et al., 2009) or 0.5 μM N to 1 μg Chl *a* l^{-1} (Maar et al., 2011). Based on the analysis of Ferrybox nutrient data from the period of 1993 to 2009, it was suggested that spring bloom phytoplankton have the ability to excessively uptake phosphorus in relation to nitrogen (Raateoja et al., 2011). To match the model outputs with observations, it was suggested that the classical Redfield ratio should be replaced with a constant but lower ratio for the N:P uptake, e.g., 10:1 (Wan et al., 2011). In addition, the use of constant conversion factors under changing nutrient and light conditions in natural systems has been questioned (Mateus et al., 2012), and high-resolution data appear to be essential to understand the links between the phytoplankton dynamics and the environmental conditions and to suggest relevant approaches that should be used in ecological models.

The main aim of the present paper was to describe the dynamics of the spring bloom in the Gulf of Finland based on high-resolution measurements and sampling in 2009 and 2010 and to correlate the observed features and the temporal and spatial variability of the bloom to physical and chemical patterns. Employing new technologies and high-resolution sampling, we linked the dynamics of the spring bloom, e.g., the dominance and peaking of different species and the related nutrient dynamics, to the environmental conditions and physical processes. Based on the observational results, we also discuss several key concepts and recent suggestions, such as a shift toward the dominance of dinoflagellates and the use of a non-Redfield ratio for the uptake rates of nitrogen and phosphorus.

2. Materials and methods

The study was conducted in the Gulf of Finland of the Baltic Sea. The sampling transect was located in the central part of the gulf between Tallinn and Helsinki (Fig. 1). The width of the gulf in the study area is less than 80 km, and the measurements were collected in a 72-km wide area along the ferry route (excluding an area of approximately 4 km close to each harbour).

The Ferrybox system, which was installed aboard the passenger ferry "Baltic Princess" (AS Tallink Grupp) that travels between Tallinn and Helsinki, was used for the measurements and sampling in the surface layer in 2009 and 2010. Water was pumped through the measuring system as the ferry travelled. The water intake was located at a depth of approximately 4 m. The temperature (T; PT-100 sensor), salinity (S; FSI Excell thermosalinograph), and Chl *a* fluorescence (SCUFA Turner Design) were recorded twice a day along the ferry route (Fig. 1) with a time resolution of 20 s, which corresponds approximately to a spatial resolution of 150 m between each collected data point. The water sampling from up to 17 locations along the ferry route was conducted using an automatic refrigerating (4 °C) sampler (Sigma 900 MAX) on the dates shown in Tables 1–3. The collected water samples were analysed to determine the concentrations of PO$_4^{3-}$, NO$_2^-$ + NO$_3^-$, and Chl *a*, the phytoplankton species composition, wet weight, and carbon (C) biomass. The success of sampling during early spring is dependent on the ice conditions because the system may automatically switch off if even small pieces of ice are detected in the debubbling chamber. Because there were relatively heavy ice conditions in the Gulf of Finland, the sampling was less successful in March 2010.

CTD measurements using an Ocean Seven 320*plus* CTD probe (Idronaut S.r.l.) equipped with a Seapoint Chl *a* fluorometer and water sampling aboard the research vessel were performed at Station AP5 on 8, 14, 21, and 26 April and 5, 11, and 21 May in 2010 (Fig. 1). The vertical resolution of the water sampling was in the range of 5 to 10 m. The water samples were analysed to determine the inorganic nutrient (PO$_4^{3-}$ and NO$_2^-$ + NO$_3^-$) concentrations and the Chl *a* content. Samples were also collected on 9, 17, and 30 June to describe the nutrient and phytoplankton dynamics during the summer. These results are not shown in the present paper but are partly used in the discussion to support a suggestion.

The samples collected for nutrient analysis were deep-frozen at −20 °C after collection and analysed at the shore-based laboratory using the automatic nutrient analysers μMac 1000 (Systea S.r.l.) and Lachat QuikChem 8500 Series 2 (Lachat Instruments, Hach Company). The nutrient analyses were performed according to the guidelines of the American Public Health Association (APHA, 1992; methods 4500-NO3 F and 4500-P F for μMac 1000) and recommendations made by USEPA, ISO, and DIN standards (methods 31-107-04-1-D NO3 (Lachat Instruments, 2000) and 31-115-01-1-I PO4 (Lachat Instruments, 2001) for the Lachat instrument). The lower detection range for PO$_4^{3-}$ and NO$_2^-$ + NO$_3^-$ using the μMac 1000 was 1 ppb (parts per billion; 0.03 and 0.07 μM, respectively; with a measurement uncertainty of
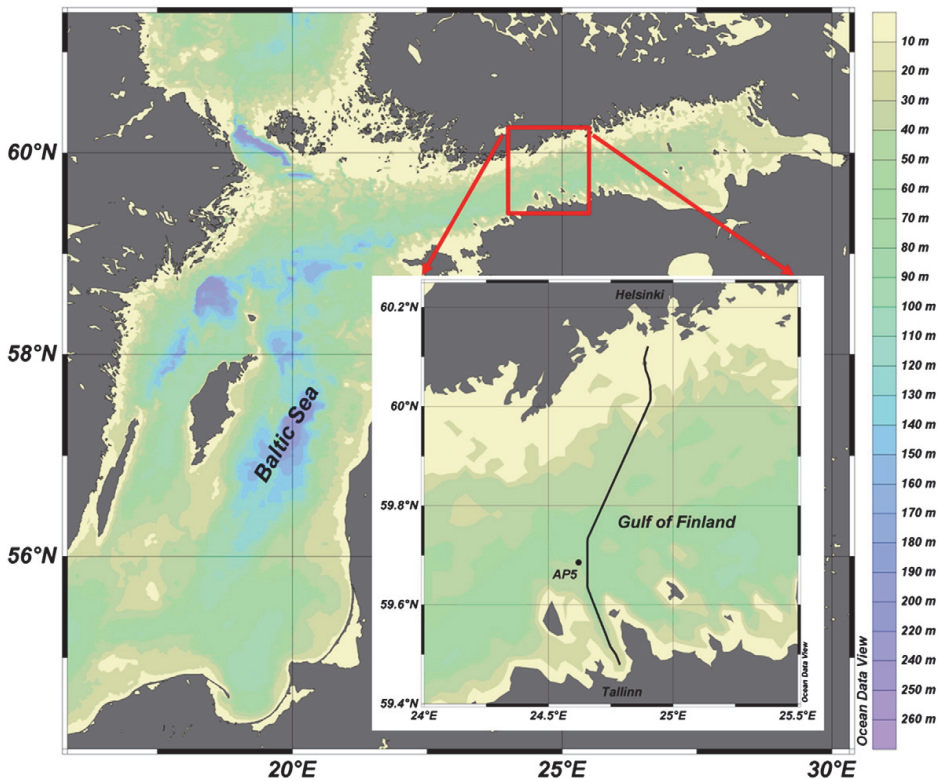
Fig. 1. Map of the study area. The Ferrybox line between Tallinn and Helsinki and station AP5 are shown.

20% near the detection limit). The corresponding parameters for the Lachat instrument were 0.008 and 0.014 μM, respectively.

The Chl *a* concentration in the water samples was determined using Whatman GF/F glass fibre filters following extraction at room temperature in the dark with 96% ethanol for 24 h. The Chl *a* content from the extract was measured spectrophotometrically (Thermo Helios γ) in the laboratory (HELCOM, 1988).

Phytoplankton sub-samples (100 ml) were preserved with an acid Lugol solution (HELCOM recommendations and EVS-EN 15972:2011 standard) and analysed using the technique developed by Utermöhl (1958) and the PhytoWin software (Kahma Ky). The wet weight biomasses calculated according to Olenina et al. (2006), which are shown in Tables 1–3, were compared with historical records (e.g., HELCOM, 1996). The phytoplankton carbon content was calculated using C: biovolume factors according to Menden-Deuer and Lessard (2000). Different C:biovolume relationships were used for diatoms and other protist plankton. However, instead of invoking differences between different sizes of diatoms, the following formula was used for all of the cells (including cells with a volume greater than 3000 μm³; ESD = 17 μm): pgC cell^{-1} = 0.288 × volume$^{0.811}$. The use of this formula may cause a 20 to 30% underestimation of the C biomass of bigger cells. However, the only species in our samples that had larger cells was *Thalassiosira baltica*. C biomass of naked ciliates was calculated according to the method described by Putt and Stoecker (1989).

The proportion of dinoflagellates was calculated by dividing the C biomass of dinoflagellates by the total C biomass of dinoflagellates and diatoms.

The consumption rates of nutrients were estimated using a simple linear regression model: $N = b \times day + a$, where N is the nutrient concentration ($NO_2^- + NO_3^-$ or PO_4^{3-}), *day* is the day of the year, *b* is the slope of the regression line, and *a* is the intercept of the regression line. The absolute value of the estimated slope is considered the consumption rate, i.e., the amount of consumed nutrients in μM per day. Thus, the ratio of the slopes of the two regression lines is an estimate of the ratio of the nitrogen:phosphorus (N:P) uptake rates. Depending on the objective, different periods for the regression analysis and the estimation of the consumption rate were used.

3. Results

3.1. Hydrophysical background

The Gulf of Finland was partially ice-covered in the winter of 2009 and almost fully ice-covered in the winter of 2010. In March 2009, the ice was mostly found in the northern part of the gulf, whereas, in March 2010, the ice was present along almost the whole cross-section and occasionally caused breaks in the measurements. In 2009, the temperature of maximum density (2.5 °C) was reached in the surface waters on 5 April in the southern part, between 10 and 12 April in the central part, and between 19 and 21 April in the northern part of the gulf (Fig. 2). In 2010, the temperature increase started later and exhibited a different pattern: the increase was faster in the coastal zones compared with the open waters. The temperature of maximum density was reached on 11 April in the southern part, on 14 April in the northern part, and between 19 and 21 April in the central part of the gulf. By the end of May, the surface water temperature along the cross section was 12–13 °C in 2009 and approximately 10 °C in 2010 (Fig. 2).

Table 1
Average concentrations ± standard deviation of $NO_2^- + NO_3^-$, PO_4^{3-}, Chl a, phytoplankton carbon biomass, and carbon to Chl a ratio along the ferry route from Tallinn to Helsinki in March 2009 and 2010. The five dominant species (according to the wet weight biomass) with their corresponding average and maximum biomass values (shown in brackets) at each sampling date are listed. N — number of samples analysed, n — number of stations where a species was among the five dominant species.

	March				
2009	01.03.	10.03.	16.03.	22.03.	29.03.
$NO_2^- + NO_3^-$ (µM)	–	–	–	–	7.2 ± 1.6 (N = 17)
PO_4^{3-} (µM)	0.83 ± 0.06 (N = 17)	0.82 ± 0.03 (N = 11)	0.79 ± 0.04 (N = 14)	0.82 ± 0.03 (N = 15)	0.71 ± 0.06 (N = 17)
Chl a (mg m^{-3})	2.42 ± 1.30 (N = 17)	1.34 ± 0.47 (N = 11)	2.80 ± 1.79 (N = 14)	2.76 ± 0.89 (N = 15)	6.38 ± 1.91 (N = 17)
Carbon biomass (mg m^{-3})	47 ± 23 (N = 17)	16 ± 7 (N = 11)	53 ± 62 (N = 14)	66 ± 25 (N = 14)	130 ± 68 (N = 14)
Mean C:Chl a ratio	19.4	11.8	18.8	23.9	20.4
Wet weight biomass (mg m^{-3})	365 ± 181 (N = 17)	141 ± 69 (N = 11)	451 ± 503 (N = 14)	541 ± 202 (N = 15)	1098 ± 532 (N = 17)
	Scri/Biech 191 (350, n = 17)	*Scri/Biech* 50 (85, n = 11)	*Scri/Biech* 164 (1059, n = 14)	*Scri/Biech* 171 (345, n = 15)	*Scri/Biech* 472 (1345, n = 17)
	P. catenata 99 (235, n = 17)	*P. catenata* 29 (64, n = 11)	*P. catenata* 118 (687, n = 14)	*P. catenata* 114 (217, n = 15)	*P. catenata* 202 (738, n = 16)
	M. rubra 28 (85, n = 14)	*T. levanderi* 14 (36, n = 11)	*T. levanderi* 33 (79, n = 14)	*M. rubra* 92 (198, n = 15)	*T. levanderi* 160 (323, n = 16)
	Aphaniz. 12 (85, n = 12)	*T. baltica* 11 (44, n = 7)	*P. taeniata* 26 (177, n = 3)	*T. levanderi* 57 (81, n = 15)	*M. rubra* 87 (214, n = 13)
	T. levanderi 6 (18, n = 12)	*M. arctica* 6 (46, n = 3)	*M. arctica* 19 (63, n = 6)	*T. baltica* 29 (110, n = 12)	*T. baltica* 52 (101, n = 16)
2010	–	–	–	25.03.	31.03.
$NO_2^- + NO_3^-$ (µM)	–	–	–	7.3 ± 1.3 (N = 14)	6.9 ± 1.3 (N = 10)
PO_4^{3-} (µM)	–	–	–	0.90 ± 0.05 (N = 14)	0.78 ± 0.05 (N = 10)
Chl a (mg m^{-3})	–	–	–	2.91 ± 1.58 (N = 14)	3.40 ± 0.73 (N = 10)
Carbon biomass (mg m^{-3})	–	–	–	71 ± 80 (N = 16)	53 ± 15 (N = 10)
Mean C:Chl a ratio	–	–	–	24.4	15.6
Wet weight biomass (mg m^{-3})	–	–	–	557 ± 594 (N = 16)	449 ± 111 (N = 10)
				Scri/Biech 196 (1405, n = 16)	*Scri/Biech* 105 (242, n = 10)
				M. rubra 135 (758, n = 16)	*T. levanderi* 82 (147, n = 10)
				P. catenata 83 (307, n = 15)	*M. rubra* 70 (126, n = 9)
				T. levanderi 49 (97, n = 16)	*P. catenata* 67 (119, n = 10)
				P. taeniata 30 (125, n = 11)	*P. taeniata* 31 (50, n = 8)

The surface layer salinity was lower in spring 2009 than in spring 2010: in the central part of the gulf, the salinity was mostly below 5.5 in March and April 2009 and close to 6 in March and April 2010 (Fig. 2). In 2009, the surface layer salinity decreased from April to May over the whole cross section. In contrast, in 2010, an increase in the salinity was observed near the southern coast in early May. Starting from mid-May (both in 2009 and in 2010), less saline waters appeared in the central part of the gulf, which altered the ordinary salinity distribution (a north–south salinity gradient) observed in March and April.

In spring 2010, the vertical profiles of temperature and salinity were measured at station AP5 close to the ferry line (see location in Fig. 1). According to the data acquired at this station, the temperature of maximum density was reached in the surface layer on 26 April.

Table 2
Average concentrations ± standard deviation of $NO_2^- + NO_3^-$, PO_4^{3-}, Chl a, phytoplankton carbon biomass, and carbon to Chl a ratio along the ferry route from Tallinn to Helsinki in April 2009 and 2010. The five dominant species (according to the wet weight biomass) with their corresponding average and maximum biomass values (shown in brackets) at each sampling date are listed. N — number of samples analysed, n — number of stations where a species was among the five dominant species.

	April			
2009	05.04.	12.04.	19.04.	26.04.
$NO_2^- + NO_3^-$ (µM)	5.6 ± 1.4 (N = 17)	2.7 ± 2.5 (N = 17)	2.0 ± 1.4 (N = 17)	0.2 ± 0.2 (N = 17)
PO_4^{3-} (µM)	0.55 ± 0.08 (N = 17)	0.38 ± 0.12 (N = 17)	0.45 ± 0.06 (N = 17)	0.20 ± 0.02 (N = 17)
Chl a (mg m^{-3})	11.58 ± 2.72 (N = 17)	20.20 ± 4.96 (N = 17)	14.55 ± 1.41 (N = 17)	14.34 ± 1.83 (N = 16)
Carbon biomass (mg m^{-3})	234 ± 117 (N = 17)	307 ± 97 (N = 17)	226 ± 50 (N = 17)	283 ± 53 (N = 17)
Mean C:Chl a ratio	20.2	15.2	15.5	19.7
Wet weight biomass (mg m^{-3})	2062 ± 913 (N = 17)	2717 ± 702 (N = 17)	2327 ± 558 (N = 17)	2717 ± 516 (N = 17)
	Scri/Biech 746 (2892, n = 17)	*Scri/Biech* 831 (3425, n = 17)	*T. baltica* 566 (863, n = 17)	*T. baltica* 870 (1052, n = 17)
	T. levanderi 478 (941, n = 17)	*T. levanderi* 614 (1254, n = 15)	*T. levanderi* 536 (889, n = 17)	*P. catenata* 388 (734, n = 17)
	P. catenata 341 (1632, n = 17)	*P. catenata* 307 (879, n = 17)	*Scri/Biech* 301 (569, n = 16)	*M. rubra* 366 (667, n = 16)
	T. baltica 150 (241, n = 17)	*T. baltica* 234 (588, n = 16)	*P. catenata* 269 (636, n = 17)	*P. taeniata* 279 (748, n = 17)
	M. rubra 128 (272, n = 9)	*P. taeniata* 177 (511, n = 14)	*P. taeniata* 265 (587, n = 16)	*Scri/Biech* 254 (491, n = 13)
2010	04.04.	12.04.	19.04.	27.04.
$NO_2^- + NO_3^-$ (µM)	6.1 ± 2.6 (N = 15)	3.9 ± 2.9 (N = 16)	1.8 ± 2.1 (N = 17)	0.4 ± 0.8 (N = 15)
PO_4^{3-} (µM)	0.78 ± 0.11 (N = 17)	0.51 ± 0.12 (N = 17)	0.50 ± 0.09 (N = 17)	0.38 ± 0.07 (N = 15)
Chl a (mg m^{-3})	8.91 ± 1.71 (N = 17)	14.94 ± 3.85 (N = 17)	19.43 ± 4.51 (N = 17)	18.47 ± 2.72 (N = 15)
Carbon biomass (mg m^{-3})	265 ± 59 (N = 17)	261 ± 48 (N = 17)	322 ± 95 (N = 17)	328 ± 71 (N = 15)
Mean C:Chl a ratio	29.7	17.5	16.6	17.7
Wet weight biomass (mg m^{-3})	2258 ± 511 (N = 17)	2357 ± 436 (N = 17)	2955 ± 855 (N = 17)	2816 ± 685 (N = 15)
	Scri/Biech 757 (1429, n = 17)	*T. levanderi* 668 (960, n = 17)	*Scri/Biech* 591 (1335, n = 17)	*Scri/Biech* 668 (1090, n = 15)
	T. levanderi 413 (677, n = 17)	*Scri/Biech* 448 (737, n = 16)	*T. levanderi* 572 (804, n = 17)	*P. catenata* 478 (838, n = 13)
	M. rubra 352 (740, n = 16)	*P. catenata* 311 (586, n = 16)	*P. catenata* 486 (1088, n = 17)	*P. taeniata* 470 (957, n = 15)
	P. catenata 312 (536, n = 17)	*P. taeniata* 305 (667, n = 17)	*P. taeniata* 483 (817, n = 17)	*T. baltica* 283 (583, n = 12)
	P. taeniata 115 (386, n = 12)	*M. rubra* 187 (345, n = 12)	*T. baltica* 327 (1810, n = 15)	*Gymnod.* 192 (478, n = 17)

Table 3
Average concentrations $\pm$ standard deviation of $NO_2^- + NO_3^-$, PO_4^{3-}, Chl a, phytoplankton carbon biomass, and carbon to Chl a ratio along the ferry route from Tallinn to Helsinki in May 2009 and 2010. The five dominant species (according to the wet weight biomass) with their corresponding average and maximum biomass values (shown in brackets) at each sampling date are listed. N — number of samples analysed, n — number of stations where a species was among the five dominant species.

	May				
2009	03.05.	10.05.	17.05.	24.05.	31.05.
$NO_2^- + NO_3^-$ (µM)	0.2 ± 0.2 (N = 17)	0.0 ± 0.0 (N = 17)	0.4 ± 0.3 (N = 17)	–	–
PO_4^{3-} (µM)	0.18 ± 0.06 (N = 17)	0.13 ± 0.02 (N = 17)	0.10 ± 0.03 (N = 17)	0.10 ± 0.02 (N = 17)	0.01 ± 0.03 (N = 17)
Chl a (mg m^{-3})	10.45 ± 3.07 (N = 17)	8.58 ± 3.50 (N = 17)	9.40 ± 3.14 (N = 17)	4.99 ± 1.53 (N = 17)	2.42 ± 0.94 (N = 17)
Carbon biomass (mg m^{-3})	263 ± 77 (N = 17)	310 ± 140 (N = 17)	439 ± 162 (N = 17)	178 ± 69 (N = 17)	43 ± 30 (N = 17)
Mean C:Chl a ratio	25.2	36.1	46.7	35.7	17.8
Wet weight biomass (mg m^{-3})	2478 ± 1031 (N = 17)	2159 ± 931 (N = 17)	2919 ± 1062 (N = 17)	1221 ± 468 (N = 17)	299 ± 195 (N = 17)
	M. rubra 578 (848, n = 17)	*M. rubra* 1325 (2788, n = 17)	*M. rubra* 1964 (3086, n = 17)	*M. rubra* 737 (1481, n = 17)	*M. rubra* 128 (750, n = 17)
	T. baltica 976 (2568, n = 17)	*P. catenata* 412 (899, n = 17)	*P. catenata* 672 (1477, n = 17)	*P. catenata* 192 (564, n = 17)	*Aphaniz.* 40 (80, n = 17)
	P. catenata 340 (602, n = 16)	*T. baltica* 198 (617, n = 17)	*Gymnod.* 73 (159, n = 17)	*T. baltica* 59 (158, n = 14)	*D. acuminata* 35 (116, n = 16)
	P. taeniata 197 (280, n = 17)	*Gymnod.* 30 (66, n = 11)	*T. baltica* 64 (190, n = 17)	*Gymn.* HET 45 (159, n = 11)	*P. brevipes* 13 (31, n = 11)
	S. marinoi 154 (381, n = 15)	*Pyramim.* 26 (41, n = 13)	*Aphaniz.* 15 (60, n = 8)	*D. acuminata* 34 (102, n = 9)	*P. granii* 8 (27, n = 8)
2010	03.05.	10.05.	17.05.	24.05.	31.05.
$NO_2^- + NO_3^-$ (µM)	0.1 ± 0.0 (N = 17)	0.2 ± 0.2 (N = 17)	0.3 ± 0.3 (N = 17)	0.1 ± 0.1 (N = 17)	–
PO_4^{3-} (µM)	0.35 ± 0.05 (N = 17)	0.37 ± 0.08 (N = 17)	0.36 ± 0.08 (N = 17)	0.26 ± 0.09 (N = 17)	–
Chl a (mg m^{-3})	18.64 ± 4.52 (N = 17)	14.30 ± 5.63 (N = 17)	6.06 ± 1.95 (N = 17)	6.69 ± 2.58 (N = 17)	2.96 ± 0.68 (N = 17)
Carbon biomass (mg m^{-3})	463 ± 156 (N = 17)	418 ± 209 (N = 17)	184 ± 61 (N = 17)	325 ± 233 (N = 17)	144 ± 67 (N = 17)
Mean C:Chl a ratio	24.8	29.2	30.3	48.7	48.5
Wet weight biomass (mg m^{-3})	3763 ± 968 (N = 17)	3319 ± 1596 (N = 17)	1519 ± 439 (N = 17)	2568 ± 1791 (N = 17)	973 ± 414 (N = 17)
	Scri/Biech 1361 (3123, n = 15)	*P. catenata* 1662 (4388, n = 17)	*P. catenata* 752 (1585, n = 17)	*P. catenata* 1982 (3943, n = 17)	*M. rubra* 517 (1143, n = 17)
	P. catenata 1114 (2018, n = 15)	*Scri/Biech* 851 (1352, n = 17)	*M. rubra* 252 (746, n = 16)	*M. rubra* 214 (948, n = 16)	*P. catenata* 204 (551, n = 13)
	P. taeniata 319 (1173, n = 15)	*M. rubra* 309 (694, n = 14)	*T. baltica* 210 (411, n = 17)	*Gymn.* HET 83 (203, n = 13)	*Gymn.* HET 48 (111, n = 15)
	M. rubra 277 (640, n = 14)	*P. taeniata* 129 (585, n = 13)	*P. taeniata* 74 (418, n = 15)	*T. baltica* 82 (215, n = 13)	Unid. dinof. 29 (57, n = 10)
	T. baltica 196 (688, n = 14)	*T. baltica* 112 (421, n = 14)	*Ch. holsaticus* 31 (318, n = 4)	*Gymnod.* 46 (81, n = 15)	*P. brevipes* 21 (69, n = 9)

Before this date, the vertical stratification was maintained by the vertical salinity distribution (Fig. 3). The upper mixed layer depth was approximately 15 m in general. In the period from 26 April to 11 May, strong vertical gradients appeared at a depth of 20 m, and only weak stratification was observed in the layer above. A clear decrease in the salinity of the upper layer with a concurrent upward shift of saltier waters at intermediate depths was revealed by 21 May.

3.2. Nutrient dynamics

In both years, the measurement of the nutrient concentrations in the Ferrybox samples started in March and ended in May, when the $NO_2^- + NO_3^-$ concentrations were below or close to the detection limit. At the end of March, the $NO_2^- + NO_3^-$ values in the surface layer along the cross section were similar in both years: in the range of 4.6 to 9.3 µM in 2009 (average = 7.2 µM; see Table 1) and in the range of 5.7 to 9.4 µM in 2010 (average = 6.9 µM). In general, the $NO_2^- + NO_3^-$ concentrations were higher and stayed above the detection limit longer near the northern coast of the gulf (Fig. 4). The system reached the N-limitation in the southern and central part of the gulf at approximately the same time in both years (26–27 April).

The PO_4^{3-} concentrations in the surface layer of the study area in late March were slightly lower in 2009 (in the range of 0.58 to 0.79 µM; average = 0.71 µM) compared with 2010, when these were in the range of 0.70 to 0.85 µM (average = 0.78 µM). The concentrations started to decrease at the beginning of April in both years (Fig. 4). The main difference in the PO_4^{3-} dynamics between the years was related to the higher concentrations clearly observed in late April and May 2010 compared with the concentrations obtained at same period in 2009. Whereas the PO_4^{3-} concentrations varied from 0.12 to 0.16 µM on 10 May 2009, concentrations as high as 0.23–0.48 µM were measured on 10 May 2010.

The consumption rates of nutrients from the surface layer were estimated for the spring bloom period from the end of March until nitrogen

($NO_2^- + NO_3^-$) depletion. Thus, data from 29 March 2009 to 26 April 2009 and from 31 March 2010 to 27 April 2010 were taken into account. Consumption rates of $NO_2^- + NO_3^-$ as high as 0.250 µM day^{-1} ($n = 84$, standard error of the slope estimate (se_b) = 0.018 µM day^{-1}) and 0.251 µM day^{-1} ($n = 73$, se_b = 0.026 µM day^{-1}) were estimated in 2009 and 2010, respectively. The consumption rate of PO_4^{3-} was 0.0160 µM day^{-1} ($n = 84$, se_b = 0.0011 µM day^{-1}) in spring 2009 and 0.0158 µM day^{-1} ($n = 76$, se_b = 0.0013 µM day^{-1}) in spring 2010. These results yield a ratio of nutrient consumption close to the Redfield ratio (16:1) in both springs: 15.7:1 in 2009 and 15.9:1 in 2010. If the data from May were taken into account, the estimates of the consumption rates (especially for nitrogen) and the ratios of nutrient consumption were lower. For instance, the ratios of nutrient consumption were 11.7:1 from 29 March to 17 May 2009 and 13.8:1 from 31 March to 24 May 2010. Furthermore, if alterations in the nutrient concentrations between consecutive sampling days (time step of 7 days) were used in the regression analysis, the estimates of the consumption rates and the corresponding ratios of the nutrient consumption varied widely: between 7.2 and 18.0 in 2009 and between 9.2 and 17.9 in 2010 (only data that exhibited a decrease in both nutrients were considered).

The measurements at station AP5 (Fig. 1) on 8 April 2010 showed $NO_2^- + NO_3^-$ concentrations as high as 5.1–5.3 µM in the upper 10-m layer (Fig. 3). By 14 April, the values in the same layer decreased to 0.2–0.4 µM, but relatively high concentrations were measured at depths of 15 and 20 m (1.7 and 6.8 µM, respectively). A significant deepening of the nitracline took place in the first half of May. At the end of May, the rise of the thermocline (Fig. 3) reintroduced higher $NO_2^- + NO_3^-$ concentrations into the depths of 10–15 m. The PO_4^{3-} concentrations in the upper 10-m layer were between 0.71 and 0.75 µM on 8 April and decreased to 0.48–0.51 µM by 14 April. At depths below 20 m, the concentrations were greater than 0.9 µM. In the beginning of May, the PO_4^{3-} concentrations in the upper 10-m layer were between 0.24 and 0.33 µM, and, due to the occurrence of slightly saltier waters and the observed change in the stratification
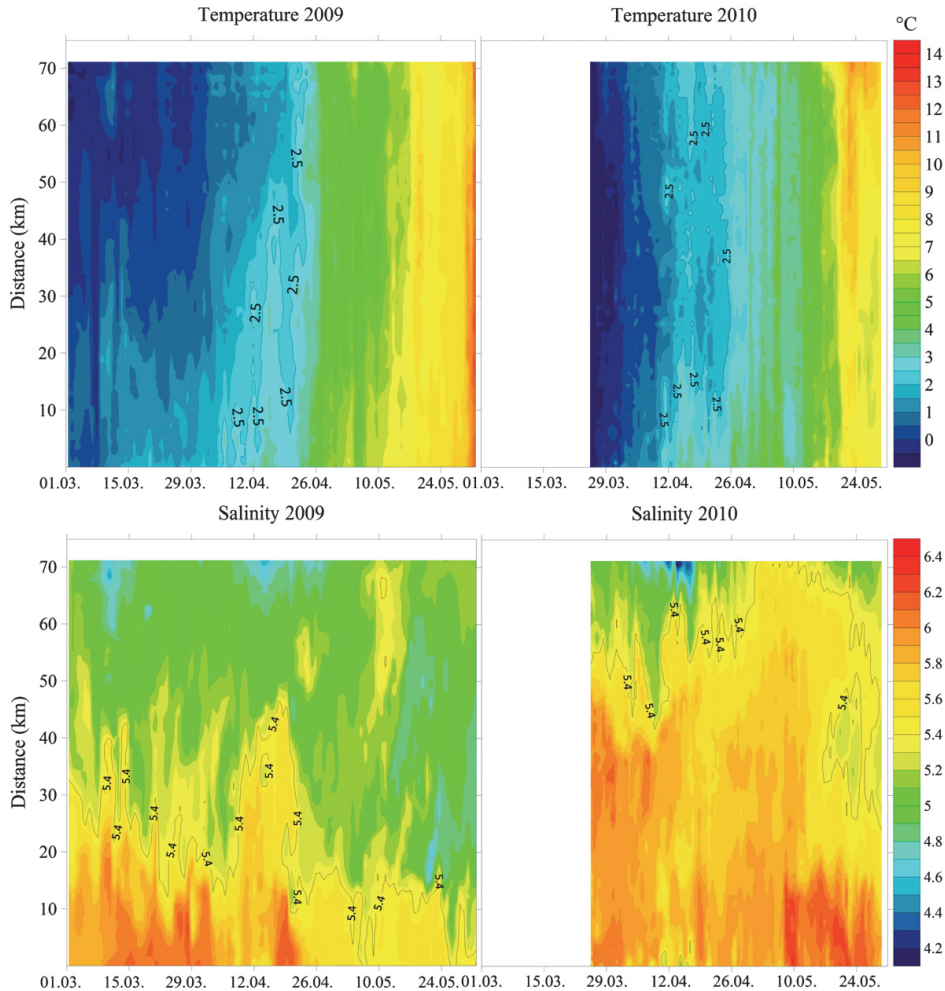
Fig. 2. Temporal variation of the horizontal distribution of temperature and salinity in the surface layer along the ferry route from Tallinn to Helsinki in the springs of 2009 and 2010. The daily measurements of the surface layer with a spatial resolution of 150 m are plotted.

(Fig. 3), increases in the concentrations in this layer were evident on 11 and 21 May (to 0.32–0.41 μM and 0.35–0.48 μM, respectively).

3.3. Dynamics of phytoplankton chlorophyll a and biomass

In both years, the Chl *a* concentrations along the entire cross section were mostly less than 3 μg l^{-1} in March (Fig. 5; Tables 1–3). In 2009, an increase in the Chl *a* concentrations to 6.38 ± 1.91 μg l^{-1} was observed at the end of March, whereas, in 2010, the concentrations remained less than 3.5 μg l^{-1} on 31 March. On average, the spring bloom developed earlier (by a couple of days to a week) in 2009 compared with 2010. The maximum values of Chl *a* were measured on 12 April (13.3–32.2 μg l^{-1}) in 2009 and on 19 April (10.5–26.3 μg l^{-1}) in 2010. In addition, the spring bloom lasted longer in 2010. If a threshold value of 5 μg l^{-1} is used, the spring bloom continued from 29 March to 17 May in 2009 and from 4 April to 24 May in 2010. Before the bloom termination, a secondary peak of relatively high Chl *a* concentrations was observed in both years: on 10–17 May in the central part of the gulf in 2009 and on 24

May in the northern part of the gulf in 2010. By 31 May, the Chl *a* concentrations decreased to 1.5–4.9 μg l^{-1} in 2009 and to 2.4–4.2 μg l^{-1} in 2010. In general, the spring bloom period (with Chl *a* values greater than 5 μg l^{-1}) lasted longer in the northern part of the study area than in the southern half.

According to the phytoplankton C and wet weight biomass, the spring bloom was more heterogeneous compared with the dynamics of the Chl *a* concentrations (Fig. 5, Tables 1–3). In both years, relatively fast biomass growth was observed concurrently with the Chl *a* increase in the first half of April. However, after the Chl *a* maximum had been reached, the biomass did not decrease accordingly. The highest phytoplankton biomass values were observed on 17 May in 2009 in the central part of the gulf, which coincides with the secondary Chl *a* peak, and on 3–10 May in 2010 in the southern and central parts of the gulf. A secondary biomass peak on 24 May 2010 in the northern part of the gulf was also clearly distinguished (Fig. 5).

In both years, the carbon to Chl *a* ratio (C:Chl), which was estimated based on the daily average values of the phytoplankton C content and the Chl *a* concentration, varied between 11.8 and 48.7 in the
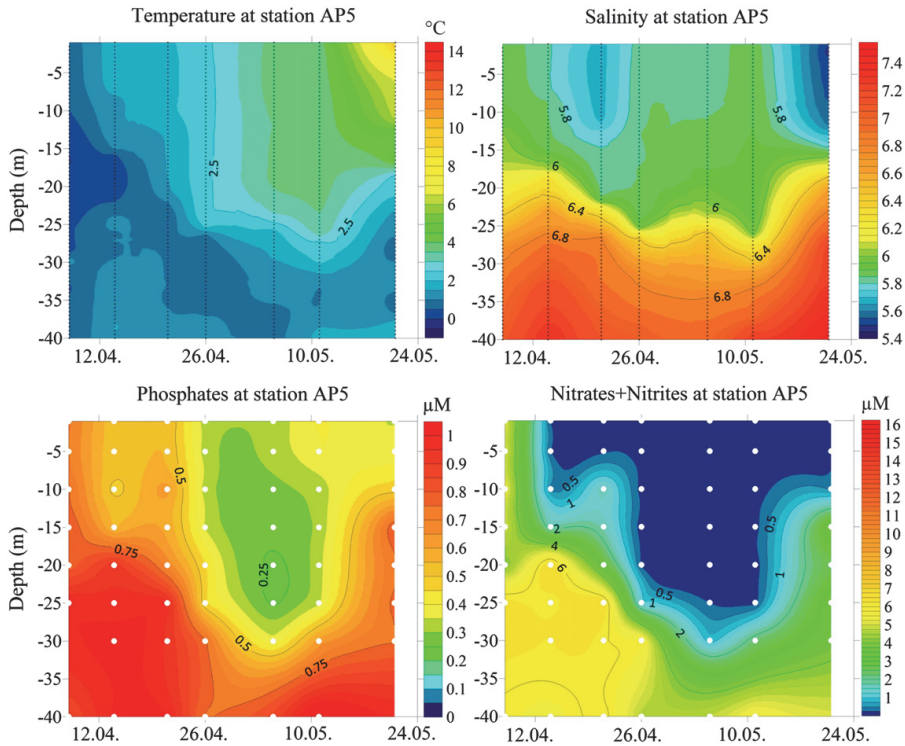
Fig. 3. Temporal variation of the vertical distribution of temperature, salinity, nitrates – nitrites, and phosphates at station AP5 in the spring of 2010. The vertical profiles of the temperature and the salinity are shown as black dots, and sampling depths for the nutrient analyses are shown as white dots.

period from March to May and exhibited clear and similar dynamics during the spring bloom (Tables 1–3). On average, the C:Chl ratio was lower in March to April than in May, when the Chl *a* concentration started to decrease and the biomass reached its maximum. If the spring bloom period (Chl *a* > 5 μg l^{-1}) is taken into account, the C:Chl ratios for the first and last four weeks were 17.6 ± 4.8 and 32.5 ± 13.3 in 2009 (29 March to 19 April and 26 April to 17 May, respectively) and 20.4 ± 7.0 and 33.1 ± 13.1 in 2010 (4 April to 27 April and 3 May to 24 May, respectively). An exception with regard to this pattern was observed in the early phase of the spring bloom in 2010, when a C:Chl ratio of 30.2 ± 6.5 was estimated on 4 April. The lowest C:Chl values during the spring bloom period coincided with the Chl *a* peak on 12 April in 2009 (C:Chl ratio was 15.5 ± 3.8) and on 19 April in 2010 (C:Chl ratio was 16.5 ± 2.4).

3.4. Dynamics of phytoplankton groups and species

In this paper, mainly two major groups (diatoms and dinoflagellates) and some dominating species of those groups were analysed. The overall timing of the diatom bloom was similar in both years studied (Fig. 6). The biomass of diatoms started to increase at the end of March along the entire cross section. In the southern and central gulf, the diatom bloom lasted 1–2 weeks longer in 2009 compared with 2010. The spring of 2010 was characterised by a longer period of diatom bloom in the northern part, which coincided well with the decline/dynamics of the $NO_2^- + NO_3^-$ concentration in the surface layer of this region.

The main diatom biomass during both springs was composed of *T. baltica* (Grunow) Ostenfeld 1901, *Thalassiosira levanderi* van Goor

1924, and *Pauliella taeniata* (Grunow) Round and Basson 1997 (Tables 1–3). The higher biomass values of *T. levanderi* were restricted to the southern and central gulf in both years. In addition, the bloom period of the latter species was strictly defined within 1 month. The distribution of *P. taeniata* followed well the distribution of diatom bloom, but the biomass values were lower in 2009. *T. baltica* was found in the surface layer during a period of two months and exhibited its maximum biomass in the second half of April in both years (Fig. 7), although the bloom of *T. baltica* was more intensive in 2009.

Whereas the diatom biomass in the study area was well correlated with the Chl *a* distribution, the dinoflagellate biomass coincided with the overall phytoplankton biomass distribution. The dinoflagellate spring bloom was more intensive in 2010 (Fig. 6), and the bloom was more concentrated in the southern and central part of the cross section, where the biomass maximum was reached later in 2010. The dinoflagellate bloom was mainly composed of *Peridiniella catenata* (Levander) Balech 1977 and the *Scrippsiella/Biecheleria* complex (Tables 1–3). The latter showed different bloom intensities and distribution patterns in the consecutive springs (Fig. 7). In 2009, the biomass of the *Scrippsiella/Biecheleria* complex was on average lower and more concentrated in the northern part and decreased at the end of April. In 2010, an intensive bloom of the complex was observed during a one-and-a-half-month period in the central part of the cross section, and the bloom maximum appeared in the beginning of May in the southern and central part of the study area. The decrease in the *Scrippsiella/Biecheleria* complex bloom in 2010 was very sudden and occurred at the same time along the whole cross section. *P. catenata* was present in the surface layer throughout the
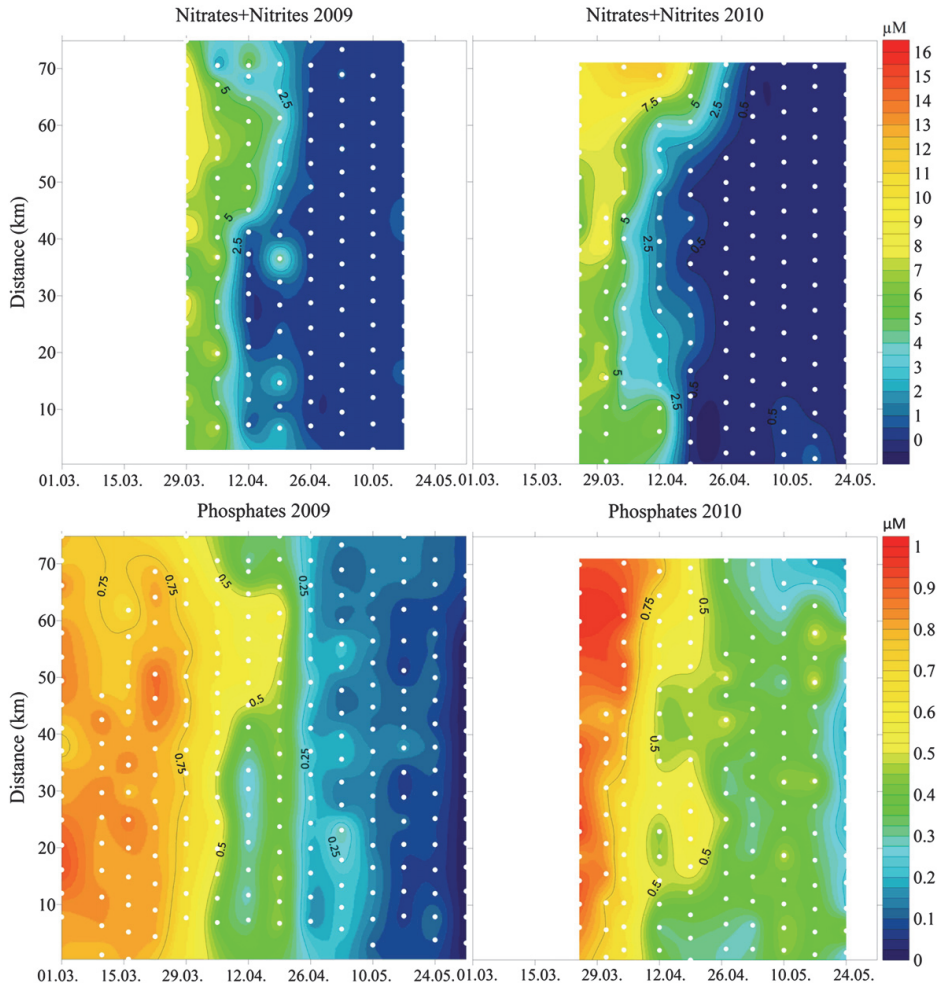
Fig. 4. Temporal variation of the horizontal distribution of the nitrates–nitrites and phosphates in the surface layer along the ferry route from Tallinn to Helsinki in the springs of 2009 and 2010. The sampling sites are indicated as white dots.

spring bloom period (from the melting of the ice cover) and had its biomass maximum after the *Scrippsiella*/*Biecheleria* complex bloom in both years (Fig. 7), although the intensity of the *P. catenata* bloom was significantly higher in 2010.

When calculating the proportion of dinoflagellates in the dinoflagellate-diatom community, one can clearly observe the distinct periods of dominance of diatoms (values below 0.5 in Fig. 6) in both years. The intensity and dominance of diatoms in 2009 was greater, and the period of diatom dominance lasted longer in 2009 compared with 2010. Furthermore, based on the carbon biomass, the dinoflagellates dominated in the central gulf during the entire study period in 2010. During the spring bloom period (Chl $a > 5$ μg l^{-1}), the average proportion of dinoflagellates in the dinoflagellate–diatom community was 0.64 ± 0.23 in 2009 and 0.73 ± 0.23 in 2010. The daily average dinoflagellate:diatom ratio, which was calculated based on 17 samples along the study transect, was less than 0.5 (indicates diatom dominance in the dinoflagellate–diatom community) during three sampling days in 2009 (19 April, 26 April, and 3 May). This ratio exhibited a minimum of 0.42 ± 0.11 on 19 April in 2009. Diatom dominance was detected only

during one sampling day in 2010: the dinoflagellate:diatom ratio was 0.49 ± 0.13 on 12 April, whereas it was already 0.52 ± 0.12 on 19 April.

Remarkable differences in the biomass of the photosynthetic ciliate *M. rubra* were observed in the two studied spring periods (Fig. 8). As observed from the data (Tables 1–3), this species was present among the five dominants almost during the entire study period in both years. However, the biomass of *M. rubra* reached values greater than 200 μg C l^{-1} only in May 2009, when approximately 2/3 of the total carbon biomass of autotrophic organisms was composed of this species. A relatively high biomass of *M. rubra* for the early phase of the spring bloom was detected on 4 April 2010. Because this high biomass value coincided with a peak in the *Scrippsiella*/*Biecheleria* complex bloom, a relatively high C:Chl ratio was estimated for this sampling day (see above).

4. Discussion

A few decades ago, it was generally accepted that the vernal phytoplankton bloom occurs in the second half of April in the southern
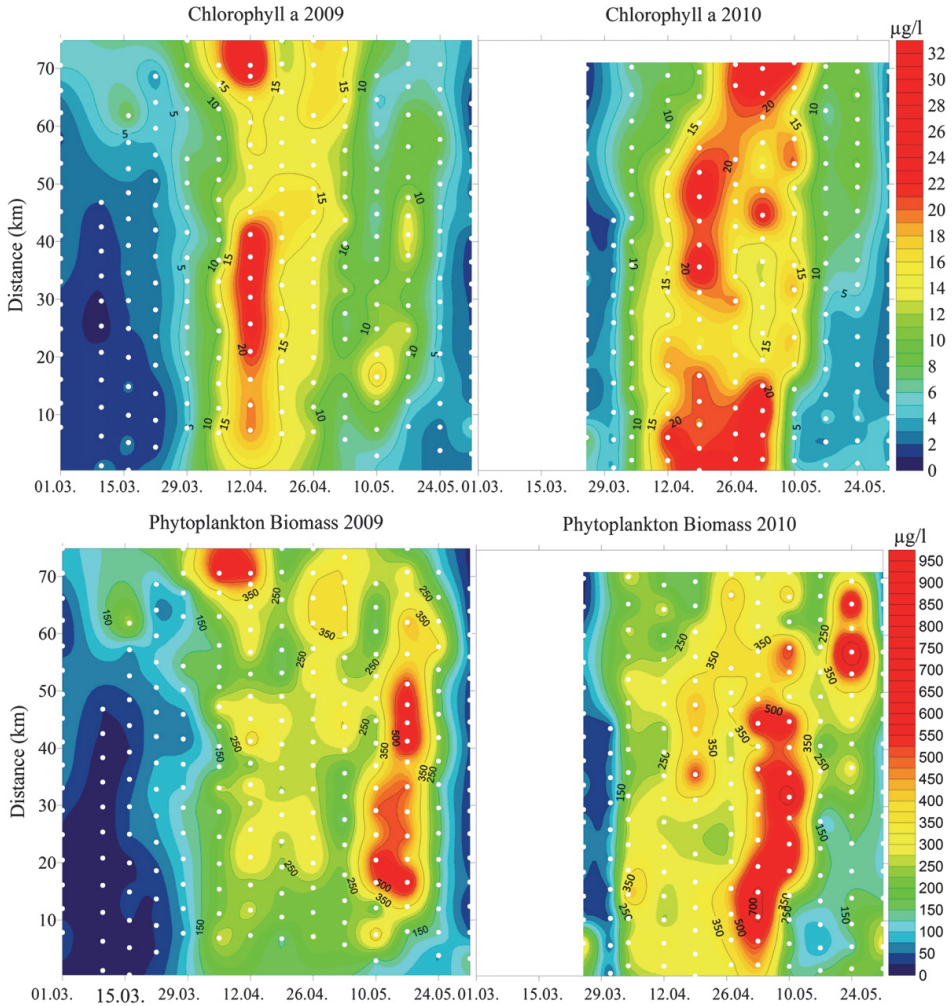
Fig. 5. Temporal variation of the horizontal distribution of the chlorophyll *a* concentration and the phytoplankton carbon biomass along the ferry route from Tallinn to Helsinki in the springs of 2009 and 2010. The sampling sites are indicated as white dots.

and central part of the Baltic Proper and in early May in the northern part of the Baltic Proper and in the Gulf of Finland (Edler, 1979; Hällfors et al., 1981). From our data, it can be observed that the commencement and culmination of the bloom in the Gulf of Finland occurred a few weeks earlier in 2009–2010 compared with the 1970s. The ensemble forecast for the sea surface temperature (SST) in the Baltic Sea predicts that the annual mean SST will increase by 2.9 °C from 1961–1990 to 2071–2100, whereas the greatest increase will be observed in May and June (BACC, 2008). The change in SST will influence various processes in the marine ecosystem, mostly through the changes in trophic interactions (Alheit et al., 2005; Sommer and Lengfellner, 2008; Vehmaa et al., 2011). Two of the predicted changes in the Baltic Sea area are the earlier onset of the spring bloom (Wasmund and Uhlig, 2003) and the increased dinoflagellate:diatom ratio (Wasmund et al., 1998). Increased winter temperatures and changed mixing conditions mainly explain the latter.

In earlier publications (e.g., Hällfors et al., 1981), the availability of light and thermal stratification have been regarded as the main

regulators of bloom development. Kahru and Nõmmann (1990) showed that the water temperature does not determine the commencement of the spring bloom and that the restriction of vertical mixing is provided by the much stronger influence of the salinity stratification. Based on the Ferrybox data collected in 2009 and 2010, the spring bloom (Chl *a* concentration $>5 \mu g \, l^{-1}$) in the Gulf of Finland started before the temperature of maximum density had been reached in the surface layer (2.5 °C in the study area). The earlier bloom development in 2009 compared with 2010 was most likely related to the slightly earlier warming of the surface waters in 2009, but might also have been indirectly influenced by the salinity stratification. The latter suggestion assumes that the lower salinity in the surface layer in the spring of 2009 indicates a stronger vertical stratification.

Based on unattended monitoring data from the period of 1993 to 2009, Raateoja et al. (2011) suggested that the spring bloom takes up dissolved inorganic nitrogen (DIN) and dissolved inorganic phosphorus (DIP) at a ratio lower than that suggested by the Redfield
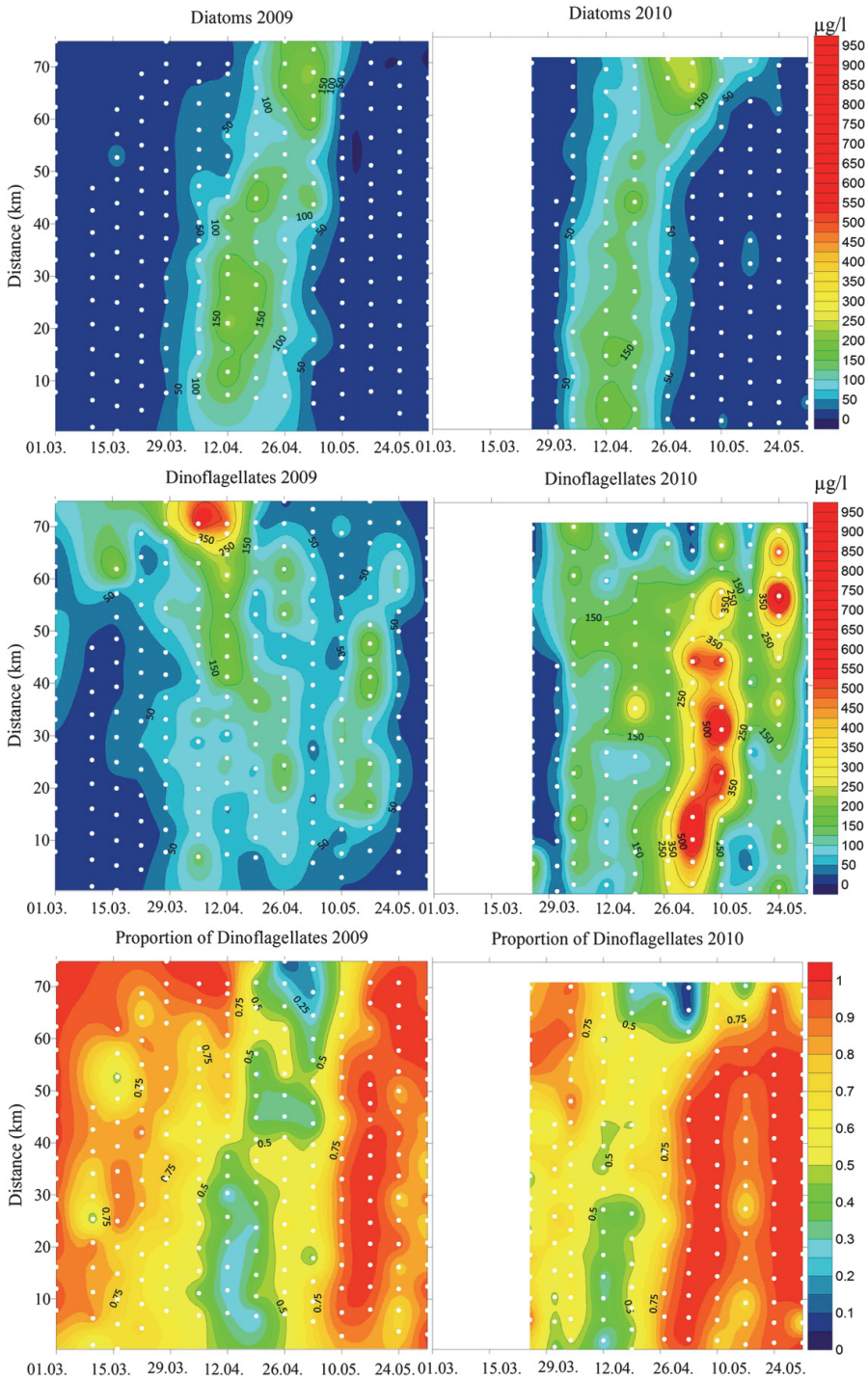
Fig. 6. Temporal variation of the horizontal distribution of the carbon biomass of diatoms and dinoflagellates and the proportion of dinoflagellates in the diatom–dinoflagellate community along the ferry route from Tallinn to Helsinki in the springs of 2009 and 2010. The sampling sites are indicated as white dots.
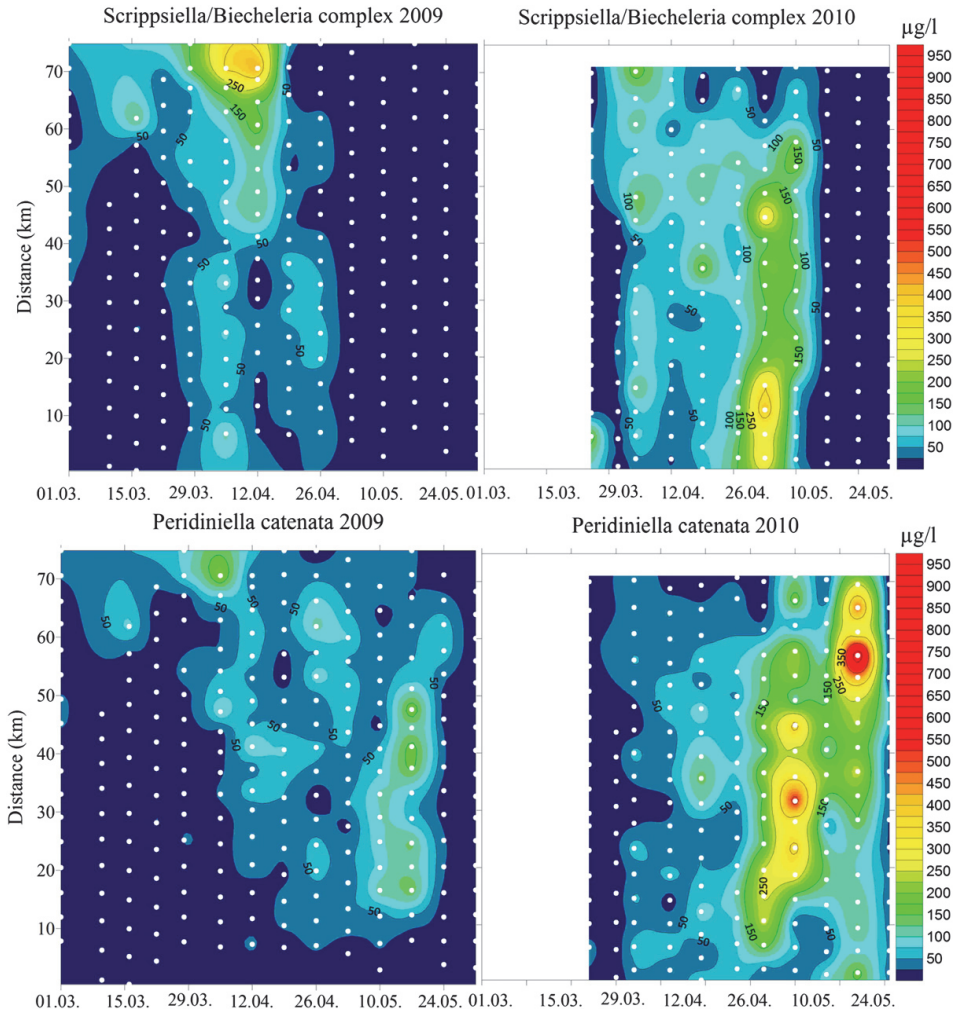
Fig. 7. Temporal variation of the horizontal distribution of the carbon biomass of the *Scrippsiella*/*Biecheleria* complex and *Peridiniella catenata* along the ferry route from Tallinn to Helsinki in the springs of 2009 and 2010. The sampling sites are indicated as white dots.

ratio. These researchers used a time period of 60 days around the bloom peak in their estimates. In the present analysis, we showed that the estimated ratio of the nutrient consumption was close to the Redfield ratio if the growth phase of the spring bloom (i.e., both nutrients are available in the surface layer) was considered. If a time period of two months was used in the analysis, the estimated ratio of the nutrient consumption was lower than the Redfield ratio. However, in addition to a non-Redfield uptake ratio, additional nitrogen sources, such as remineralisation, vertical transport by migrating species, and horizontal transport of water masses with different DIN and DIP concentrations, have to be assessed.

The nutrient concentrations from winter to early spring in the surface layer of the Gulf of Finland have distinct gradients from west to east: the DIN varies from 7 μM to 21 μM and the DIP varies from 0.7 μM to 1.3 μM (Pitkänen et al., 2008). This yields a corresponding gradient of the DIN:DIP ratio from 10:1 in the western and central gulf to 16:1 in the eastern gulf. If the approach described in the

present paper is used to estimate the nutrient uptake, the N:P uptake ratio is underestimated in the case of prevailing westward flow in the surface layer of the Gulf of Finland. Thus, we argue that estimates of the uptake ratios based on changes in the nutrient concentrations in the surface layer are applicable for the growth period of fast nutrient uptake. However, as a result of vertical mixing and advection (e.g., related to mesoscale processes), which introduce phosphates into the Gulf of Finland surface layer in excess compared with the Redfield ratio, these estimates might also be biased for shorter periods due to the low DIN:DIP ratio in the sub-surface layer (Laanemets et al., 2011). In accordance with this assumption, the different rates of the decrease of phosphates in the surface layer that were observed in 2009 and 2010 could be attributed to the upward movement of the thermocline and sub-surface waters with higher nutrient concentrations in May 2010.

The observed decrease in the phosphate concentrations in the surface layer after nitrogen ($NO_2^- + NO_3^-$) depletion could be supported
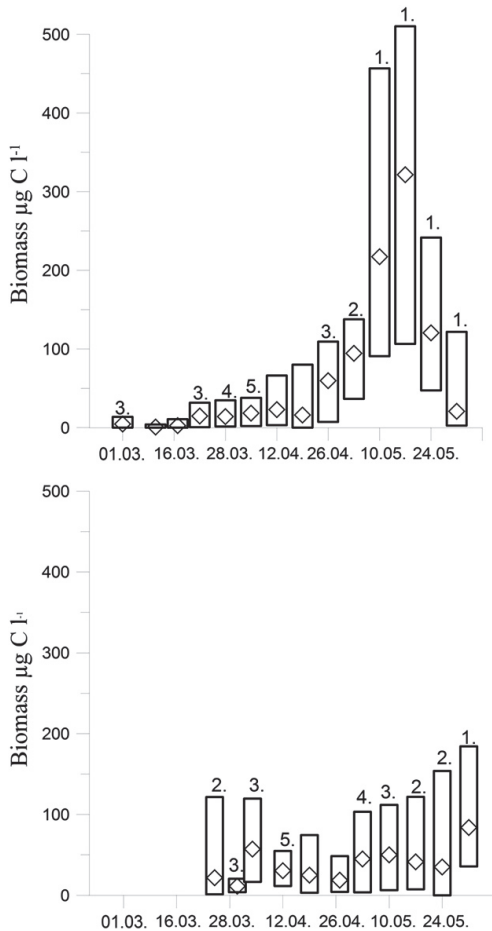
Fig. 8. Carbon biomass of *M. rubra* in 2009 (upper panel) and 2010 (lower panel). Each box represents the range of values observed at different stations on different dates (x-axis). The diamonds in the boxes show the average biomass value of all of the stations across the gulf at the indicated date. The order numbers at the top of the boxes show the position of this species among the five dominant species at the indicated sampling date.

by the processes that make additional nitrogen sources available for the phytoplankton growth, e.g., remineralisation of nitrogen. We also hypothesise that the vertical transport of nitrates–nitrites from the sub-surface layers by migrating dinoflagellates (Fraga et al., 1989) and the photosynthetic ciliate *M. rubra* (Crawford and Lindholm, 1997) could be considered an additional nitrogen source. Lindholm and Mörk (1990) observed that *M. rubra* can migrate vertically over tens of metres per day and exploit layers rich in nutrients. These researchers suggested that *M. rubra* may form a significant mechanism for the transport of nutrients from deep layers into the euphotic zone when this ciliate is found at high abundances in stratified waters. The faster decrease of phosphates after the DIN depletion in the surface layer in late April to early May 2009, when the photosynthetic ciliate *M. rubra* exhibited a high biomass (compared with the slower decrease of phosphates and the lower biomass *M. rubra* in April to May 2010) supports these hypotheses. A further indication that the migrating species could contribute as an additional nitrogen source was provided by the measurements at station AP5 in late May and June 2010 (on 21 May and 9, 17, and 30

June). The estimates of the consumption rates of nutrients in the surface layer (samples taken from depths of 1, 5, and 10 m) and in the sub-surface layer (samples taken from depths of 25 and 30 m) were the following: the decrease of $NO_2^- + NO_3^-$ was not significant in the surface layer and 0.072 μM day^{-1} ($n = 8$, $se_b = 0.018$ μM day^{-1}) in the sub-surface layer, and the decrease of PO_4^{3-} was 0.0049 μM day^{-1} ($n = 8$, $se_b = 0.0011$ μM day^{-1}) in the surface layer and not significant in the sub-surface layer. According to the Ferrybox sampling on 31 May and 7, 14, and 21 June the migrating photosynthetic ciliate *M. rubra* exhibited relatively high biomass (up to 232 μg C l^{-1}). In contrast, on 30 June, when the surface layer had become depleted of phosphates, this species was almost absent from the samples (data from June are not included in the present paper).

The observed spring blooms can be divided into two phases: the growth phase, when both the Chl *a* and the biomass increase, which approximately coincides with the period when both DIN and DIP are available in the surface layer, and the second phase, when Chl *a* starts to decrease and the biomass continues to grow until the rapid decay of the bloom. Clearly lower estimates of the C:Chl ratio were obtained for the first period (17.6 in 2009 and 20.4 in 2010) compared with the second period (32.5 in 2009 and 33.1 in 2010). This result is consistent with earlier findings that lower C:Chl ratios exist when diatoms dominate in the community and higher ratios are found when flagellates prevail (e.g., Eker-Develi et al., 2008). Additionally, large cells have a relatively higher C:Chl ratio (Malone, 1980) compared with smaller cells. Hence, the increase in the Chl *a* concentration caused by the increase of small-cell diatoms will not give a similar increase in the phytoplankton C if the biomass growth is formed by larger cells. The nutrient depletion may reduce the cellular chlorophyll content and hence affect pigment ratios. The most pronounced effects of nutrient depletion have been found to be related to N-depletion (Goericke and Montoya, 1998) because Chl synthesis is closely coupled to the internal N pool (Staehr et al., 2002). The observed large variations in the C:Chl ratio during the spring bloom show that the measurement of Chl *a* is often insufficient to describe the fluctuations in the phytoplankton standing stock. Furthermore, it is clear that the models that use constant values for the conversion factors that link the carbon to the nitrogen and the phosphorus contents and the nutrients to the Chl *a* content cannot reproduce the observed dissimilar dynamics of the Chl *a* concentration and the phytoplankton biomass during the spring bloom.

The carbon bound to the phytoplankton biomass increases as the community transitions from diatoms to dinoflagellates during the spring bloom. The major part of the annual new production and sedimentation of organic matter in the Northern Baltic Sea occurs during the spring bloom in April–May (Heiskanen, 1998). The dinoflagellate: diatom ratio during the spring bloom is important because diatom-dominated blooms provide a fresh supply of organic matter to the benthos, whereas dinoflagellate-dominated blooms lead to a greater retention of organic matter in the water column. Because diatom-bound C will sink out of the water column and is impounded to sediments for long periods of time, a higher diatom contribution in the spring bloom biomass will affect the overall C budget through rapid C loss from the water column. Although most of the dinoflagellate biomass is found to be disintegrated in the water column, the formation and sedimentation of cysts in the *Scrippsiella/Biecheleria* complex has been estimated to be approximately 45% of the maximum sedimentation of particulate organic C during this period of the year (Heiskanen, 1993). Hence, the cyst-forming dinoflagellates also strongly influence the total carbon sedimentation in the late part of the spring bloom but the sedimentation of cysts might have a different biogeochemical effect on nutrient cycling compared with sedimentation of diatom cells (Spilling and Lindström, 2008).

Our results clearly show the different patterns in the diatom and dinoflagellate temporal distributions in the spring (Figs. 6 and 7). Diatoms have a more distinct high-biomass period compared with dinoflagellates

and exhibit their biomass maximum in mid-April. The diatom dominance before the peak of the dinoflagellate biomass was observed by Tamelander and Heiskanen (2004) in the Finnish coastal waters, and by Edler (1979) and Wasmund et al. (1998) in the Baltic Proper. Our two years of observations are probably too short to support this as in some years (e.g. 2009, Fig. 6) the dinoflagellate peak may form clearly before the diatom maximum. Additionally, a longer bloom period of dinoflagellates was evident from historical data (Edler, 1979), which demonstrated the presence and significant abundance of dinoflagellates, e.g., *P. catenata* (*Gonyaulax catenata* in the referenced publication), from early April until late May. Kononen and Niemi (1984) observed apparent changes in the dominance of diatoms and dinoflagellates during the spring bloom in a long-term trend analysis of the entrance area of the Gulf of Finland. These researchers concluded that dinoflagellates dominated during the spring bloom in the period of 1968 to 1975 and that there was a shift to diatom dominance in the late 1970s. However, it is possible that the recent reported decrease in spring diatoms and coincident increase in dinoflagellates might often be a result of a sparse spatial and temporal sampling. Because the diatom peak appears in a narrower time window compared with that of dinoflagellates (Fig. 6), undersampling might lead to the wrong conclusion. For instance, sampling once a month during a fixed week combined with the time-shifts in the development of the spring bloom due to the inter-annual or long-term variation in meteorological conditions could miss the short period of diatom dominance. Furthermore, our data showed that the period when diatoms were dominant in the community (Fig. 6) occurred in the northern and southern parts of the gulf at different time periods. Thus, depending on the sampling week, the north–south gradient of the dinoflagellate:diatom ratio could be different or even opposite.

It is possible to reveal species-level changes by comparing our observational results with the historical data on the dominant species during the spring bloom. Between 1979 and 1993, *S. marinoi* (formerly identified as *S. costatum*) has often been reported as the most important diatom species during the spring bloom (e.g., HELCOM, 1996). Although we confirmed this result with regard to the abundance of the organism, the cell size of this species was very small during both years (predominant size class = 3×6–8 μm), which implies that its contribution to the overall bloom biomass was not significant. Hence, this species was only once included in the list of the five dominants species (Tables 1–3). The diatom *T. levanderi* has not been mentioned among the dominant diatoms in earlier publications and periodic assessments of the Gulf of Finland. In the years 2009 and 2010, this species was among the dominants from the beginning of March to the second half of April, at which point it rapidly disappeared from the spring bloom community. *P. taeniata*, which was often mentioned among the bloom-forming species, does not appear to build a high biomass each year. The proportion of this species in the spring bloom community was relatively modest in 2009.

P. catenata continues to be the dominant dinoflagellate, as demonstrated through the analysis of historical records (e.g., HELCOM, 1996). However, the abundance and biomass of the *Scrippsiella/Biecheleria* complex have made these species one of the most dominant during the entire spring bloom period. The regular occurrence and blooms of single-celled dinoflagellates in winter and spring have often been reported in the Gulf of Finland since the early 1980s (Jaanus et al., 2006; Kremp et al., 2005). Because the classification of these species has been under review and their identification using a light microscope is difficult, several species are often counted and reported as the *Scrippsiella* or *Biecheleria* complex (including *Scrippsiella hangoei* (Schiller) Larsen, *Biecheleria baltica* Moestrup, Lindberg, and Daugbjerg, and *Gymnodinium corollarium* A. M. Sundström, Kremp, and Daugbjerg). According to our data, these single-celled dinoflagellate species appear in the water during the entire spring bloom period from March to May. The maximum biomass of the *Scrippsiella/Biecheleria* complex was observed in different spring bloom stages during the two studied years. In 2009, the highest biomass was

found at the end of March and was clearly limited to the northern part of the Gulf (Fig. 7). In 2010, the biomass maximum occurred after the diatom peak in the beginning of May, and high biomass values were measured along the whole cross section of the gulf. The slightly different temperature and salinity preferences of the species in the *Scrippsiella/Biecheleria/Gymnodinium* complex (Kremp et al., 2005; Sundström et al., 2009; Sundström et al., 2010) might explain the temporally wide window of occurrence of this complex during the spring bloom. Further field studies on succession of different species of this complex are needed. The decline of the *Scrippsiella/Biecheleria* complex bloom was very sharp in 2010.

The last phase of the spring bloom was dominated by dinoflagellates and photosynthetic ciliates that are potentially capable of performing vertical migrations. The ability for diel vertical migration is widely known in *M. rubra* (Crawford, 1989; Passow, 1991; Smayda, 2010) and *P. catenata* (Heiskanen, 1995; Passow, 1991; Spilling et al., 2006). There is no strong evidence of migration behaviour of the *Scrippsiella/Biecheleria* complex. The vertical migration of *P. catenata* becomes more important as the bloom progresses. However, if the nitrate concentration is depleted below a threshold concentration in the migrating range of *P. catenata*, its vertical migration can no longer compensate the assimilation of the limiting nutrient. The more intensive growth of *P. catenata* in 2010 might be explained by the change in the stratification in the second half of May and the concurrent rise of the nitracline to the euphotic layer.

The remarkable dominance of the migrating photosynthetic ciliate *M. rubra* most likely caused the depletion of phosphates in the surface layer by the end of May in 2009. This species is known as the fastest autotroph in the sea and is characterised by a swimming velocity that is reported to reach 8.5 mm s^{-1} (30 m h^{-1}; Smayda, 2010). This species can swim to the surface layer within 1–2 h from anywhere within a 40-m water column. *M. rubra* is also known for its direct utilisation of nitrate, ammonium, and dissolved organic nitrogen (Wilkerson and Grunseich, 1990). Its dominance, migration behaviour, and phosphate utilisation in the surface layer will not only prolong the autotrophic production in the nutrient-depleted upper layer but will also strongly influence the amount of excess phosphorus that is usually regarded to support the summer cyanobacterial bloom development. The observed different dynamics of this species in the two studied years and the reasons behind this inter-annual variation still need to be investigated and are not discussed in the present paper.

5. Conclusions

High-resolution measurements and sampling revealed the high spatial and temporal variability of the phytoplankton community composition and distribution in the Gulf of Finland during the spring. To analyse the related nutrient dynamics in the surface layer, we divided the bloom period into two parts: the growth period, in which both phosphates and nitrates–nitrites are available, and the period after the depletion of the nitrates–nitrites. During the first period, the ratio of nutrient consumption was close to the Redfield ratio. We suggest that the decrease in the excess phosphate concentrations in the surface layer after the depletion of nitrates–nitrites could be partly related to the vertical transport of nitrates from the sub-surface layers by migrating species. Clearly lower estimates of the C:Chl ratio were obtained for the growth period of the spring bloom (17.6 in 2009 and 20.4 in 2010) compared with the second half of the bloom (32.5 in 2009 and 33.1 in 2010). During this second half of the bloom, the Chl *a* concentration started to decrease, but the phytoplankton biomass continued to grow until the rapid decay of the bloom. As a result, the phytoplankton-bound carbon stock increased with the succession of the spring bloom and the transition from diatom to dinoflagellate dominance in the community. Diatoms exhibited a relatively narrow and more distinct period of high biomass compared with dinoflagellates, and we argue that this period of diatom dominance in the Gulf of Finland might be overlooked

by measurements with low temporal resolution. The second phase of the spring bloom was dominated by dinoflagellates, including the *P. catenata* and single-celled species reported as the *Scrippsiella/Biecheleria* complex, and the ciliate *M. rubra*. The dominance of both dinoflagellates and the photosynthetic ciliate increases the retention time for newly produced material and might have a substantial biogeochemical impact on the nutrient-limited upper layer of the Gulf of Finland in late spring.

References

Alheit, J., Möllmann, C., Dutz, J., Kornilovs, G., Loewe, P., Mohrholz, V., Wasmund, N., 2005. Synchronous ecological regime shifts in the central Baltic and the North Sea in the late 1980s. ICES J. Mar. Sci. 62, 1205–1215.

APHA, 1992. APHA, AWWA, and WPCF standard methods for the examination of water and wastewater, 18th edn. American Public Health Association, Washington.

BACC Author Team, 2008. Assessment of Climate Change from the Baltic Sea Basin. Regional Climate Studies. Springer Verlag 1–473.

Crawford, D.W., 1989. *Mesodinium rubrum*: the phytoplankter that wasn't. Mar. Ecol. Prog. Ser. 58, 161–174.

Crawford, D.W., Lindholm, T., 1997. Some observations on the vertical distribution and vertical migration of the phototrophic ciliate *Mesodinium rubrum* (= *Myrionecta rubra*) in a stratified brackish inlet. Aquat. Microb. Ecol. 13, 267–274.

Edler, L., 1979. Phytoplankton succession in the Baltic Sea. Acta Bot. Fenn. 110, 75–78.

Eilola, K., Meier, M.H.E., Almroth, E., 2009. On the dynamics of oxygen, phosphorus and cyanobacteria in the Baltic Sea: a model study. J. Mar. Syst. 75, 163–184.

Eker-Develi, E., Berthon, J.-F., van der Linde, D., 2008. Phytoplankton class determination by microscopic and HPLC-CHEMTAX analyses in the southern Baltic Sea. Mar. Ecol. Prog. Ser. 359, 69–87.

Fleming, V., Kaitala, S., 2006. Phytoplankton spring bloom intensity index for the Baltic Sea estimated for the years 1992 to 2004. Hydrobiologia 554, 57–65.

Fraga, S., Gallager, S.M., Anderson, D.M., 1989. Chain-forming dinoflagellates: An adaptation to red tides. In: Anderson, D.M., Nemoto, T. (Eds.), Red Tides: Biology, Environmental Science and Toxicology: Proceedings of the First International Symposium on Red Tides, pp. 281–284 (Takamatsu, Japan).

Goericke, R., Montoya, J.P., 1998. Estimating the contribution of microalgal taxa to chlorophyll a in the field – variations of pigment ratios under nutrient- and light-limited growth. Mar. Ecol. Prog. Ser. 169, 97–112.

Grayek, S., Staneva, J., Schulz-Stellenfleth, J., Petersen, W., Stanev, E.V., 2011. Use of FerryBox surface temperature and salinity measurements to improve model based state estimates for the German Bight. J. Mar. Syst 88 (1), 45–59.

Hällfors, G., Niemi, Å., Ackefors, H., Lassig, J., Leppäkoski, E., 1981. Biological oceanography. In: Voipio, A. (Ed.), The Baltic Sea: Elsevier Oceanography Series, 30, pp. 219–274.

Heiskanen, A.S., 1993. Mass encystment and sinking of dinoflagellates during a spring bloom. Mar. Biol. 116, 161–167.

Heiskanen, A.S., 1995. Contamination of sediment trap fluxes by vertically migrating phototrophic micro-organisms in the coastal Baltic Sea. Mar. Ecol. Prog. Ser. 122, 45–58.

Heiskanen, A.S., 1998. Factors governing sedimentation and pelagic nutrient cycles in the northern Baltic Sea. Boreal Environ. Res. 8 (80 pp.).

HELCOM, 1988. Guidelines for the Baltic monitoring programme for the third stage. Part D. Biological determinants. Balt. Sea Environ. Proc. 27D, 1–161.

HELCOM, 1996. Third periodic assessment of the state of the marine environment of the Baltic Sea, 1989–1993; Background document. Balt. Sea Environ. Proc. 64B, 1–252.

Jaanus, A., Hajdu, S., Andersson, A., Kaitala, S., Kaljurand, K., Ledaine, I., Lips, I., Olenina, I., 2006. Distribution patterns of the red tide dinoflagellate *Scripsiella hangoei* in the Baltic Sea. Hydrobiologia 554, 137–146.

Jaanus, A., Toming, K., Hällfors, S., Kaljurand, K., Lips, I., 2009. Potential phytoplankton indicator species for monitoring Baltic coastal waters in the summer period. Hydrobiologia 629, 157–168.

Johansson, M., Gorokhova, E., Larsson, U., 2004. Annual variability in ciliate community structure, potential prey and predators in the open northern Baltic Sea proper. J. Plankton Res. 26, 67–80.

Kahru, M., Nõmmann, S., 1990. The phytoplankton spring bloom in 1985, 1986: multitude of spatio-temporal scales. Cont. Shelf Res. 10, 329–354.

Klais, R., Tamminen, T., Kremp, A., Spilling, K., Olli, K., 2011. Decadal-scale changes of dinoflagellates and diatoms in the anomalous Baltic Sea spring bloom. PLoS One 6 (6), e21567.

Kononen, K., Niemi, Å., 1984. Long-term variation of the phytoplankton composition at the entrance of the Gulf of Finland. Ophelia Suppl. 3, 101–110.

Kremp, A., Elbrächter, M., Schweikert, M., Wolny, J.L., Gottschling, M., 2005. *Woloszynskia halophila* (Biecheler) comb. nov.: a bloom-forming cold-water dinoflagellate co-occurring with *Scripsiella hangoei* (Dinophyceae) in the Baltic Sea. J. Phycol. 41, 629–642.

Laanemets, J., Väli, G., Zhurbas, V., Elken, J., Lips, I., Lips, U., 2011. Simulation of mesoscale structures and nutrient transport during summer upwelling events in the Gulf of Finland in 2006. Boreal Environ. Res. 16A, 15–26.

Lachat Instruments, 2000. QuikChem method number 31–107–04–1-D - Determination of nitrate and/or nitrite in the brackish waters by flow injection analysis. Revision date: 20 November 2000.

Lachat Instruments, 2001. QuikChem method number 31–115–01–1-I - Determination of ortophosphate by flow injection analysis. Revision date: 27 June 2001.

Lignell, R., Heiskanen, A.-S., Kuosa, H., Gundersen, K., Kuuppo-Leinilcki, P., Pajuniemi, R., Uitto, A., 1993. Fate of a phytoplankton spring bloom: sedimentation and carbon flow in the planktonic food web in the northern Baltic. Mar. Ecol. Prog. Ser. 94, 239–252.

Lindholm, T., Mork, A.-C., 1990. Depth maxima of *Mesodinium rubrum* (Lohmann) Hamburger and Buddenbrock – examples from a stratified Baltic Sea inlet. Sarsia 75, 53–64.

Lips, I., Lips, U., 2008. Abiotic factors influencing cyanobacterial bloom development in the Gulf of Finland (Baltic Sea). Hydrobiologia 614, 133–140.

Lips, U., Lips, I., Liblik, T., Kikas, V., Altoja, K., Buhhalko, N., Rünk, N., 2011. Vertical dynamics of summer phytoplankton in a stratified estuary (Gulf of Finland, Baltic Sea). Ocean Dyn. 61, 903–915.

Maar, M., Moller, E.F., Larsen, J., Madsen, K.S., Wan, Z., She, J., Jonasson, L., Neumann, T., 2011. Ecosystem modelling across a salinity gradient from the North Sea to the Baltic Sea. Ecol. Model. 222, 1696–1711.

Malone, T.C., 1980. Algal size. In: Morris, I. (Ed.), The Physiological Ecology of Phytoplankton. Blackwell Scientific Publications, Oxford, pp. 433–463.

Mateus, M., Leitão, P.C., de Pablo, H., Neves, R., 2012. Is it relevant to explicitly parametrize chlorophyll synthesis in marine ecological models? J. Mar. Syst. 94, S23–S33.

Menden-Deuer, S., Lessard, E.J., 2000. Carbon to volume relationships for dinoflagellates, diatoms, and other protist plankton. Limnol. Oceanogr. 45, 569–579.

Müller-Karulis, B., Aigars, J., 2011. Modeling the long-term dynamics of nutrients and phytoplankton in the Gulf of Riga. J. Mar. Syst. 87, 161–176.

Olenina, I., Hajdu, S., Edler, L., Andersson, A., Wasmund, N., Busch, S., Göbel, J., Gromisz, S., Huseby, S., Huttunen, M., Jaanus, A., Kokkonen, P., Ledaine, I., Niemkiewicz, E., 2006. Biovolumes and size-classes of phytoplankton in the Baltic Sea. HELCOM Balt. Sea Environ. Proc. 106 (144 pp.).

Passow, U., 1991. Vertical migration of *Gonyaulax catenata* and *Mesodinium rubrum*. Mar. Biol. 110, 455–463.

Pitkänen, H., Lehtoranta, J., Peltonen, H., 2008. The Gulf of Finland. In: Schiewer, U. (Ed.), Ecology of Baltic Coastal Waters: Ecological Studies, 197, pp. 285–308.

Putt, M., Stoecker, D.K., 1989. An experimentally determined carbon: volume ratio for marine 'oligotrichous' ciliates from estuarine and coastal waters. Limnol. Oceanogr. 34, 1097–1103.

Raateoja, M., Kuosa, H., Hällfors, S., 2011. Fate of excess phosphorus in the Baltic Sea: a real driving force for cyanobacterial blooms? J. Sea Res. 65, 315–321.

Rantajärvi, E., Gran, V., Hällfors, S., Olsonen, R., 1998. Effects of environmental factors on the phytoplankton community in the Gulf of Finland — unattended high frequency measurements and multivariate analyses. Hydrobiologia 363, 127–139.

Roiha, P., Westerlund, A., Nummelin, A., Stipa, T., 2010. Ensemble forecasting of harmful algal blooms in the Baltic Sea. J. Mar. Syst. 83, 210–220.

Rychert, K., 2004. The size structure of the *Mesodinium rubrum* population in the Gdańsk Basin. Oceanologia 46, 439–444.

Schneider, B., Kaitala, S., Maunula, P., 2006. Identification and quantification of plankton bloom events in the Baltic Sea by continuous *p*CO2 and chlorophyll *a* measurements on a cargo ship. J. Mar. Syst. 59, 238–248.

Smayda, T.J., 2010. Adaptations and selections of harmful and other dinoflagellate species in upwelling systems. 2. Motility and migratory behaviour. Prog. Oceanogr. 85, 71–91.

Sommer, U., Lengfellner, K., 2008. Climate change and the timing, magnitude, and composition of the phytoplankton spring bloom. Glob. Chang. Biol. 14, 1199–1208.

Spilling, K., Lindström, M., 2008. Phytoplankton life cycle transformations lead to species-specific effects on sediment processes in the Baltic Sea. Cont. Shelf Res. 28, 2488–2495.

Spilling, K., Kremp, A., Tamelander, T., 2006. Vertical distribution and cyst production of *Peridiniella catenata* (Dinophyceae) during a spring bloom in the Baltic Sea. J. Plankton Res. 28, 659–665.

Staehr, P.A., Henriksen, P., Markager, S., 2002. Photoacclimation of four marine phytoplankton species to irradiance and nutrient availability. Mar. Ecol. Prog. Ser. 238, 47–59.

Stipa, T., 2004. The vernal bloom in heterogeneous convection: a numerical study of Baltic restratification. J. Mar. Syst. 44, 19–30.

Sundström, A.M., Kremp, A., Daugbjerg, N., Moestrup, Ø., Ellegaard, M., Hansen, R., Hajdu, S., 2009. *Gymnodinium corollarium* sp. nov. (Dinophyceae) — a new cold-water dinoflagellate responsible for cyst sedimentation events in the Baltic Sea. J. Phycol. 45, 938–952.

Sundström, A.M., Kremp, A., Tammilehto, A., Tuimala, J., Larsson, U., 2010. Detection of the bloom-forming cold-water dinoflagellate *Biecheleria baltica* in the Baltic Sea using LSU rRNA probes. Aquat. Microb. Ecol. 61, 129–140.

Sverdrup, H., 1953. On conditions for the vernal blooming of phytoplankton. J. Cons. Explor. Mer 18, 287–295.

Tamelander, T., Heiskanen, A.S., 2004. Effects of spring bloom phytoplankton dynamics and hydrography on the composition of settling material in the coastal northern Baltic Sea. J. Mar. Syst. 52, 217–234.

Thamm, R., Schernewski, G., Wasmund, N., Neumann, T., 2004. Spatial phytoplankton pattern in the Baltic Sea. In: Schernewski, G., Wielgat, M. (Eds.), Baltic Sea Typology: Coastline Reports, 4, pp. 85–109.

Utermöhl, H., 1958. Zur Vervollkommnung der quantitativen Phytoplanktonmetodic. Mittelungen des Internationale Vereinigung für Theoretische und Angewandte Limnologie. : , 9 1–38.

Vehmaa, A., Kremp, A., Tamminen, T., Hogfors, H., Spilling, K., Engström-Öst, J., 2011. Copepod reproductive success in spring-bloom communities with modified diatom and dinoflagellate dominance. ICES J. Mar. Sci. http://dx.doi.org/10.1093/icesjms/fsr138.

Vepsäläinen, J., Pyhälahti, T., Rantajärvi, E., Kallio, K., Pertola, S., Stipa, T., 2005. The combined use of optical remote sensing data and unattended flow-through fluorometer measurements in the Baltic Sea. Int. J. Remote Sens. 26, 261–282.

Wan, Z., Jonasson, L., Bi, H., 2011. N/P ratio of nutrient uptake in the Baltic Sea. Ocean Sci. 7, 693–704.

Wasmund, N., Uhlig, S., 2003. Phytoplankton trends in the Baltic Sea. ICES J. Mar. Sci. 60, 177–186.

Wasmund, N., Nausch, G., Matthäus, W., 1998. Phytoplankton spring blooms in the southern Baltic Sea — spatio-temporal development and long-term trends. J. Plankton Res. 20, 1099–1117.

Wasmund, N., Tuimala, J., Suikkanen, S., Vandepitte, L., Kraberg, A., 2011. Long-term trends in phytoplankton composition in the western and central Baltic Sea. J. Mar. Syst. 87, 145–159.

Wasmund, N., Nausch, G., Feistel, R., 2013. Silicate consumption: an indicator for long-term trends in spring diatom development in the Baltic Sea. J. Plankton Res. http://dx.doi.org/10.1093/plankt/fbs101.

Wilkerson, F.P., Grunseich, G., 1990. Formation of blooms by the symbiotic ciliate *Mesodinium rubrum*: the significance of nitrogen uptake. J. Plankton Res. 12, 973–989.

Paper V

Lips, U., Lips, I., Kikas, V., Kuvaldina, N. (2008). Ferrybox measurements: a tool to study meso-scale processes in the Gulf of Finland (Baltic Sea). *IEEE Conference Publications: 2008 IEEE/OES US/EU–Baltic International Symposium, Tallinn, 27–29 May 2008*, 1–6, doi: 10–1109/BALTIC.2008. 4625536.

Ferrybox Measurements: a Tool to Study Meso-Scale Processes in the Gulf of Finland (Baltic Sea)

Urmas Lips, Inga Lips, Villu Kikas and Natalja Kuvaldina
Marine Systems Institute, Tallinn University of Technology
Akadeemia tee 21
12618 Tallinn, Estonia

Abstract- **Ferrybox measurements are carried out in the Gulf of Finland (Baltic Sea) in a regular basis since 1997. Routines for data acquisition are developed enabling near real-time data delivery for operational models. Cross-gulf high-resolution temperature, salinity and chlorophyll *a* fluorescence profiles collected in 2007 are used to describe meso-scale variability of hydrophysical and -biological fields in the gulf. It is shown that higher values of chlorophyll a concentration are more often observed in the coastal areas and in the vicinity of a quasi-permanent salinity front in the central Gulf of Finland.**

I. INTRODUCTION

Meso-scale physical features (fronts, eddies, upwelling, downwelling) are known to be determinant for biological production, retention and transport. To assess and quantify the influence of these processes on the functioning of pelagic ecosystem, measurements with high enough resolution, duration and extent have to be conducted. Conventional monitoring programs have too low resolution of sampling while special investigations using the research vessels are conducted episodically. Therefore, new methods such as remote sensing, measurements at autonomous buoy stations and voluntary platforms such as ferries have to be applied. Only using these methods we could be able to monitor the variability of environmental parameters in the spatial and temporal scales in order of 10 km and of a few days.

The Gulf of Finland lies in the northeastern part of the Baltic Sea. It is an elongated basin with a length of about 400 km and a maximum width of 140 km. The large freshwater inflow in the eastern end of Gulf (the Neva River) leads to a surface-layer salinity decrease from 6 at its entrance to 1 in the easternmost area. The vertical stratification is characterized by a permanent halocline at depths of 60-80 m, and a seasonal thermocline, which forms at the depths of 10-30 m in summer. The long-term residual circulation in the surface layer of the Gulf is characterized by a relatively low speed and by a cyclonic pattern (e.g. [1,2] and references therein). According to the latter, the saltier water of the northern Baltic Proper intrudes to the Gulf along the Estonian coast and the seaward flow of fresher gulf water occurs along the Finnish coast.

The circulation is more complex at time scales from days to weeks due to the variable wind forcing. A variety of mesoscale processes (fronts, eddies, upwelling/downwelling) have been observed [3,4,5]. Due to the dominating southwesterly winds, the Finnish coastal sea is one of the main upwelling areas in the Baltic Sea in summer, from May to September [6]. In case of easterly winds, upwelling events are observed in the Estonian coastal sea area near the southern coast of the Gulf (e.g. [7]).

The nutrient concentrations in the surface layer of the Gulf of Finland reveal pronounced seasonal variation. Maximal dissolved inorganic nitrogen (DIN) and phosphorus (DIP) concentrations are observed in winter while in summer, the concentrations of DIN and DIP are usually close to the detection limit in the upper layer. However, higher concentrations are observed just below the seasonal thermocline [8]. The seasonal dynamics of phytoplankton species composition and biomass in the Gulf of Finland is characterised by spring bloom in April-May dominated by dinoflagellates (and diatoms), summer minimum from late May to late June and late summer bloom in July (or late June to mid August) dominated by cyanobacteria. The latter is often causing public concern about the status of the sea environment.

The main aim of the present paper is to show how Ferrybox measurements can be used for the monitoring of meso-scale processes in the Gulf of Finland. On the basis of data collected from May to September 2007, the meso-scale dynamics in the study area and influence of observed processes to the chlorophyll *a* distribution in the surface layer will be described.

II. MATERIAL AND METHODS

A. Measurements

Temperature (T), salinity (S) and chlorophyll *a* fluorescence data and water samples for chlorophyll *a* (Chl *a*) analysis are collected unattended on passenger ferries, travelling between Tallinn and Helsinki (Fig. 1) since 1997. In 2006 a new flow-through system (see Fig. 2; 4H-Jena, Germany) was installed onboard ferry Galaxy (Tallink Group). It is able to measure in addition to T, S and fluorescence also turbidity and nutrient concentrations. The system and sensors are kept clean by an acid washing procedure performed autonomously every evening.
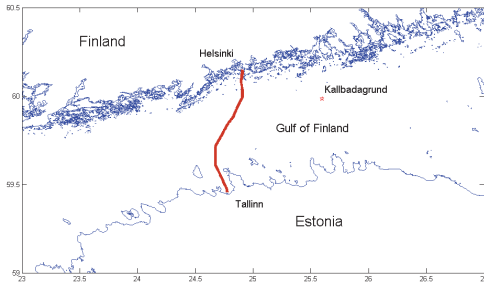
Figure 1. Map of the study area, ferry route between Tallinn and Helsinki and location of Kalbådagrund meteorological station.

Figure 2. Measurement system onboard passenger ferry Galaxy.

The water intake for measurements and sampling is located at 3-4 m depth. To restrict larger particles to get into the measurement system a mud filter is used just after the intake. For temperature measurements a sensor PT100 is used that is installed also close to the water intake to diminish the effect of warming of water while flowing through the tubes onboard. Prior to the other sensors a debubbler is installed to avoid air bubbles to influence the measurements of conductivity, turbidity and Chl *a* fluorescence. For salinity measurements a FSI temperature and conductivity meter is used. The performance of these sensors is checked by taking water samples and analyzing them using a high-precision salinometer AUTOSAL. Temperature and salinity profiles along the ferry route have been compared also with the results of CTD measurements from research vessel.

For Chl *a* fluorescence measurements a SCUFA submersible fluorometer (Turner Designs) with a flow-through cap is used. The fluorometer is equipped also with a turbidity sensor, and a temperature sensor to correct the fluorescence values for temperature. While T, S, Chl *a* fluorescence and turbidity data are recorded every 20 seconds (corresponding to a horizontal resolution of approximately 200 m) every crossing, 14 water samples (1 litre per a sampling) are automatically collected once a week with a predefined time interval of 10 minutes, when ferry is travelling from Helsinki to Tallinn. For water sampling a refrigerated water sampler Hach Sigma 900 MAX is used and the samples are kept in cool (4 °C) and dark conditions until analysis (after 12 hours). To calibrate the measured fluorescence values against Chl *a* content in the water, samples are analyzed using a spectrophotometer Thermo Helios γ. The concentration of Chl *a* is determined by filtering the water samples through Millipore APFF glassfibre filters (pore size 0.7 □m), extracting the pigments 24 hours at room temperature with ethanol (96%) and measuring the absorption at the wavelength of 665 nm. The Fluorometer is calibrated once a year in an onshore laboratory as well.

B. Preliminary processing, quality check and transfer of data

Data are stored in an onboard terminal and delivered automatically to the on-shore ftp-server once a day. In order to use the data for assimilation into operational models automatic procedures for preliminary processing and quality check have to be applied. The quality of data is checked for unrealistic data values as well as the performance parameters of the system are validated. These parameters are flow speed of water and pressure in the system. If the values of these parameters exceed certain limits then the data points are marked by a flag.

One of the procedures which have to be carried out is shifting of data points to the actual positions of water intake. While water is taken in and it flows through the tubes and debubbler with a flow speed of 6-7 liters per minute, the ferry moves on. The position (defined using a GPS) is attached to a data record at the time of measurement. Analysis of data from forth- and backward journeys allowed introducing a very rough position-correction procedure: a constant shift in latitude and longitude is applied for all recorded data points (Fig. 3).

To convert fluorescence values to the Chl a concentrations a linear regression between fluorescence and Chl a content detected spectrophotometrically is found. An example of comparison between these two data sets from 8 July 2007 is shown in Fig. 3.

Chl *a* fluorescence, raw positions

Chl *a* fluorescence, corrected positions
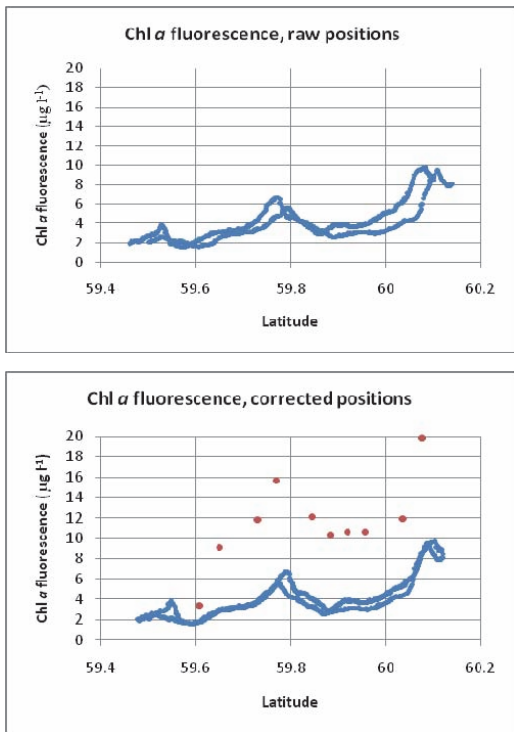
Figure 3. Horizontal profiles of Chl *a* fluorescence along the ferry route on 8 July 2007 (both crossings are shown). In upper panel raw positions of measurements and in the lower panel corrected positions are shown. Red dots indicate Chl *a* concentrations detected from the water samples in the on-shore laboratory.

III   RESULTS

A. Spatial and temporal variability of T, S and Chl a fluorescence along the ferry route in May-September 2007

Seasonal variation of water temperature in the study area was characterized by a relatively slow increase in spring and June – the surface layer temperature exceeded 10 °C in the beginning of June and 15 °C in the beginning of July only. The maximum values of surface layer temperature > 20 °C were observed in mid August.

Meso-scale variability of temperature field was related mainly to the coastal upwelling events observed near the both coasts. An upwelling event occurred near the Estonian coast in the beginning of June when temperature fall about 4-5 degrees. In July, first an upwelling event was observed near the Estonian coast and after that near the Finnish coast. This latter event was a dominating meso-scale feature in the study area during a more than two weeks period. However, the temperature difference between upwelled waters and the rest of the transect fairly exceeded 5 degrees. One of the horizontal profiles from this period is shown in Fig. 5.

Appearance of coastal upwelling events is explained quite well by the variations of the wind speed and direction in the region (Fig. 6). Easterly winds prevailed in the beginning of June and in the first half of July; as a result upwelling events occurred near the Estonian coast. Two-week period with dominating westerly winds in July-August coincided with the upwelling event near the northern coast.

Salinity distribution revealed a seasonal variation of salinity as well. In June – first half of July a low salinity water mass was present in the study area. In mid July salinity values rose along the entire transect.

Spatial distribution of salinity was characterized by a salinity front that almost permanently was observed in the central part of the transect. The two horizontal profiles presented in Fig. 6 expose that even though salinity values increased along the entire transect from 16 to 23 July a front separating more saline southern gulf waters and fresher northern gulf waters did not move away from the region.

Chlorophyll *a* fluorescence distribution in the study area in July-August was very patchy. High Chl *a* concentrations were observed near the coast opposite to the upwelling events (in the downwelling areas). A remarkable feature of the Chl *a* distribution is frequently observed high concentrations in the central part of the transect close to the described quasi-permanent salinity front. Somewhat higher number of days with Chl *a* fluorescence exceeding 4 mg m^{-3} was found there as well (Fig. 7).

A few-day period was observed in the second half of August when along the entire ferry route the fluorescence values were > 6 mg m^{-3}. According to the Kalbådagrund wind data weak south-easterly winds prevailed during this period.
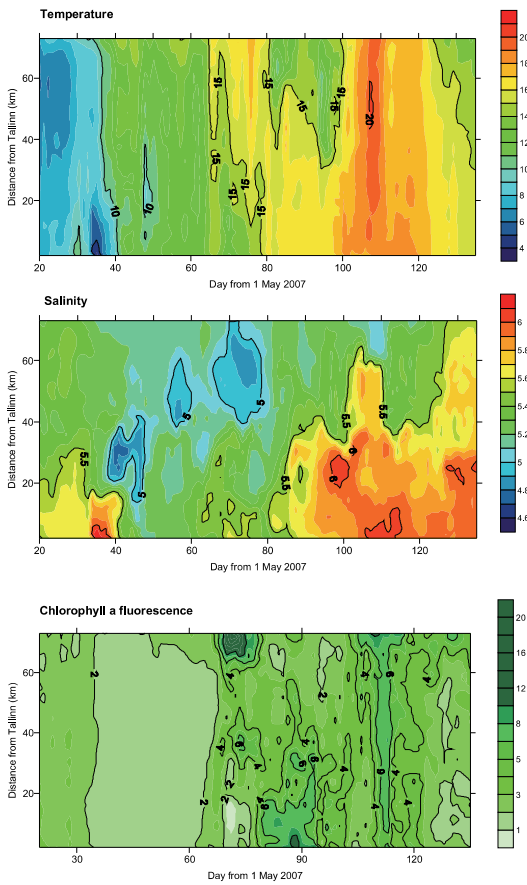
Figure 4. Spatial and temporal variations of temperature, salinity and chlorophyll *a* fluorescence (mg m^{-3}) along the ferry route Tallinn – Helsinki in May-September 2007.
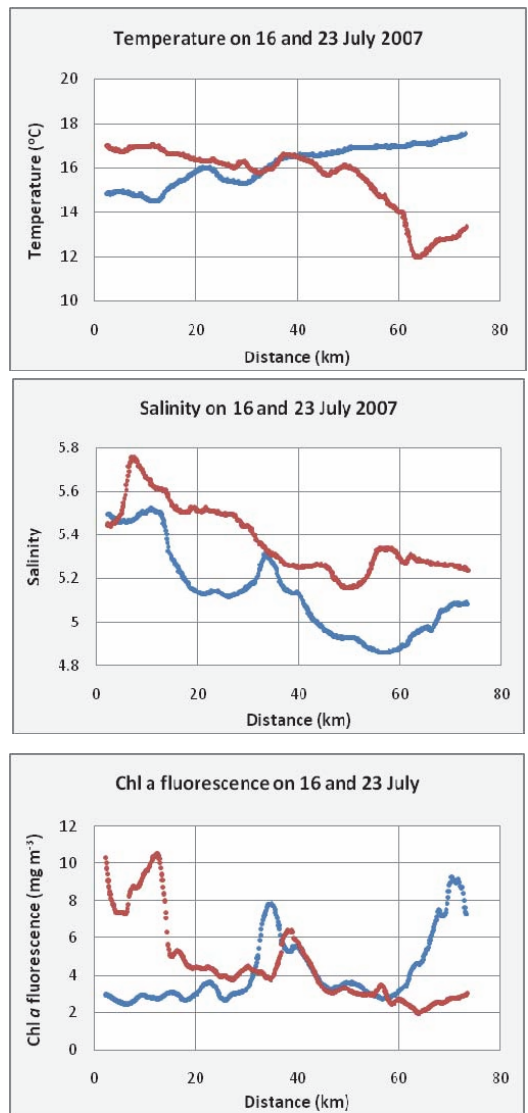
Figure 5. Horizontal profiles of temperature, salinity and chlorophyll *a* fluorescence (mg m^{-3}) along the ferry route Tallinn – Helsinki on 16 July (blue dots) and on 23 July (red dots) 2007.

Figure 6. Time series of wind speed and direction at the Kalbådagrund meteorological station from May to September 2007.
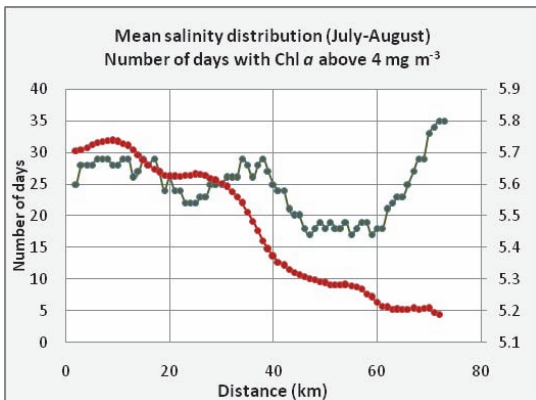
Figure 7. Average salinity distribution along the ferry route (red dots and line) and number of days when Chl a fluorescence value exceeded 4 mg m⁻³ in July-August 2007.

IV   APPLICATION OF MESO-SCALE INDEXES

An upwelling intensity index is developed on the basis of unattended measurements along the ferry route (along a cross-gulf transect) as a mean temperature difference between coastal waters and gulf waters [10]. It is shown that estimated intensities of upwelling events are well correlated with the cross-gulf Ekman transport estimates. Upwelling index can be used as a measure of vertical transport of nutrients into the depleted surface layer of the gulf. The integrated upwelling index for a period starting from 1 May until a selected date is finally obtained summing up all values of indexes for days when upwelling was present either near the southern coast or near the northern coast (when index is below 0). It is shown that the estimated upwelling index and off coast 10-day average Ekman transport values correlate very well.

Analysis of Ferrybox data from 1997-2004 showed that an integrated intensity of pre-bloom upwelling events (sum of upwelling indexes in May-June) is well correlated with the cyanobacterial bloom intensity in the Gulf of Finland in July-August (r^2 = 0.66, p = 0.01; [11]).

CONCLUSIONS

High meso-scale variability of temperature and salinity fields in the Gulf of Finland can be related to the coastal upwelling events, fronts and eddies. Depending on the wind speed and direction coastal upwelling appears either off southern coast (when easterly winds prevail, in 2007 – in June and beginning of July) or off northern coast (when westerly winds prevail, in 2007 – second half of July and beginning of August). Quasi-permanent salinity front exists between saltier waters of southern gulf and fresher waters of northern coast.

Ferrybox measurements enable to monitor the occurrence and estimate the intensity of meso-scale physical processes/ structures influencing the pelagic ecosystem. An introduced upwelling index can be used in operational forecasts of cyanobacterial blooms in the Gulf of Finland [12].

REFERENCES

[1] P. Alenius, K. Myrberg and A. Nekrasov. "The physical oceanography of the Gulf of Finland: a review." *Boreal Env. Res.,* 3, pp. 97-125, 1998.
[2] O. Andrejev, K. Myrberg, P. Alenius and P. Lundberg. "Mean circulation and water exchange in the Gulf of Finland - a study based on three-dimensional modeling", *Boreal Env. Res.,* 6, pp. 1-16, 2004.
[3] L. Talpsepp, T. Nõges, T. Raid and T. Kõuts, "Hydrophysical and hydrobiological processes in the Gulf of Finland in summer 1987 –

characterization and relationship.", *Cont. Shelf Res.,* 14, pp. 749-763, 1994.

[4] J. Pavelson, J. Laanemets, K. Kononen and S. Nõmman, "Quasi-permanent density front at the entrance to the Gulf of Finland: Response to wind forcing.", *Cont. Shelf Res.,* 17, pp. 253-265, 1997.

[5] J. Laanemets, J. Pavelson, U. Lips and K. Kononen. "Downwelling related meso-scale motions at the entrance to the Gulf of Finland: observations and diagnosis.", *Oceanological and Hydrobiological Studies*, 34, pp. 15-36, 2005.

[6] I. Lips, U. Lips, T. Liblik and N. Kuvaldina "Consequences of summer upwelling events on hydrophysical and biogeochemical patterns in the western Gulf of Finland (Baltic Sea)", 2008, manuscript.

[7] K. Myrberg and O. Andrejev, "Main upwelling regions in the Baltic Sea – a statistical analysis based on three-dimensional modeling," *Boreal Environ. Res.*, vol. 8, pp. 97-112, 2003.

[8] J. Laanemets, K. Kononen, J. Pavelson, and E.-L. Poutanen « Vertical location of seasonal nutriclines in the western Gulf of Finland." *J. Mar. Sys.*, 52, pp. 1-13, 2004.

[9] I. Kanoshina, U. Lips and J.-M. Leppänen „The influence of weather conditions (temperature and wind) on cyanobacterial bloom development in the Gulf of Finland (Baltic Sea)." *Harmful Algae*, 2, pp. 29-41, 2003.

[10] U. Lips, I. Lips, L. London, V. Kikas and T. Liblik. "Upwelling index based on Ferrybox measurements in the Gulf of Finland: a tool to assess meso-scale physical forcing on the pelagic ecosystem." *Baltic Sea Science Congress, March 19-23, Rostock, Germnay. Abstract Volume, lectures –CBO Session, Topic B: Upwelling events, coastal offshore exchange, links to biogeochemical processes,* pp. 53, 2007.

[11] I. Lips. "An analysis of factors controlling the development of cyanobacterial blooms in the Gulf of Finland (Baltic Sea)." (PhD thesis, Tartu Ülikool) Tartu: Tartu University Press, 2005.

[12] J. Laanemets, J., M.-J. Lilover, U. Raudsepp, R. Autio, E. Vahtera, I. Lips and U. Lips. (2006). "A fuzzy logic model to describe the cyanobacteria *Nodularia spumigena* bloom in the Gulf of Finland, Baltic Sea." *Hydrobiologia*, 554, pp. 31-45.

ACKNOWLEDGEMENTS

ABSTRACT

The main aim of this thesis is to describe surface layer dynamics and physical processes driving them in the highly stratified Gulf of Finland in spring–summer period. The Gulf of Finland is an estuarine-like basin, with the eastern end being closed and having significant freshwater input, through western boundary almost non-restricted water exchange with the more saline Baltic Proper takes place. In addition to the quasi-permanent halocline at the depths of 60–70 m, a seasonal thermocline forms in the Gulf of Finland in spring-summer at the depths of 10–20 m.

The present study is based on high-resolution data collected (2007–2013 May–September) with Ferrybox system installed on board a passenger ferry traveling between Tallinn and Helsinki (regularly crossing the gulf twice a day). In addition to Ferrybox measurements, water samples are collected to calibrate the sensors, analyze nutrient concentrations and phytoplankton species composition and biomass. In this study temperature, salinity and Chl *a* data from over 1000 crossings is used, measured in 4 m depth with a spatial resolution of ~160 m. Additionally, to analyze the surface and sub-surface layer dynamics, temperature, salinity, and Chl *a* data from autonomous buoy profiler, research-vessel-based devices, towed undulating instruments (Scanfish), remote sensing and wind data were applied in the present study.

An average cross-gulf salinity distribution in the surface layer with the salinity minimum in the northern gulf confirms that in general, an outflow of fresher waters dominates along the northern coast (with the core at a distance of 20 km from the northern shore) in summer. Average cross-gulf temperature distribution did not show significant gradients, but high standard deviations approximately 20 km from both shores compared to the middle section, implies great impact of upwelling events in coastal areas.

One of the main scientific questions of the study is related to the coastal upwelling events. Coastal upwelling events are generated in the Gulf of Finland by strong enough wind impulses from west – south-west near the northern coast and from east – north-east near the southern coast. Previous analyses based on remote sensing, wind and numerical modeling data have indicated more frequent upwelling events near northern coast. It has been suggested that a greater impact (salt and nutrients transport to upper layer) of upwellings in the southern part is related to steeper bottom slope. Upwelling index, a method for detection and quantitative description of coastal upwelling events was developed and used to describe statistically the occurrence of coastal upwelling events and their characteristic parameters along the two opposite coasts of the gulf. The analysis of Ferrybox data revealed that the upwelling occurrences and average intensities of the events are similar near the northern and southern coasts while the wind impulse needed to generate an upwelling event of certain intensity differs between the two coastal areas. This different response to the wind forcing in the southern and northern coastal areas could be related to the estuarine character of the basin with only one open border in the west and prevailing winds from west

– south-west. The resulting deeper position of the thermocline in the northern gulf could be a reason why a stronger wind impulse is needed to initiate the upwelling by the westerly (up-estuary) winds near the northern coast than in the case of the easterly (down-estuary) winds and the upwelling near the southern coast. Additionally, the results suggest that dominating long-term easterly and westerly winds have a different impact on the surface layer dynamics. In the case of easterly winds, the surface layer waters are transported out of the gulf, this has to be compensated by an upward movement of the thermocline and intensifies upwelling near the southern coast. The effect is reversed in the case of long-term westerly winds, working against intensifying upwelling events near the northern coast.

Two types of upwelling events were identified – one characterized by a strong temperature (upwelling) front and the other revealing a gradual decrease in temperature from the open sea to the coastal area, with a maximum temperature deviation very close to the shore. The spatial variations in temperature with scales of a few kilometers, which were characteristic for the second type, could be signs of the sub-mesoscale features (filaments and squirts) associated with the upwelling dynamics. The spectral analysis of high-resolution temperature data revealed pronounced sub-mesoscale features in the surface and subsurface layer. The horizontal wavenumber spectra of temperature variance estimated between the lateral scales of 10 and 0.5 km had the slopes close to –2 both in the surface layer and the seasonal thermocline. It shows that the ageostrophic sub-mesoscale processes contribute considerably to the energy cascade from larger to smaller spatial scales in this stratified sea basin.

Analysis of the Ferrybox data showed that spring bloom peaks coincide with a relatively fast temperature increase in the surface layer, indicating a strengthening of stratification.

Ferrybox long-term and high-resolution measurements from Tallinn to Helsinki can be successfully used to describe physical and biogeochemical processes in the surface layer, supplementing significantly existing field measurements.

RESÜMEE

Käesoleva töö eesmärgiks on kevadise ja suvise mere pinnakihi muutlikkuse ja muutlikkust põhjustavate füüsikaliste protsesside selgitamine tugevalt stratifitseeritud Soome lahes. Soome laht on estuaari tüüpi bassein, mille idaosa on suletud ja suure mageda vee sissevooluga ning avatud lääneosas toimub veevahtus Läänemere avaosaga. Soome lahe stratifikatsiooni iseloomustavad kvaasi-permanentne halokliin sügavuste vahemikus 60–70 m ja suvisel perioodil sesoone termokliin, mis paikneb 10–20 m sügavusel.

Töö põhineb Tallinna–Helsingi vahel kurseerivale parvlaevale (regulaarselt kaks korda päevas) paigaldatud Ferryboxi süsteemi abil aastatel 2007–2013 (perioodil mai-september) kogutud kõrglahutusega andmetel. Lisaks mõõtmistele võimaldab Ferrybox süsteem koguda veeproove andurite kalibreerimiseks, toiainete ja fütoplanktoni koosluse määramiseks. Kokku on töös kasutatud üle 1000 temperatuuri, soolsuse ja klorofülli andmerea, mis on mõõdetud 4 m sügavusel horisontaalse sammuga ~160 m. Täiendavalt on mere pinnakihi andmete analüüsiks kasutatud veesamba autonoomse profileerija ja pukseeritava aparatuuri temperatuuri, soolsuse ja klorofülli vertikaalseid profiile, samuti kaugseire (klorofüll) ja tuule andmeid.

Soolsuse suvine mitmeaastane keskmine jaotus lõikel Tallinn–Helsingi kinnitas Soome lahe üldist tsirkulatsiooni: magedam vesi voolab lahest välja lahe põhjaosas, tuumaga ligikaudu 20 km rannikust. Temperatuuri keskmine jaotus ei näidanud olulisi gradiente kuid on märkimisväärne, et temperatuuri standard hälbed olid 20 km tsoonis mõlemast rannikust palju suuremad võrreldes lahe avaosaga, mis viitab rannikumere apvellingute (süvavee kerge) mõjule.

Töö üks peamisi teaduslikke küsimusi oli seotud rannikumere apvellingute dünaamikaga. Apvellinguid tekitavad piki lahte puhuvad tuuled – idatuuled tekitavad apvellinguid lõunaranniku ja läänetuuled põhjaranniku läheduses. Senised hinnangud, kasutades kaugseire, tuule ja numbrilise modelleerimise andmeid, näitasid sagedasemat apvellingute esinemist lahe põhjaosas. Lahe lõunaosa apvellingute suuremat mõju (soola ja toitainete transport ülakihti) on seostatud järsuma põhjakaldega. Apvellingu parameetrite ja nende seose leidmiseks mõjuva tuule impulsiga töötati välja spetsiaalne apvellingu indeks. Ferrybox'i andmete analüüs näitas, et apvellingute sagedus mõlemas rannikumeres on samasugune, kuid tuule impulss samasuguse intensiivsusega apvellingu tekitamiseks on erinev. Tuulepingele erineva reaktsiooni selgitamiseks lahe lõuna ja põhja osas vaadeldi Soome lahte estuaarina, millest tulenevalt on termokliin lahe põhjaosas keskmiselt sügavamal kui lõunaosas. Seega, termokliini kalle nõrgendab läänetuule poolt tekitatud apvellingut lahe põhjaosas ja soodustab idatuule poolt tekitatud apvellingut lahe lõunaosas. Lisaks on töös välja pakutud selgitus, et pikema aja jooksul domineerivad ida- ja läänetuuled mõjutavad lahe ülemise veekihi dünaamikat erinevalt. Idatuulte mõjul transporditakse

ülemise kihi vett lahest välja ja selle kompenseerimiseks peab termokliin lahes tõusma, mis soodustab apvellingut lõunaranniku lähedal. Pikaajaliste läänetuulte puhul on mõju vastupidine, mis töötab vastu apvellingu intensiivistumisele põhjaranniku lähedal.

Ferrybox'i andmete analüüs näitas kahte tüüpi apvellingute esinemist Soome lahes: tugeva temperatuuri frondiga ja järkjärgulise temperatuuri vähenemisega ranniku suunas. Viimasel juhul esinesid temperatuuri ridades fluktuatsioonid mastaabiga paar kilomeetrit, mis viitab apvellingu dünaamikaga seotud sub-mesomastaapsetele protsessidele. Temperatuuri ridade spektraalanalüüs kinnitas sub-mesomastaapsete protsesside rolli temperatuuri välja struktuuride formeerumisel. Temperatuuri dispersiooni spektrite kalle ruumi mastaapides 10–0.5 km oli lähedane –2, mis näitab sub-mesomastaapsete protsessid olulisust energia ülekandel suurematelt ruumi mastaapidelt väiksematele mastaapidele.

Ferrybox'i andmete analüüs näitas, et kevadise fütoplanktoni õitsengu maksimumid langevad kokku pinnakihi temperatuuri kiire tõusuga, st mere ülemise kihi stratifikatsiooni tugevnemisega.

Ferrybox süsteemi abil lõikel Tallinn–Helsingi kogutud kõrglahutusega pikaajaliste andmeridade analüüs näitas nende sobivust pinnakihis toimuvate füüsikaliste ja biogeokeemiliste protsesside uurimiseks, täiendades oluliselt traditsiooniliste välimõõtmistega kogutud andmeid.

ELULOOKIRJELDUS

1. Isikuandmed
   Ees- ja perekonnanimi   Villu Kikas
   Sünniaeg ja -koht   08.02.1982, Tallinn, Eesti
   Kodakondsus   Eesti
   E-posti aadress   villu.kikas@msi.ttu.ee

2. Hariduskäik

Õppeasutus (nimetus lõpetamise ajal)	Lõpetamise aeg	Haridus (eriala/kraad)
TTÜ	2008	Loodusteaduse magistrikraad
Eesti Mereakadeemia	2006	Rakenduskõrgharidus, hüdrograafia
TTÜ	2002	Tootearendus (lõpetamata)
Tallinna Nõmme Gümnaasium	2000	Keskharidus

3. Keelteoskus (alg-, kesk- või kõrgtase)

Keel	Tase
Eesti	Emakeel
Inglise	Kõrgtase
Soome	Kesktase

4. Teenistuskäik

Töötamise aeg	Tööandja nimetus	Ametikoht
2006 - …	TTÜ MSI	Insener
2004 - 2006	Veeteede Amet	Hüdrograaf

5. Publikatsioonid Eesti Teadusinfosüsteemi klassifikaatori järgi

1.1.

- Lips, Urmas; Kikas, Villu; Liblik, Taavi; Lips, Inga (2016). Multi-sensor in situ observations to resolve the sub-mesoscale features in the stratified Gulf of Finland, Baltic Sea. Ocean Science, 12 (3), 715−732, 10.5194/os-12-715-2016.
- Kikas, Villu; Lips, Urmas (2016). Upwelling characteristics in the Gulf of Finland (Baltic Sea) as revealed by Ferrybox measurements in 2007–2013. Ocean Science, 12, 843−859, 10.5194/os-12-843-2016.
- Lips, Inga; Rünk, Nelli; Kikas, Villu; Meerits, Aet; Lips, Urmas (2014). High-resolution dynamics of spring bloom in the Gulf of Finland, Baltic Sea. Journal of Marine Systems, 129, 135−149.
- Lips, Urmas; Lips, Inga; Liblik, Taavi; Kikas, Villu; Altoja, Kristi; Buhhalko, Natalja; Rünk, Nelli (2011). Vertical dynamics of summer phytoplankton in

a stratified estuary (Gulf of Finland, Baltic Sea). Ocean Dynamics, 61, 903−915, s10236-011-0421-8.

3.1.

- Kikas, V., Norit, N., Meerits, A., Kuvaldina, N., Lips, I., Lips, U. (2010). High-resolution monitoring of environmental state variables in the surface layer of the Gulf of Finland (during a dynamic spring bloom in March–May 2010). In: 4th IEEE/OES Baltic Symposium, Riga, 24-27 August 2010 (1−9). IEEE.
- Lips, Urmas; Lips, Inga; Kikas, Villu; Kuvaldina, Natalja (2008). Ferrybox measurements: a tool to study meso-scale processes in the Gulf of Finland (Baltic Sea). *US/EU-Baltic Symposium "Ocean Observations, Ecosystem-Based Management & Forecasting", Tallinn, 27-29 May, 2008.* IEEE, 1−6. (IEEE Conference Proceedings).

3.4.

- Lips, U.; Lips, I.; Liblik, T.; Kikas, V.; Altoja, K.; Kuvaldina, N.; Norit, N. (2010). Multiparametric in situ observations in the Gulf of Finland. In: Proceedings of the 2nd International Conference (school) on DYNAMICS OF COASTAL ZONE OF NON-TIDAL SEAS, Baltiysk, 26-30 June 2010 (284−289). Kaliningrad: Terra Baltica.

5.2.

- Lips, Urmas; Lips, Inga; London, Lauri; Kikas, Villu; Liblik, Taavi (2007). Upwelling index based on Ferrybox measurements in the Gulf of Finland: a tool to assess meso-scale physical forcing on the pelagic ecosystem. *Abstract Volume: Baltic Sea Science Congress, Rostock, March 19-22, 2007.* 53.
- Raudsepp, U.; Elken, J.; Kõuts, T.; Liblik, T.; Kikas, V.; Lagemaa, P.; Uiboupin, R. (2007). Forecasting skills of the HIROMB in the Gulf of Finland. *Geophysical Research Abstracts, 9: EGU General Assembly, 2007.* European Geosciences Union, 10617.
- Rünk, Nelli; Meerits, Aet; Buhhalko, Natalja; Lips, Inga; Kikas, Villu; Liblik, Taavi; Lips, Urmas (2011). Dynamics of nutrients and phytoplankton Chl *a* influenced by mesoscale and sub-mesoscale physical processes in the Gulf of Finland (Baltic Sea). *Geophysical Research Abstracts, 13: European Geosciences Union General Assembly 2011, Vienna, Austria, May 3 – 8.*
- Norit, Nelli; Kikas, Villu; Lips, Inga; Kuvaldina, Natalja; Lips, Urmas (2009). Spatio-temporal variability of environmental parameters in the surface layer of the Gulf of Finland in spring (on the basis of Tallinn–Helsinki FerryBox data 2007–2009). *Abstract Book: Baltic Sea Science Congress, Tallinn, August 17-21, 2009.* Tallinn University of Technology, 211.

CURRICULUM VITAE

1. Personal data
   Name   Villu Kikas
   Date and place of birth   08.02.1982, Tallinn, Estonia
   E-mail address   villu.kikas@msi.ttu.ee

2. Education

Educational institution	Graduation year	Education (field of study/degree)
TUT	2008	Master's degree
Maritime Academy	2006	Hydrographer
TUT	2002	(unfinished)
TNG	2000	Secondary

3. Language competence/skills (fluent, average, basic skills)

Language	Level
Estonian	Native
English	Fluent
Finnish	Average

4. Professional employment

Period	Organization	Position
2008 – …	MSI at TUT	Engineer
2004 – 2006	Maritime Administration	Hydrographer

5. Publications according ETIS

   1.1.

- Lips, Urmas; Kikas, Villu; Liblik, Taavi; Lips, Inga (2016). Multi-sensor in situ observations to resolve the sub-mesoscale features in the stratified Gulf of Finland, Baltic Sea. Ocean Science, 12 (3), 715−732, 10.5194/os-12-715-2016.
- Kikas, Villu; Lips, Urmas (2016). Upwelling characteristics in the Gulf of Finland (Baltic Sea) as revealed by Ferrybox measurements in 2007–2013. Ocean Science, 12, 843−859, 10.5194/os-12-843-2016.
- Lips, Inga; Rünk, Nelli; Kikas, Villu; Meerits, Aet; Lips, Urmas (2014). High-resolution dynamics of spring bloom in the Gulf of Finland, Baltic Sea. Journal of Marine Systems, 129, 135−149.
- Lips, Urmas; Lips, Inga; Liblik, Taavi; Kikas, Villu; Altoja, Kristi; Buhhalko, Natalja; Rünk, Nelli (2011). Vertical dynamics of summer phytoplankton in

a stratified estuary (Gulf of Finland, Baltic Sea). Ocean Dynamics, 61, 903−915, s10236-011-0421-8.

3.1.

- Kikas, V., Norit, N., Meerits, A., Kuvaldina, N., Lips, I., Lips, U. (2010). High-resolution monitoring of environmental state variables in the surface layer of the Gulf of Finland (during a dynamic spring bloom in March–May 2010). In: 4th IEEE/OES Baltic Symposium, Riga, 24-27 August 2010 (1−9). IEEE.
- Lips, Urmas; Lips, Inga; Kikas, Villu; Kuvaldina, Natalja (2008). Ferrybox measurements: a tool to study meso-scale processes in the Gulf of Finland (Baltic Sea). *US/EU-Baltic Symposium "Ocean Observations, Ecosystem-Based Management & Forecasting", Tallinn, 27-29 May, 2008.* IEEE, 1−6. (IEEE Conference Proceedings).

3.4.

- Lips, U.; Lips, I.; Liblik, T.; Kikas, V.; Altoja, K.; Kuvaldina, N.; Norit, N. (2010). Multiparametric in situ observations in the Gulf of Finland. In: Proceedings of the 2nd International Conference (school) on DYNAMICS OF COASTAL ZONE OF NON-TIDAL SEAS, Baltiysk, 26-30 June 2010 (284−289). Kaliningrad: Terra Baltica.

5.2.

- Lips, Urmas; Lips, Inga; London, Lauri; Kikas, Villu; Liblik, Taavi (2007). Upwelling index based on Ferrybox measurements in the Gulf of Finland: a tool to assess meso-scale physical forcing on the pelagic ecosystem. *Abstract Volume: Baltic Sea Science Congress, Rostock, March 19-22, 2007.* 53.
- Raudsepp, U.; Elken, J.; Kõuts, T.; Liblik, T.; Kikas, V.; Lagemaa, P.; Uiboupin, R. (2007). Forecasting skills of the HIROMB in the Gulf of Finland. *Geophysical Research Abstracts, 9: EGU General Assembly, 2007.* European Geosciences Union, 10617.
- Rünk, Nelli; Meerits, Aet; Buhhalko, Natalja; Lips, Inga; Kikas, Villu; Liblik, Taavi; Lips, Urmas (2011). Dynamics of nutrients and phytoplankton Chl *a* influenced by mesoscale and sub-mesoscale physical processes in the Gulf of Finland (Baltic Sea). *Geophysical Research Abstracts, 13: European Geosciences Union General Assembly 2011, Vienna, Austria, May 3 – 8.*
  - Norit, Nelli; Kikas, Villu; Lips, Inga; Kuvaldina, Natalja; Lips, Urmas (2009). Spatio-temporal variability of environmental parameters in the surface layer of the Gulf of Finland in spring (on the basis of Tallinn–Helsinki FerryBox data 2007–2009). *Abstract Book: Baltic Sea Science Congress, Tallinn, August 17-21, 2009.* Tallinn University of Technology, 211.

DISSERTATIONS DEFENDED AT
TALLINN UNIVERSITY OF TECHNOLOGY ON
NATURAL AND EXACT SCIENCES

1. **Olav Kongas**. Nonlinear Dynamics in Modeling Cardiac Arrhytmias. 1998.

2. **Kalju Vanatalu**. Optimization of Processes of Microbial Biosynthesis of Isotopically Labeled Biomolecules and Their Complexes. 1999.

3. **Ahto Buldas**. An Algebraic Approach to the Structure of Graphs. 1999.

4. **Monika Drews**. A Metabolic Study of Insect Cells in Batch and Continuous Culture: Application of Chemostat and Turbidostat to the Production of Recombinant Proteins. 1999.

5. **Eola Valdre**. Endothelial-Specific Regulation of Vessel Formation: Role of Receptor Tyrosine Kinases. 2000.

6. **Kalju Lott**. Doping and Defect Thermodynamic Equilibrium in ZnS. 2000.

7. **Reet Koljak**. Novel Fatty Acid Dioxygenases from the Corals *Plexaura homomalla* and *Gersemia fruticosa.* 2001.

8. **Anne Paju**. Asymmetric oxidation of Prochiral and Racemic Ketones by Using Sharpless Catalyst. 2001.

9. **Marko Vendelin**. Cardiac Mechanoenergetics *in silico*. 2001.

10. **Pearu Peterson**. Multi-Soliton Interactions and the Inverse Problem of Wave Crest. 2001.

11. **Anne Menert**. Microcalorimetry of Anaerobic Digestion. 2001.

12. **Toomas Tiivel**. The Role of the Mitochondrial Outer Membrane in *in vivo* Regulation of Respiration in Normal Heart and Skeletal Muscle Cell. 2002.

13. **Olle Hints**. Ordovician Scolecodonts of Estonia and Neighbouring Areas: Taxonomy, Distribution, Palaeoecology, and Application. 2002.

14. **Jaak Nõlvak**. Chitinozoan Biostratigrapy in the Ordovician of Baltoscandia. 2002.

15. **Liivi Kluge**. On Algebraic Structure of Pre-Operad. 2002.

16. **Jaanus Lass**. Biosignal Interpretation: Study of Cardiac Arrhytmias and Electromagnetic Field Effects on Human Nervous System. 2002.

17. **Janek Peterson**. Synthesis, Structural Characterization and Modification of PAMAM Dendrimers. 2002.

18. **Merike Vaher**. Room Temperature Ionic Liquids as Background Electrolyte Additives in Capillary Electrophoresis. 2002.

19. **Valdek Mikli**. Electron Microscopy and Image Analysis Study of Powdered Hardmetal Materials and Optoelectronic Thin Films. 2003.

20. **Mart Viljus**. The Microstructure and Properties of Fine-Grained Cermets. 2003.

21. **Signe Kask**. Identification and Characterization of Dairy-Related *Lactobacillus.* 2003.

22. **Tiiu-Mai Laht**. Influence of Microstructure of the Curd on Enzymatic and Microbiological Processes in Swiss-Type Cheese. 2003.

23. **Anne Kuusksalu**. 2–5A Synthetase in the Marine Sponge *Geodia cydonium.* 2003.

24. **Sergei Bereznev**. Solar Cells Based on Polycristalline Copper-Indium Chalcogenides and Conductive Polymers. 2003.

25. **Kadri Kriis**. Asymmetric Synthesis of C_2-Symmetric Bimorpholines and Their Application as Chiral Ligands in the Transfer Hydrogenation of Aromatic Ketones. 2004.

26. **Jekaterina Reut**. Polypyrrole Coatings on Conducting and Insulating Substracts. 2004.

27. **Sven Nõmm**. Realization and Identification of Discrete-Time Nonlinear Systems. 2004.

28. **Olga Kijatkina**. Deposition of Copper Indium Disulphide Films by Chemical Spray Pyrolysis. 2004.

29. **Gert Tamberg**. On Sampling Operators Defined by Rogosinski, Hann and Blackman Windows. 2004.

30. **Monika Übner**. Interaction of Humic Substances with Metal Cations. 2004.

31. **Kaarel Adamberg**. Growth Characteristics of Non-Starter Lactic Acid Bacteria from Cheese. 2004.

32. **Imre Vallikivi**. Lipase-Catalysed Reactions of Prostaglandins. 2004.

33. **Merike Peld**. Substituted Apatites as Sorbents for Heavy Metals. 2005.

34. **Vitali Syritski**. Study of Synthesis and Redox Switching of Polypyrrole and Poly(3,4-ethylenedioxythiophene) by Using *in-situ* Techniques. 2004.

35. **Lee Põllumaa**. Evaluation of Ecotoxicological Effects Related to Oil Shale Industry. 2004.

36. **Riina Aav**. Synthesis of 9,11-Secosterols Intermediates. 2005.

37. **Andres Braunbrück**. Wave Interaction in Weakly Inhomogeneous Materials. 2005.

38. **Robert Kitt**. Generalised Scale-Invariance in Financial Time Series. 2005.

39. **Juss Pavelson**. Mesoscale Physical Processes and the Related Impact on the Summer Nutrient Fields and Phytoplankton Blooms in the Western Gulf of Finland. 2005.

40. **Olari Ilison**. Solitons and Solitary Waves in Media with Higher Order Dispersive and Nonlinear Effects. 2005.

41. **Maksim Säkki**. Intermittency and Long-Range Structurization of Heart Rate. 2005.

42. **Enli Kiipli**. Modelling Seawater Chemistry of the East Baltic Basin in the Late Ordovician–Early Silurian. 2005.

43. **Igor Golovtsov**. Modification of Conductive Properties and Processability of Polyparaphenylene, Polypyrrole and polyaniline. 2005.

44. **Katrin Laos**. Interaction Between Furcellaran and the Globular Proteins (Bovine Serum Albumin β-Lactoglobulin). 2005.

45. **Arvo Mere**. Structural and Electrical Properties of Spray Deposited Copper Indium Disulphide Films for Solar Cells. 2006.

46. **Sille Ehala**. Development and Application of Various On- and Off-Line Analytical Methods for the Analysis of Bioactive Compounds. 2006.

47. **Maria Kulp**. Capillary Electrophoretic Monitoring of Biochemical Reaction Kinetics. 2006.

48. **Anu Aaspõllu.** Proteinases from *Vipera lebetina* Snake Venom Affecting Hemostasis. 2006.

49. **Lyudmila Chekulayeva**. Photosensitized Inactivation of Tumor Cells by Porphyrins and Chlorins. 2006.

50. **Merle Uudsemaa**. Quantum-Chemical Modeling of Solvated First Row Transition Metal Ions. 2006.

51. **Tagli Pitsi**. Nutrition Situation of Pre-School Children in Estonia from 1995 to 2004. 2006.

52. **Angela Ivask**. Luminescent Recombinant Sensor Bacteria for the Analysis of Bioavailable Heavy Metals. 2006.

53. **Tiina Lõugas**. Study on Physico-Chemical Properties and Some Bioactive Compounds of Sea Buckthorn (*Hippophae rhamnoides* L.). 2006.

54. **Kaja Kasemets**. Effect of Changing Environmental Conditions on the Fermentative Growth of *Saccharomyces cerevisae* S288C: Auxo-accelerostat Study. 2006.

55. **Ildar Nisamedtinov**. Application of ^{13}C and Fluorescence Labeling in Metabolic Studies of *Saccharomyces* spp. 2006.

56. **Alar Leibak**. On Additive Generalisation of Voronoï's Theory of Perfect Forms over Algebraic Number Fields. 2006.

57. **Andri Jagomägi**. Photoluminescence of Chalcopyrite Tellurides. 2006.

58. **Tõnu Martma**. Application of Carbon Isotopes to the Study of the Ordovician and Silurian of the Baltic. 2006.

59. **Marit Kauk**. Chemical Composition of $CuInSe_2$ Monograin Powders for Solar Cell Application. 2006.

60. **Julia Kois**. Electrochemical Deposition of $CuInSe_2$ Thin Films for Photovoltaic Applications. 2006.

61. **Ilona Oja Açik**. Sol-Gel Deposition of Titanium Dioxide Films. 2007.

62. **Tiia Anmann**. Integrated and Organized Cellular Bioenergetic Systems in Heart and Brain. 2007.

63. **Katrin Trummal**. Purification, Characterization and Specificity Studies of Metalloproteinases from *Vipera lebetina* Snake Venom. 2007.

64. **Gennadi Lessin**. Biochemical Definition of Coastal Zone Using Numerical Modeling and Measurement Data. 2007.

65. **Enno Pais**. Inverse problems to determine non-homogeneous degenerate memory kernels in heat flow. 2007.

66. **Maria Borissova**. Capillary Electrophoresis on Alkylimidazolium Salts. 2007.

67. **Karin Valmsen**. Prostaglandin Synthesis in the Coral *Plexaura homomalla*: Control of Prostaglandin Stereochemistry at Carbon 15 by Cyclooxygenases. 2007.

68. **Kristjan Piirimäe**. Long-Term Changes of Nutrient Fluxes in the Drainage Basin of the Gulf of Finland – Application of the PolFlow Model. 2007.

69. **Tatjana Dedova**. Chemical Spray Pyrolysis Deposition of Zinc Sulfide Thin Films and Zinc Oxide Nanostructured Layers. 2007.

70. **Katrin Tomson**. Production of Labelled Recombinant Proteins in Fed-Batch Systems in *Escherichia coli*. 2007.

71. **Cecilia Sarmiento**. Suppressors of RNA Silencing in Plants. 2008.

72. **Vilja Mardla**. Inhibition of Platelet Aggregation with Combination of Antiplatelet Agents. 2008.

73. **Maie Bachmann**. Effect of Modulated Microwave Radiation on Human Resting Electroencephalographic Signal. 2008.

74. **Dan Hüvonen**. Terahertz Spectroscopy of Low-Dimensional Spin Systems. 2008.

75. **Ly Villo**. Stereoselective Chemoenzymatic Synthesis of Deoxy Sugar Esters Involving *Candida antarctica* Lipase B. 2008.

76. **Johan Anton**. Technology of Integrated Photoelasticity for Residual Stress Measurement in Glass Articles of Axisymmetric Shape. 2008.

77. **Olga Volobujeva**. SEM Study of Selenization of Different Thin Metallic Films. 2008.

78. **Artur Jõgi**. Synthesis of 4'-Substituted 2,3'-dideoxynucleoside Analogues. 2008.

79. **Mario Kadastik**. Doubly Charged Higgs Boson Decays and Implications on Neutrino Physics. 2008.

80. **Fernando Pérez-Caballero**. Carbon Aerogels from 5-Methylresorcinol-Formaldehyde Gels. 2008.

81. **Sirje Vaask**. The Comparability, Reproducibility and Validity of Estonian Food Consumption Surveys. 2008.

82. **Anna Menaker**. Electrosynthesized Conducting Polymers, Polypyrrole and Poly(3,4-ethylenedioxythiophene), for Molecular Imprinting. 2009.

83. **Lauri Ilison**. Solitons and Solitary Waves in Hierarchical Korteweg-de Vries Type Systems. 2009.

84. **Kaia Ernits**. Study of In_2S_3 and ZnS Thin Films Deposited by Ultrasonic Spray Pyrolysis and Chemical Deposition. 2009.

85. **Veljo Sinivee**. Portable Spectrometer for Ionizing Radiation "Gammamapper". 2009.

86. **Jüri Virkepu**. On Lagrange Formalism for Lie Theory and Operadic Harmonic Oscillator in Low Dimensions. 2009.

87. **Marko Piirsoo**. Deciphering Molecular Basis of Schwann Cell Development. 2009.

88. **Kati Helmja**. Determination of Phenolic Compounds and Their Antioxidative Capability in Plant Extracts. 2010.

89. **Merike Sõmera**. Sobemoviruses: Genomic Organization, Potential for Recombination and Necessity of P1 in Systemic Infection. 2010.

90. **Kristjan Laes**. Preparation and Impedance Spectroscopy of Hybrid Structures Based on $CuIn_3Se_5$ Photoabsorber. 2010.

91. **Kristin Lippur**. Asymmetric Synthesis of 2,2'-Bimorpholine and its 5,5'-Substituted Derivatives. 2010.

92. **Merike Luman**. Dialysis Dose and Nutrition Assessment by an Optical Method. 2010.

93. **Mihhail Berezovski**. Numerical Simulation of Wave Propagation in Heterogeneous and Microstructured Materials. 2010.

94. **Tamara Aid-Pavlidis**. Structure and Regulation of BDNF Gene. 2010.

95. **Olga Bragina**. The Role of Sonic Hedgehog Pathway in Neuro- and Tumorigenesis. 2010.

96. **Merle Randrüüt**. Wave Propagation in Microstructured Solids: Solitary and Periodic Waves. 2010.

97. **Marju Laars**. Asymmetric Organocatalytic Michael and Aldol Reactions Mediated by Cyclic Amines. 2010.

98. **Maarja Grossberg**. Optical Properties of Multinary Semiconductor Compounds for Photovoltaic Applications. 2010.

99. **Alla Maloverjan**. Vertebrate Homologues of Drosophila Fused Kinase and Their Role in Sonic Hedgehog Signalling Pathway. 2010.

100. **Priit Pruunsild**. Neuronal Activity-Dependent Transcription Factors and Regulation of Human *BDNF* Gene. 2010.

101. **Tatjana Knjazeva**. New Approaches in Capillary Electrophoresis for Separation and Study of Proteins. 2011.

102. **Atanas Katerski**. Chemical Composition of Sprayed Copper Indium Disulfide Films for Nanostructured Solar Cells. 2011.

103. **Kristi Timmo.** Formation of Properties of $CuInSe_2$ and $Cu_2ZnSn(S,Se)_4$ Monograin Powders Synthesized in Molten KI. 2011.

104. **Kert Tamm**. Wave Propagation and Interaction in Mindlin-Type Microstructured Solids: Numerical Simulation. 2011.

105. **Adrian Popp**. Ordovician Proetid Trilobites in Baltoscandia and Germany. 2011.

106. **Ove Pärn**. Sea Ice Deformation Events in the Gulf of Finland and This Impact on Shipping. 2011.

107. **Germo Väli**. Numerical Experiments on Matter Transport in the Baltic Sea. 2011.

108. **Andrus Seiman**. Point-of-Care Analyser Based on Capillary Electrophoresis. 2011.

109. **Olga Katargina**. Tick-Borne Pathogens Circulating in Estonia (Tick-Borne Encephalitis Virus, *Anaplasma phagocytophilum*, *Babesia* Species): Their Prevalence and Genetic Characterization. 2011.

110. **Ingrid Sumeri**. The Study of Probiotic Bacteria in Human Gastrointestinal Tract Simulator. 2011.

111. **Kairit Zovo**. Functional Characterization of Cellular Copper Proteome. 2011.

112. **Natalja Makarytsheva**. Analysis of Organic Species in Sediments and Soil by High Performance Separation Methods. 2011.

113. **Monika Mortimer**. Evaluation of the Biological Effects of Engineered Nanoparticles on Unicellular Pro- and Eukaryotic Organisms. 2011.

114. **Kersti Tepp**. Molecular System Bioenergetics of Cardiac Cells: Quantitative Analysis of Structure-Function Relationship. 2011.

115. **Anna-Liisa Peikolainen**. Organic Aerogels Based on 5-Methylresorcinol. 2011.

116. **Leeli Amon**. Palaeoecological Reconstruction of Late-Glacial Vegetation Dynamics in Eastern Baltic Area: A View Based on Plant Macrofossil Analysis. 2011.

117. **Tanel Peets**. Dispersion Analysis of Wave Motion in Microstructured Solids. 2011.

118. **Liina Kaupmees**. Selenization of Molybdenum as Contact Material in Solar Cells. 2011.

119. **Allan Olspert**. Properties of VPg and Coat Protein of Sobemoviruses. 2011.

120. **Kadri Koppel**. Food Category Appraisal Using Sensory Methods. 2011.

121. **Jelena Gorbatšova**. Development of Methods for CE Analysis of Plant Phenolics and Vitamins. 2011.

122. **Karin Viipsi**. Impact of EDTA and Humic Substances on the Removal of Cd and Zn from Aqueous Solutions by Apatite. 2012.

123. **David Schryer**. Metabolic Flux Analysis of Compartmentalized Systems Using Dynamic Isotopologue Modeling. 2012.

124. **Ardo Illaste**. Analysis of Molecular Movements in Cardiac Myocytes. 2012.

125. **Indrek Reile**. 3-Alkylcyclopentane-1,2-Diones in Asymmetric Oxidation and Alkylation Reactions. 2012.

126. **Tatjana Tamberg**. Some Classes of Finite 2-Groups and Their Endomorphism Semigroups. 2012.

127. **Taavi Liblik**. Variability of Thermohaline Structure in the Gulf of Finland in Summer. 2012.

128. **Priidik Lagemaa**. Operational Forecasting in Estonian Marine Waters. 2012.

129. **Andrei Errapart**. Photoelastic Tomography in Linear and Non-linear Approximation. 2012.

130. **Külliki Krabbi**. Biochemical Diagnosis of Classical Galactosemia and Mucopolysaccharidoses in Estonia. 2012.

131. **Kristel Kaseleht**. Identification of Aroma Compounds in Food using SPME-GC/MS and GC-Olfactometry. 2012.

132. **Kristel Kodar**. Immunoglobulin G Glycosylation Profiling in Patients with Gastric Cancer. 2012.

133. **Kai Rosin**. Solar Radiation and Wind as Agents of the Formation of the Radiation Regime in Water Bodies. 2012.

134. **Ann Tiiman**. Interactions of Alzheimer's Amyloid-Beta Peptides with Zn(II) and Cu(II) Ions. 2012.

135. **Olga Gavrilova**. Application and Elaboration of Accounting Approaches for Sustainable Development. 2012.

136. **Olesja Bondarenko**. Development of Bacterial Biosensors and Human Stem Cell-Based *In Vitro* Assays for the Toxicological Profiling of Synthetic Nanoparticles. 2012.

137. **Katri Muska**. Study of Composition and Thermal Treatments of Quaternary Compounds for Monograin Layer Solar Cells. 2012.

138. **Ranno Nahku**. Validation of Critical Factors for the Quantitative Characterization of Bacterial Physiology in Accelerostat Cultures. 2012.

139. **Petri-Jaan Lahtvee**. Quantitative Omics-level Analysis of Growth Rate Dependent Energy Metabolism in *Lactococcus lactis*. 2012.

140. **Kerti Orumets**. Molecular Mechanisms Controlling Intracellular Glutathione Levels in Baker's Yeast *Saccharomyces cerevisiae* and its Random Mutagenized Glutathione Over-Accumulating Isolate. 2012.

141. **Loreida Timberg**. Spice-Cured Sprats Ripening, Sensory Parameters Development, and Quality Indicators. 2012.

142. **Anna Mihhalevski**. Rye Sourdough Fermentation and Bread Stability. 2012.

143. **Liisa Arike**. Quantitative Proteomics of *Escherichia coli*: From Relative to Absolute Scale. 2012.

144. **Kairi Otto**. Deposition of In_2S_3 Thin Films by Chemical Spray Pyrolysis. 2012.

145. **Mari Sepp**. Functions of the Basic Helix-Loop-Helix Transcription Factor TCF4 in Health and Disease. 2012.

146. **Anna Suhhova**. Detection of the Effect of Weak Stressors on Human Resting Electroencephalographic Signal. 2012.

147. **Aram Kazarjan**. Development and Production of Extruded Food and Feed Products Containing Probiotic Microorganisms. 2012.

148. **Rivo Uiboupin**. Application of Remote Sensing Methods for the Investigation of Spatio-Temporal Variability of Sea Surface Temperature and Chlorophyll Fields in the Gulf of Finland. 2013.

149. **Tiina Kriščiunaite**. A Study of Milk Coagulability. 2013.

150. **Tuuli Levandi**. Comparative Study of Cereal Varieties by Analytical Separation Methods and Chemometrics. 2013.

151. **Natalja Kabanova**. Development of a Microcalorimetric Method for the Study of Fermentation Processes. 2013.

152. **Himani Khanduri**. Magnetic Properties of Functional Oxides. 2013.

153. **Julia Smirnova**. Investigation of Properties and Reaction Mechanisms of Redox-Active Proteins by ESI MS. 2013.

154. **Mervi Sepp**. Estimation of Diffusion Restrictions in Cardiomyocytes Using Kinetic Measurements. 2013.

155. **Kersti Jääger**. Differentiation and Heterogeneity of Mesenchymal Stem Cells. 2013.

156. **Victor Alari**. Multi-Scale Wind Wave Modeling in the Baltic Sea. 2013.

157. **Taavi Päll**. Studies of CD44 Hyaluronan Binding Domain as Novel Angiogenesis Inhibitor. 2013.

158. **Allan Niidu**. Synthesis of Cyclopentane and Tetrahydrofuran Derivatives. 2013.

159. **Julia Geller**. Detection and Genetic Characterization of *Borrelia* Species Circulating in Tick Population in Estonia. 2013.

160. **Irina Stulova**. The Effects of Milk Composition and Treatment on the Growth of Lactic Acid Bacteria. 2013.

161. **Jana Holmar**. Optical Method for Uric Acid Removal Assessment During Dialysis. 2013.

162. **Kerti Ausmees**. Synthesis of Heterobicyclo[3.2.0]heptane Derivatives *via* Multicomponent Cascade Reaction. 2013.

163. **Minna Varikmaa**. Structural and Functional Studies of Mitochondrial Respiration Regulation in Muscle Cells. 2013.

164. **Indrek Koppel**. Transcriptional Mechanisms of BDNF Gene Regulation. 2014.

165. **Kristjan Pilt**. Optical Pulse Wave Signal Analysis for Determination of Early Arterial Ageing in Diabetic Patients. 2014.

166. **Andres Anier**. Estimation of the Complexity of the Electroencephalogram for Brain Monitoring in Intensive Care. 2014.

167. **Toivo Kallaste**. Pyroclastic Sanidine in the Lower Palaeozoic Bentonites – A Tool for Regional Geological Correlations. 2014.

168. **Erki Kärber**. Properties of ZnO-nanorod/In_2S_3/$CuInS_2$ Solar Cell and the Constituent Layers Deposited by Chemical Spray Method. 2014.

169. **Julia Lehner**. Formation of Cu_2ZnSnS_4 and $Cu_2ZnSnSe_4$ by Chalcogenisation of Electrochemically Deposited Precursor Layers. 2014.

170. **Peep Pitk**. Protein- and Lipid-rich Solid Slaughterhouse Waste Anaerobic Co-digestion: Resource Analysis and Process Optimization. 2014.

171. **Kaspar Valgepea**. Absolute Quantitative Multi-omics Characterization of Specific Growth Rate-dependent Metabolism of *Escherichia coli*. 2014.

172. **Artur Noole**. Asymmetric Organocatalytic Synthesis of 3,3'-Disubstituted Oxindoles. 2014.

173. **Robert Tsanev**. Identification and Structure-Functional Characterisation of the Gene Transcriptional Repressor Domain of Human Gli Proteins. 2014.

174. **Dmitri Kartofelev**. Nonlinear Sound Generation Mechanisms in Musical Acoustic. 2014.

175. **Sigrid Hade**. GIS Applications in the Studies of the Palaeozoic Graptolite Argillite and Landscape Change. 2014.

176. **Agne Velthut-Meikas**. Ovarian Follicle as the Environment of Oocyte Maturation: The Role of Granulosa Cells and Follicular Fluid at Pre-Ovulatory Development. 2014.

177. **Kristel Hälvin**. Determination of B-group Vitamins in Food Using an LC-MS Stable Isotope Dilution Assay. 2014.

178. **Mailis Päri**. Characterization of the Oligoadenylate Synthetase Subgroup from Phylum Porifera. 2014.

179. **Jekaterina Kazantseva**. Alternative Splicing of *TAF4*: A Dynamic Switch between Distinct Cell Functions. 2014.

180. **Jaanus Suurväli**. Regulator of G Protein Signalling 16 (RGS16): Functions in Immunity and Genomic Location in an Ancient MHC-Related Evolutionarily Conserved Synteny Group. 2014.

181. **Ene Viiard**. Diversity and Stability of Lactic Acid Bacteria During Rye Sourdough Propagation. 2014.

182. **Kristella Hansen**. Prostaglandin Synthesis in Marine Arthropods and Red Algae. 2014.

183. **Helike Lõhelaid**. Allene Oxide Synthase-lipoxygenase Pathway in Coral Stress Response. 2015.

184. **Normunds Stivrinš**. Postglacial Environmental Conditions, Vegetation Succession and Human Impact in Latvia. 2015.

185. **Mary-Liis Kütt**. Identification and Characterization of Bioactive Peptides with Antimicrobial and Immunoregulating Properties Derived from Bovine Colostrum and Milk. 2015.

186. **Kazbulat Šogenov**. Petrophysical Models of the CO_2 Plume at Prospective Storage Sites in the Baltic Basin. 2015.

187. **Taavi Raadik**. Application of Modulation Spectroscopy Methods in Photovoltaic Materials Research. 2015.

188. **Reio Põder**. Study of Oxygen Vacancy Dynamics in Sc-doped Ceria with NMR Techniques. 2015.

189. **Sven Siir**. Internal Geochemical Stratification of Bentonites (Altered Volcanic Ash Beds) and its Interpretation. 2015.

190. **Kaur Jaanson**. Novel Transgenic Models Based on Bacterial Artificial Chromosomes for Studying BDNF Gene Regulation. 2015.

191. **Niina Karro**. Analysis of ADP Compartmentation in Cardiomyocytes and Its Role in Protection Against Mitochondrial Permeability Transition Pore Opening. 2015.

192. **Piret Laht**. B-plexins Regulate the Maturation of Neurons Through Microtubule Dynamics. 2015.

193. **Sergei Žari**. Organocatalytic Asymmetric Addition to Unsaturated 1,4-Dicarbonyl Compounds. 2015.

194. **Natalja Buhhalko**. Processes Influencing the Spatio-temporal Dynamics of Nutrients and Phytoplankton in Summer in the Gulf of Finland, Baltic Sea. 2015.

195. **Natalia Maticiuc**. Mechanism of Changes in the Properties of Chemically Deposited CdS Thin Films Induced by Thermal Annealing. 2015.

196. **Mario Öeren**. Computational Study of Cyclohexylhemicucurbiturils. 2015.

197. **Mari Kalda**. Mechanoenergetics of a Single Cardiomyocyte. 2015.

198. **Ieva Grudzinska**. Diatom Stratigraphy and Relative Sea Level Changes of the Eastern Baltic Sea over the Holocene. 2015.

199. **Anna Kazantseva**. Alternative Splicing in Health and Disease. 2015.

200. **Jana Kazarjan**. Investigation of Endogenous Antioxidants and Their Synthetic Analogues by Capillary Electrophoresis. 2016.

201. **Maria Safonova**. SnS Thin Films Deposition by Chemical Solution Method and Characterization. 2016.

202. **Jekaterina Mazina**. Detection of Psycho- and Bioactive Drugs in Different Sample Matrices by Fluorescence Spectroscopy and Capillary Electrophoresis. 2016.

203. **Karin Rosenstein**. Genes Regulated by Estrogen and Progesterone in Human Endometrium. 2016.

204. **Aleksei Tretjakov**. A Macromolecular Imprinting Approach to Design Synthetic Receptors for Label-Free Biosensing Applications. 2016.

205. **Mati Danilson**. Temperature Dependent Electrical Properties of Kesterite Monograin Layer Solar Cells. 2016.

206. **Kaspar Kevvai**. Applications of ^{15}N-labeled Yeast Hydrolysates in Metabolic Studies of *Lactococcus lactis* and *Saccharomyces Cerevisiae*. 2016.

207. **Kadri Aller**. Development and Applications of Chemically Defined Media for Lactic Acid Bacteria. 2016.

208. **Gert Preegel**. Cyclopentane-1,2-dione and Cyclopent-2-en-1-one in Asymmetric Organocatalytic Reactions. 2016.

209. **Jekaterina Služenikina**. Applications of Marine Scatterometer Winds and Quality Aspects of their Assimilation into Numerical Weather Prediction Model HIRLAM. 2016.

210. **Erkki Kask**. Study of Kesterite Solar Cell Absorbers by Capacitance Spectroscopy Methods. 2016.

211. **Jürgen Arund**. Major Chromophores and Fluorophores in the Spent Dialysate as Cornerstones for Optical Monitoring of Kidney Replacement Therapy. 2016.

212. **Andrei Šamarin**. Hybrid PET/MR Imaging of Bone Metabolism and Morphology. 2016.

213. **Kairi Kasemets**. Inverse Problems for Parabolic Integro-Differential Equations with Instant and Integral Conditions. 2016.

214. **Edith Soosaar**. An Evolution of Freshwater Bulge in Laboratory Scale Experiments and Natural Conditions. 2016.

215. **Peeter Laas**. Spatiotemporal Niche-Partitioning of Bacterioplankton Community across Environmental Gradients in the Baltic Sea. 2016.

216. **Margus Voolma**. Geochemistry of Organic-Rich Metalliferous Oil Shale/Black Shale of Jordan and Estonia. 2016.

217. **Karin Ojamäe**. The Ecology and Photobiology of Mixotrophic Alveolates in the Baltic Sea. 2016.

218. **Anne Pink**. The Role of CD44 in the Control of Endothelial Cell Proliferation and Angiogenesis. 2016.

219. **Kristiina Kreek**. Metal-Doped Aerogels Based on Resorcinol Derivatives. 2016.

220. **Kaia Kukk**. Expression of Human Prostaglandin H Synthases in the Yeast Pichia pastoris. 2016.

221. **Martin Laasmaa**. Revealing Aspects of Cardiac Function from Fluorescence and Electrophysiological Recordings. 2016.